5.0 SUMMARY

The IH2VOF model was used to assess the potential overtopping during extreme conditions including the 15, 25 and 50 years return period waves and water levels. Two profiles were analyzed, one without a seawall (R131) and one with a seawall (R137). The wave data and storm profiles were obtained from previous SBEACH modeling. The water level was considered constant during the simulation period (30 minutes). To analyze comparatively, three wave cases were simulated on each profile for two alternatives (Alternatives 2 and 6).

Seven probes were placed within the model across the beach profiles to analyze the evolution of wave propagation toward the coast. The probes showed a reduction in wave height as the waves propagated through shallower waters depths and the transfer of wave energy from higher to lower frequencies due to wave breaking. The transfer of energy can eventually generate infragravity waves, which depending on a variety of factors including profile shape and elevation, can be more important than wave height on causing overtopping, as described by Suzuki et al. (2012). As the waves approach the beach, the presence of the beach fill from Alternatives 2 and 6 reduced wave height, the likelihood of the waves reaching the dune crest, and the frequency of overtopping. It was also observed that as the waves and water levels increase, the overtopping thickness increases.

- <u>15 Year Return Period Storm:</u> At R131, the Alternatives 2/6 resulted in a 67% reduction in the mean overtopping discharge as compared to the existing conditions. At R137, the volume of water overtopping the seawall was reduced by 25% for Alternative 2 and 88% for Alternative 6 as compared to the existing conditions.

- <u>25 Year Return Period Storm:</u> At R131, the overtopping discharge for Alternatives 2/6 is reduced by 75% as compared to the existing conditions. At R137, overtopping discharge is similar for existing conditions and Alternative 2, while a 22% reduction was simulated for Alternative 6.

- <u>50 Year Return Period Storm:</u> At R131, the overtopping discharge for Alternatives 2/6 is reduced by 67% as compared to the existing conditions. At R137, the reduction is observed, but at a smaller magnitude. For Alternatives 2 and 6 the mean overtopping discharges are reduced by 8% and 16% as compared to the existing conditions.

The top 1-3 feet of the seawall is exposed for the existing condition and buried for the alternatives. For the exposed portion under the existing conditions, the results showed that the maximum horizontal forces at the seawall vary from 41.8, 53.3 to 69.1 kN/m for 15, 25 and 50 year return period waves, respectively. The maximum horizontal momentum for existing conditions with return period waves of 15, 25, and 50 years was 25.6, 37.2 and 52.2 kN/m, respectively. The wave forces and momentums to which the seawall is exposed increases with higher return period waves. Sand fill placed in front of the seawalls may reduce this effect.

The overtopping discharge was used to categorize the anticipated safety during the storm events. Regardless of the return period storm event, the overtopping is expected to be “unsafe at any speed” for vehicle safety and “very dangerous” pedestrian safety. At R137 when the seawall is exposed under the existing conditions, “damage if back slope is not protected” should be expected for the 15 year return period storm event and “damage even if fully protected” should be expected for the 25 and 50 year events. At R131 and at R137 (for the alternatives), the dune is expected to incur “damage” except during the 15 year return period storm event for Alternative 6. During this scenario, the additional protection provided by the increased fill volume would reduce the expectation to “start of damage.”

6.0 CONCLUSIONS

While considering the findings of this study, it is important to emphasize that the simulated conditions represent extreme storm events, but there is considerable variability among events that may be encountered. Based on the modeling, the following conclusions were made:

- The existing beach conditions are susceptible to wave overtopping during 15, 25 and 50 year return period storms. Overtopping increases as wave and water level conditions increase. This is attributed to the reduction in dry beach width and the dune crest (or seawall) height above the waves and water level.

- For the return period storms, the alternatives provide a reduction in overtopping and consequently an increase in storm protection as compared to the existing conditions.

    - At R131, the overtopping during the 15 year storm was reduced up to 67% for the alternatives as compared to the existing conditions. Similarly, the overtopping during 25 and 50 year storms were reduced up to 75% and 58%, respectively.

    - At R137, the larger fill volume associated with Alternative 6 provided greater storm protection by reducing overtopping as compared to Alternative 2. The incremental benefit of Alternative 6 above the protection as compared to the existing conditions was 50% less overtopping for the 15 year return period storm, 22% less for the 25 year storm, and 8% less for the 50 year storm. Alternative 2 provided 25% less overtopping for the 15 year storm, 0% for the 25 year storm, and 8% for the 50 year storm.

- Given the existing conditions, seawalls are subject to wave attack during storm events. These wave forces that the seawalls are exposed to increase with the intensity of the storm events. The exposure of seawalls to waves can cause damage thereby reducing the designed level of protection and/or increasing the frequency and need for structural repairs in order to maintain their integrity. Sand fill placed in front of the seawalls may offer additional protection.

- According to the USACE safety criteria, the mean overtopping discharge during the storm events is expected to cause some level of damage to the dune (or seawall) and create unsafe, dangerous situations for vehicles and pedestrians at the point of overtopping. Overtopping was not eliminated by having the alternatives in place. However, the alternatives did reduce overtopping, which would in turn reduce damage and unsafe, dangerous situations during storm events.

The results of this numerical modeling study should be used in conjunction with other coastal engineering assessments and prudent engineering judgment.

7.0 LITERATURE CITED

CB&I Coastal Planning & Engineering, Inc., 2014. Southern Palm Beach Island Comprehensive Shoreline Stabilization Project Environmental Impact Statement (EIS) SBEACH Analysis Report. Prepared for U.S. Army Corps of Engineers (USACE) 131 p.

EurOtop Manual. 2007. Overtopping Manual; Wave Overtopping of Sea Defences and Related Structures – Assessment Manual. UK: N.W.H. Allsop, T. Pullen, T. Bruce. NL: J.W. van der Meer. DE: H. Schüttrumpf, A. Kortenhaus. www.overtopping-manual.com.

Hirt, C.W., Nichols, B.D., 1981. Volume of Fluid (VOF) method for dynamics of the Free boundaries. Journal of Computation Physic, 39: 201-225.

Hsu, T-J., Sakakiyama, T., Liu, P.L.-F., 2002. A Numerical Model for Wave Motions and Turbulence flows in Front of a Composite Breakwater. Coastal Engineerint, 46: 25-50.

Lara, J.L., Garcia, N e Lossada, I.J., 2006. RANS Modelling applied to Random Wave Interaction With Submerged Permeable Structures. Coastal Engineering, Vol. 53 (5-6), 395-417. ELSEVIER.

Lara, J.L., Ruju, A., Losada, I.J., 2011. RANS Modeling of Long Waves Induced By a Transient Wave Group on Beach. Pro. Of Royal Society A-Mathematical, Physical and Engineering Sciences. 467 (2129), 1215-1242.

Lin, P.,1998. Numerical Modeling of Breaking Waves. Ph.D. Thesis, Cornell University.

Lykke Andersen, T. 2006. Hydraulic Response of Rubble Mound Breakwaters. Scale Effects – Berm Breakwaters, Ph.D. Thesis, Department of Civil Engineering, Aalborg University, Denmark.

Peng Z, Zou Q-P. 2011. Spatial distribution of wave overtopping water behind coastal structures. Coastal Engineering. 58: 489–498.

Schüttrumpf, H. and Oumeraci, H. 2005. Layer Thickness and Velocities of Overtopping at Seadikes. Journal of Coastal Engineering. No. 52. Pp 473-495.

Suzuki, T. • Verwaest, T. • Veale, W. • Trouw, K. • Zijlema, M., 2012. A Numerical Study on the Effect of the Beach Nourishment on Wave Overtopping in Shallow Foreshores. Coastal Engineering 2012. 12 pp.

Torres-Freyermuth, A., Lara, J.L., Lossada, I.J., 2010. Numerical Modelling of Short-and-Long-Wave transformation on barred beach. Coastal Engineering. 57, pp 317-330.

U.S. Army Corps of Engineers, 2006. Coastal Engineering Manual, Engineer Manual 1110-2-1100, U.S. Army Corps of Engineers, Washington, D.C. (in 6 volumes).

Van der Meer, J.W., R. Schrijver, B. Hardeman, A. van Hoven, H. Verheij and G.J. Steendam. 2009. Guidance on erosion resistance of inner slopes of dikes from three years of testing with the Wave Overtopping Simulator. Proc. ICE, Coasts, Marine Structures and Breakwaters 2009, Edinburgh, UK.

SUB-APPENDIX G-3

DRAFT DELFT3D MODELING REPORT

This page intentionally left blank.

SOUTHERN PALM BEACH ISLAND COMPREHENSIVE SHORELINE STABILIZATION PROJECT DRAFT DELFT3D MODELING REPORT

TABLE OF CONTENTS

LIST OF FIGURES

Figure No.

LIST OF TABLES

Table No.

1.0 INTRODUCTION

Under direction of the U.S. Army Corps of Engineers (USACE), CB&I Coastal Planning & Engineering, Inc. (CB&I) assisted in the development of the Southern Palm Beach Island Comprehensive Shoreline Stabilization Project Environmental Impact Statement (EIS). The initial tasks associated with the effort included public scoping and agency coordination to determine what data was necessary to develop the EIS. After review of the data and previous work, the USACE has determined that numerical modeling of sediment transport was required to obtain necessary data that is not currently available.

The Project Area for the Southern Palm Beach Island Comprehensive Shoreline Stabilization Project (the Project) comprises approximately 2.07 miles of shoreline and nearshore environment. The north and south limits are Florida Department of Environmental Protection (FDEP) range monuments (R-monuments) R-129-210 (south end of Lake Worth Municipal Beach) and R-138+551 (south of the Eau Palm Beach Resort and Spa in Manalapan), respectively (Figure 1-1). The Project Area's beaches provide storm protection to residential and public infrastructure and serve as nesting areas for marine turtles.

A numerical modeling study was conducted to assess the potential impacts to hardbottom as a result of the proposed alternatives. Morphology and sediment transport analysis of proposed alternatives for the EIS Project Area was conducted using the Delft3D model. The simulation of nearshore hardbottom is included in the model.

As part of a previous study conducted for Palm Beach County, a Delft3D numerical model (CPE, 2013) was developed, calibrated and applied to evaluate Project alternatives along the shoreline of South Palm Beach, Lantana, and Manalapan. The setup, initially focused on the South Palm Beach project area, was expanded for this study to include the Town of Palm Beach in evaluating the combined project area.

The study presented herein builds upon the following series of earlier reports:

- Coastal Planning & Engineering, Inc., 2007a. Town of South Palm Beach/Town of Lantana Erosion Control Study, Coastal Planning & Engineering, Inc., Boca Raton, FL.

- Coastal Planning & Engineering, Inc., 2010. Central Palm Beach County Comprehensive Erosion Control Project, Numerical Calibration of Wave Propagation and Morphology Changes, Coastal Planning & Engineering, Inc., Boca Raton, FL.

- Coastal Planning & Engineering, Inc., 2011. Central Palm Beach County Comprehensive Erosion Control Project Numerical Modeling of Shore Protection Alternatives, Coastal Planning & Engineering, Inc., Boca Raton, FL.

- Coastal Planning & Engineering, Inc., 2013. Central Palm Beach County Comprehensive Erosion Control Project Reformulated Shore Protection Alternatives, Coastal Planning & Engineering, Inc., Boca Raton, FL.

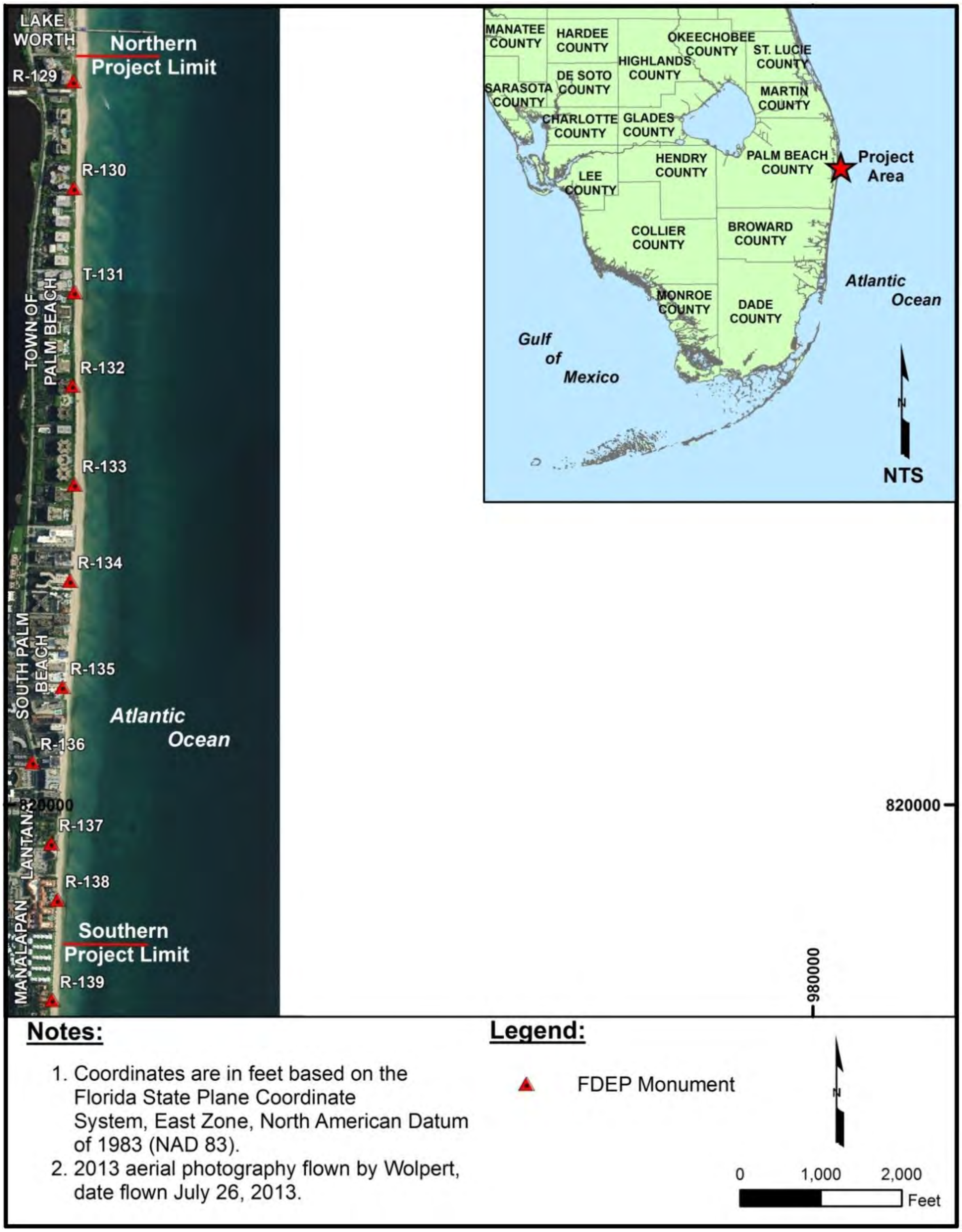

Figure 1-1. Southern Palm Beach Island Comprehensive Shoreline Stabilization Project Location.

The alternatives that were considered in the analysis included:

- Alternative 1 – No Action Alternative (Status Quo) and referenced herein as the existing conditions.
- Alternative 2 – The Applicants' Preferred Project (proposed action): Beach and Dune Fill with Shoreline Protection Structures
- Alternative 3 – The Applicants' Preferred Project without Shoreline Protection Structures
- Alternative 4 – The Town of Palm Beach Preferred Project and County Increased Sand Volume without Shoreline Protection Structures
- Alternative 5 – The Town of Palm Beach Increased Sand Volume and County Preferred Project Alternative 6 – The Town of Palm Beach Increased Sand Volume Project and County Increased Sand Volume without Shoreline Protection Structures Project
- Alternative 7 – Plan was presented by The Coalition to Save Our Shoreline, Inc. (SOS) consisting of beach fill and dune restoration between R-129+210 and R-134+135 with shoreline protection structures. The sand fill volumes required for the SOS plan are greater than the volumes for Alternative 6 over the same shoreline extents. For the purpose of modeling, Alternative 7 was defined as the SOS plan north of R-134+135 and Alternative 2 to the south.

In addition, the alternatives were separated into the Town of Palm Beach and the County projects and modeled individually to evaluate the effects/impacts attributable to the individual projects.

2.0 METHODOLOGY

The primary modeling tool used in this study was the Delft3D morphological modeling package (Deltares, 2011). This package consists of two models, which are coupled together to determine changes in a topographic and bathymetric surface based on the effects of waves, water levels, winds, and currents. Wave propagation from the offshore to the nearshore area is estimated using the Simulating Waves Nearshore Model (SWAN 40.72ABCDE, Delft University of Technology, 2008). Delft3D-FLOW utilizes the output waves from SWAN, along with the varying water levels offshore and the bathymetry, to determine the resulting currents, water levels, sediment transport, erosion, and deposition. Based on the estimated erosion and deposition at each time step, the Delft3D-FLOW model calculates the subsequent elevations of the topographic and bathymetric surface and sends the updated bathymetry back to the SWAN model. Typical time steps in Delft3D-FLOW range from 1 second to 60 seconds, while wave propagation estimates in the SWAN model are performed every 1 to 3 hours. Given the interaction between the currents, hardbottoms, and waves, Delft3D is an effective means of evaluating the performance and impact of structures, and beach fill alternatives within the Study Area.

3.0 MODEL SETUP

3.1. Grids

To perform morphological calibration and productions runs, four numerical grids were used (Figure 3-1). The following is a brief description of each grid:

1. A regional wave grid was designed to examine wave transformation processes. The regional wave grid extends from near Highland Beach to 2 miles north of Palm Beach Inlet reaching depths up to 700 feet, NAVD (Figure 3-1).

2. An intermediate wave grid was designed to examine wave propagation from deep to shallow water, transferring waves from regional to local grid (Figure 3-1). The intermediate grid was nested in regional grid.

3. A local wave grid was designed to examine detailed, shallow water wave processes along the Study Area. Near the shoreline and in the nearby area of proposed alternatives, grid resolution was increased to simulate refraction, diffraction, and breaking processes (Figure 3-2). The local wave grid was nested in intermediate wave grid.

4. A flow grid was designed to examine circulation patterns and morphological changes along the Study Area. The perimeter cells of the grid were trimmed to ensure stable coupling between the SWAN model and the Delft3D-Flow model (Figure 3-3).

All grids were constructed in Cartesian coordinates based on the Florida State Plane Coordinate System, East Zone, North American Datum of 1983 (FLE-NAD83). Grid characteristics are summarized in Table 3-1.

The model's developers (Deltares) have established guidelines for grid cell smoothing and orthogonality that were used. Smoothing represents the change in cell size between two rows of grid cells. A smoothing value of 1.1 indicates that the cell size between two rows of grid cells increases by 10%. The maximum smoothing value recommended by model developers is 1.2. Orthogonality is equivalent to the angle between the longshore and cross-shore grid lines. The angles between the longshore and cross-shore grid lines should be at least 87.7 degrees within the area of interest. All four grids follow the Deltares guidelines for smoothing and orthogonality (see Table 3-1).

Figure 3-1. Computational grids used in Delft3D-WAVE and Delft3D-FLOW calibration and production runs.

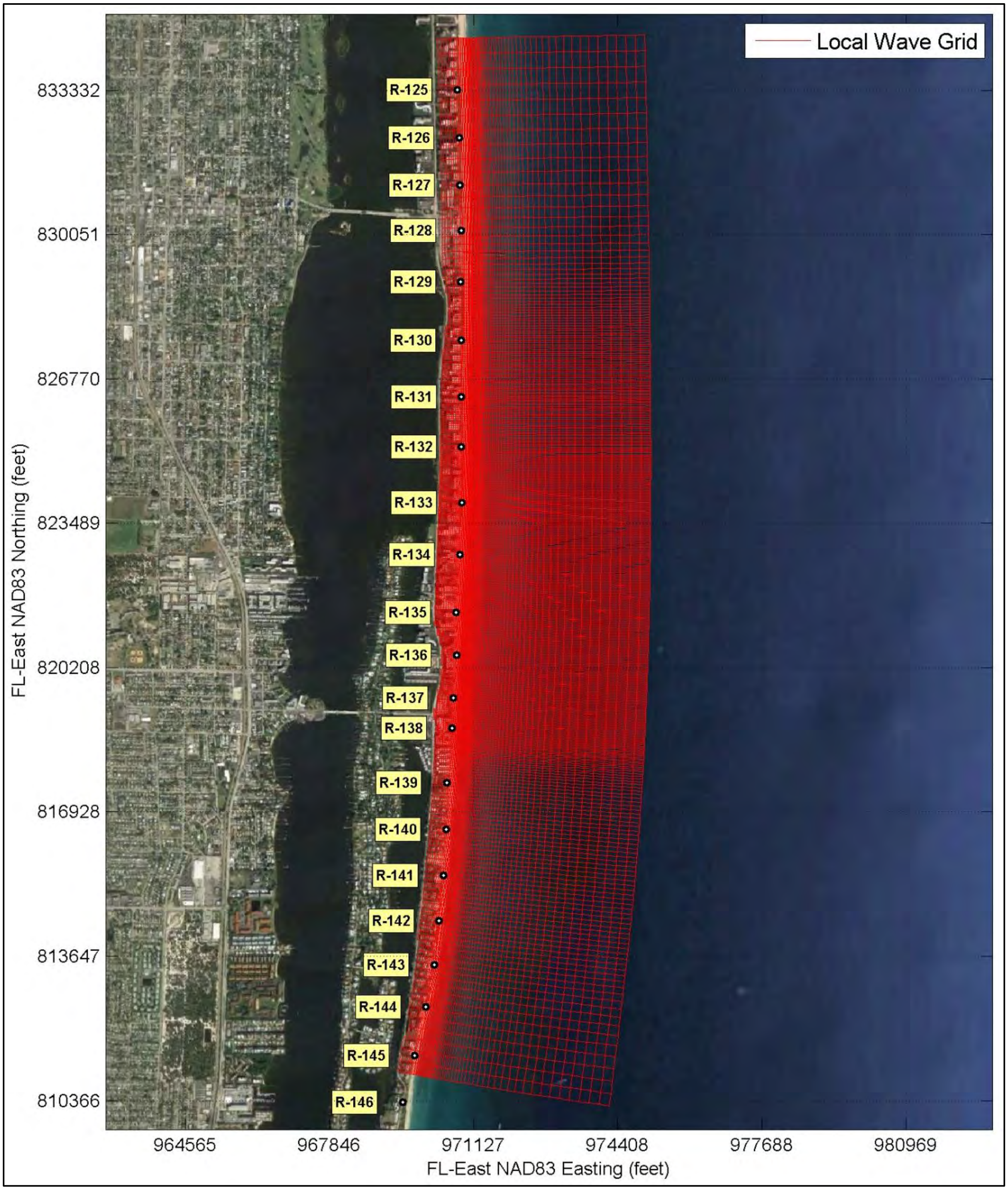

Figure 3-2. Local wave grid used in calibration and production runs.

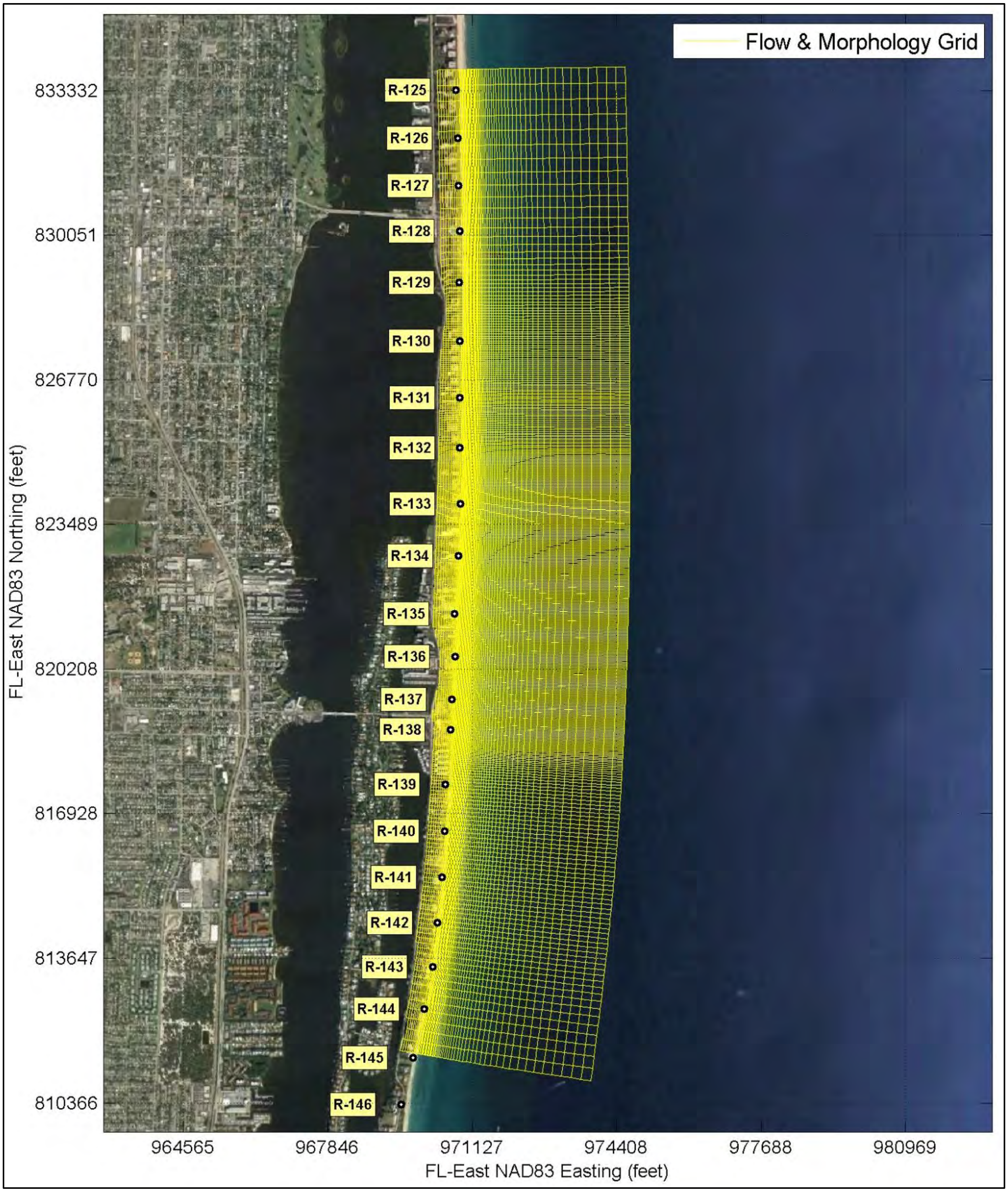

Figure 3-3. Flow and morphology grid used in calibration and production runs.

Table 3-1. South Palm Beach – Calibration Grids.

	Regional Wave Grid	Intermediate Wave Grid	Local Wave Grid	Flow Grid
# of Longshore Cells	36	49	405	401
# of Cross-Shore Cells	124	109	67	65
Longshore Spacing (feet) - Min.	1,148.00	312.00	30.00	44.69
Longshore Spacing (feet) - Max.	1,312.00	344.00	354.00	171.33
Cross-shore Spacing (feet) - Min.	623.00	164.00	20.00	50.92
Cross-shore Spacing (feet) - Max.	1227.00	328.00	233.00	211.88
Longshore Smoothness - Min.	1.00	1.00	1.00	1.00
Longshore Smoothness - Max.	1.00	1.00	1.10	1.10
Cross-shore Smoothness - Min.	1.00	1.00	1.00	1.00
Cross-shore Smoothness - Max.	1.11	1.11	1.13	1.13
Orthogonality (deg.) - Min.	90.00	90.00	89.90	89.90
Orthogonality (deg.) - Max.	90.00	90.00	90.00	90.00

3.2. Initial Bathymetry

The primary sources of topographic and bathymetric data for this model study are listed in Table 3-2. Conversions between MSL and NAVD assumed MSL = -0.28 feet NAVD. All the models were run in MSL.

Table 3-2. Bathymetric & Topographic Data Sources.

Survey Date	Area	Type	Source	Vertical Accuracy (feet)
January 2012	Beach Profiles	R-135 to R-164	FDEP (2012)	0.1 to 0.5
September-November 2011	Beach Profiles	R-73 to R-135	ATM (2012)	0.1 to 0.5
December 2008	High-Density Beach Profiles	R-132 to R-143	Sea-Diversified (2008)	0.1 to 0.5
October-December 2008	Beach Profiles	R-77 to R-135	CPE (2009)	0.1 to 0.5
January-February 2006	LIDAR	Palm Beach County	USACE (2006)	0.5
1963-1964	Hydrographic	Palm Beach County	NOAA (2006)	1.4

Bathymetry for the morphologic calibration period was based on the following data sources (see also Table 3-2):

1. December 2008 high-density beach profiles (i.e., spaced at 500 feet alongshore) (Sea-Diversified, 2008)
2. October-December 2008 beach profiles (CPE, 2009)
3. 2006 Lidar (USACE, 2006)
4. 1963-1964 hydrographic survey (NOAA, 2006)

For morphology calibration, the primary data set was the December 2008 high-density beach profiles, followed by October-December 2008 beach profiles. The 2006 Lidar data was used to represent topography beyond the beach profiles, while the hydrographic survey from 1963-1964 were used to represent the bathymetry at deeper water depths for the intermediate and regional wave grids. The resulting bathymetries for the local wave grid and the flow and morphology grid appear in Figure 3-4 and Figure 3-5. The bathymetries for the regional and intermediate grids are shown in Figure 3-6 and Figure 3-7.

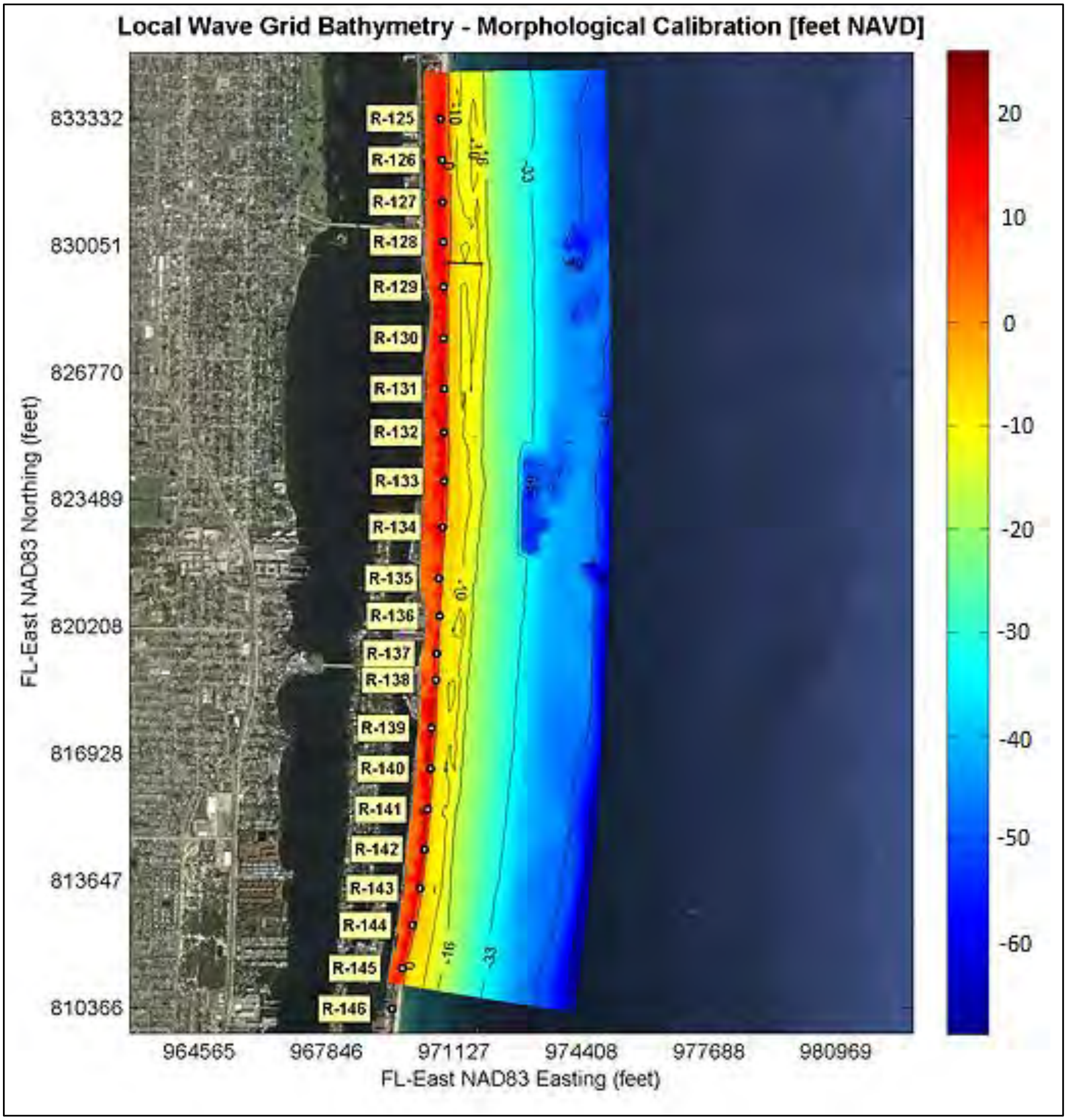

Figure 3-4. Local wave grid bathymetry (feet NAVD) used in morphological calibration run.

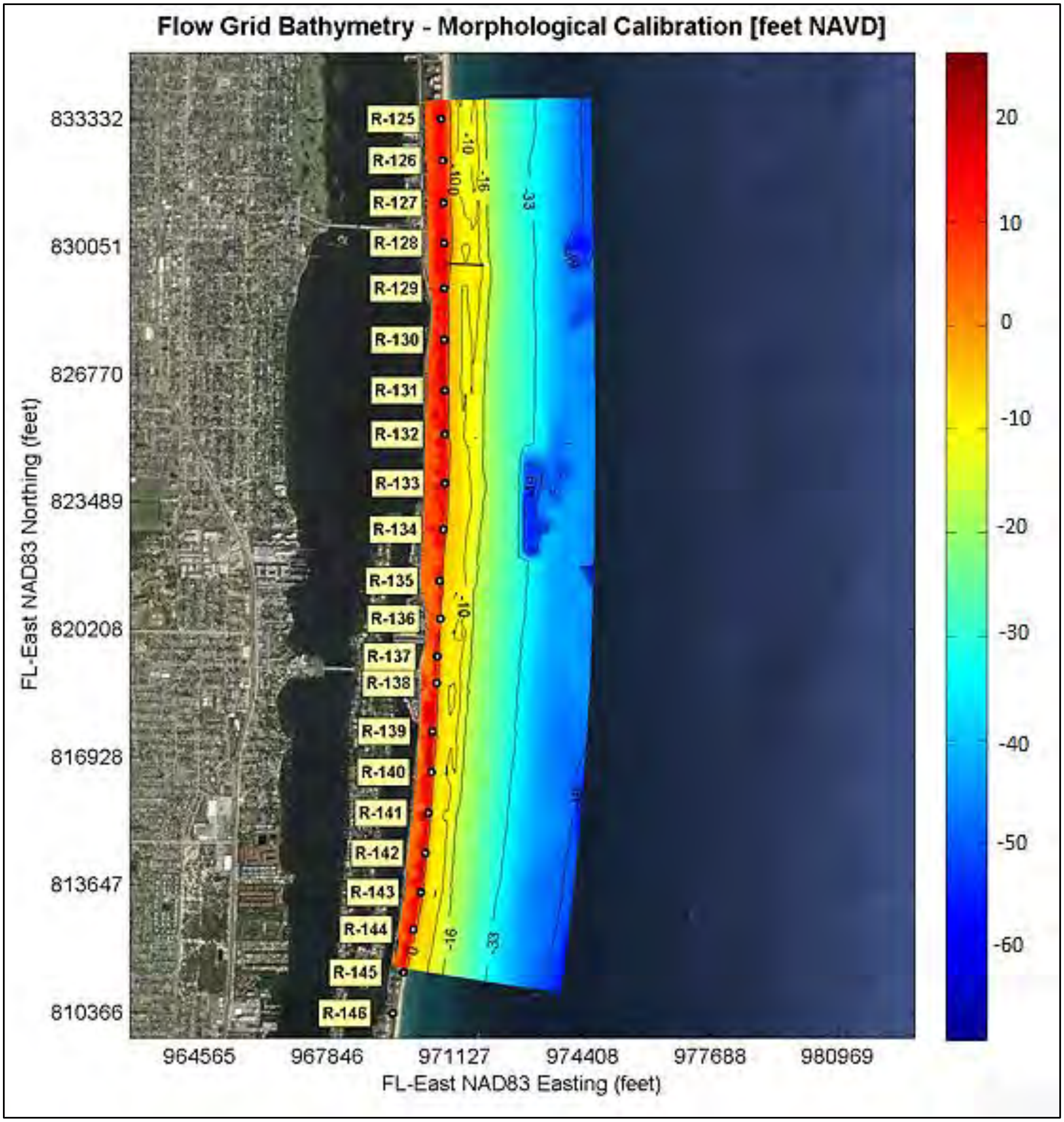

Figure 3-5. Flow and morphology grid bathymetry (feet NAVD) used in morphological calibration run.

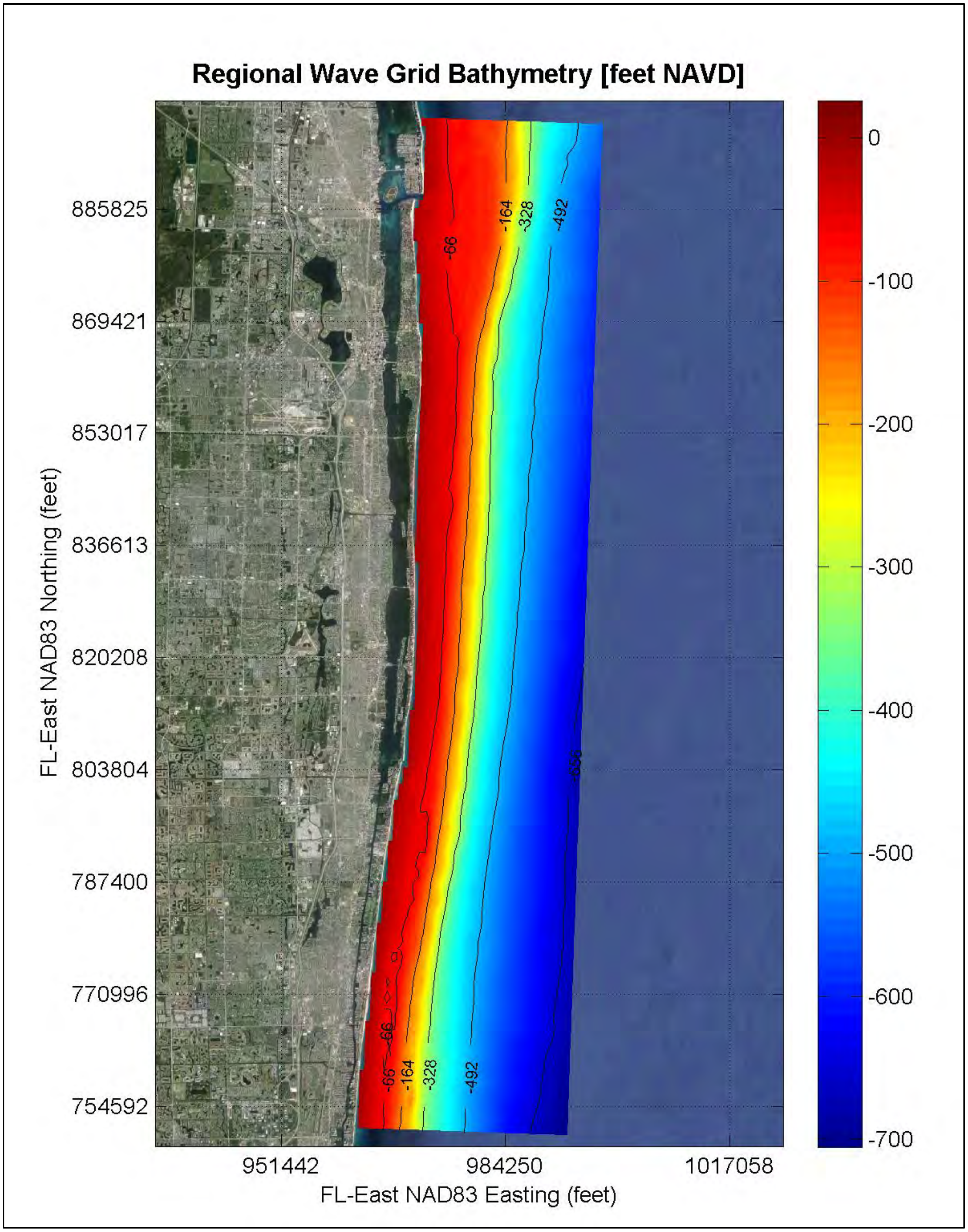

Figure 3-6. Regional wave grid bathymetry (feet NAVD) used in morphological calibration run.

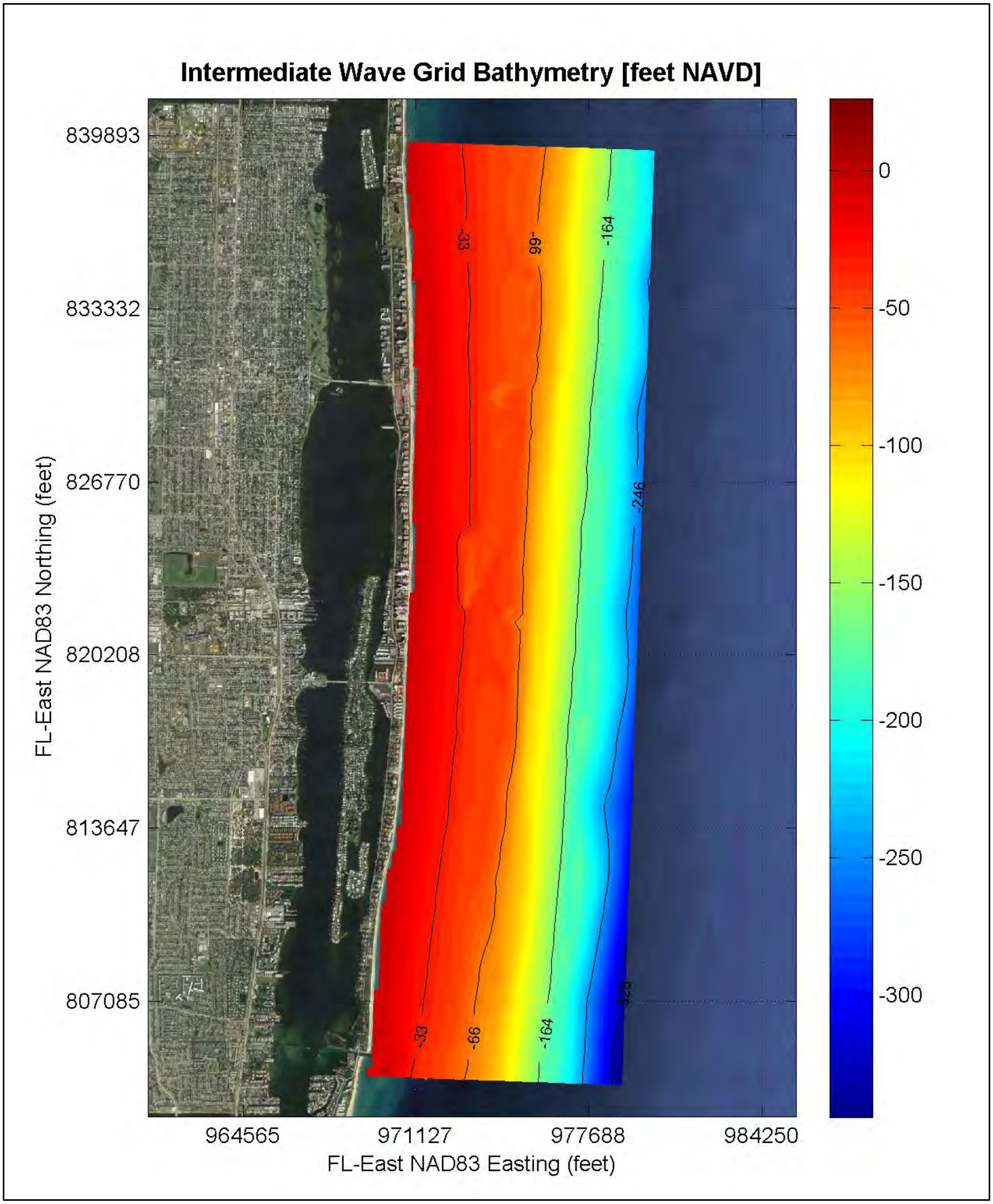

Figure 3-7. Intermediate wave grid bathymetry (feet NAVD) used in calibration runs.

3.3. Water Levels

Tides at the Project Area were based at tidal datums along Lake Worth Pier Station located at 26° 36.7' N, 80° 2.0' W (NOAA, 2011) which are presented in Table 3-3. The observed water levels from March 2014 are shown in Figure 3-8. Tides at the Project Area are semidiurnal with amplitudes averaging 2.74 feet based on the vertical difference between MHW and MLW. Tides were represented as morphological tide, described in Section 4.2.4 below.

Table 3-3: Tidal Datums, Lake Worth Pier FL, NOAA Station 8722670 (NOAA, 2011).

Datum	Abbrev.	(feet MLLW)	(feet NAVD)
MEAN HIGHER HIGH WATER	MHHW	3.01	0.58
MEAN HIGH WATER	MHW	2.87	0.44
North American Vertical Datum of 1988	NAVD88	2.42	0.00
MEAN SEA LEVEL	MSL	1.51	-0.92
MEAN TIDE LEVEL	MTL	1.50	-0.92
MEAN LOW WATER	MLW	0.13	-2.29
MEAN LOWER LOW WATER	MLLW	0.00	-2.42

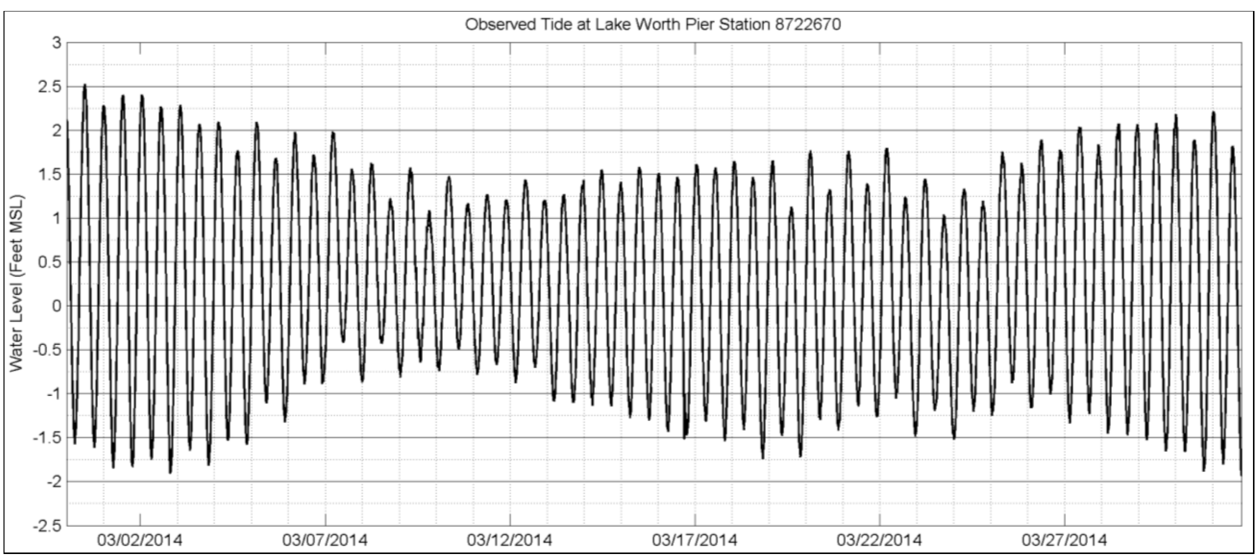

Figure 3-8. Observed water levels at Lake Worth Pier Station.

3.4. Offshore Wind and Wave Data

The wind and wave data used in this modeling study were obtained from WIS (Wave Information System) hindcast data (v02) at Station 63461 over the time period between 1980 and 2012. The data source was located approximately 12 miles offshore of the Study Area (Figure 3-9) at 26.58° N, 79.83° W. All wave and wind data was provided in SI units, with times referenced to Greenwich Mean Time (GMT). WIS Station data was given every 3 hours.

WIS Hindcast Data is generated from numerical models (WISWAVE, WAM) driven by climatological wind fields overlaid on grids containing estimated bathymetries. The WIS numerical hindcasts supply long-term wave climate information at nearshore locations (stations) of U.S. coastal waters.

Time series of significant wave height (Hs), peak period (Tp) and wave peak direction (Dirp) from WIS Station ST 63461 appear in Figure 3-10. Time series of wind velocity and wind direction from WIS Station ST 63461 appear in Figure 3-10. Directional wind and wave statistics are presented in Figure 3-12 and Figure 3-13, respectively. In general, winds come from all directions, but there are a large percentage of winds that come from E to S quadrants. The prevailing directions of waves are from NE to ESE.

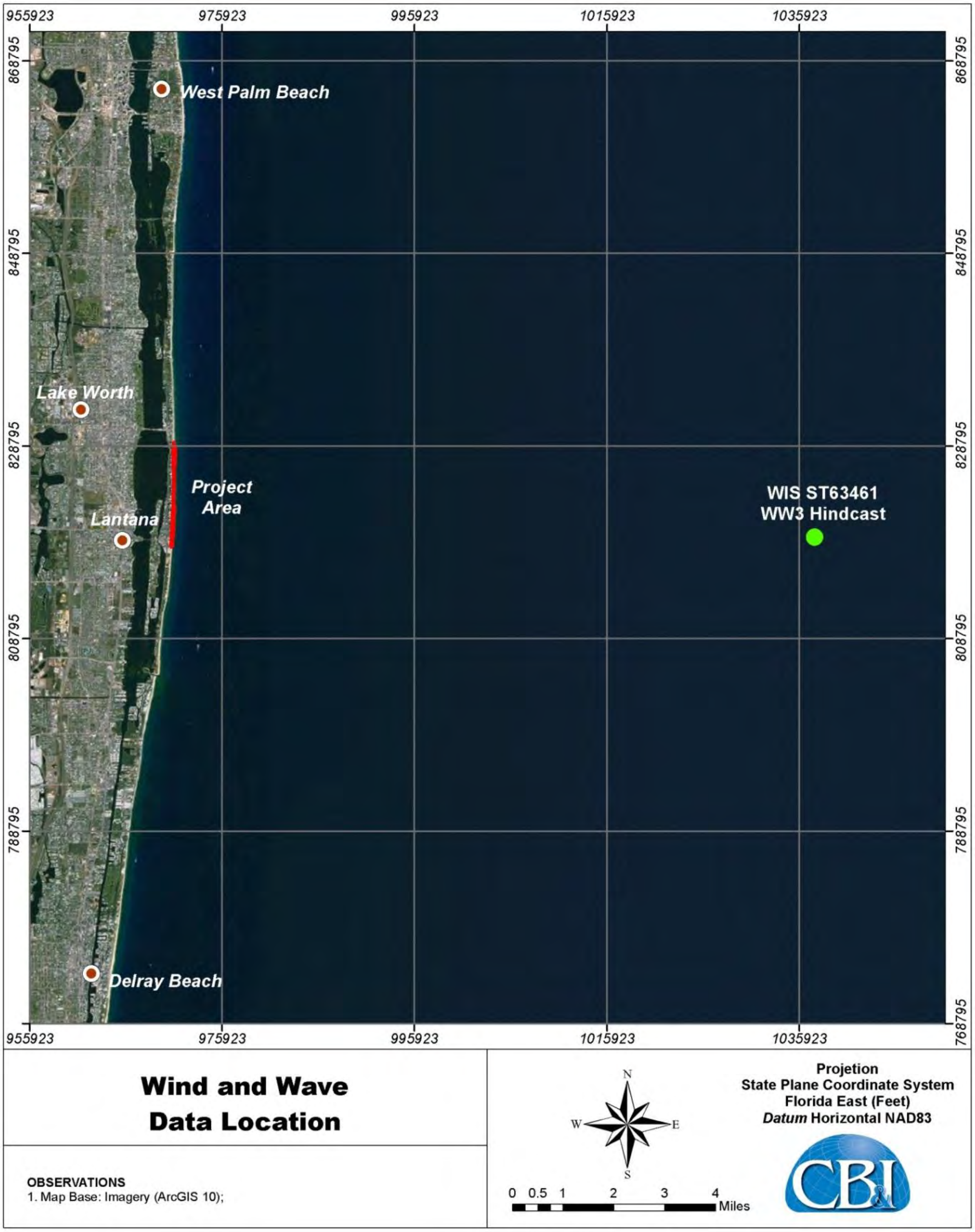

Figure 3-9. Location of the wind and wave data sources.

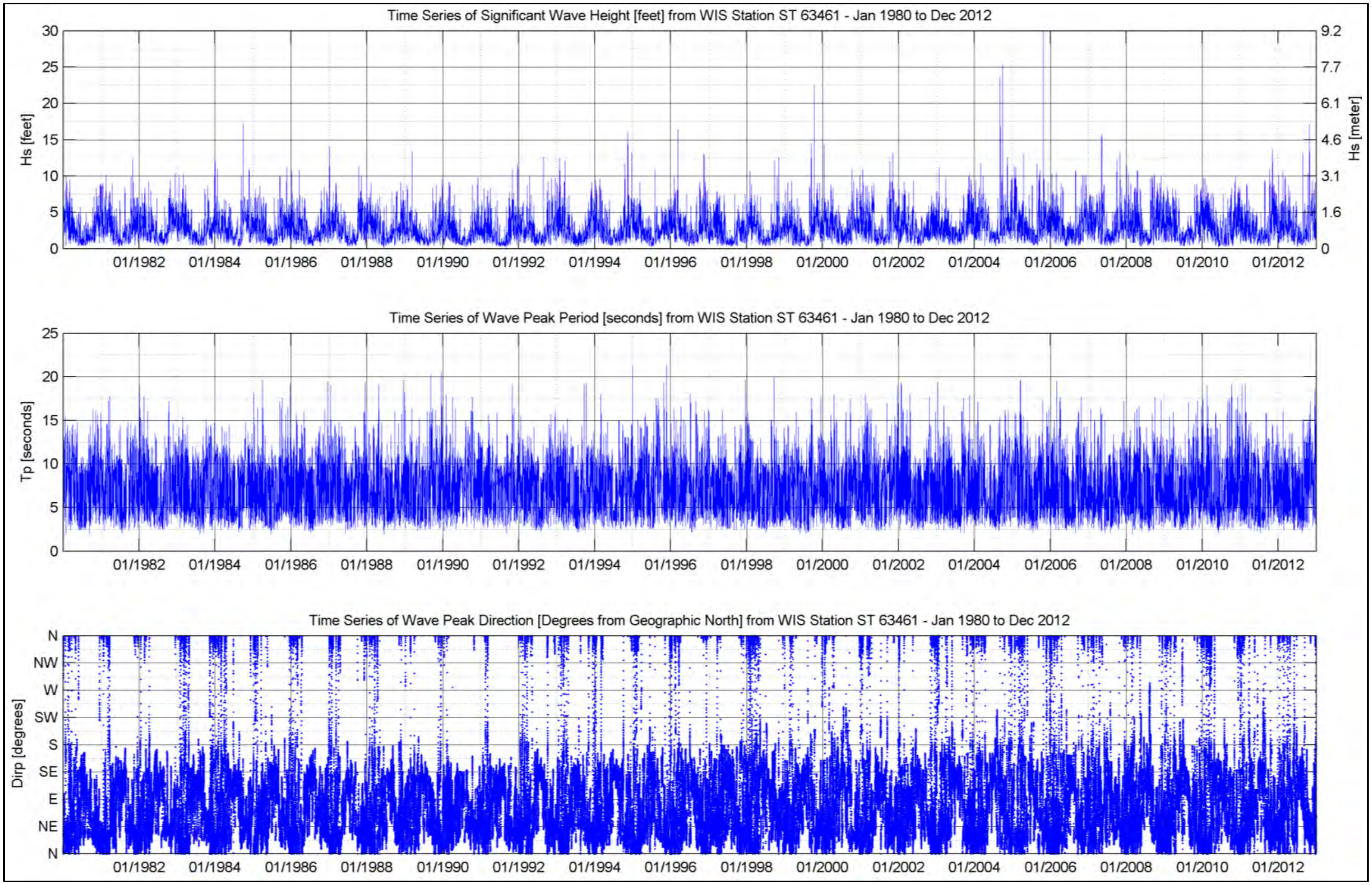

Figure 3-10. Hindcast wave height (Hs), peak period (Tp) and wave peak direction at WIS Station ST 63461.

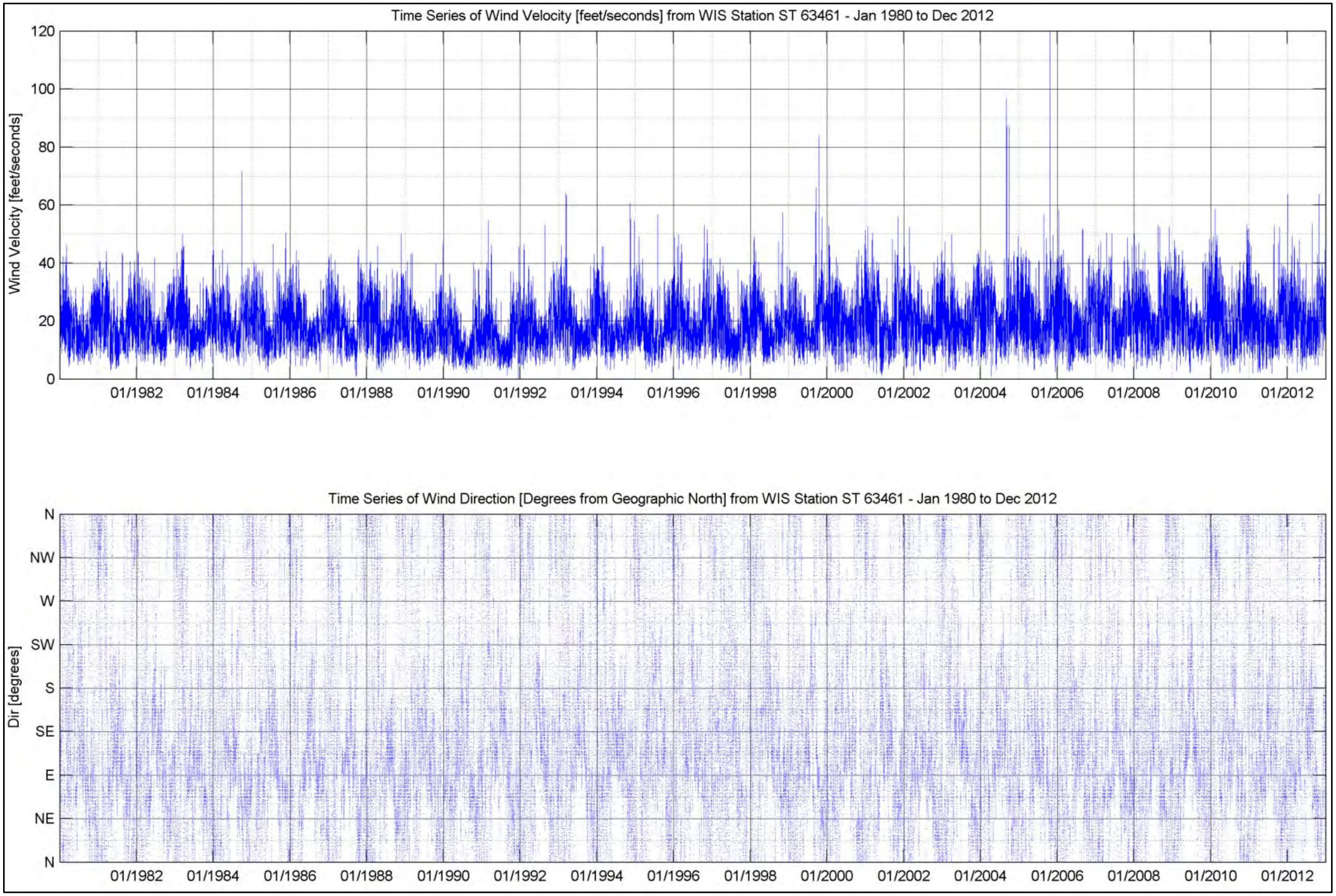

Figure 3-11. Hindcast wind velocity [feet/seconds] and wind direction [degrees] at WIS Station ST 63461.

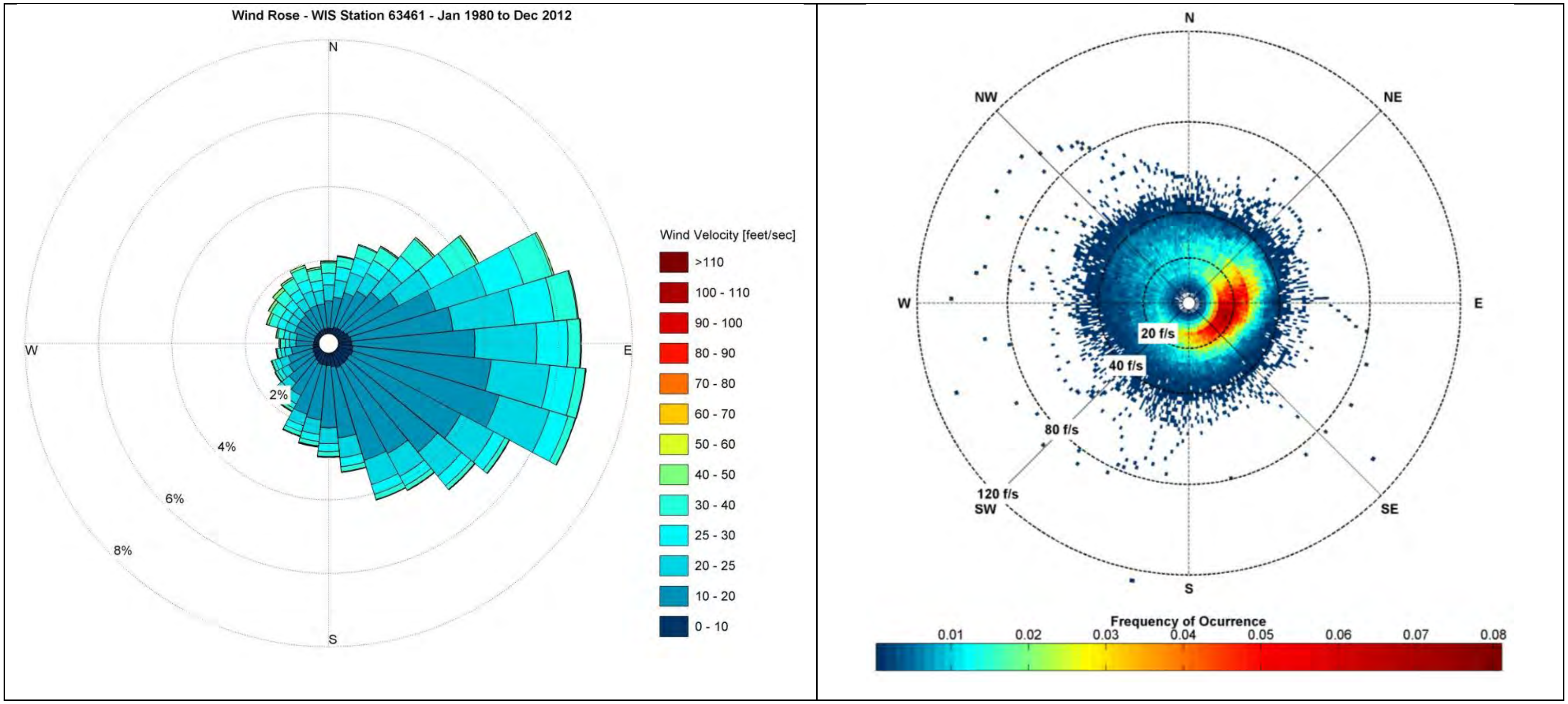

Figure 3-12. Directional wind statistics for WIS Station ST 63461 from January 1980 to December 2012.

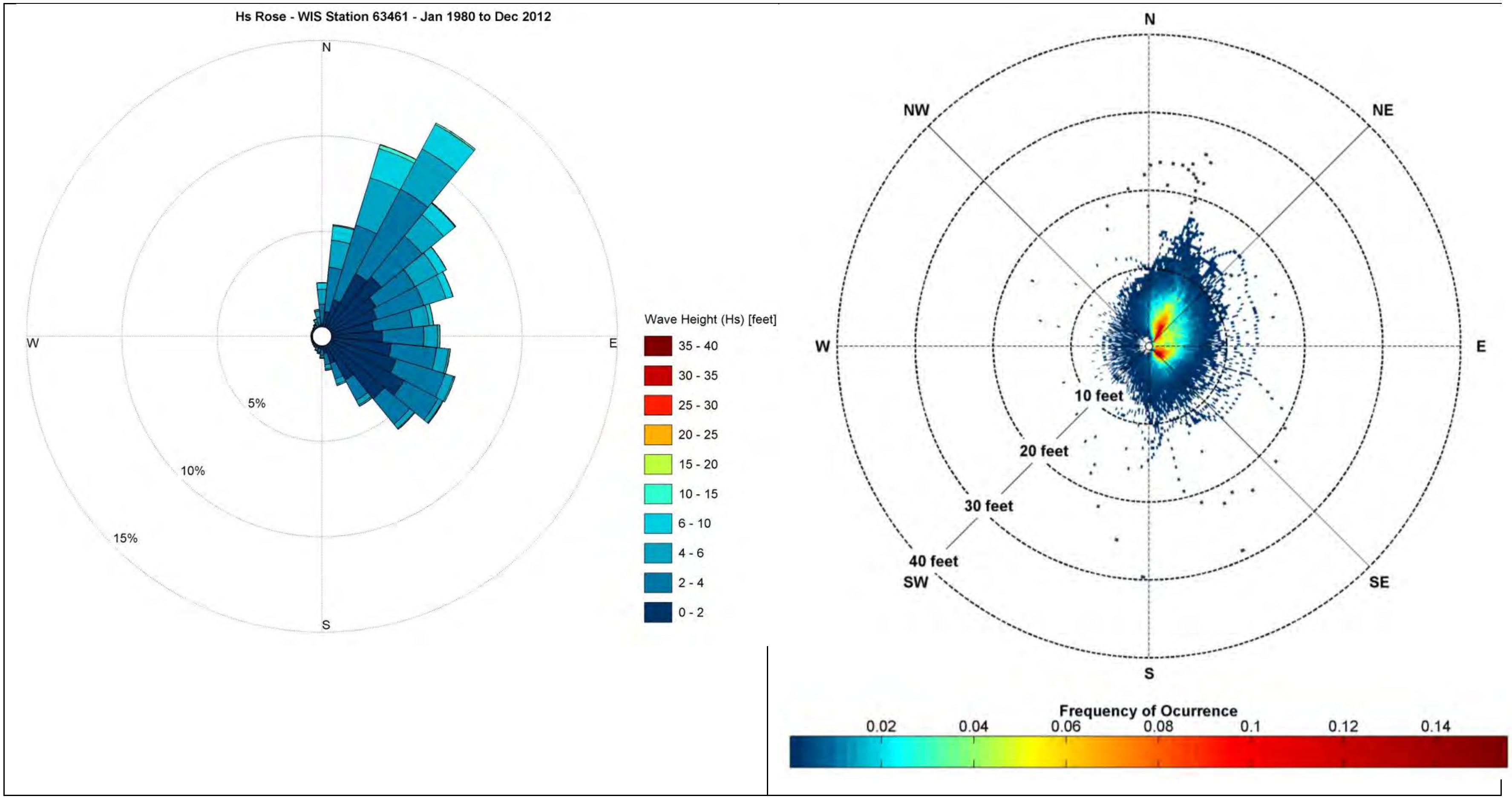

Figure 3-13. Directional wave statistics for WIS Station ST 63461 hindcast from January 1980 to December 2012.

3.5. Sediments

Sediments within the Project Area are a mixture of quartz and carbonate sands. The most recent sand samples over the entire Project Area were taken by Palm Beach County (1993). While several dune restoration projects have been constructed since that effort (see Table 3-4), no major beach nourishment projects have been constructed within the Project Area. Thus, the Palm Beach County (1993) samples were assumed to provide a reasonable characterization of the native sediments across the beach profiles (dry beach, surf zone, and submerged profile) as a whole. Based on the composite for profile lines R-124 to R-139 (Palm Beach County, 1993, p. 32), the mean grain size is approximately 0.36 mm (1.49ϕ), with a sorting value of 0.78ϕ, a silt content of 0.02%, and a carbonate content of 42%. However, it is noted that wave action has likely sorted out the finer sediments from the beach resulting in coarser sediment characteristics.

Table 3-4. Recent dune and beach nourishment projects.

Date	Volume (cy)	Extents	Sand Source
2003	1,000	R-135+460 to R-137+410	Upland
2005	3,132	R-135+460 to R-137+410	Upland
2005	5,814	R-135+460 to R-137+410	Upland
2006	141,458	R-116.5 to R-119-300; R-126 to R-127+100; R-129+200 to R-133+500	Offshore Borrow Area
2006	1,100,000	R-118+700 to R-126	Offshore Borrow Area
2007	6,750	R-135+460 to R-137+410	Upland
2008	11,000	R-135+460 to R-137+410	Upland
2009	10,000	R-135+460 to R-137+410	Upland
2011	56,000	Dune R-129 to R-133	Upland

3.6. Hardbottom

Hardbottom was incorporated into the Delft3D model by spatially varying the erodible sediment depth and sediment thickness based on physical measurements, survey data and aerial delineations. Erodible sediment depth is defined by an elevation fixed in time demarking the surface of the hardbottom such that erosion of sand cannot occur below this depth in the model. Sediment thickness varies with time based on the sand layer on top of the hardbottom resulting from model simulations. To develop the erodible sediment depth, the following steps were taken:

1. The hardbottom database was acquired from the Palm Beach County's Department of Environmental Resources Management. This database was distributed in the form of a Shape File outlining hardbottom areas appearing in the 1993, 2000, 2001, 2003, 2004, 2005, 2006, 2007, 2008, and 2009 aerials. Blue Kenue 3.3.4 was used to convert the hardbottom information into a plain-text file listing the years and coordinates of each outcropping. The database has been used by the County to assess natural habitats and permit coastal projects. In addition, the 2000-2009 mappings have been incorporated into the Beach Management Agreement dataset administered by the FDEP.

2. To supplement the information above:

    - Post-Hurricane Jeanne hardbottom areas were digitized from aerial photographs taken in January 2005 and March 2005.

    - Nearshore hardbottom areas were digitized from December 2002 aerials provided by the U.S. Geological Survey (USGS) Earth Explorer. These hardbottom areas were combined with 2002 offshore hardbottom mapping provided by the Florida Fish and Wildlife Conservation Commission (FFWCC, http://ocean.floridamarine.org/mrgis/Description_Layers_Marine.htm).

- The 1993 hardbottom mapping from FFWCC was combined with the 1993 hardbottom mapping from the Palm Beach County database.

- Vertical relief measurements of hardbottom habitat in the Project Area from R-130 to R-143 were collected in January 2009, April 2009 and April 2010 by Coastal Planning & Engineering, Inc. and CZR, Inc. (CPE, 2010a). Measurements were obtained along the nearshore and offshore edges of the hardbottom formation. These measurements along the edges were not be the highest relief areas within the formation, but provided “ground truth” data at the locations sampled. Measurements from the sand bottom to the top of hardbottom edges ranged from 1 cm to 65 cm (0 to 2 feet).

- The March 2012 hardbottom mapping was digitized from March 2012 aerial photographs flown by Aerial Cartographics of America on behalf of the Town of Palm Beach and FDEP. The quality of the photographs and the water clarity during the flight date was sufficient for this purpose.

- The July 2013 hardbottom delineation was digitized from July 25-26, 2013 aerial photographs flown by Woolpert, Inc. on behalf of Palm Beach County. The clear and shallow waters of the Study Area allowed the hardbottom resources to be delineated (CB&I, 2014).

3. Bathymetries for the Flow & Morphology Grids from 1993 to 2009 were developed from the topographic and bathymetric surveys listed in Table 3-5. For each year’s hardbottom delineation, grid points within the respective hardbottom areas were identified. The elevations of the exposed hardbottom areas at those grid points were then estimated based on the concurrent survey. For example, the elevations of the exposed hardbottom in 2002 were based on the bathymetric grid surface drawn from the November 2002 LIDAR survey.

4. To further extend the hardbottom surfaces developed above, two additional data sources were used:

    - The first reflector (seismic) mapping developed for the 2007 Town of Palm Beach borrow area investigation (Finkl, et al., 2008) was used. The seismic reflector is an indication of the first occurrence of bedrock beneath the sand. This remote sensing investigation provided data to fill the gaps between other data sets and expand the subsurface bedrock map.

    - The minimum beach profile elevations of the beach profile envelope on FDEP profiles R-124 to R-137. The beach profile envelope consists of the area bounded by the maximum and minimum elevations found at distances along a profile throughout time. This was used to estimate erodible depth elevations where neither hardbottom information nor seismic data were available. The minimum beach profile elevation was developed using physical beach surveys and the Average Profile tool in Beach Morphology Analysis Package 2.0.

Using the methods and data sources listed above, several iterations of the erodible sediment depth and sediment thickness were developed as part of the morphology model calibration process, similar to CPE (2010a).

Table 3-5. Surveys Used to Estimate Hardbottom Outcropping Elevations in Feet NAVD.

Hardbottom Mapping	Closest Survey Date(s)	Survey Data Sources*
1993	July-October 1990	FDEP - PB9008_CCC_1.PRF
2000	Fall-Winter 2000-2001	FDEP - PB0102_MAE_1.PRF
2001	August 2001	FDEP - PB0109_MAE_1.PRF
2002	Nov. 2002 LIDAR	Tenix (2003)
2004	June 2004 LIDAR	USACE (2004)
Jan.-March 2005 (Post-Jeanne)	Nov. 2004 LIDAR	USACE (2004)
2005	May-Aug. 2005	CPE (2005) FDEP - PB0507_MAE_1.PRF
2006	May 2006 – Project Area April 2006 – R-124 to R-134 Nearshore Jan.-Feb 2006 – Remaining Areas	Sea Diversified (2006) Bean-Stuyvesant (2006) USACE (2006)
2007	May-Sep. 2007	CPE (2007d) FDEP - PB0709_MAE_1.PRF
2008	Sep.-Dec. 2008	Sea Diversified (2008) CPE (2009) FDEP - PB0809_BLI_1.PRF
2009	October 2009	FDEP - PB0909_BLI_1.PRF
2012	Jan. 2012 & September-November 2011	FDEP - PB1109_SDI_1.PRF ATM (2012)
2013	July 2013	ATM (2013)

*NOTE: The FDEP surveys are taken from the FDEP Historic Shoreline Data / Profile Data database, ftp://ftp.dep.state.fl.us/pub/water/beaches/HSSD/ProfileData/prof839088/ PALPZ.ZIP.

3.7. Existing Structures and Features

Seawalls – The locations and elevations of the existing seawalls were verified based on the March 2012 aerial photograph, the Town of Lantana Seawall drawings by Taylor Engineering (2009), and the beach profile surveys listed in Table 3-2.

In the SWAN model, the seawalls were treated as vertical walls with finite heights ("dams") ranging from +12.4 to +18.7 feet NAVD. The overtopping coefficients α = 1.8 and β = 0.1 were equal to the recommended values for vertical walls (Deltares, 2011b). Reflection coefficients were assumed to be equal to 20%, similar to CPE (2010, 2011). In the Delft3D-FLOW model, the seawalls were treated as "thin-dams" that prevented flow from occurring through or over the structures regardless of water level.

Lake Worth Pier – As shown in Figure 3-14, the Lake Worth Pier has a localized influence on the shoreline shape. Accordingly, several representations of the Lake Worth Pier in the model were examined.

Figure 3-14. January 24, 2009 Aerial Photograph of the Lake Worth Pier.

The final calibration run identified the Lake Worth Pier as a structure with a permeability of 85% for modeling purposes. In the SWAN model, the pier was treated as a "sheet" of infinite height with transmission coefficients of 0.85. In the Delft3D-FLOW model, the pier was treated as a "porous plate", or a partially transparent structure that extends into the flow along one of the grid directions, with a thickness that is smaller than the grid size in the direction normal to the porous plate. Unlike other types of structures in the

Delft3D-FLOW model, mass and momentum can be exchanged through the porous plate.

Phipps Ocean Park South Borrow Area – The borrow area located south of Lake Worth Pier is represented in the model. The borrow area is located approximately 2,000 to 3,200 feet offshore at R-133 as shown in Figure 3-15. According to spatial resolution of the grid domain in this area, the edges of borrow were slightly smoothed, but in general was well represented in the numerical domain. Figure 3-16 illustrates the borrow area representation in plan view.

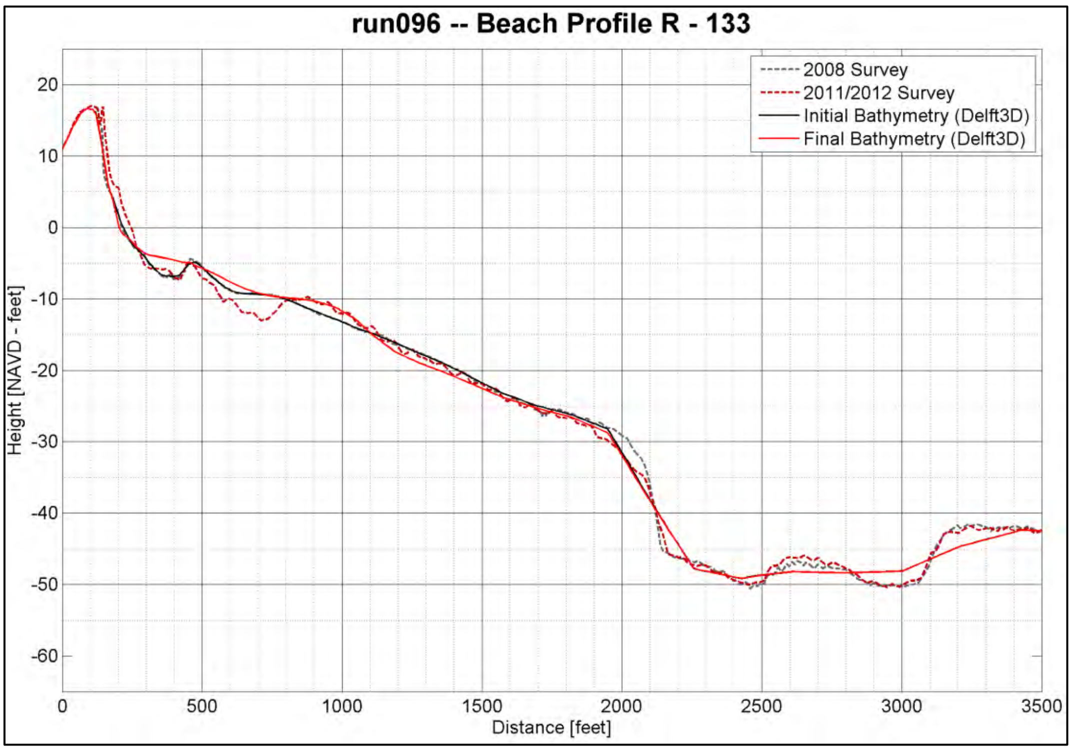

Figure 3-15. Representation of Phipps Ocean Park borrow area in numerical domain, profile from monument R-133.

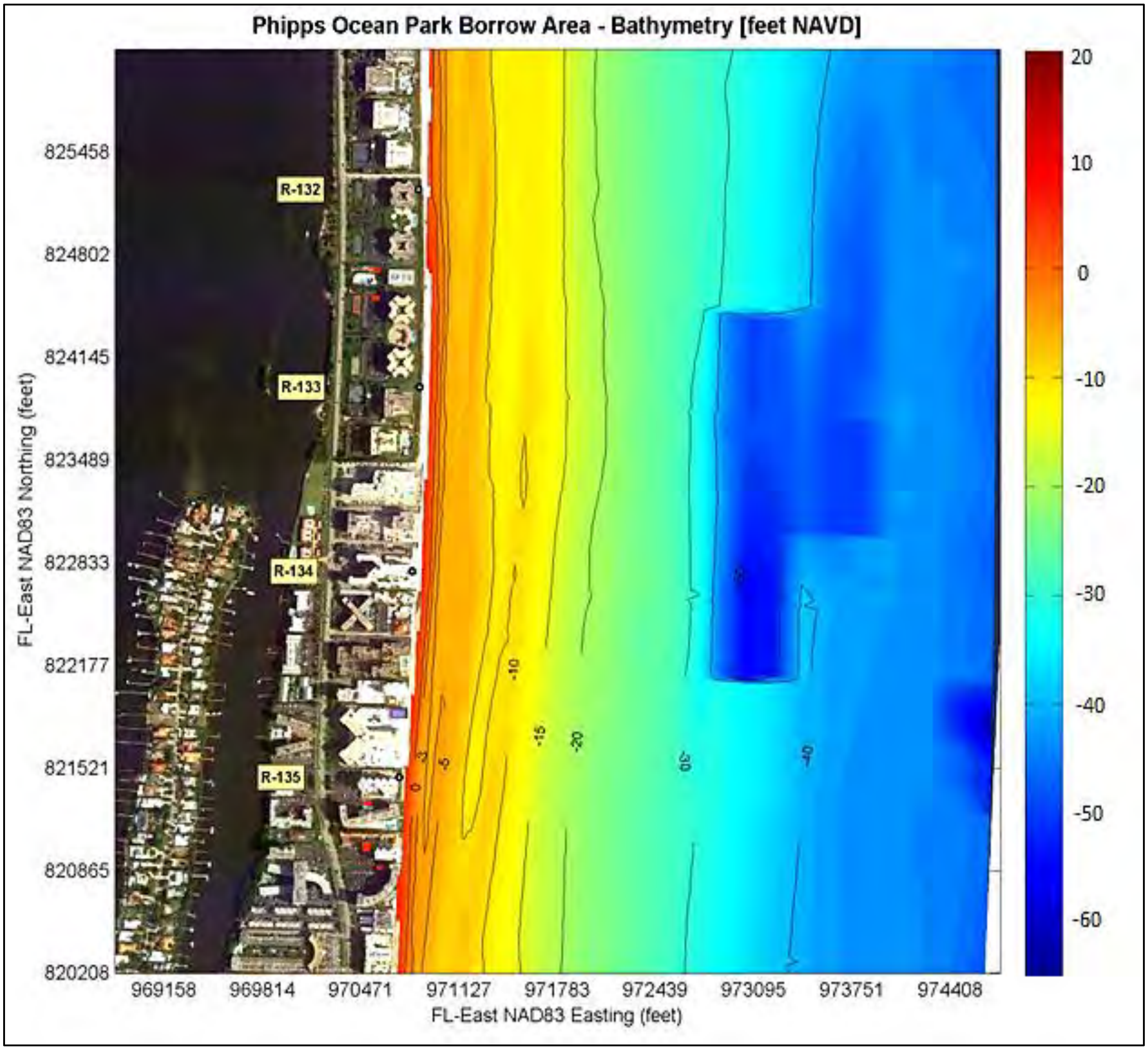

Figure 3-16. Plan view representation of Phipps Ocean Park borrow area bathymetry.

4.0 MODEL CALIBRATION

Calibration of the Delft3D model was completed in two main parts: first, through comparison and calculated hydrodynamics and secondly through comparison of morphologic changes. After the model calibration was performed, it was expected for the model to produce a close representation of the measured sediment transport and the measured morphologic changes.

4.1. Updated SWAN and Delft3D-FLOW Model Calibration

Calibration of the SWAN model was performed using wave measurements collected near the Project Area in 2008 (CPE, 2010b). SWAN model was calibrated primarily in terms of the JONSWAP bottom friction value (C_{jon}). Four values of C_{jon} were examined – the default value (0.067), a lower value (0.05), and two higher values (0.1 and 0.2). Setting the friction value to 0.2 led to the best fit between the observed wave heights and the simulated wave heights at the Offshore ADCP (Figure 4-1). The simulated waves also compared favorably with the observed waves at the Nearshore ADCP given C_{jon} = 0.2 (Figure 4-2).

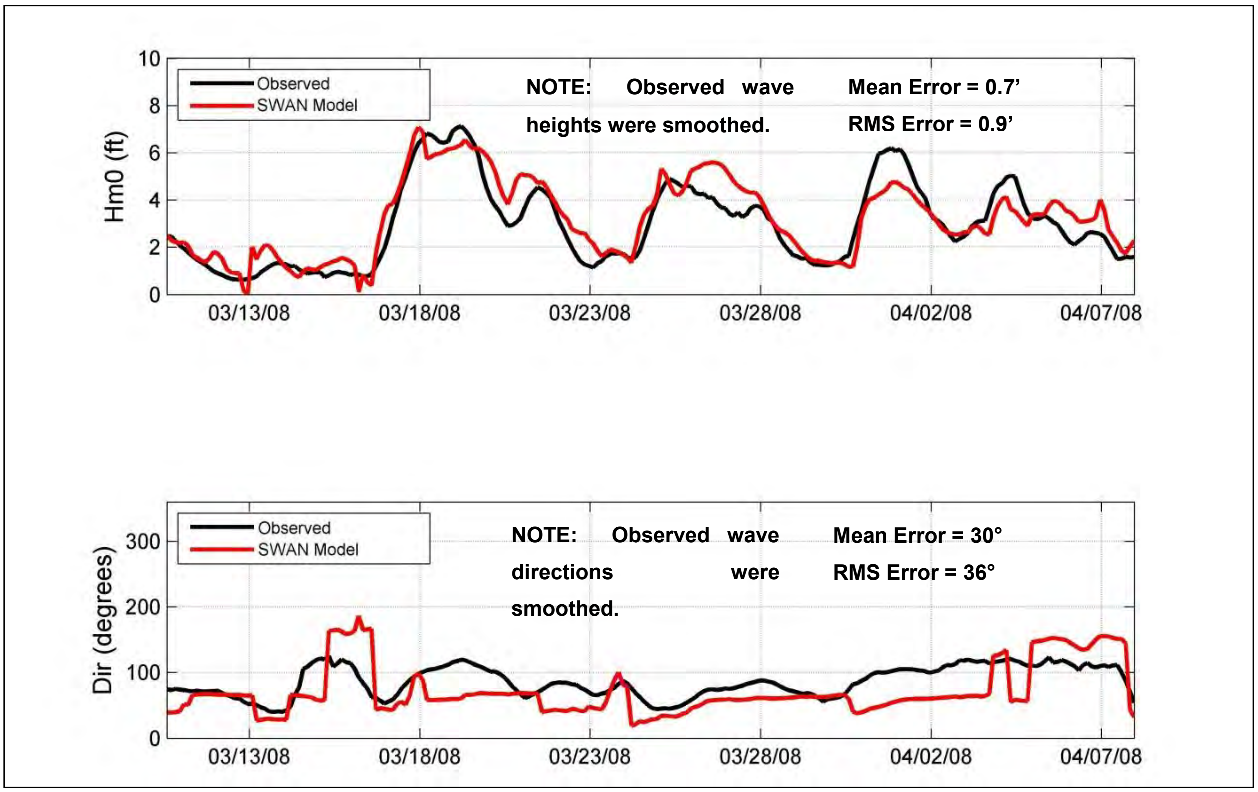

Figure 4-1. Simulated and Observed Waves at the Offshore ADCP given C_{jon} = 0.2 (CPE, 2010b).

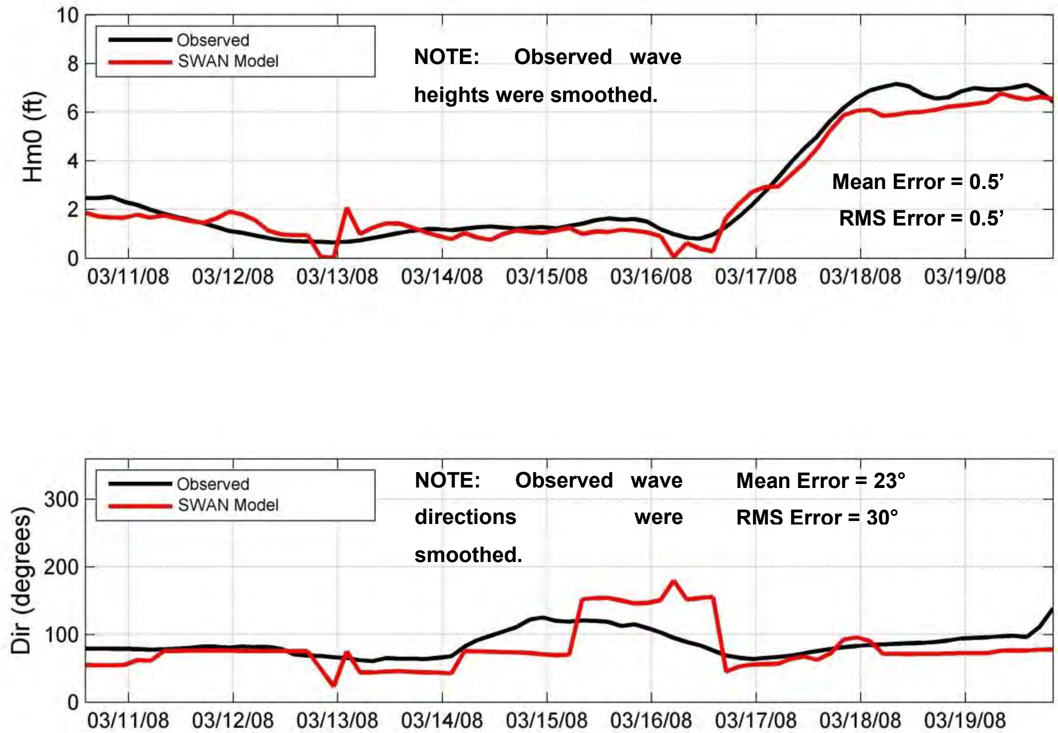

Figure 4-2. Simulated and Observed Waves at the Nearshore ADCP given Cjon = 0.2 (CPE, 2010b).

Following the calibration of SWAN model, 47 simulations were conducted in previous studies (CPE, 2010a) to calibrate the patterns within Delft3D-FLOW. The flow parameters used in the Delft3D-FLOW model were set to the values recommended by Deltares (2011) as detailed in Appendix 2 of CPE (2010b). As part of the model calibration process, longshore current velocities were reviewed to ensure that the currents were reasonable under the wave cases being utilized in the SWAN and Delft3D-FLOW models. Additional details regarding the SWAN model calibration appear in CPE (2010b).

4.2. Morphology Calibration

4.2.1. Hypercube Method for Estimating Nearshore Waves

The WIS hindcast Station (Station 63461) data was used for morphology calibration. The dataset includes both wind and wave data. A concurrent wave record in nearshore regime was developed using Delft3D and Hypercube Method. This nearshore record was called the Hypercube Output Location and located in a water depth of approximately 57 feet as shown in Figure 4-3. The Hypercube Method is briefly described below.

Due to the long time period (32 years) of wave data, modeling the wave record at a 3-hour time step using SWAN is computationally time intensive. As an alternative, the Hypercube technique developed by the Environmental Hydraulic Institute of the University of Cantabria, Spain (Instituto de Hidraulica Ambiental de la Universidad de Cantabria - IH Cantabria) was used. This Hypercube method suggests simulating a large number of deep water wave cases in SWAN using different combinations of wave height, period, and direction that cover the entire ranges of these parameters. The nearshore wave field for all the offshore wave data record can be constructed using three-dimensional (“cube”), linear interpolation based on the SWAN results for each wave case (see Figure 4-4). This procedure is similar to the lookup method used to couple GENESIS to an external wave transformation model (Hanson & Kraus, 1989, p. 74). However, the number of wave cases in this study is much larger – the total number of wave cases summarized in Table 4-1 is 1,111 (Figure 4-5).

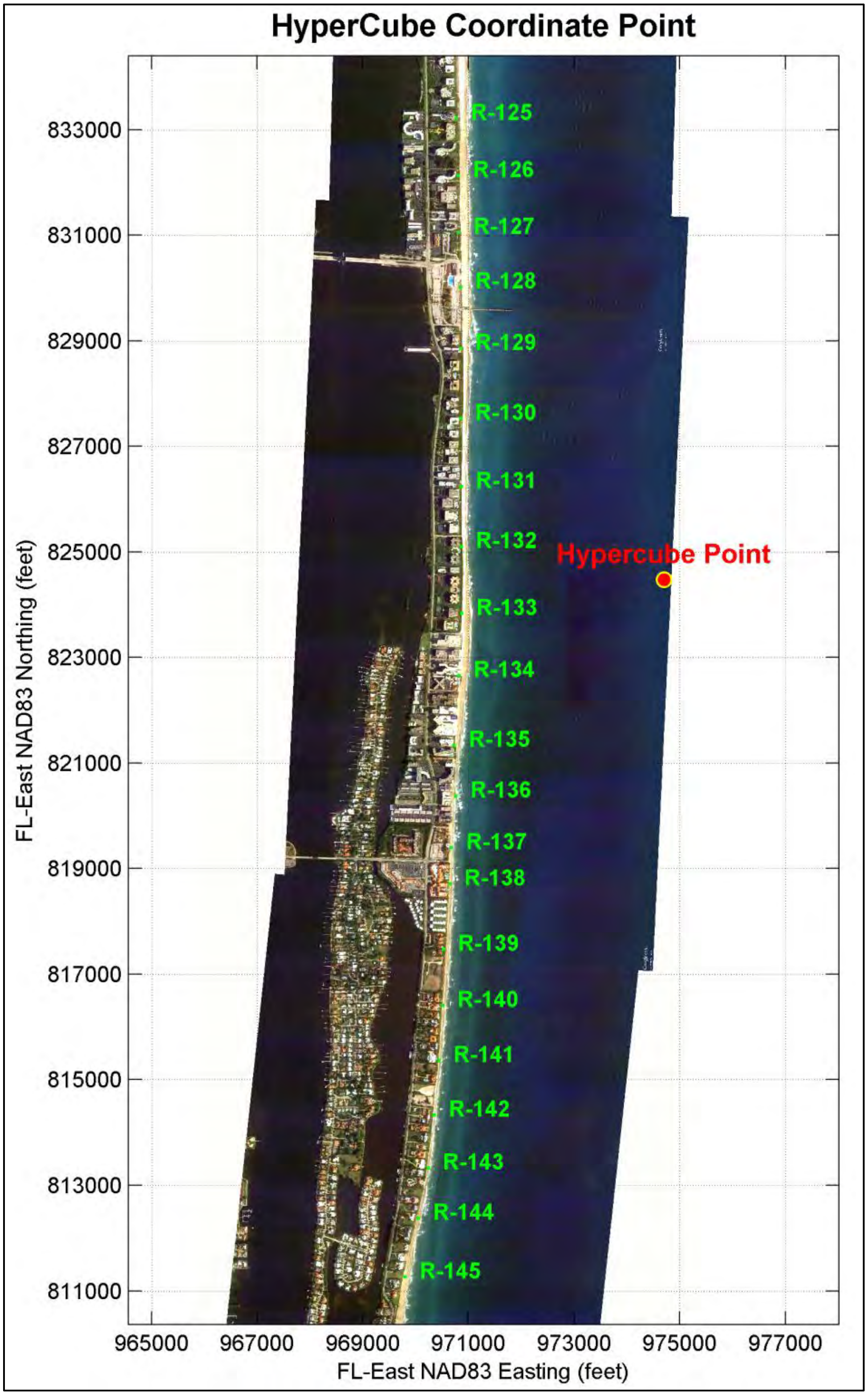

Figure 4-3. Location of Hypercube Output.

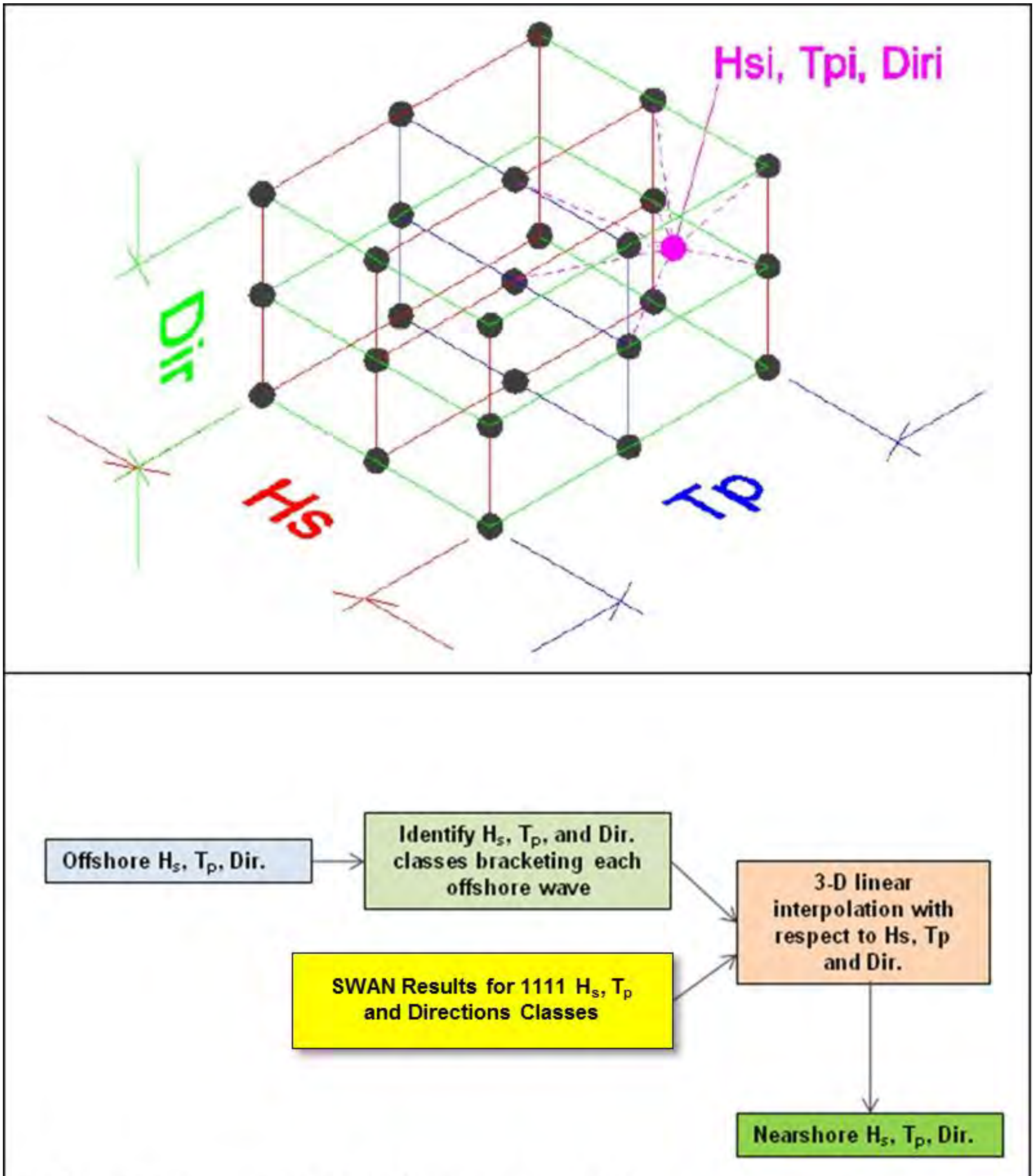

Schematic representation of the Hypercube methodology. The wave height, period, and direction can be obtained for a selected nearshore point through linear interpolation of the SWAN results for a large number of deepwater wave cases.

Figure 4-4. Schematic representation of the Hypercube methodology.

Table 4-1. Summary of Hypercube Wave Cases at WIS Station ST 63461.

Sign. Wave Height		Peak Wave Period	Wave Direction
(m)	(feet)	(sec.)	(deg.)
0.5	1.6	2	0.0
1.0	3.3	3	22.5
1.5	4.9	4	45.0
2.0	6.6	5	67.5
2.5	8.2	6	90.0
3.0	9.8	7	112.5
3.5	11.5	8	135.0
4.0	13.1	9	157.5
4.5	14.8	10	180.0
5.0	16.4	11	202.5
5.5	18.0	12	225.0
6.0	19.7	13	247.5
6.5	21.3	14	270.0
7.0	23.0	15	292.5
7.5	24.6	16	315.0
8.0	26.2	17	337.5
8.5	27.9	18	360.0
9.0	29.5	19	
10.0	32.8	20	
10.5	33.4		

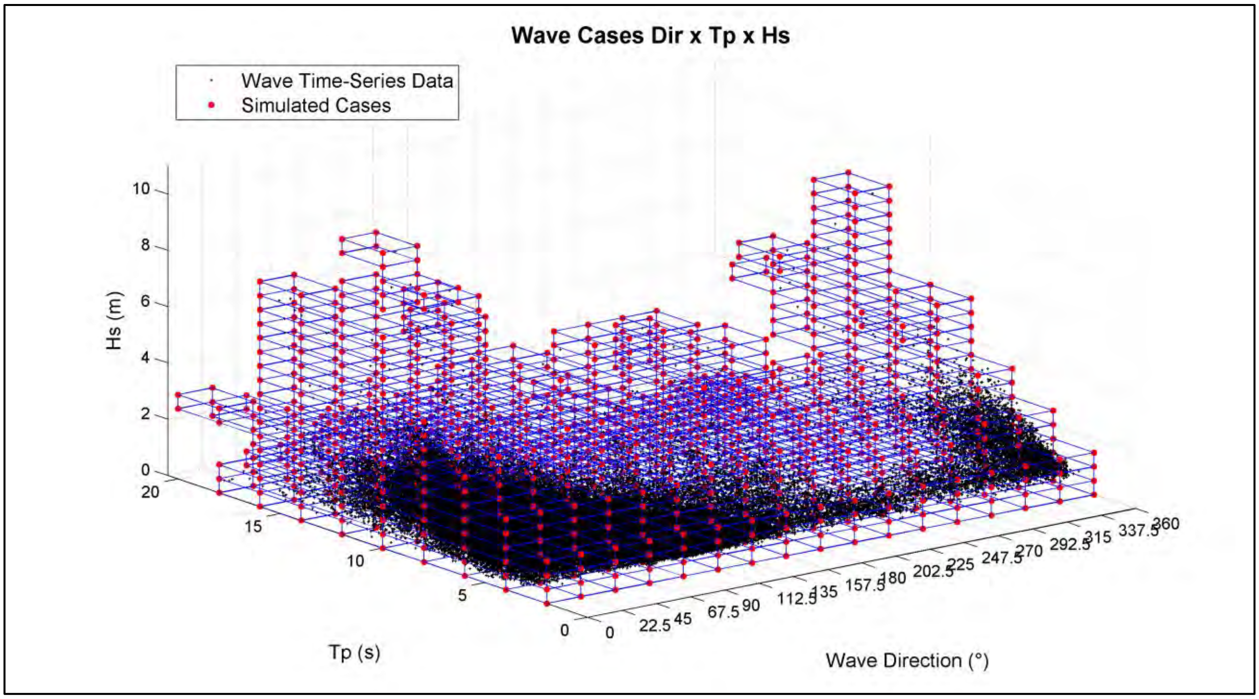

Figure 4-5. 3D plot of waves cases selected of WIS Station ST 63461.

Each of the 1,111 wave cases was then run through the SWAN model to determine the corresponding wave height, period and direction at the Hypercube Output Location. The SWAN model was run in stationary mode, which assumed that changes to the waves with respect to time were slow in comparison to the time required for a wave to travel the lengths of each grid. The multi-year wave record of WIS Station 63461 and the SWAN model results were then fed into the lookup and interpolation algorithm in Figure 4-4 to estimate the concurrent wave heights, periods and directions at the nearshore Hypercube Output Location.

Figure 4-6 presents the directional diagram frequency for the reconstructed data of wave height and wave period at the Hypercube Output Location. The reconstructed data resulted in high frequency waves at a height of 2 feet coming from northeast to southeast, while waves up to 4 feet in height dominated the northeast quadrant. The largest wave height recorded at the Hypercube Output Location had height of 16 feet from quadrant ESE. The northeast quadrant was characterized with wave periods ranging from 4.5 to 13 seconds. Waves from east and southeast had two dominant bands of wave periods ranging between 4-5 seconds and between 9-10 seconds.

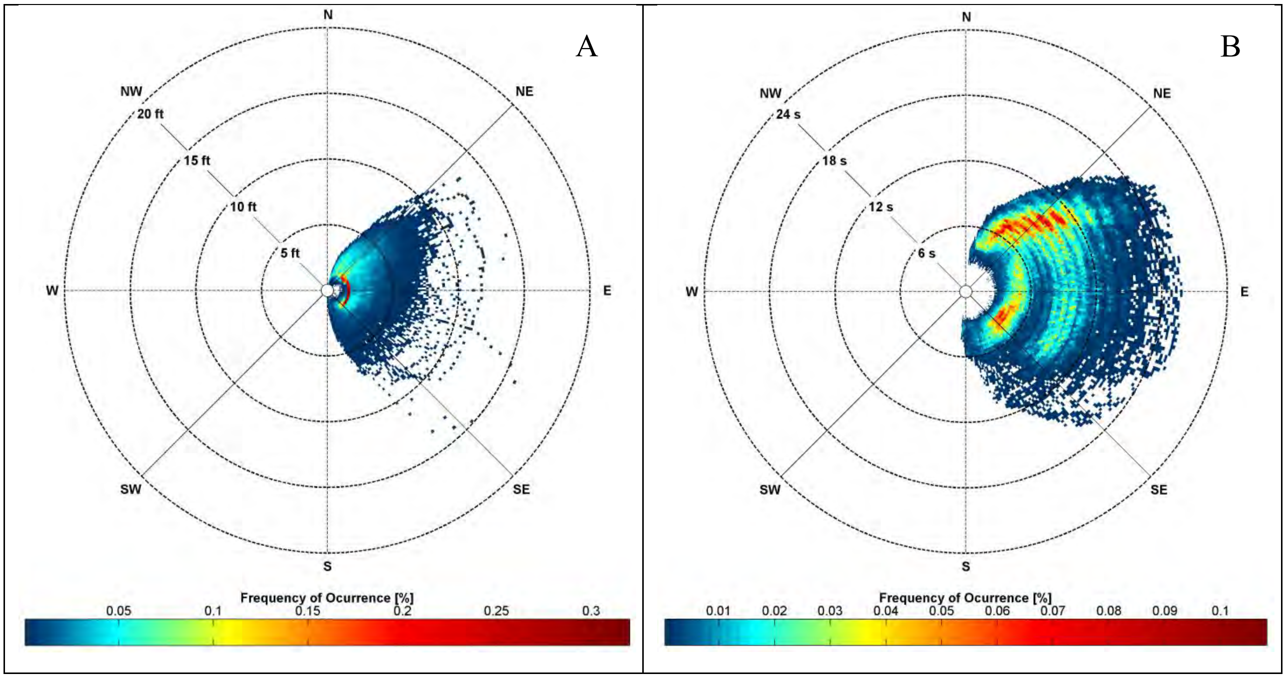

Figure 4-6. Directional diagram frequency to wave height [feet] (A) and wave period [s] (B) on Hypercube Output Location for 32 year time series.

4.2.2. Wave and Wind Cases

For morphological calibration and production runs, wave cases nearshore obtained with Hypercube were selected based on the wave energy flux:

$$E_p \approx 1.56\, T_p \rho g H_s^2 / 16$$

where

E_p = energy flux

T_p = peak wave period (seconds)

ρ = sea water density (1,025 kg/m^3)

g = gravitational acceleration (9.81 m/s^2)

H_s = significant wave height (m)

Based on the estimates above, the offshore direction bands generating 95% of the nearshore wave energy were identified, as shown in Figure 4-7. Waves originating from the north (5°) to the east-southeast (155°) of combined WIS Station ST 63461 accounted for approximately 95% of the wave energy reaching the nearshore Hypercube Output Location.

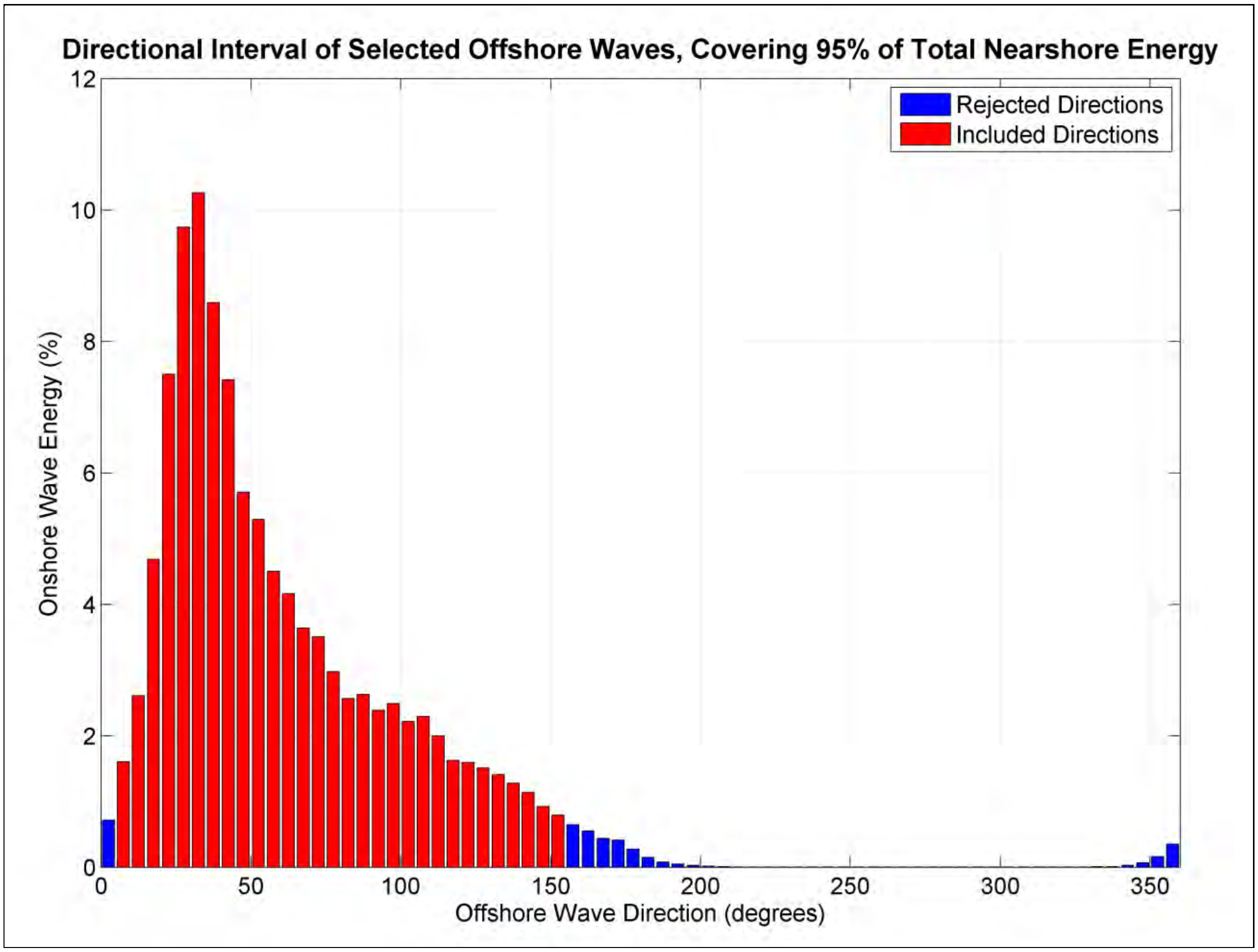

Figure 4-7. Wave record of combined WIS Station ST 63461 generating 95% of the wave energy at the nearshore Hypercube Output Location.

After selecting offshore wave cases that covers 95% of total nearshore energy, 6 directional bins were delineated. Each directional bin offshore represented a nearly equal amount of wave energy in shallow water; the 6 bins combined represented 95% of the shallow water wave energy in KW-h/m. Each of the 6 directional bins was further divided into 3 height classes, with each height class representing nearly equal amounts of wave energy in shallow water. This procedure resulted in 18 wave cases, which are presented in Figure 4-8 and Figure 4-9 and listed in Table 4-2. An additional wave case was developed representing calm conditions and times during which the predominant wave directions were towards offshore (from land to sea). Wind velocities during each wave case were averaged from the concurrent winds during each wave case at offshore location, and were assumed to be uniform over the model grids. The wave cases were organized by directional class (left to right) and increasing significant wave height within each class as shown in Figure 4-8. To avoid situations where one wave case is simulated following another wave case from the same direction, the 18 wave cases were rearranged and modeled in the order shown in Table 4-2. Alternating the wave cases allows the beach to reestablish equilibrium before subsequent wave cases from a given directional class. Repeated wave cases from the same direction without calm periods may result in morphological changes that become irreversible within the model.

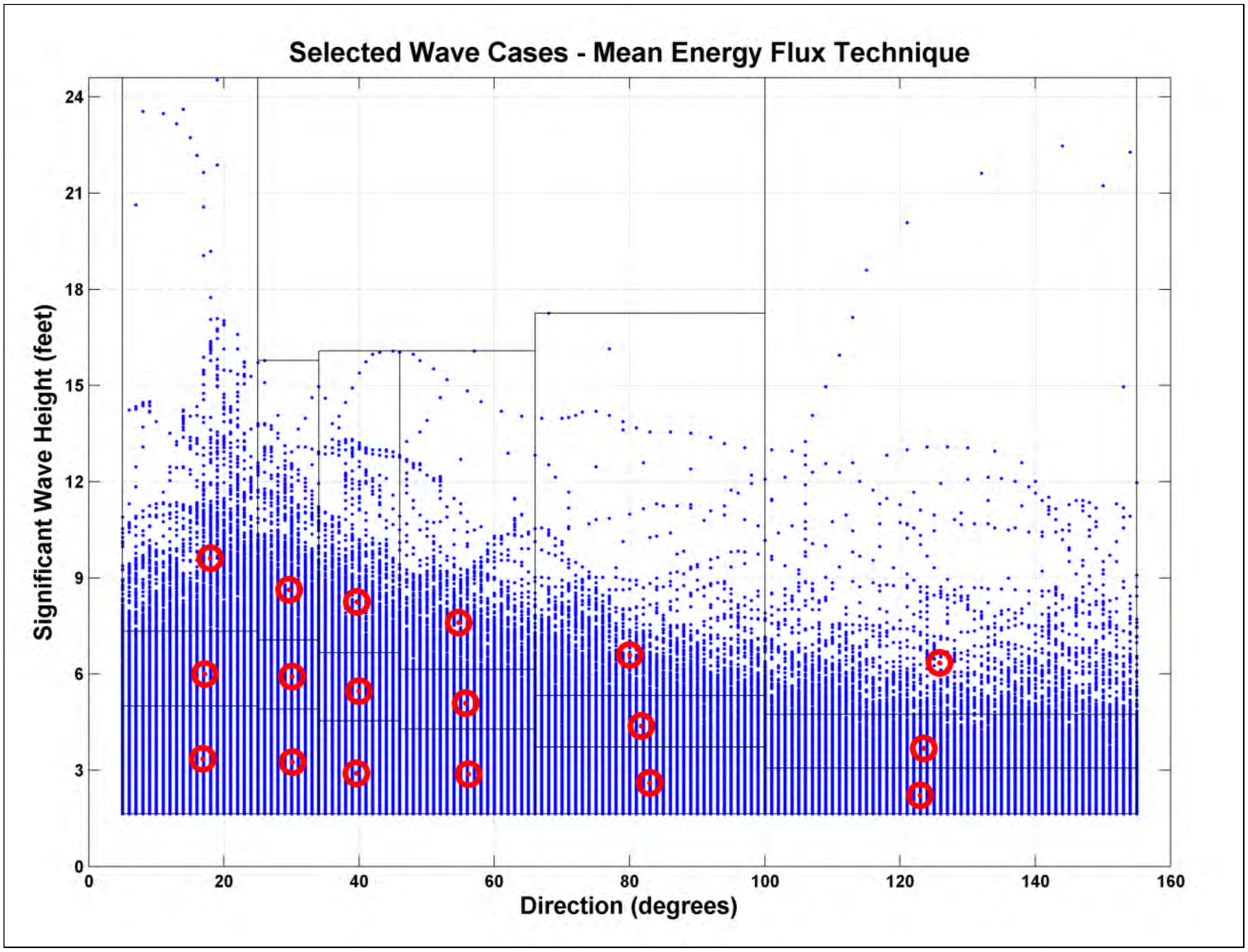

Figure 4-8. Selected wave cases using the mean energy flux technique.

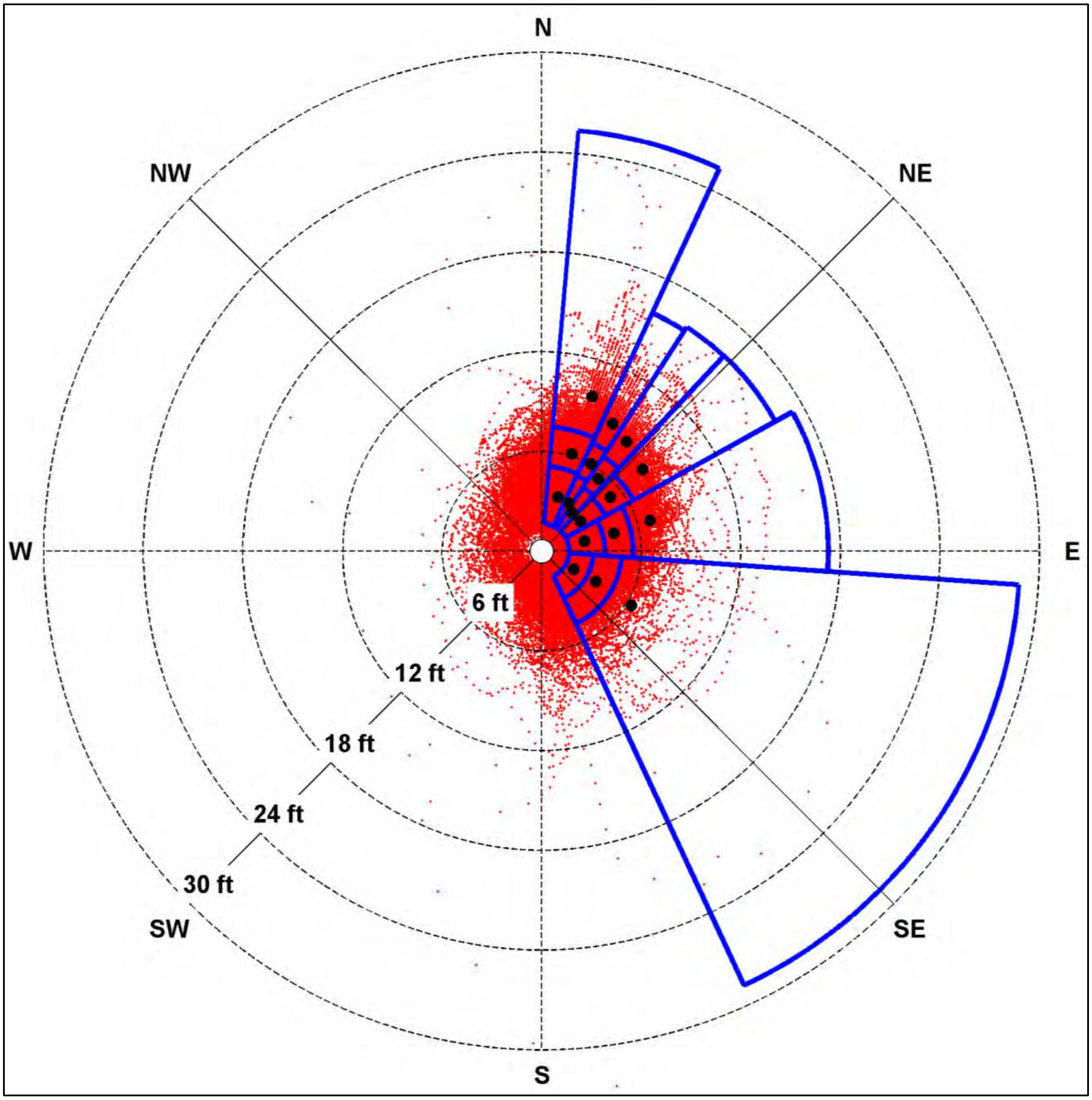

Figure 4-9. Selected wave cases using the mean energy flux technique.

Table 4-2. Wave cases selection for morphological calibration of South Palm Beach, FL.

Wave Case	Hs (feet)	Tp (sec.)	Wave Dir. (°)	Dir. Spread-ing (°)	Wind Speed (feet/s)	Wind Dir. (°)	Percent Occur. In One Year	Days in Model in One Year	Morfac (Calibration)
#1	2.92	9.35	37.93	25.00	8.11	5.12	5.52%	20.15	38.95
#2	3.72	5.64	119.07	4.00	20.98	2.14	4.11%	15.02	29.03
#3	9.78	10.09	18.06	25.00	30.40	359.45	0.93%	3.39	6.55
#4	6.03	10.10	29.55	25.00	18.60	49.36	1.53%	5.58	10.78
#5	6.77	6.98	74.42	15.00	30.54	45.22	1.11%	4.04	7.8
#6	5.23	7.80	51.83	15.00	24.29	43.27	1.84%	6.71	12.97
#7	3.40	7.60	16.90	15.00	13.28	78.74	8.26%	30.16	58.29
#8	8.34	9.87	37.90	25.00	30.69	67.54	0.67%	2.45	4.74
#9	2.23	5.30	119.89	4.00	15.10	61.35	11.75%	42.88	82.89
#10	6.11	8.72	17.13	25.00	22.68	87.42	2.44%	8.91	17.23
#11	6.30	6.51	121.16	15.00	28.66	78.31	1.17%	4.27	8.25
#12	2.65	7.01	77.08	15.00	15.82	75.02	7.45%	27.18	52.53
#13	8.77	10.84	29.20	25.00	27.66	99.22	0.70%	2.56	4.94
#14	5.52	9.58	38.03	25.00	20.76	95.84	1.57%	5.73	11.08
#15	3.32	8.78	29.61	25.00	7.86	95.78	5.31%	19.39	37.48
#16	7.81	8.56	51.10	25.00	32.37	132.86	0.75%	2.73	5.29
#17	4.49	6.51	76.13	15.00	23.65	138.21	2.91%	10.64	20.56
#18	2.91	8.36	52.20	25.00	12.98	136.62	5.43%	19.81	38.29
#CALM	0.98	6.00	20.00	15.00	6.56	20.00	36.55%	133.40	257.85

4.2.3. Morphological Acceleration Factors

To decrease the time needed for the morphological computation, morphological acceleration factors were used, as described in Lesser et al (2004) and Benedet and List (2008). The preliminary morphological acceleration factor M (Table 4-2, last column) was estimated according to the following:

$M = T_{study\ period} / T_{model\ period}$

where

$T_{study\ period}$ = (length of the study period) x (percent occurrence for each wave case)

$T_{model\ period}$ = duration of the wave case in the model simulation

For example, a wave case that occurs 14 days a year can be simulated over 24 hours with an M value of 14. It is common practice between Delft3D users to use lower M values for high wave cases, when the most significant morphological changes occur, and higher M values for smaller wave cases, where little change takes place.

4.2.4. Morphological Tides

Besides schematized wave cases, the tides must also be schematized to run the morphological model. The main purpose of reducing tidal data is to replace the complex pattern of the real tide in the Study Area by a simplified tide, also called morphological tide. The morphological tide produces the same residual sediment transport and morphological pattern of changes that the actual tide produces (LESSER, 2009).

Tidal data reduction to a sinusoidal tide with constant periodicity allows each wave case to be propagated by at least one full tidal cycle. Thus, all wave cases are influenced by the same tidal amplitude and phase.

The methodology of reduction used in this study considers a tidal wave with semi-diurnal cycle, equivalent to the lunar main component M2 (12.42107 hours or 745 minutes) and amplitude varying between MLW and MHW, oscillating around MSL.

4.3. Results of Morphological Calibration

Calibration of sediment transport, erosion and deposition within Delft3D-FLOW model was performed in terms of the volume, profile changes, and morphologic changes during the 3.3 year period between the September/October 2008 and January 2012 beach surveys. The sediment transport was also evaluated. A total of 98 test simulations and calibration runs were conducted to identify the parameters best suited to simulating the general erosion pattern along the Study Area. To improve the fit between the model results and the observed changes, the model was run with 5 vertical layers and the parameters listed below were examined. The selected values for the parameters are presented in Table 4-3.

- Vertical Eddy Viscosity and Eddy Diffusivity: The Delft3D-FLOW model has four types of turbulence formulations used to determine the vertical turbulent eddy viscosity and the vertical turbulent eddy diffusivity. The types of formulations are: Constant, Algebraic, K-L, and K-epsilon. If the constant turbulence model is selected, the background values are applied throughout the model domain. In all the other cases, the uniform values are used as the minimum value for the turbulent contribution (Deltares, 2011). This model was run using the K-epsilon formulation in which the coefficients are determined by the transport equations for both the turbulent kinetic energy and the turbulent kinetic energy dissipation. Therefore the input values for eddy viscosity and diffusivity were set to the minimum value (vertical eddy viscosity = 0; vertical eddy diffusivity = 0).

- Horizontal Eddy Viscosity and Eddy Diffusivity: These two values govern the horizontal, diffusive spreading of momentum and materials, respectively. Higher values of either parameter increase the degree of diffusive spreading. In the case of eddy diffusivity, increased spreading of material results in smoother bathymetric contours. Also, eddy diffusivity parameter is used to control the formation / destruction of bars in zone surf area.

- Sediment layer thickness at bed: In Delft3D it is possible to define space varying erodible areas, and this feature is very useful in areas with hardbottom (that are not erodible) and in areas with different thickness of sediment available to be eroded. When the sediment thickness is set equal to zero in hardbottom areas, it means the model won't erode but will be able to deposit above hardbottom. Final sediment layer thickness chosen for morphological calibration is presented in Figure 4-10.

- Bottom roughness: In order to better represent current patterns generated by hardbottom friction, different Chézy values were tested. A lower Chézy value was used in the areas mapped as hardbottom in order to increase bottom friction represented by the model.

- BED & SUS: These two values govern sediment transport due to currents, including wave-driven currents. Of the various constants in the Delft3D-FLOW model, these values have the largest influence on the sediment transport, erosion, and accretion rates. The values typically range from 0.5 to 2.0.

- BEDW & SUSW: These two values govern the sediment transport associated with the orbital motions that waves generate over the water depth at a given location. Higher values of BEDW and SUSW tend to increase onshore-directed sand transport and nearshore bar formation. Typical value of BEDW & SUSW range from 0 to 0.3.

The primary objective of the Morphology Calibration is to replicate the general trends (qualitative) and overall magnitude (quantitative) of sediment transport within the project area. Considering that the results of this analysis will be used for evaluation of potential impacts to hardbottom, the overall patterns of sediment migration were evaluated in addition to volumetric changes.

In general, the following are the calibration objectives:

- Calibration of modeled volume changes by profile line compared to measured changes within a reasonable range associated with survey error and model resolution.
- Validation of sediment transport trends through comparison of volume change magnitudes updrift, downdrift and within the project area.
- Comparison of observed and simulated beach profiles to assess general cross-shore processes and morphologic features such as and bars and troughs.
- Comparison of observed and simulated morphologic changes over time to assess the model's skill at replicating general sedimentation and erosion patterns.

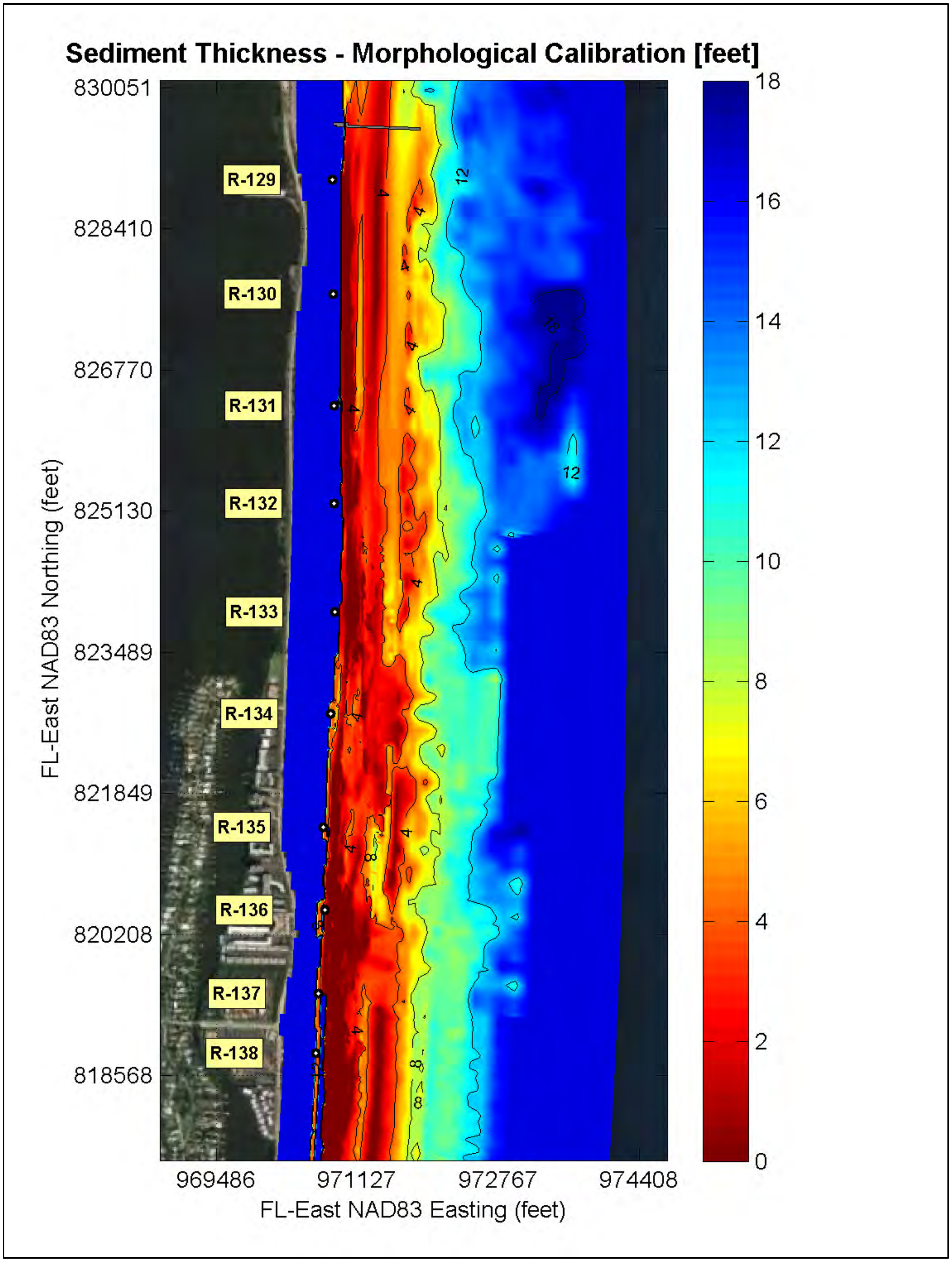

Figure 4-10. Sediment layer thickness used in morphological calibration.

Table 4-3. Summary of final calibration parameters used in morphology model.

	Min.	Default	Max.	Selected Value
SWAN Wave Transformation Model Parameters:				
Breaking Parameter γ (Hb/db)	0.55	0.73	1.20	0.73
Breaking Parameter α	0.1	1.0	10.0	1.0
Bottom Friction Coef. for Waves (Optional):				
JONSWAP Friction Value (m^2/s^3)	0.000	0.067	None	0.2
Collins Friction Value	0.000	0.015	None	Not used
Madsen Roughness Scale (m)	0.0000	0.0500	None	Not used
Triads - Energy Transfer from low to high frequencies in shallow water	-N/A-	Off	-N/A-	Off
Diffraction	-N/A-	Off	-N/A-	On
Wind Growth	-N/A-	On	-N/A-	On
JONSWAP Peak Enhancement Factor (for input waves specified in terms of height, period, and direction)	-N/A-	3.3	-N/A-	1.08
Delft3D-FLOW Model, Flow Parameters:				
Bottom Friction Coef. for Flow:				
Chezy's Friction Coef. C	0	65	1000	65
Manning's n	0.000	None	0.040	Not Used
Horiz. Eddy Viscosity (m^2/s)	0	10	100	10
Vertical Eddy Viscosity:				
Constant (m^2/s)	0	1×10^{-6}	100	Not used
Algebraic	-N/A-	-N/A-	-N/A-	Not used
K-L	-N/A-	-N/A-	-N/A-	Not used
K-Epsilon	-N/A-	-N/A-	-N/A-	Used

Table 4-3. (Cont.) Summary of final calibration parameters used in morphology model.

	Min.	Default	Max.	Selected Value
Delft3D-FLOW Model, Sediment Transport Parameters:				
Spin-up Interval - # of hours between the start of the simulation and the initiation of erosion & deposition estimates	0	6	None	12 hr
Density of sediment grains (kg/m^3)	100	2650	4000	2650
Dry bed density (kg/m^3)	Sand 500	Sand 1600	3000	1600
Median Grain Size (mm)	0.064	0.200	2.000	0.36
Horiz. Eddy Diffusivity (m^2/s)	0	10	1000	1.5
Vertical Eddy Diffusivity (m^2/s)				
Constant (m^2/s)	0	1 x 10^{-6}	100	Not used
Algebraic	-N/A-	-N/A-	-N/A-	Not used
K-L	-N/A-	-N/A-	-N/A-	Not used
K-Epsilon	-N/A-	-N/A-	-N/A-	Used
Dry Cell Erosion Factor	0	0	1	0.5
BED - Current-Related Bedload Transport Factor (including wave-driven currents)	0	1	100	0.5
SUS - Current-Related Suspended Load Transport Factor (including wave-driven currents)	0	1	100	0.5
BEDW - Wave-Related Bedload Transport Factor	0	1	100	0.02
SUSW - Wave-Related Suspended Load Transport Factor	0	1	100	0.02

Final calibration run results for volume changes (Run 96) are presented in Figure 4-11. Overall, the calibrated Delft3D-FLOW model is best suited to estimating general trends, patterns and overall sediment transport magnitudes.

The volume curves show good calibration over the Study Area. Volume changes are within the margin of error, which were based on the uncertainty associated with hydrographic surveying. The modeled curve deviates less than 10 cy/foot/year from the measured values at monuments R-128 and R-130. During the calibration period, the section that showed greater erosive tendency on the order of 10 cy/foot/year between monuments R-134 and R-138 was captured by the model. In other sections, the magnitude of the modeled volumetric changes was consistent with observed changes during the calibration period.

Based on the volumetric changes from the morphological model calibration, a sediment budget was developed to validate the longshore movement of sand within the Study Area. The Study Area was divided into three sectors (boxes) as shown in Figure 4-12.

- Updrift – north of the Project Area defined between R-126 and R-129-210
- Project Area – defined between R-129-210 and R-138+510
- Downdrift – south of the Project Area defined between R-138+551 and R-141

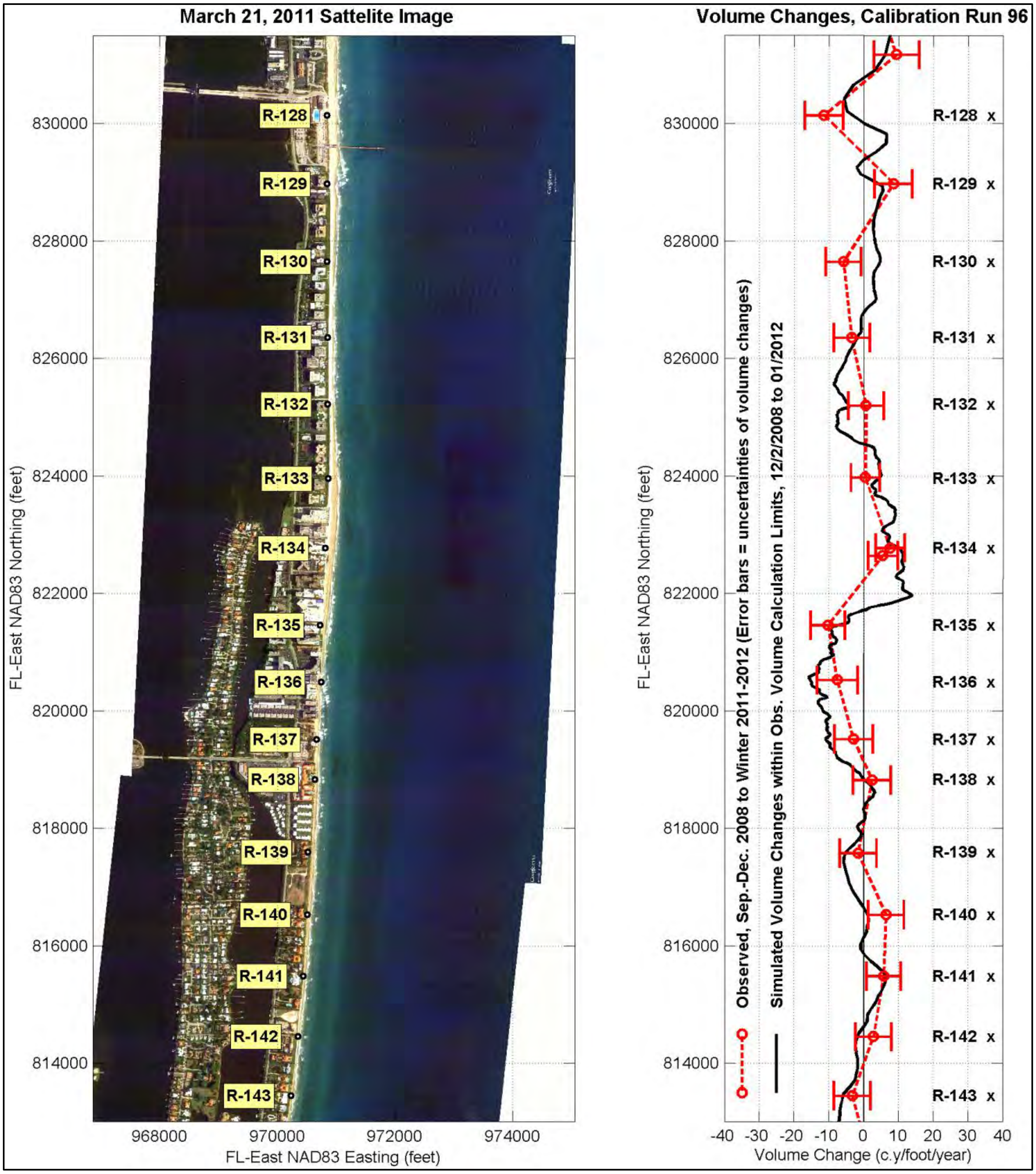

Figure 4-11. Simulated and observed volume changes between October 2008 and January 2012 given selected calibration run (Run 96).

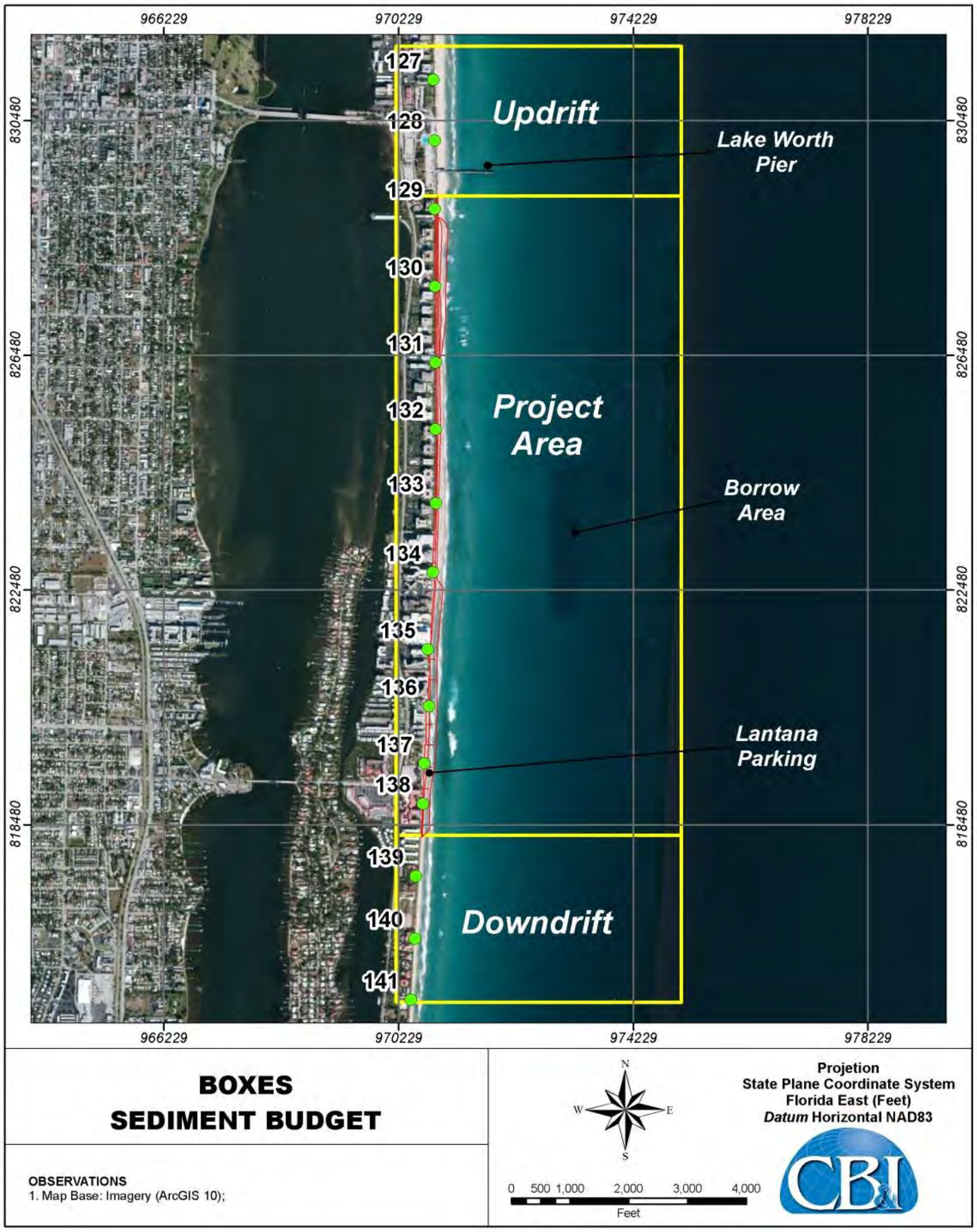

Figure 4-12. Boxes location used for sediment budget validation.

As validation that the model represents actual conditions, Figure 4-13 shows that the modeled (simulated) sediment budget analysis and the rate of transport (cy/year) agreed well with the observed values. Red arrows represent net transport. The values (bold) in boxes represent the sediment budget within each sector. Initial net sediment transport updrift (57,000 cy/yr) was obtained from the sediment transport results of the calibrated model. The simulated and observed data confrimed the erosional trend within the Project Area with a difference in magnitude of 800 cy/yr (5%). Over the length of the Project Area, this equates to a difference of approximately 0.1 cy/yr/ft of shoreline, which is trival in terms of coastal processes.

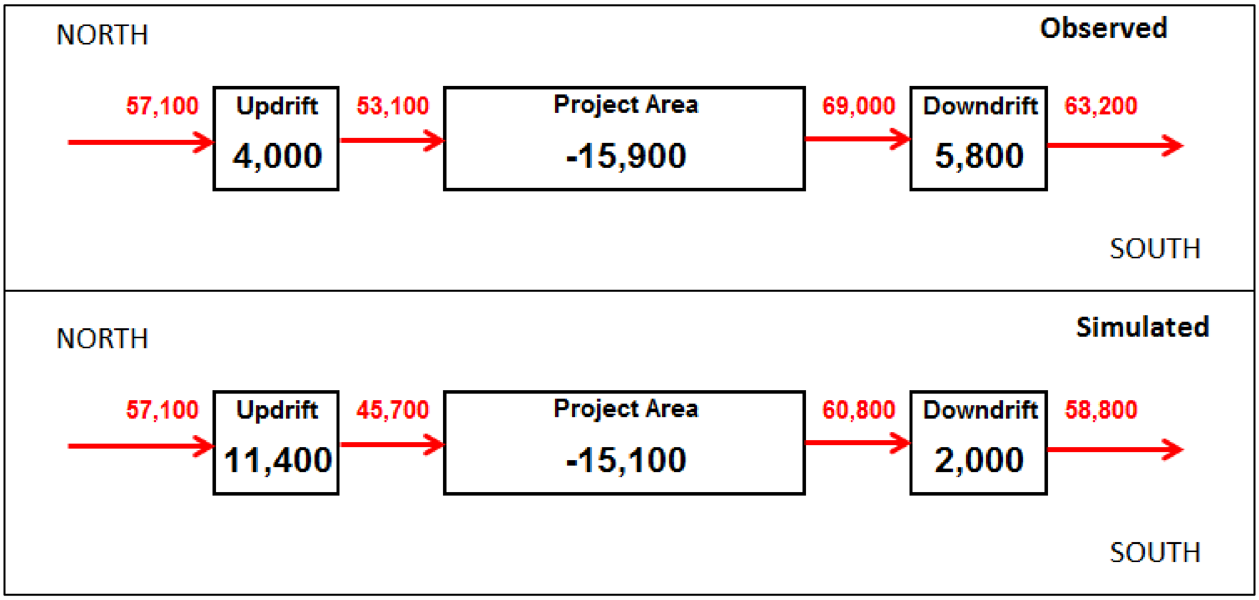

Figure 4-13. Simulated and observed sediment budget (cy/yr) between October 2008 and January 2012 given selected calibration run (Run 96). Red arrows indicate net sediment transport (cy/yr).

Comparisons between observed and modeled beach profiles are presented in Figure 4-14 through Figure 4-17 provides further validation of cross-shore processes and morphologic features. The profiles illustrate that the modeled morphology represents the observed changes between the 2008 and 2011/2012 surveys. In particular the model was able to reproduce the evolution of the offshore bar formations between -5 and -15 feet, NAVD within the surf zone.

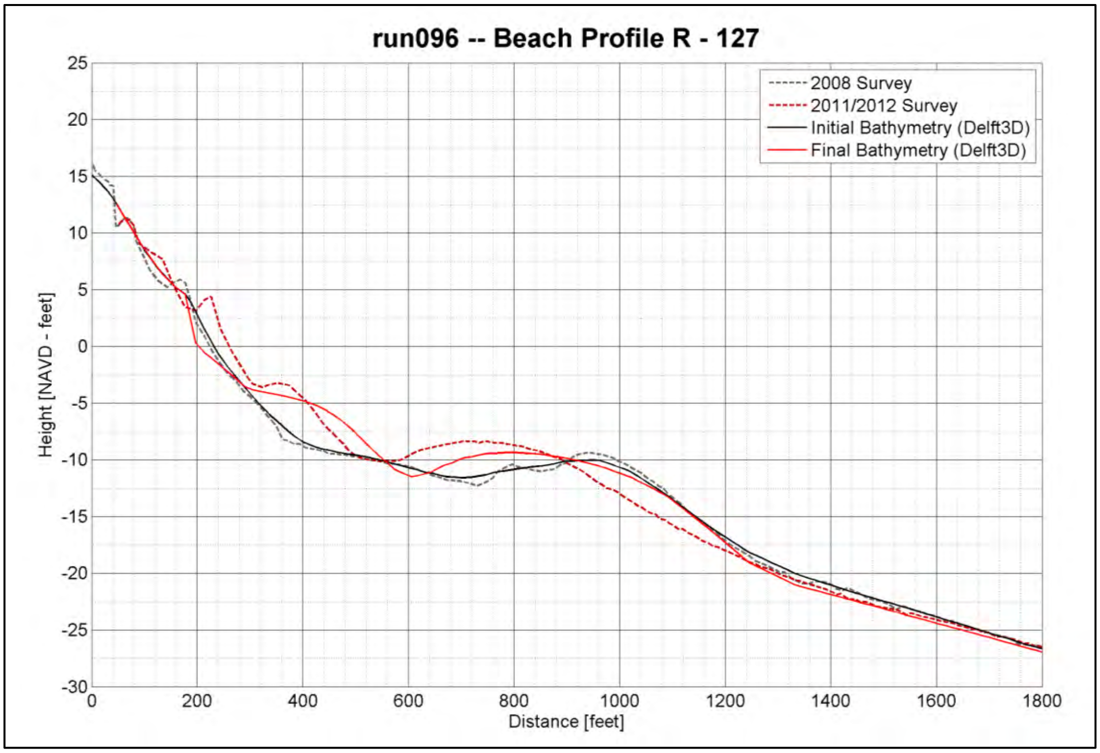

Figure 4-14. Comparison of observed and modeled beach profile R-127 for the initial and final bathymetry considered in the calibration period.

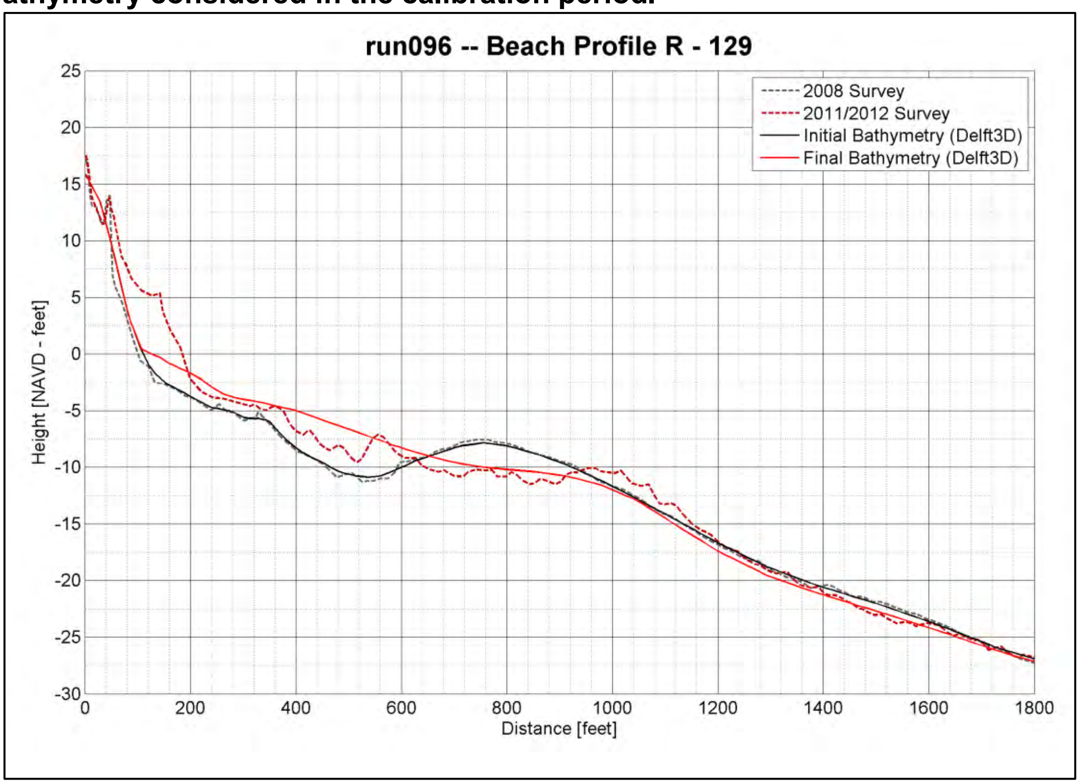

Figure 4-15. Comparison of observed and modeled beach profile R-129 for the initial and final bathymetry considered in the calibration period.

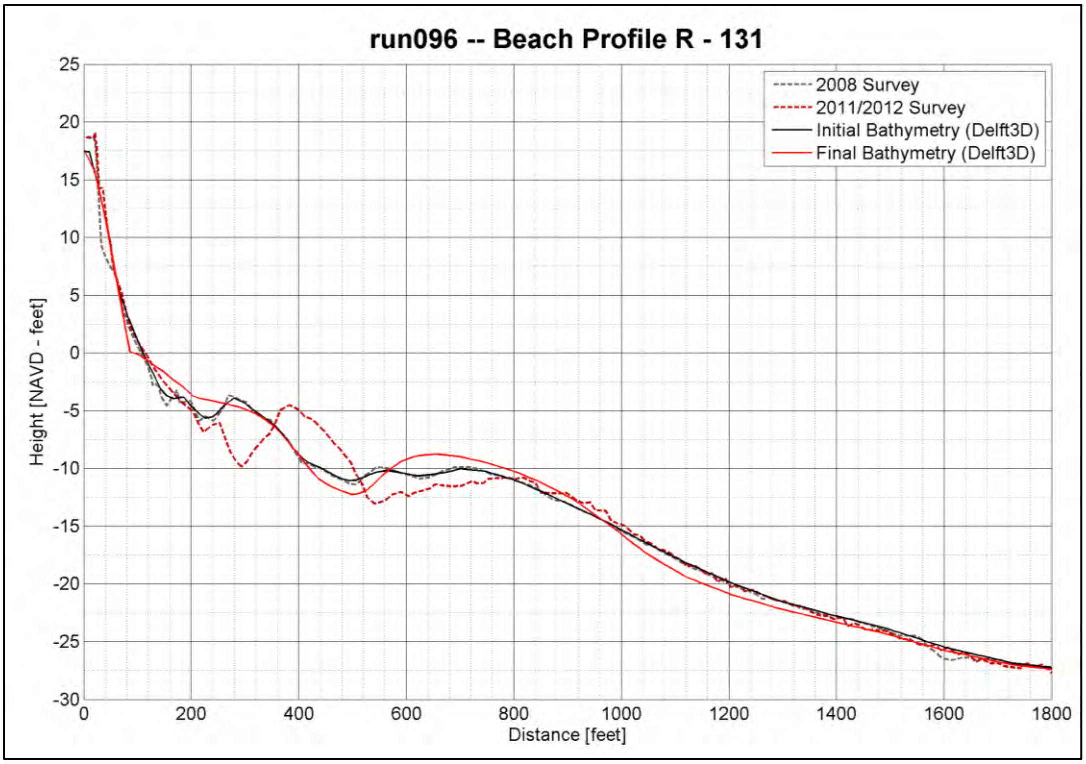

Figure 4-16. Comparison of observed and modeled beach profile R-131 for the initial and final bathymetry considered in the calibration period.

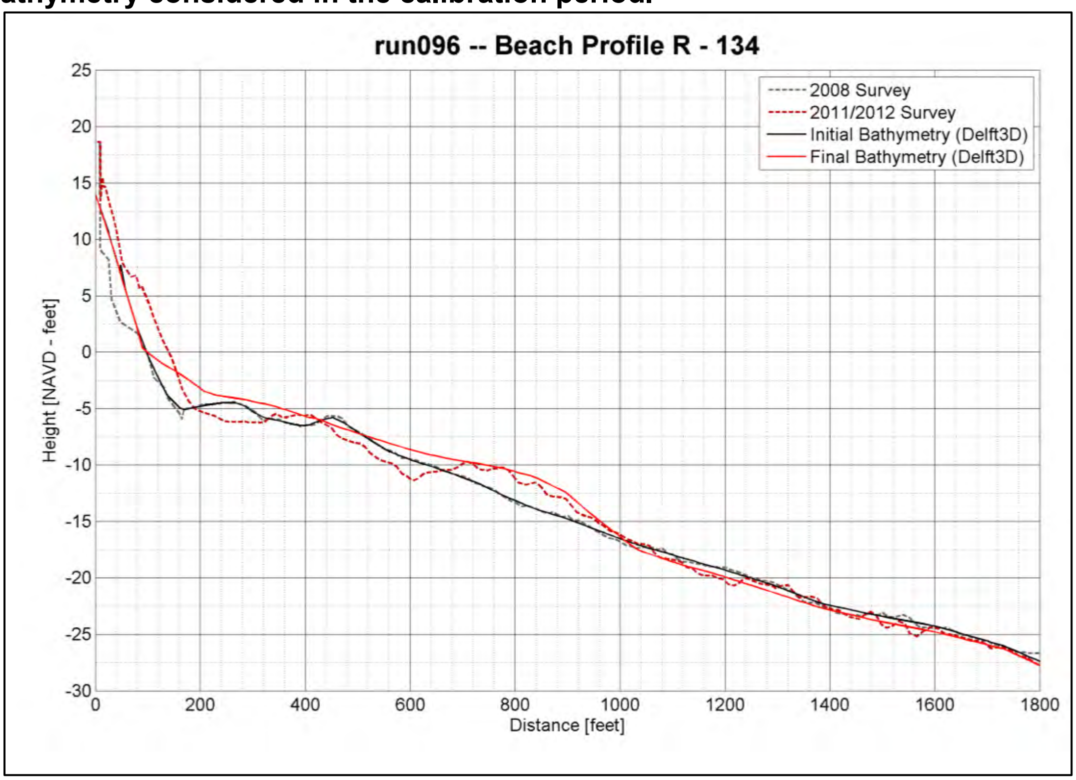

Figure 4-17. Comparison of observed and modeled beach profile R-134 for the initial and final bathymetry considered in the calibration period.

Model performance was also verified by comparing the simulated morphology changes and measured morphology changes over the 3.3 year period between the September/October 2008 and January 2012. The comparison is shown in Figure 4-18 with red shaded areas representing erosion and green shaded areas representing sedimentation. The model captures the overall morphologic changes that were measured during the calibration period. Specifically, the model was able to replicate the general locations and patterns of shifts and reversals between nearshore and offshore sedimentation/erosion patterns within the project. Qualitative comparisons are provided below:

- General onshore migration of sand into nearshore bar formations throughout study area.
- Sedimentation and erosion along bars and troughs throughout study area.
- Nearshore sedimentation occurred between R-129 and R-131.
- Sedimentation shifted offshore between R-131 to R-R-135.
- Sedimentation reversed shifting onshore between R-135 and R-137.
- Sedimentation shifted offshore between R-137 and R-144.

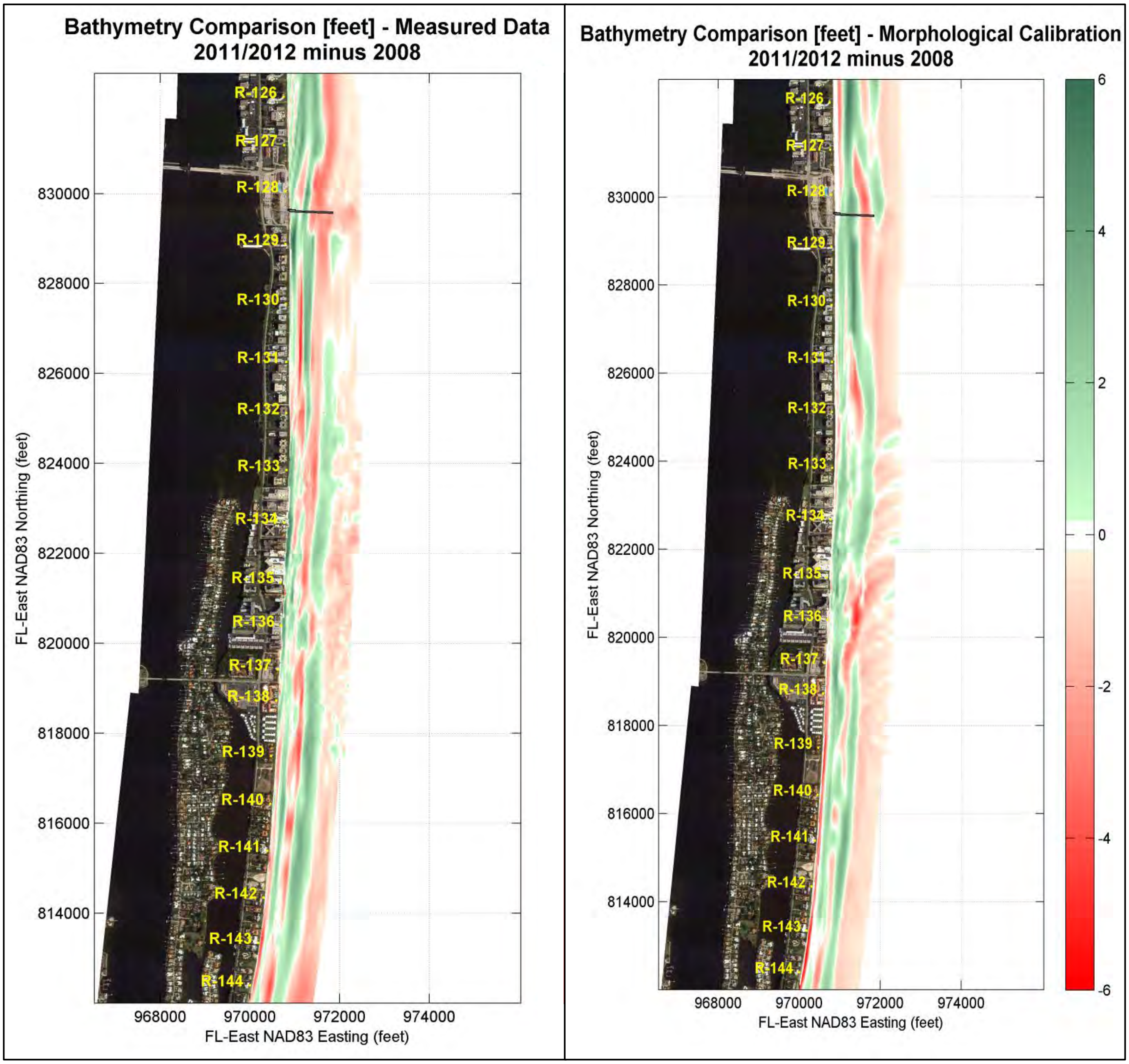

Figure 4-18. Bathymetry Comparison of Measured and Modeled Morphological Changes.

4.4. Model Calibration Summary

Calibration of the model resulted in reasonable agreement between the simulated and measured morphological changes for the expectations and intended use of the model results. Agreement was demonstrated during the calibration period based on the following:

- Volume changes showed that the magnitude of the modeled volumetric changes was consisted with the measured changes.
- Sediment budget analysis demonstrated that the modeled and measured changes have similar erosional trends within the project area. In addition it showed that the modeled transport rate was in agreement with the measured rates.
- Measured and modeled beach profiles illustrate that the modeled morphology represents cross-shore features such as the evolution of the offshore bar formations within the surf zone.
- The modeled morphologic changes captured the overall measured erosion and sedimentation demonstrating the model's skill in simulating the general patterns occurring within the project area.

5.0 ALTERNATIVES ANALYSIS

The calibrated model was used to assess the performance of several alternatives and track the movement of sand within the littoral system over a three year simulation period. A total of seven alternatives were considered. An additional six "separated" alternatives (i.e. Alternative 2T and Alternative 2C) were modeled in order to identify the individual project related effects/impacts associated with the Town of Palm Beach (T) and the County (C) fill templates as "stand-alone" projects. It should be noted that "separated" alternatives were not modeled for every combined alternative as the separated fill templates were captured within other model runs.

- <u>Alternative 1</u> – No Action Alternative (Status Quo) and referenced herein as the existing conditions.

- Alternative 2 – The Applicants' Preferred Project (proposed action) with Beach and Dune Fill with Shoreline Protection Structures. From north to south, the project would include placing sand to enhance the dune from R-129-210 to R-129+150, dune and beach berm from R-129+150 to R-131, dune from R-131 to R-134+135 (Town of Palm Beach southern limit), and beach berm from R-134+135 to R-188+551 (Figure 1-1. Southern Palm Beach Island Comprehensive Shoreline Stabilization Project Location.). South of the Town of Palm Beach seven (7) low-profile groins were included from R-134+135 to R-138+551.
    - Alternative 2T – The portion of Alternative 2 between R-129-210 and R-134+135 within the Town of Palm Beach.
    - Alternative 2C – The portion of Alternative 2 between R-134+135 and R-138+551 within the County project area.
- Alternative 3 – The Applicants' Preferred Project (proposed action) without Shoreline Protection Structures.
    - Alternative 3C – The portion of Alternative 3 between R-134+135 and R-138+551 within the County project area.
- Alternative 4 – The Town of Palm Beach Preferred Project and County Increased Sand Volume without Shoreline Protection Structures. The sand volume within the County was increased by advancing the beach berm on average 50 feet seaward as compared to Alternative 2.
- Alternative 5 – The Town of Palm Beach Increased Sand Volume and County Preferred Project. The sand volume within the Town of Palm Beach was increased by advancing the dune and beach berm on average 10 feet seaward from R-129-210 to R-131 and the dune on average 50 feet seaward from R-132 to R-134+135 (Town of Palm Beach southern limit) as compared to Alternative 2.

- Alternative 6 – The Town of Palm Beach Increased Sand Volume Project and County Increased Sand Volume without Shoreline Protection Structures. The volume was increased by advancing the dune and beach berm on average 10 feet seaward from R-129-210 to R-131, the dune on average 50 feet seaward from R-132 to R-134+135 (Town of Palm Beach southern limit), and the beach berm on average 50 feet seaward from R-134+135 to R-138+551 as compared to Alternative 2.
  - Alternative 6T – The portion of Alternative 6 between R-129-210 and R-134+135 within the Town of Palm Beach.
  - Alternative 6C – The portion of Alternative 6 between R-134+135 and R-138+551 within the County project area.
- Alternative 7 – Plan was presented by The Coalition to Save Our Shoreline, Inc. (SOS) consisting of beach fill and dune restoration between R-129+210 and R-134+135 with shoreline protection structures. The sand fill volumes required for the SOS plan are greater than the volumes for Alternative 6 over the same shoreline extents. For the purpose of modeling, Alternative 7 was defined as the SOS plan north of R-134+135 and Alternative 2 to the south.
  - Alternative 7T – The portion of Alternative 7 between R-129+210 and R-134+135 within the Town of Palm Beach.

The fill volumes required to construct the templates for each of the alternatives were estimated based on the 2011-2012 beach profile surveys. Table 5-1 and Table 5-2 summarize the alternatives and the design fill volumes. Table 5-3 summarizes the volumetric fill densities (cy/ft) by alternative. The volumes and dimensions present in Table 5-1 through Table 5-3 were estimated based beach profiles surveys at the FDEP R-monuments. The location and elevation of the fill templates were maintained within the model, but due to linear interpolation of the bathymetry between R-monuments and the size of the numerical grid, the volume of fill included in the model may differ.

Table 5-1. Summary of Alternatives.

	Design Fill Volumes	Shoreline Protection Structures
Alternative 1	No Action Scenario	
Alternative 2	Total volume of 117,300 cy	7 groins between R-135+160 and R-137+422
Alternative 2T	Total volume of 53,800 cy	Alternative 2 Town only (no groins)
Alternative 2C	Total volume of 63,500 cy	Alternative 2 County only (with 7 groins)
Alternative 3	Total volume of 117,300 cy	no structures
Alternative 3C	Total volume of 63,500 cy	Alternative 2 County only (no structures)
Alternative 4	Total volume of 225,900 cy	no structures
Alternative 5	Total volume of 164,500 cy	7 groins between R-135+160 and R-137+422
Alternative 6	Total volume of 273,000 cy	no structures
Alternative 6T	Total volume of 101,000 cy	Alternative 6 Town only (no structures)
Alternative 6C	Total volume of 172,000 cy	Alternative 6 County only (no structures)
Alternative 7	Total volume of 401,600 cy	7 groins between R-135+160 and R-137+422 and 2 T-head between R-132+556 and R-133+269
Alternative 7T	Total volume of 338,100 cy	Alternative 7 Town only (2 T-head between R-132+556 and R-133+269)

Table 5-2. Summary of Alternatives (continued). Volume expressed in cubic yards.

	Total CY	Above HTL CY	Between MHW and HTL CY	Below MHW CY
Alt 2	117,300	67,700	20,100	29,500
Alt 2T	53,755	34,470	9,300	9,960
Alt 2C	63,545	33,230	10,800	19,540
Alt 3	117,300	67,700	20,100	29,500
Alt 3C	63,545	33,230	10,800	19,540
Alt 4	225,900	113,200	37,000	75,700
Alt 5	164,500	108,300	22,600	33,600
Alt 6	273,000	153,800	39,400	79,800
Alt 6T	101,000	75,100	11,800	14,000
Alt 6C	172,000	78,700	27,600	65,800
Alt 7	401,600	187,100	60,300	154,200
Alt 7T	338,072	153,881	49,518	134,674

Table 5-3. Summary of volumetric fill densities by monuments and alternatives.

	Volumetric Fill Density (cy/ft)					
Monuments	Alternative 2	Alternative 3	Alternative 4	Alternative 5	Alternative 6	Alternative 7
R-129	0.0	0.0	0.0	12.6	12.6	25.5
R-130	16.3	16.3	16.3	22.5	22.5	65.8
R-131	9.2	9.2	9.2	9.1	9.1	68.2
R-132	8.5	8.5	8.5	8.5	8.5	61.4
R-133	0.0	0.0	0.0	19.1	19.1	53.4
R-134	7.6	7.6	7.6	22.8	22.8	7.6
R-135	10.7	10.7	31.9	10.7	31.8	10.7
R-136	27.9	27.9	53.8	27.9	53.8	27.9
R-137	13.1	13.1	54.0	13.1	54.0	13.1
R-138	10.4	10.4	28.2	10.4	28.2	10.4

5.1. Setup

Model calibration was based on the initial 2008 conditions and replicating the observed 2011-2012 conditions after the 3.3 year simulation period. For the alternatives analysis, the 2011-2012 conditions were used as the initial input into the model. While the parameters (Table 4-3) established during calibration of the model were used, three inputs were updated for the analysis.

- Bathymetry
- Hardbottom and Sediment Layer Thickness
- Shoreline Protection Structures

5.1.1. Bathymetry

Bathymetries for the local wave grid and the flow and morphology grid were updated based on the following data sources (see also Table 3-2):

1. January 2012 beach profiles (FDEP, 2012).
2. September-November 2011 beach profiles (ATM, 2012).
3. 2006 Lidar (USACE, 2006).

4. 1963-1964 hydrographic survey (NOAA, 2006).

The primary data set was January 2012 beach profiles, followed by the September-November 2011 beach profiles. Lidar data from 2006 was used to represent topography of inland area beyond the beach profiles, while the hydrographic survey from 1963-1964 was used to represent the deeper water depths extending to the intermediate and regional wave grids. The resulting bathymetry of the flow and morphology grid appears in Figure 5-1. This bathymetry represents the existing conditions for comparison with the alternatives.

The fill proposed for each of the alternatives was added to the existing conditions to create the initial input bathymetries for the alternatives.

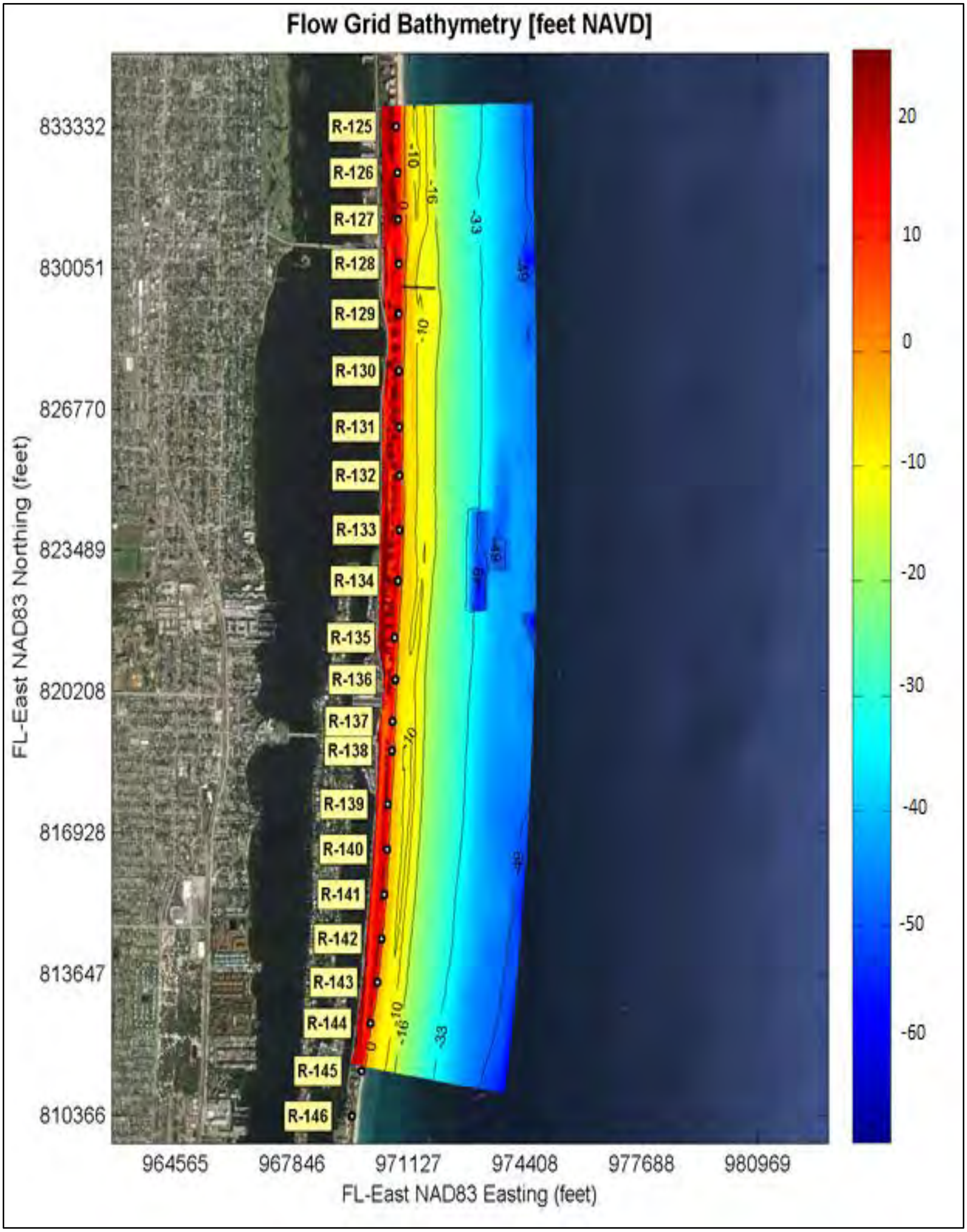

Figure 5-1. Flow and morphology grid bathymetry (feet NAVD) used in production runs.

5.1.2. Hardbottom and Sediment Thickness

The thickness of sediment used in alternatives runs was updated from the morphological calibration using the 2011-2012 surveys and 2012 hardbottom mapping. Areas where the 2012 survey was shallower than the hardbottom depth established during calibration were verified throughout the numeric domain. In these regions, the difference between the 2011-2012 survey and calibrated hardbottom elevation was added to the sediment thickness, thus setting an initial thickness for the alternatives analysis that corresponded to the 2011-2012 bathymetry. These sediment thicknesses represent the existing conditions (Figure 5-2).

Similarly, the thicknesses were updated to account for the proposed fill for each of the alternatives. The thickness of the fill was determined by subtracting 2011-2012 bathymetry from the fill bathymetry. The differences were added to the sediment thicknesses to create the initial input for the alternatives.

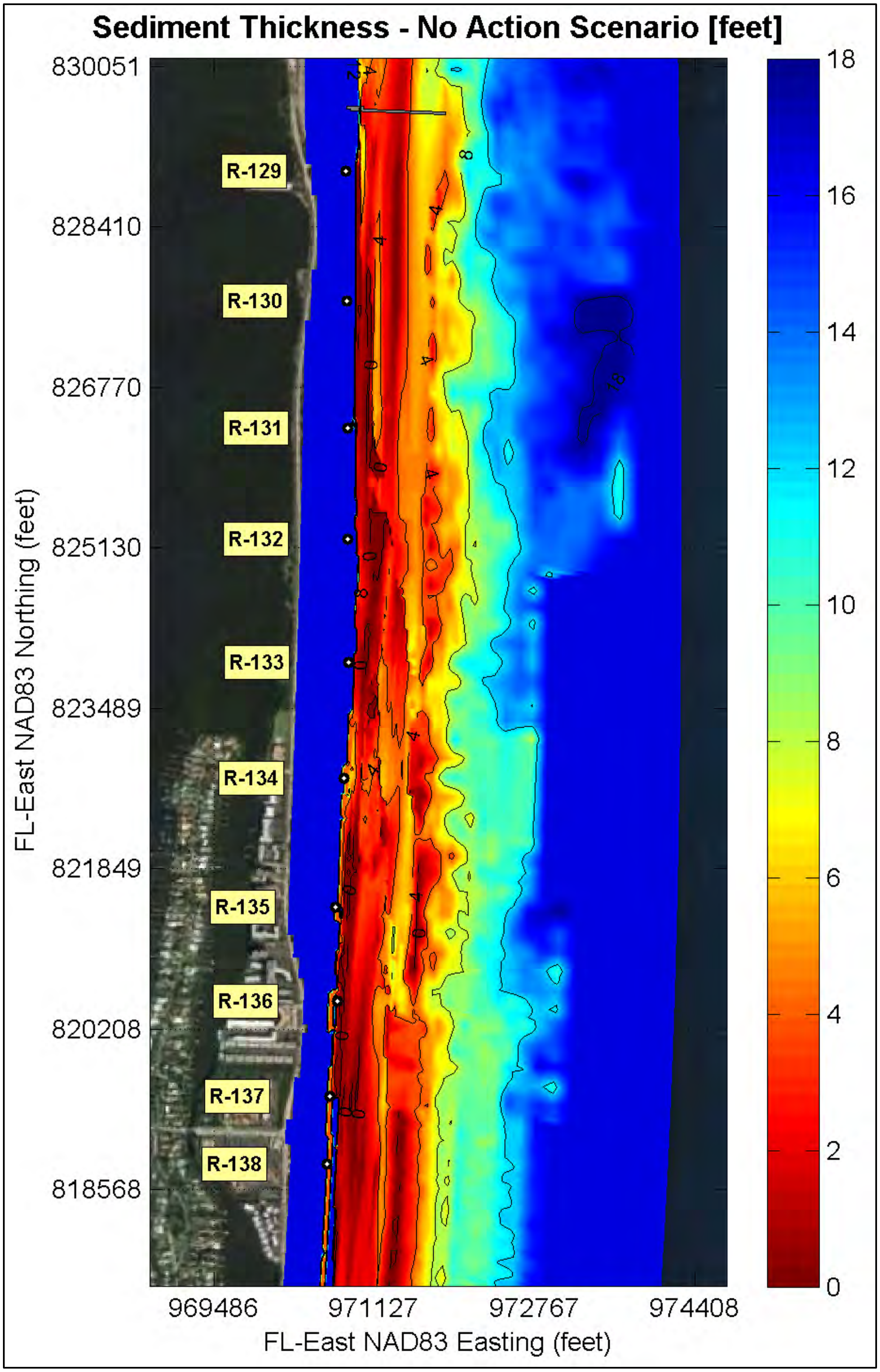

Figure 5-2. Initial sediment thickness of No Action scenario.

5.1.3. Shoreline protection structures

Alternatives 2, 5, and 7 proposed shoreline protection structures as outlined in Table 5-1. As discussed above in Section 3.7 for the Lake Worth Pier, a coefficient was required to account for the porosity of the structures. In the Delft3D-Flow model, these structures were represented as porous plates with a value of 1.0 (permeable).

5.2. Alternative 1 – No Action Alternative (Status Quo)

Alternative 1 is the No-Action Alternative. The bathymetry for this alternative is based on the existing conditions as discussed above. The evolution of the existing conditions after the 3 year simulation period is shown Figure 5-3. Included in the figure, the graphic on the right shows the erosional areas (red areas) and sedimentation areas (green areas) during this period. The graphic depicts the dynamic nature of the Project Area with sand generally accumulating within the offshore bar and trough features, which parallel the shoreline. Sand eroded from the dry beach is transported alongshore and seaward, while sand offshore of the bar is transported alongshore and landward. The hardbottom delineated represents exposed hardbottom digitized from aerial photography collected March 30, 2012.

Figure 5-4 shows the annual rate of sediment transport for each alternatives and no action scenario. Positive values denote north to south transport. This analysis highlights the change in the sediment transport rate at R-135 where there is an approximate 5° change in coastline orientation (89° to the north and 94° to the south relative to Geographical north). The details of the model runs for each alternative are described in the following sections.

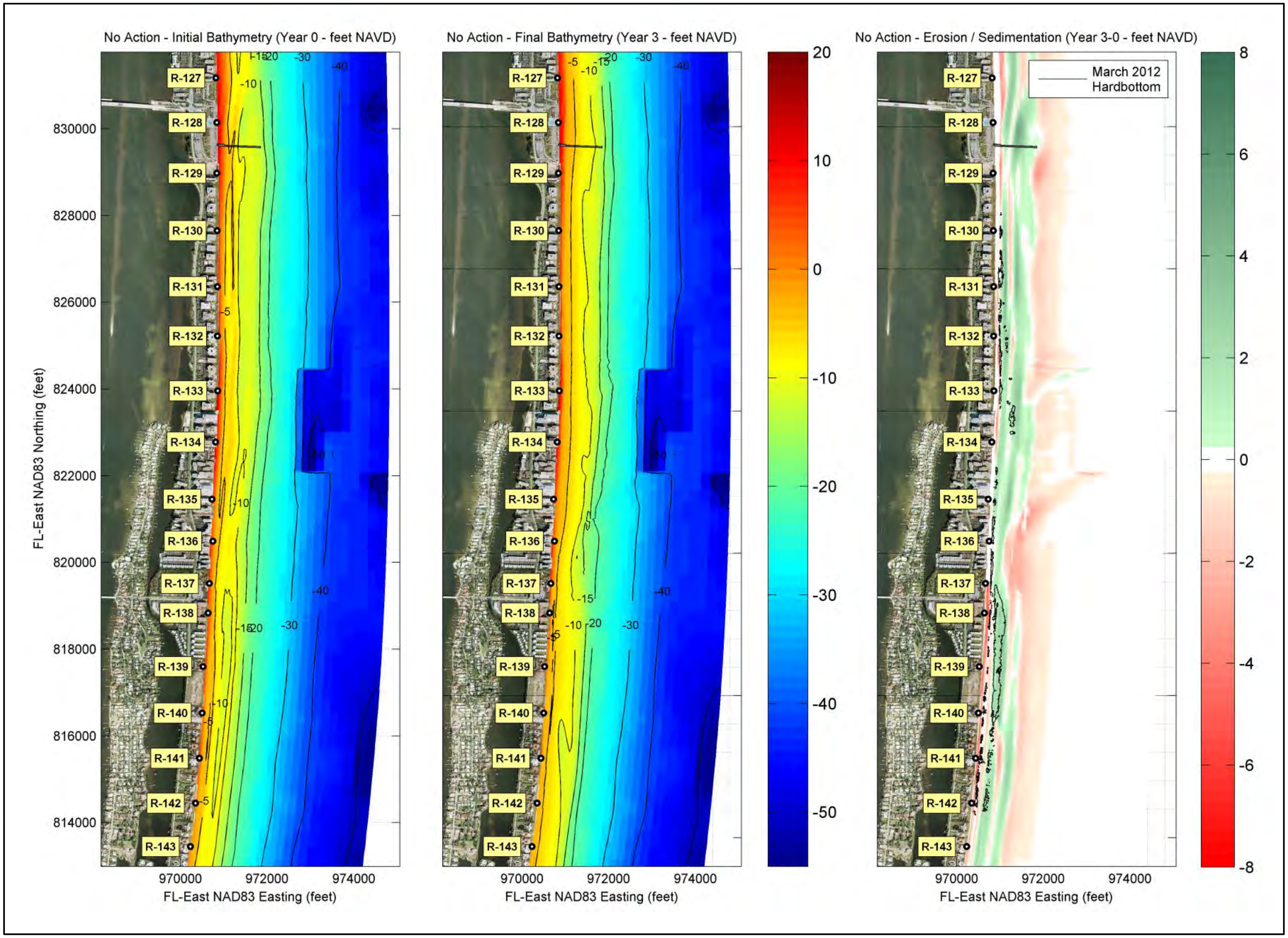

Figure 5-3. Initial bathymetry, final bathymetry and erosion sedimentation after 3 years of simulation, No Action scenario.

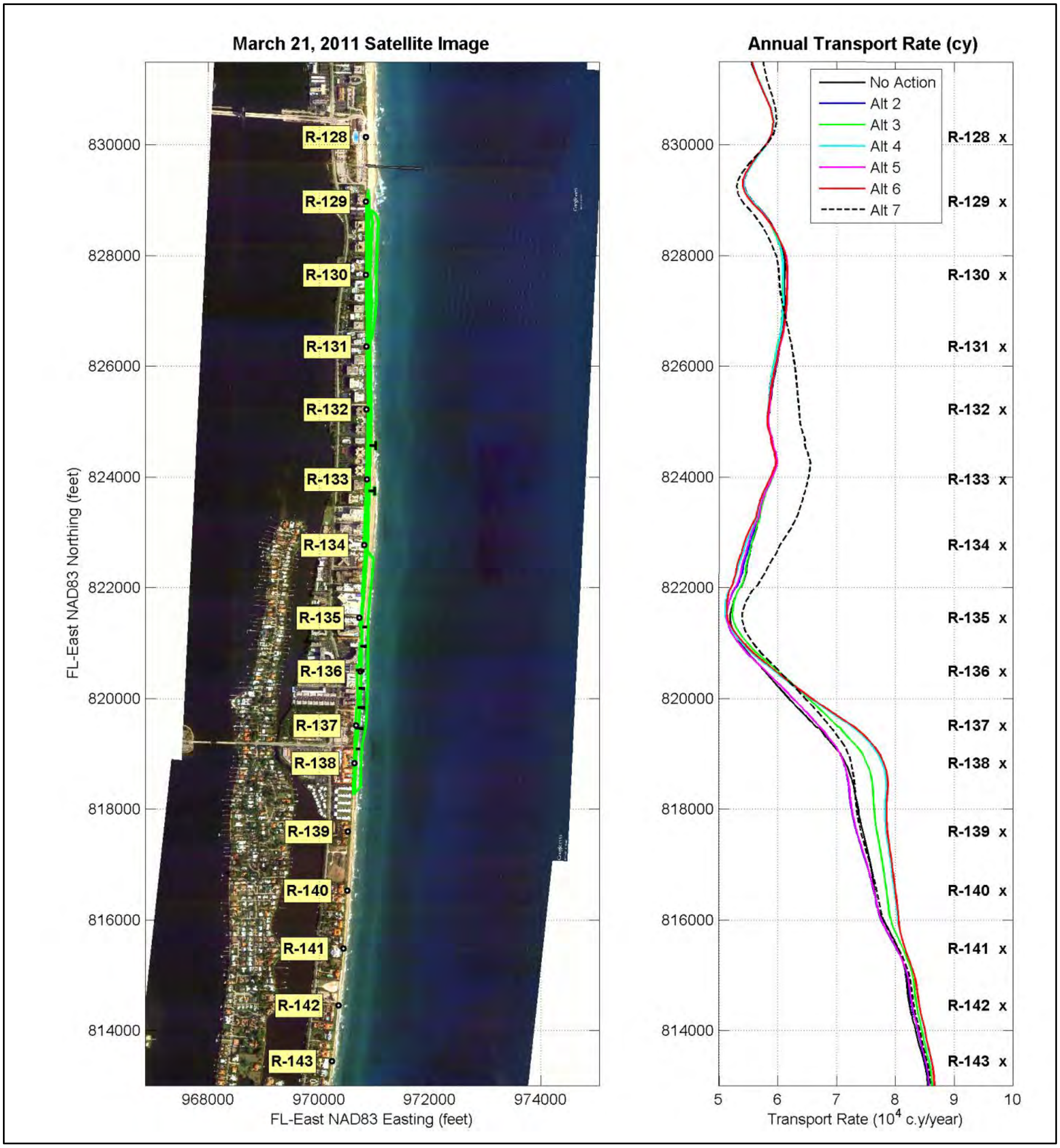

Figure 5-4. Annual transport rate (cy) for Alternatives and No Action Alternative.

5.3. Alternative 2 - The Applicants' Preferred Alternative (proposed action): Beach and Dune Fill with Shoreline Protection Structures Project

5.3.1. Combined Action

Alternative 2 includes seven groins south of R-135 and the placement of approximately 117,300 cubic yards of fill material between R-129-210 and R-138+551.

The volumetric changes for the alternative after 3 years compared to the No Action scenario are shown in Figure 5-5. The yellow line shows the volume change for the No Action Scenario (initial existing bathymetry subtracted from the final No Action bathymetry). The blue line shows the volume change for the alternative (initial existing bathymetry subtracted from the final alternative bathymetry). The black line shows the initial fill volume placed for the alternative. The volumetric impacts/benefits associated with the alternative are denoted by the red line, which is the difference between the yellow and blue lines. Locations where the red line is positive denote benefits provided by the alternative in that there is more volume at a particular location as compared to the No Action scenario after the 3 year simulation period. Likewise, locations where the red line is negative denote impacts associated with the alternative in that there is less volume at a particular location as compared to the No Action. North of R-139 the alternative shows benefits, while to the south there are impacts extending to approximately R-142. This impact may be attributed to the retention of sand within the groin field between R-135 and R-138.

The initial bathymetry for the alternative compared to the final bathymetry for the alternative after the 3 year simulation period is shown in Figure 5-6. Similar to the No Action alternative, the fill from the upper portion of the profile is eroded and deposited within the offshore bar and trough. Sand landward of the bar is transported landward.

The temporal evolution of the fill at one year time steps is tracked in Figure 5-7. The erosion and sedimentation represents the change between the alternative bathymetry as compared to the No Action bathymetry at a given time step. The movement of sand within the study area is depicted by the areas of sedimentation (green shaded areas) and areas of scour (red shaded areas). Hardbottom exposure and subsequent burial occurs naturally within the study area. The model suggests that areas of exposed hardbottom may be covered as a result of the alternative, while other areas may scour increasing hardbottom exposure.

Within the areas of sand movement, hardbottom coverage is delineated by the green outlines, while hardbottom exposure is delineated by the red outlines. The areas of sedimentation/scour and areas of coverage/exposure migrate over time as sand is redistributed during the 3 year simulation period. At the end of the 3 years, there was an estimated coverage of 8.62 acres of hardbottom and an exposure of 3.84 acres attributed to the alternative. The net change in hardbottom at the end of the simulation period (exposure minus coverage) as a result of the project is estimated to be -4.78 acres.

To assess time-dependent changes, areas of sedimentation greater than 0.2 feet for years 0, 1, 2 and 3 are highlighted in Figure 5-8. Changes less than 0.2 feet were not considered, to account for potential survey error and limits of model precision. The model suggested that the fill is transported to the south as it is redistributed offshore.

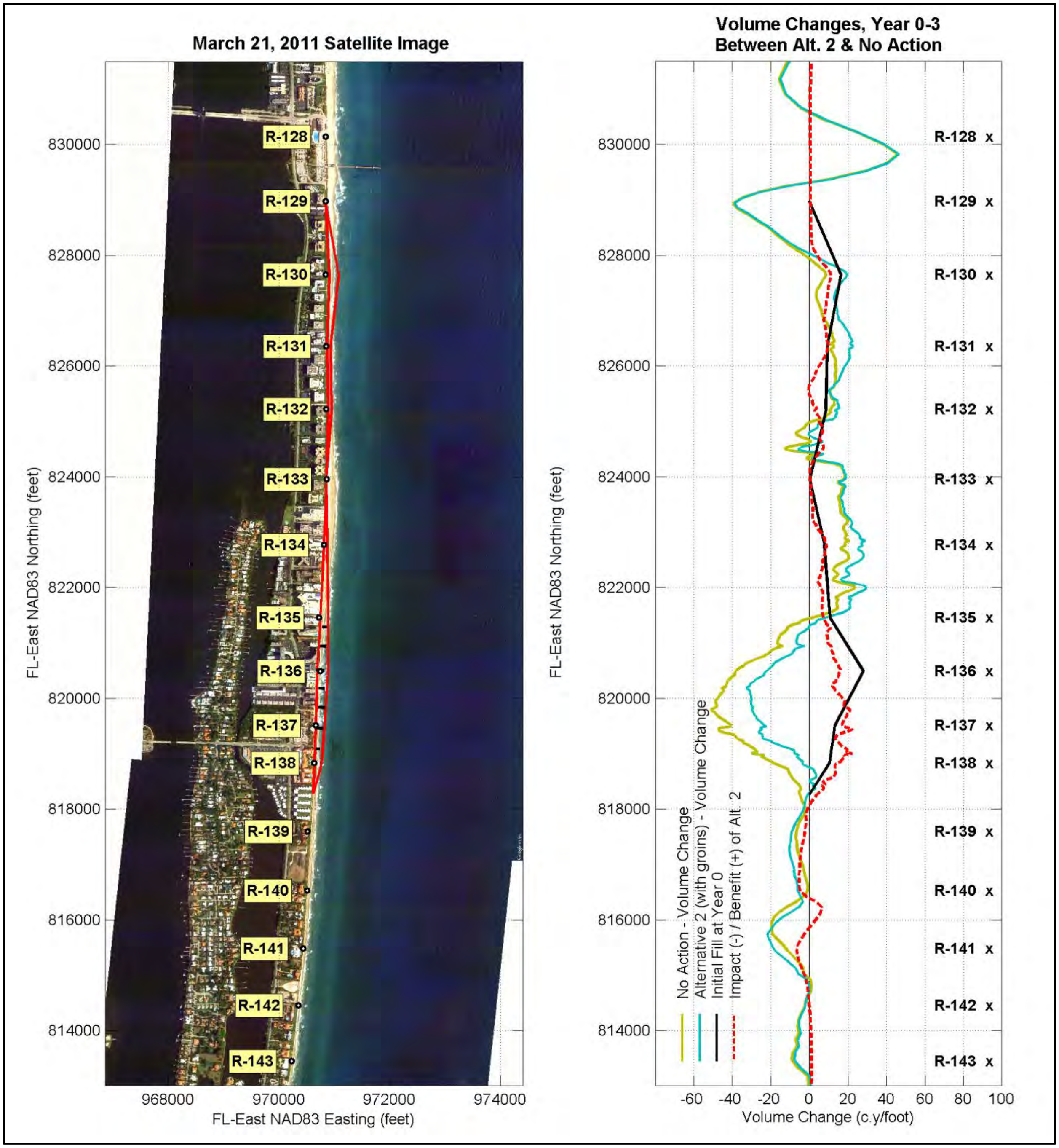

Figure 5-5. Volume Changes for Alternative 2.

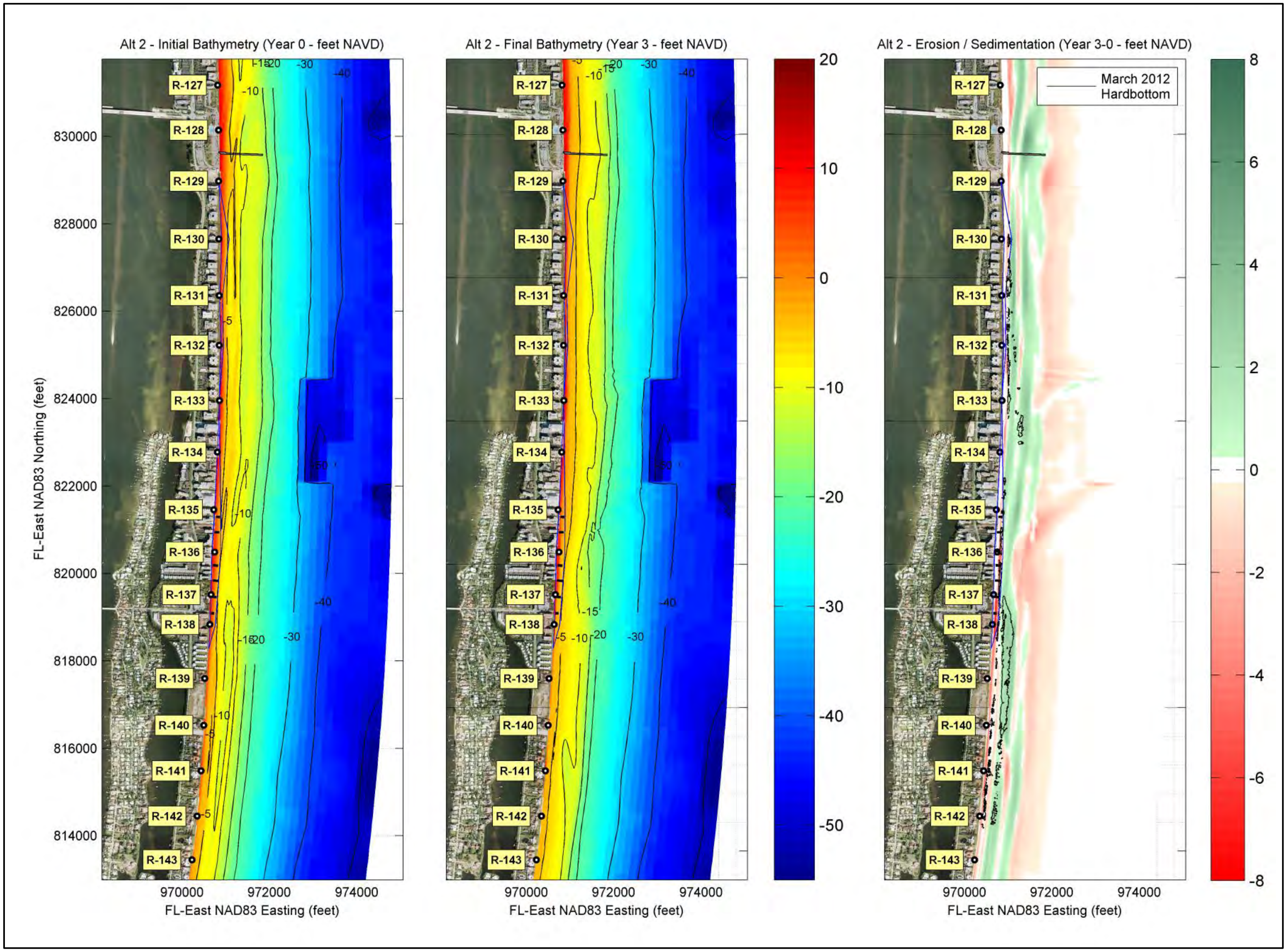

Figure 5-6. Erosion/Sedimentation after 3 years of simulation, Alternative 2.

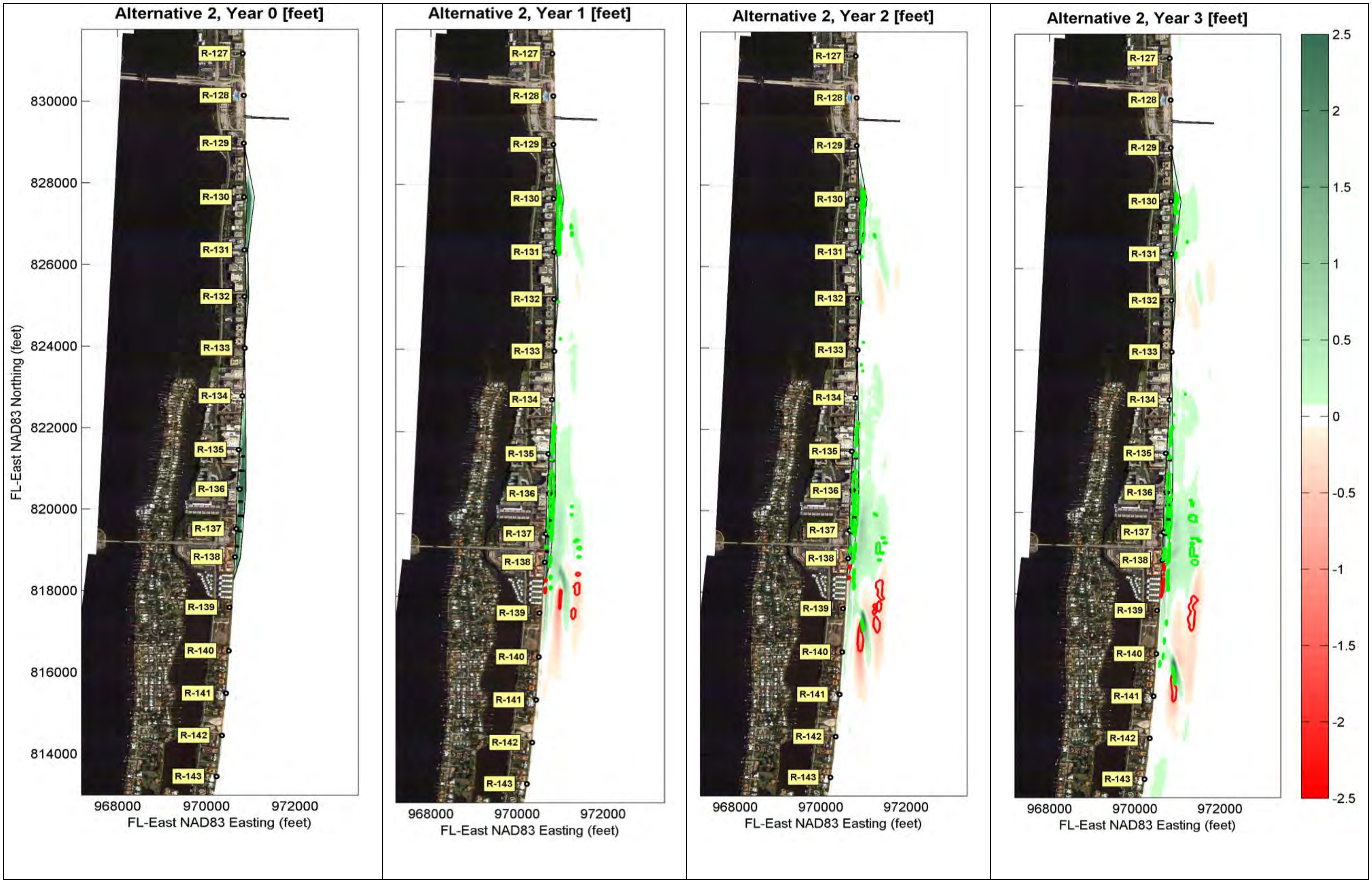

Figure 5-7. Temporal evolution of beach nourishment for Alternative 2, compared to No Action scenario.

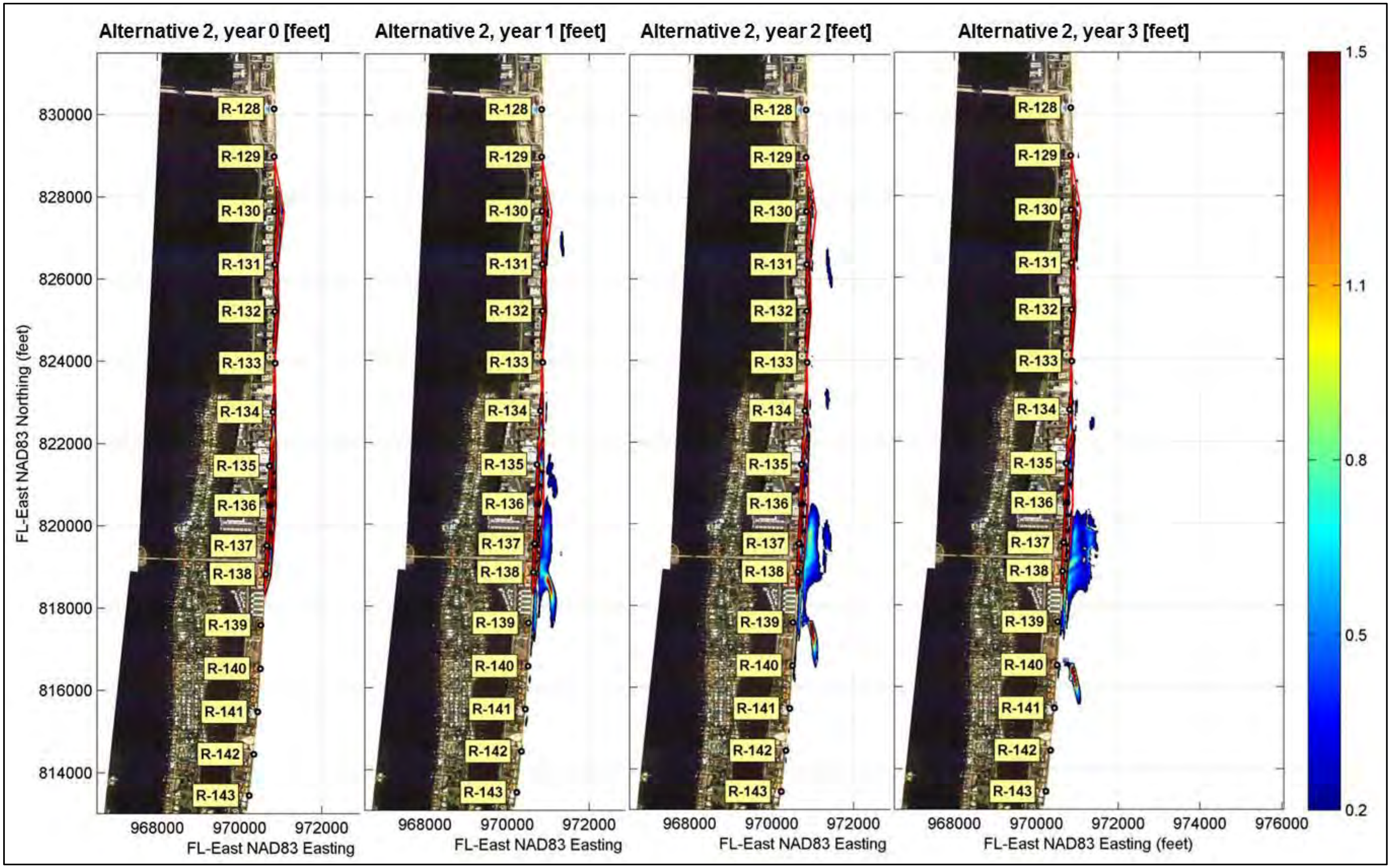

Figure 5-8. Sediment Accumulation greater than 0.2 ft for Alternative 2.

5.3.2. Separated Actions

Alternative 2T (Town of Palm Beach portion of alternative)

Alternative 2T represents the same conditions as Alternative 2 but for the Town of Palm Beach portion only. Alternative 2T consisted of the placement of 53,800 cubic yards of sand between R-129 to R-134+135. Model results for Alternative 2T are shown in Figure 5-9 through Figure 5-12.

At the end of the 3 year simulation period, there was an estimated coverage of 1.24 acres of hardbottom and an exposure of 0.20 acres attributed to the alternative as depicted in Figure 5-11. The net change in hardbottom at the end of the simulation period (exposure minus coverage) as a result of the project is estimated to be -1.04 acres.

Areas of sedimentation with thicknesses greater than 0.2 feet (Figure 5-12) are shown at approximately R-131 during Year 1 and Year 2, while the areas have diffused by Year 3. The areas of sedimentation coincide with the highest fill density for the alternative at R-131. Sedimentation is not apparent outside the alongshore extents of the Project Area for Alternative 2T.

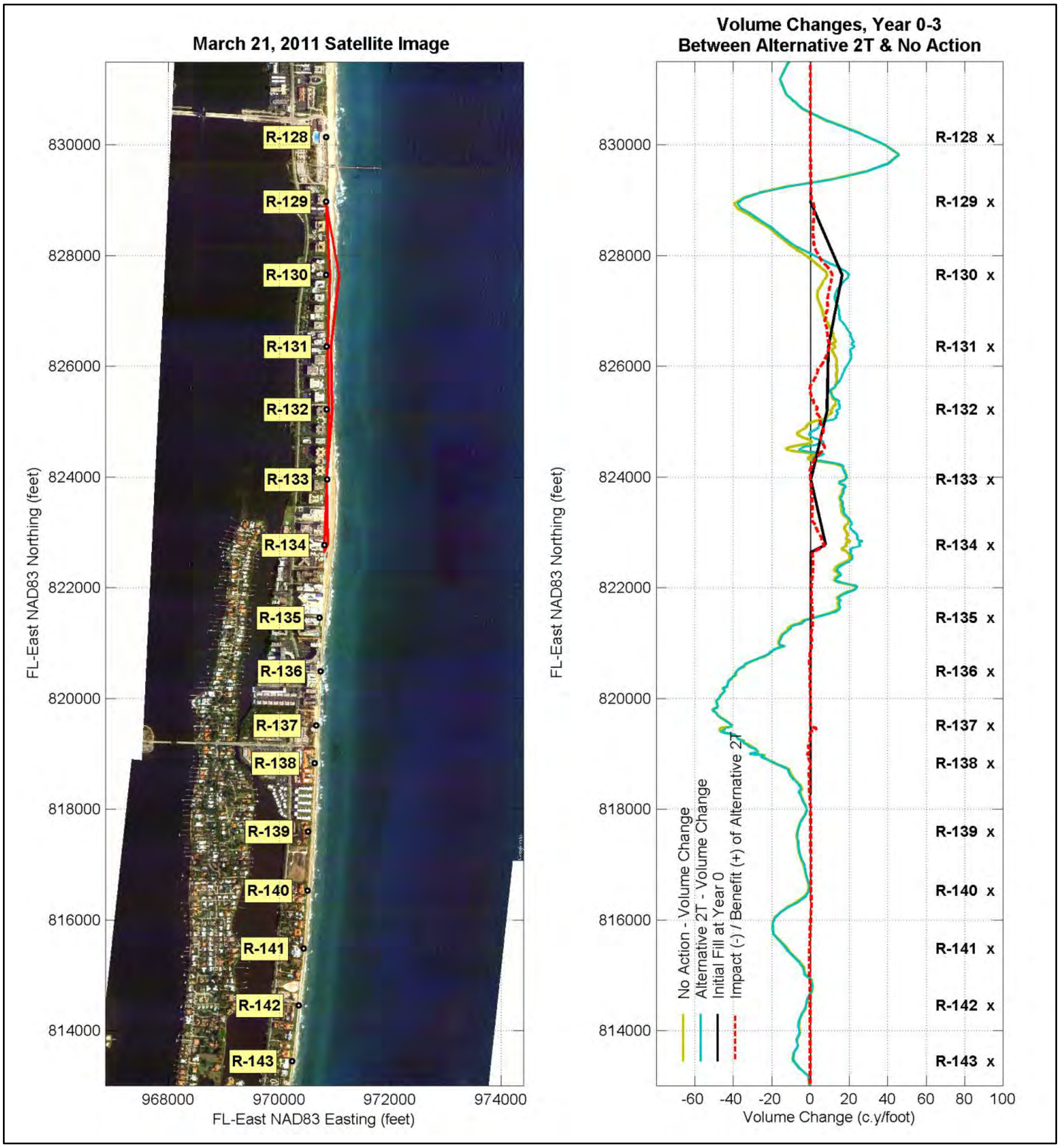

Figure 5-9. Volume Changes to Alternative 2T.

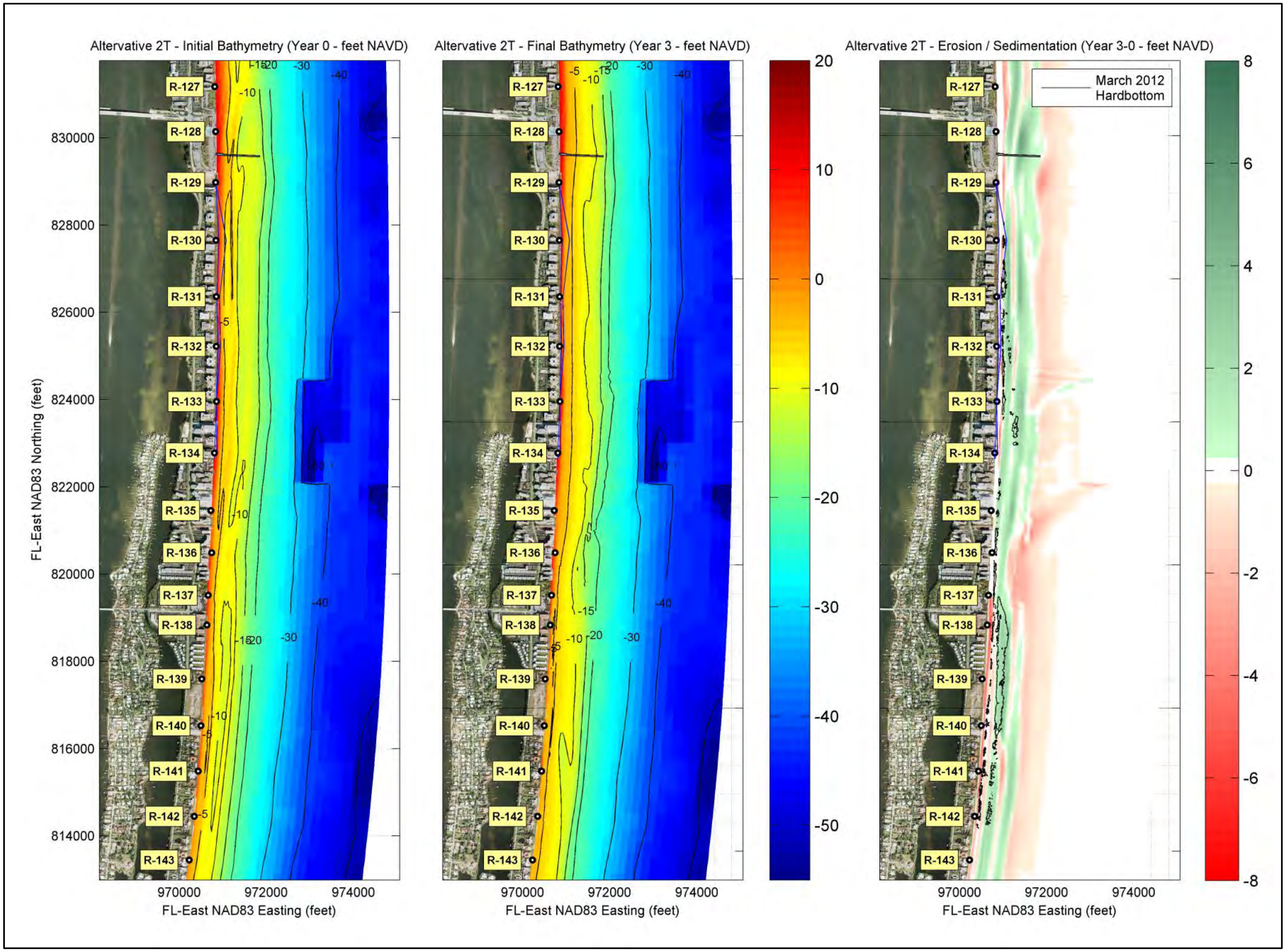

Figure 5-10. Erosion/Sedimentation after 3 years of simulation, Alternative 2T.

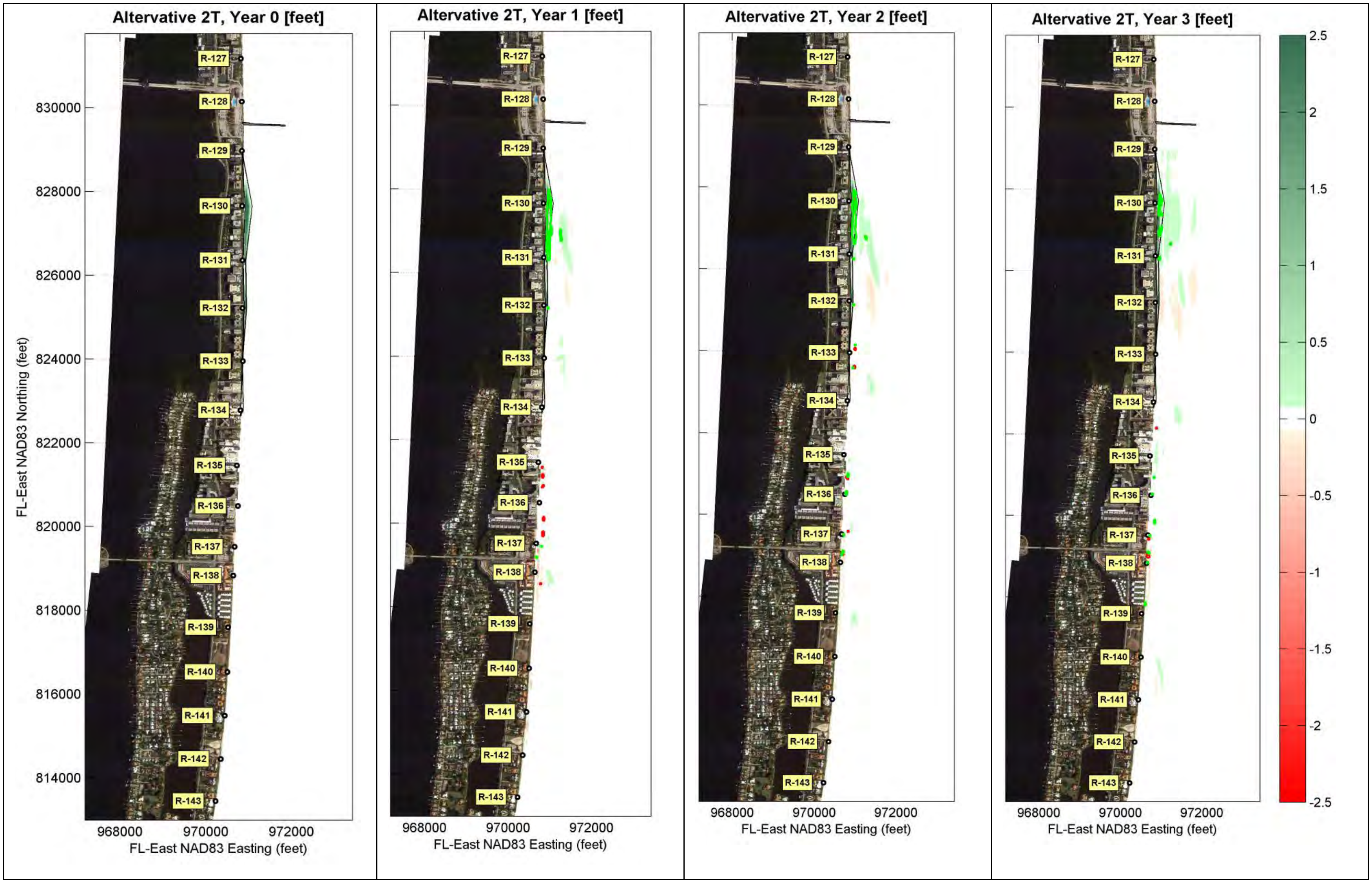

Figure 5-11. Temporal evolution of beach nourishment for Alternative 2T, compared to No Action scenario.

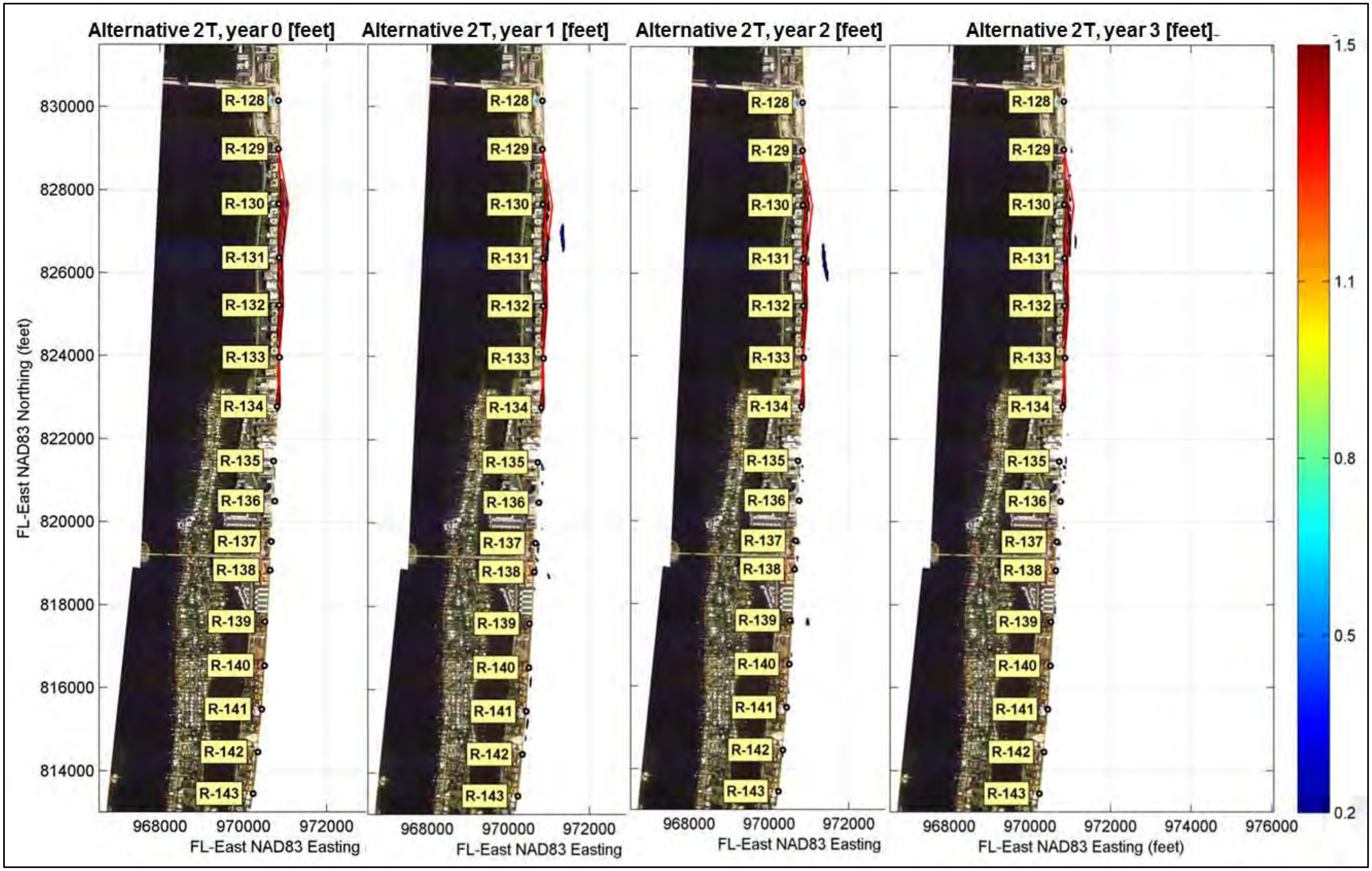

Figure 5-12. Sediment Accumulation greater than 0.2 ft for Alternative 2T.

Alternative 2C (County portion of alternative)

Alternative 2C presents a sand placement of 63,500 cubic yards between R-134+135 and R-138+551 in combination with seven groins between R-135+160 and R-137+422. Model results for Alternative 2C are shown in Figure 5-13 through Figure 5-16.

At the end of the 3 year simulation period, there was an estimated coverage of 7.76 acres of hardbottom and an exposure of 3.55 acres attributed to the alternative as depicted in Figure 5-15. The net change in hardbottom at the end of the simulation period (exposure minus coverage) as a result of the project is estimated to be -4.21 acres.

Model results suggest that the behavior of Alternative 2C is similar to Alternative 2, within County's project area. Areas of sedimentation greater than 0.2 (Figure 5-16) are located at the southern half of the project area for Alternative 2C and by Year 3 extend downdrift to approximately R-141.

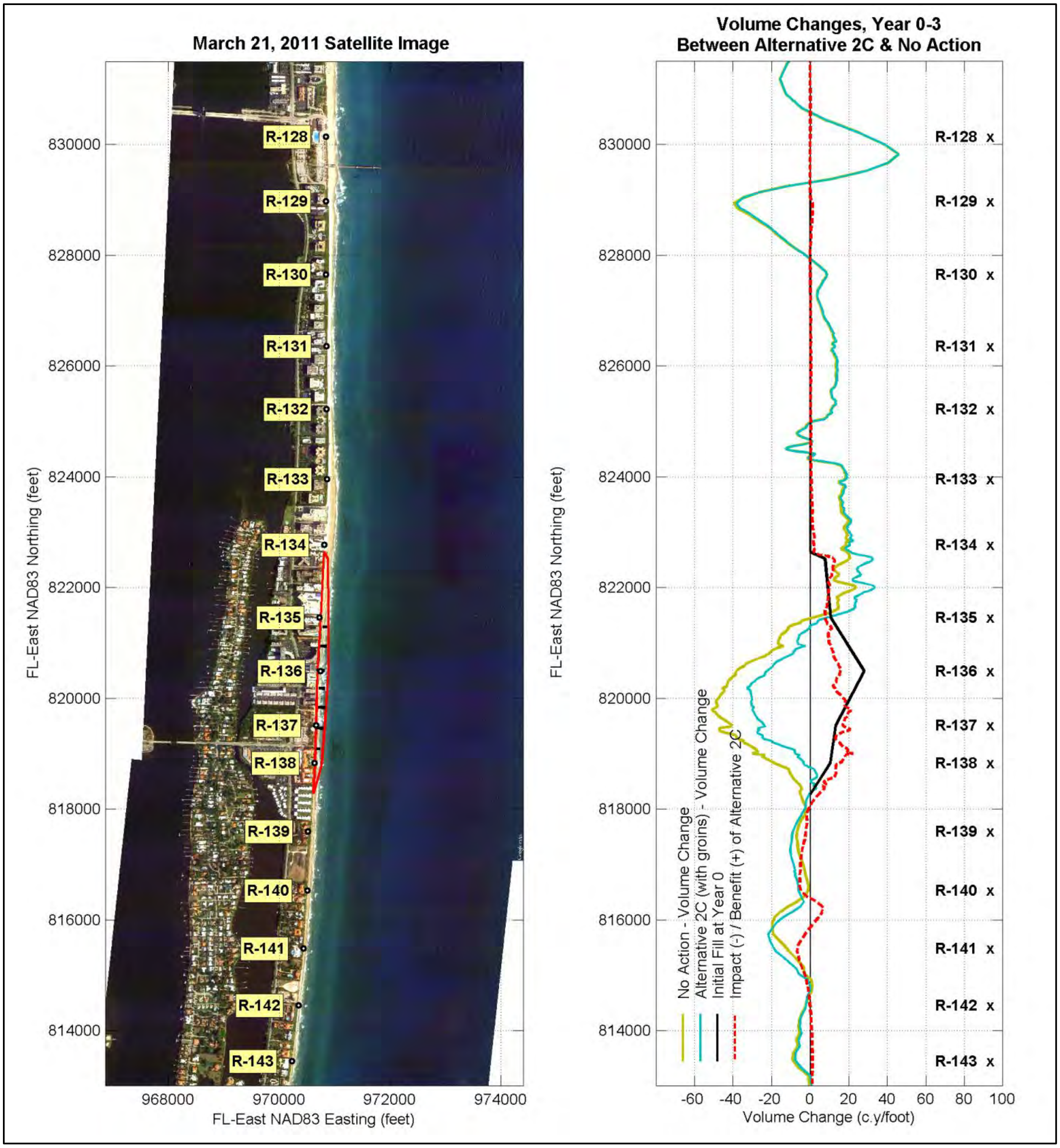

Figure 5-13. Volume Changes to Alternative 2C.

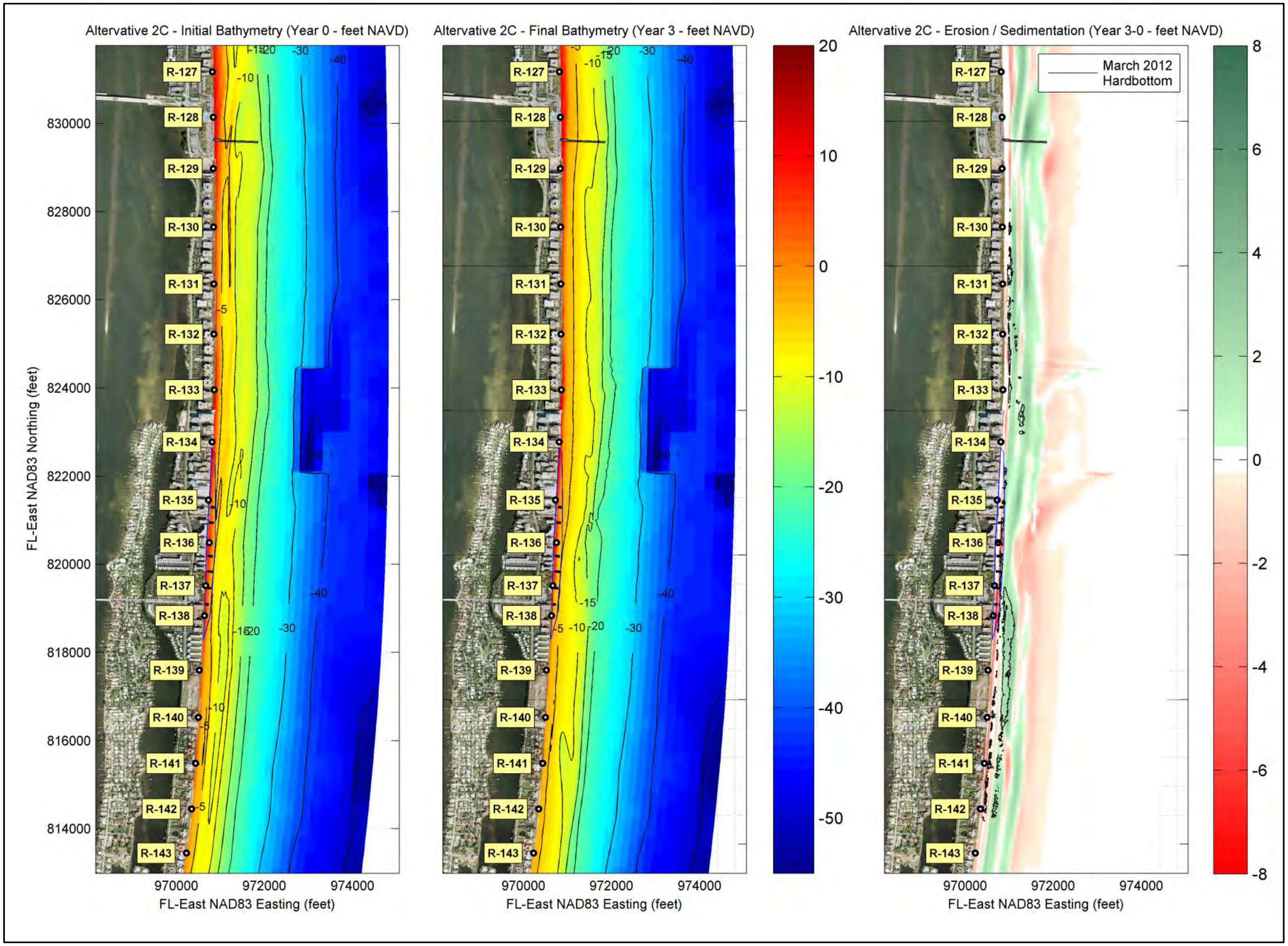

Figure 5-14. Erosion/Sedimentation after 3 years of simulation, Alternative 2C.

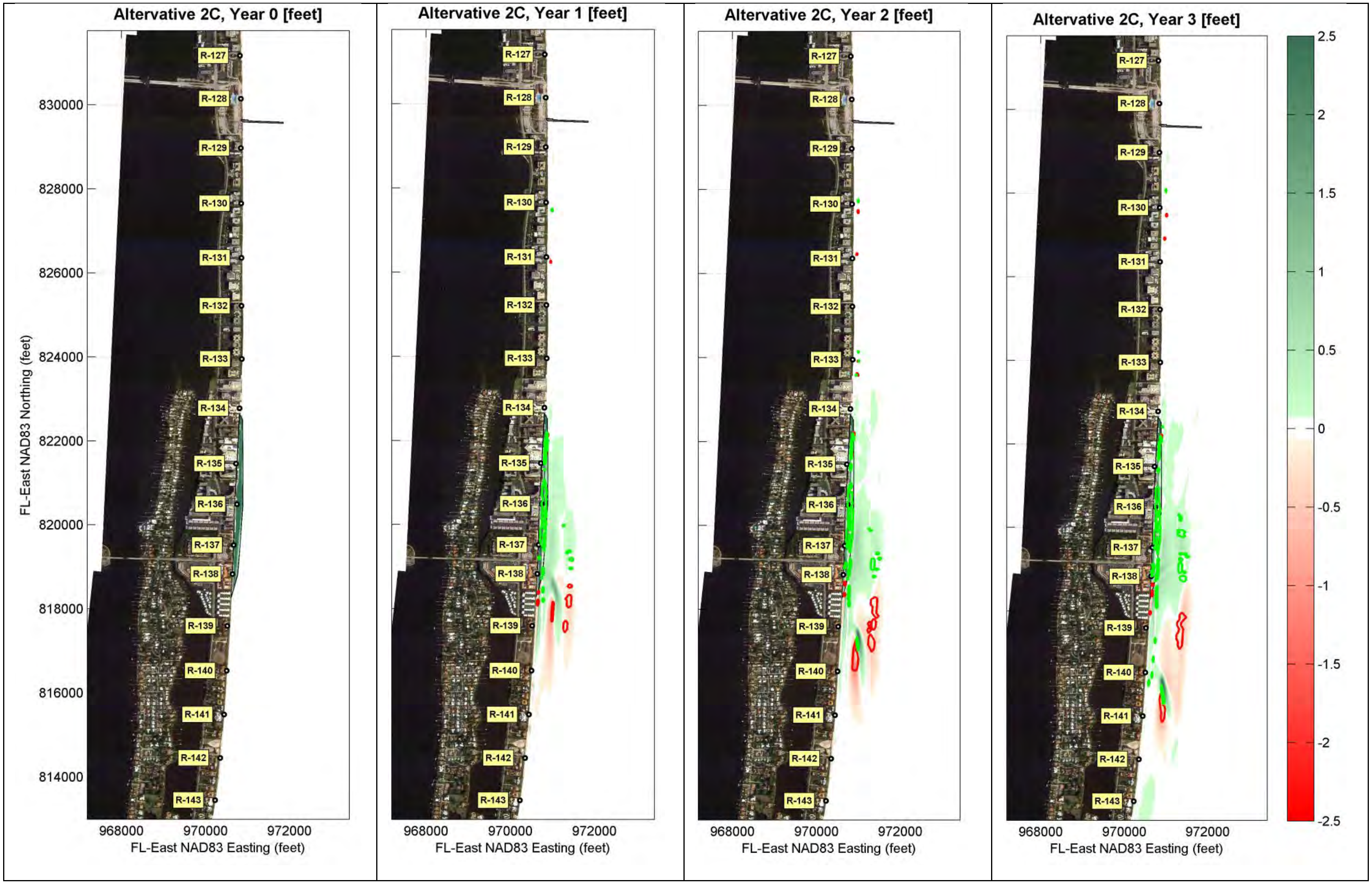

Figure 5-15. Temporal evolution of beach nourishment for Alternative 2C, compared to No Action scenario.

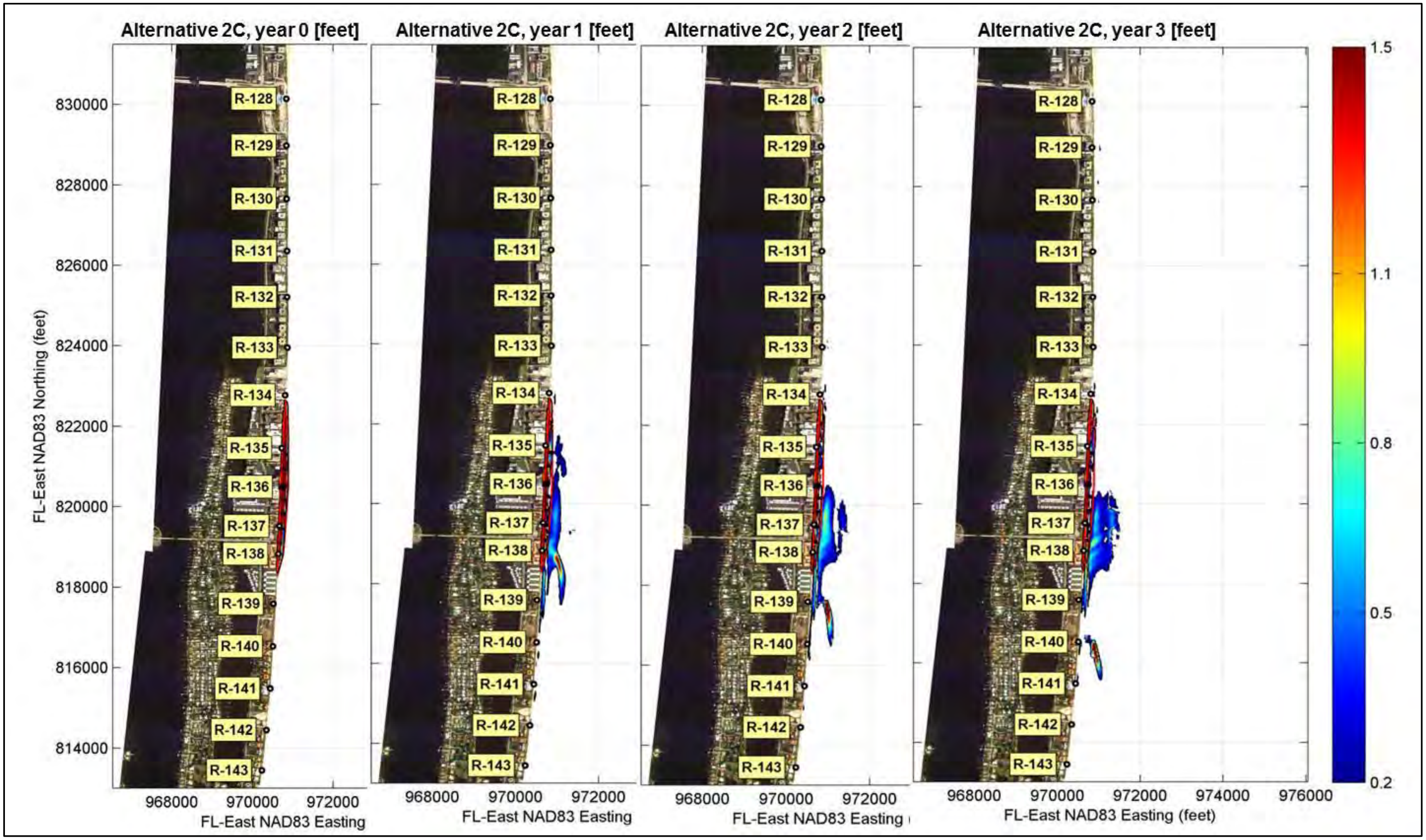

Figure 5-16. Sediment Accumulation greater than 0.2 ft for Alternative 2C.

5.4. Alternative 3 - The Applicants' Preferred Project without Shoreline Protection Structures

5.4.1. Combined Action

Alternative 3 features the same fill layout as Alternative 2, however groins were not included. Model results given in Alternative 3 appear in Figure 5-17 through Figure 5-20.

The model results show behaviors similar to Alternative 2, but Alternative 3 results in greater erosion of fill volume in between R-134 and R-138 monuments and accretion downdrift as shown in Figure 5-18. This indicates that in the absence of the groins, greater spreading in the longshore direction could be anticipated for Alternative 3 as compared to Alternative 2. Figure 5-19 and Figure 5-20 show the temporal evolution of the fill from year 0 to year 3. Compared to Alternative 2, Alternative 3 shows less cross shore spreading of the fill. This is attributed to the fill being transported downdrift in the absence of the groins.

The main difference compared to Alternative 2 was the movement of fill between monuments R-135 and R-140. Alternative 3 showed greater alongshore spreading extending downdrift R-141.

At the end of the 3 year simulation period, there was an estimated coverage of 8.09 acres of hardbottom and an exposure of 0.80 acres attributed to the alternative as depicted in Figure 5-19. The net change in hardbottom at the end of the simulation period (exposure minus coverage) as a result of the project is estimated to be -7.29 acres.

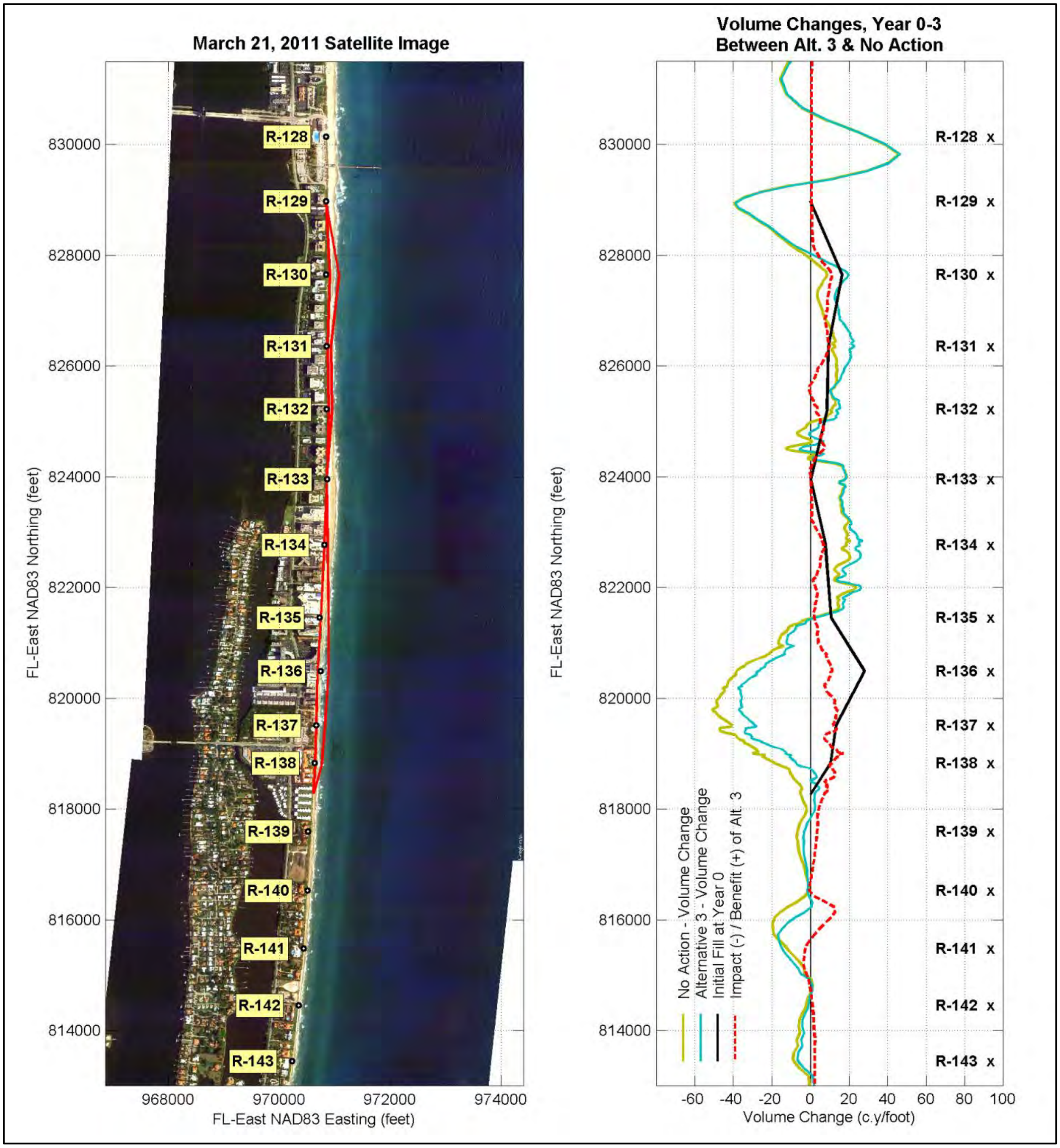

Figure 5-17. Volume Changes to Alternative 3.

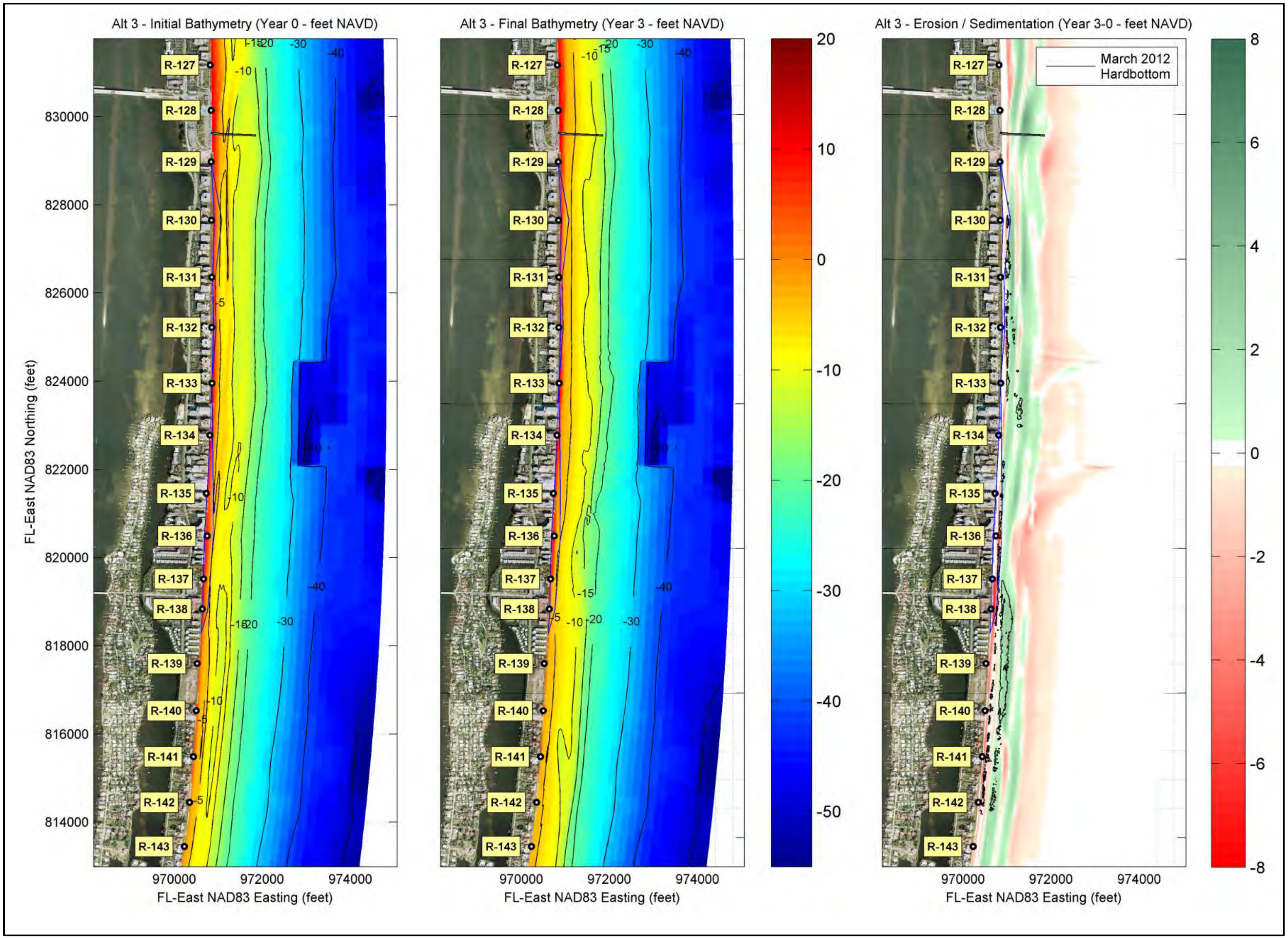

Figure 5-18. Erosion/Sedimentation after 3 years of simulation, Alternative 3.

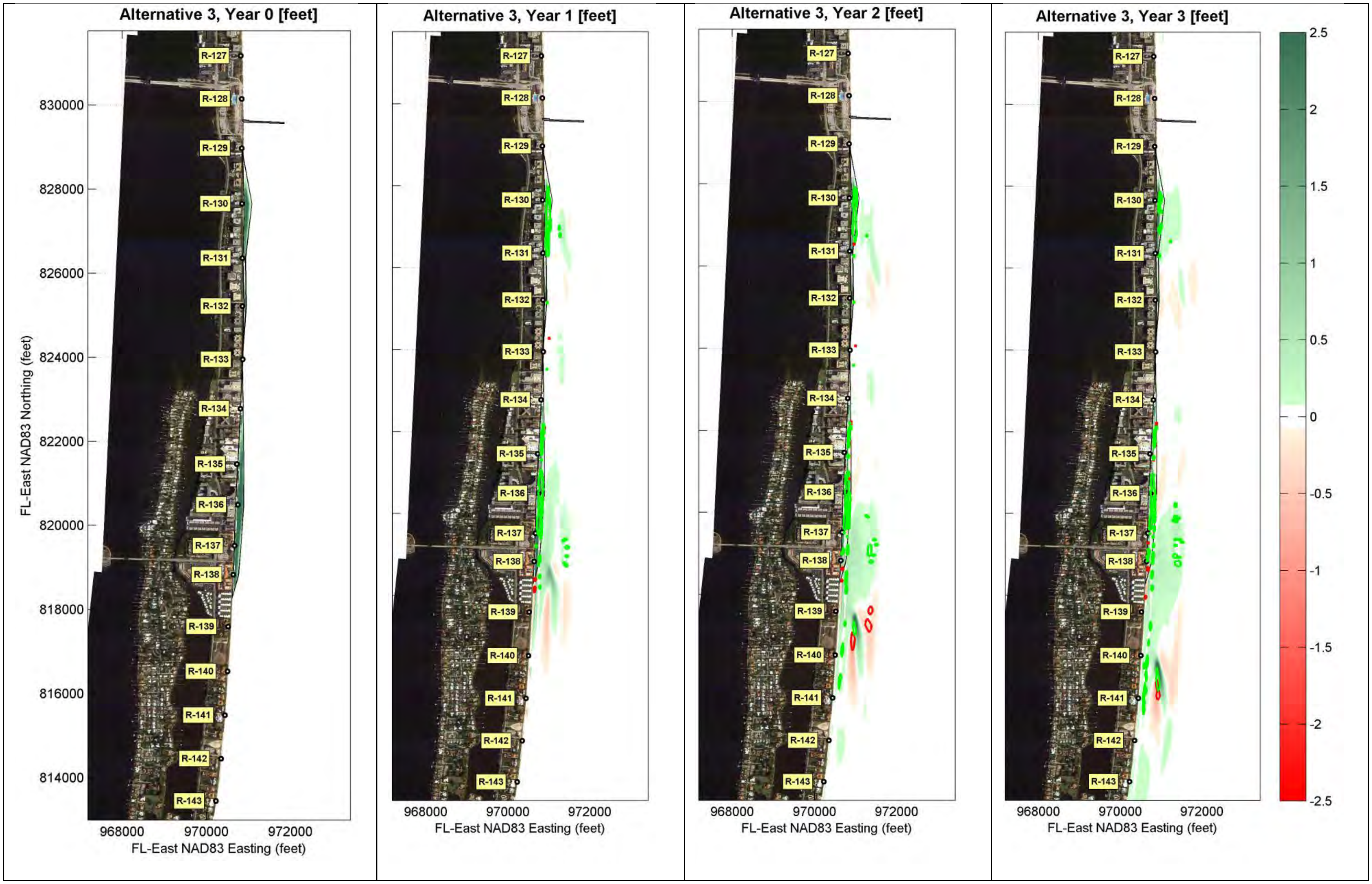

Figure 5-19. Temporal evolution of erosion (red) / sedimentation (green) for Alternative 3, compared to No Action scenario.

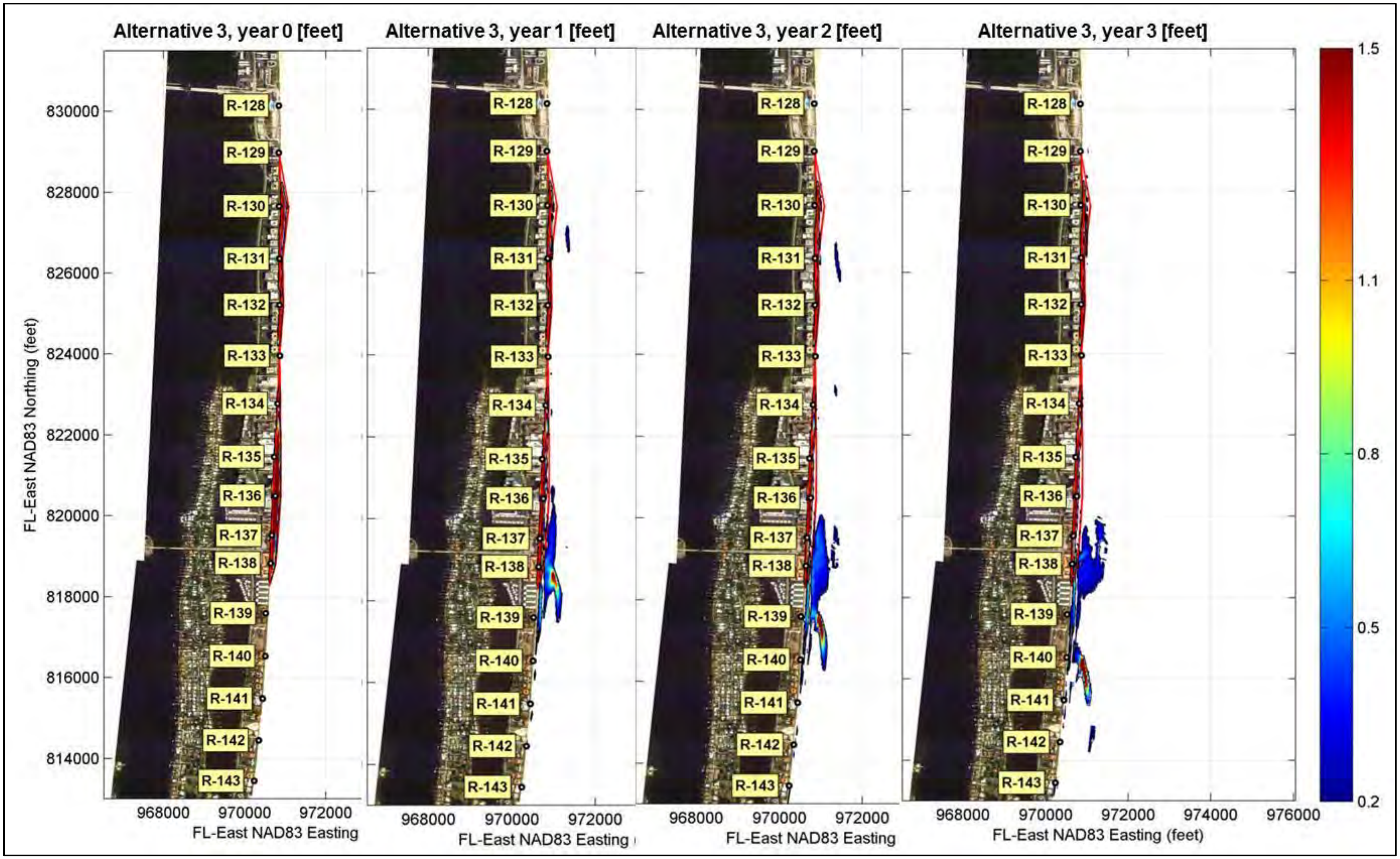

Figure 5-20. Sediment Accumulation greater than 0.2 ft for Alternative 3.

5.4.2. Separated Actions

Alternative 3C (County portion of alternative)

Alternative 3C presents the same fill configuration as Alternative 2C, but without structures. Model results given Alternative 3C are shown in Figure 5-21 through Figure 5-24. The model shows similar patterns of sedimentation as Alternative 3, which included the Town of Palm Beach's portion of the project.

At the end of the 3 year simulation period, there was an estimated coverage of 7.15 acres of hardbottom and an exposure of 0.90 acres attributed to the alternative as depicted in Figure 5-23. The net change in hardbottom at the end of the simulation period (exposure minus coverage) as a result of the project is estimated to be -6.25 acres.

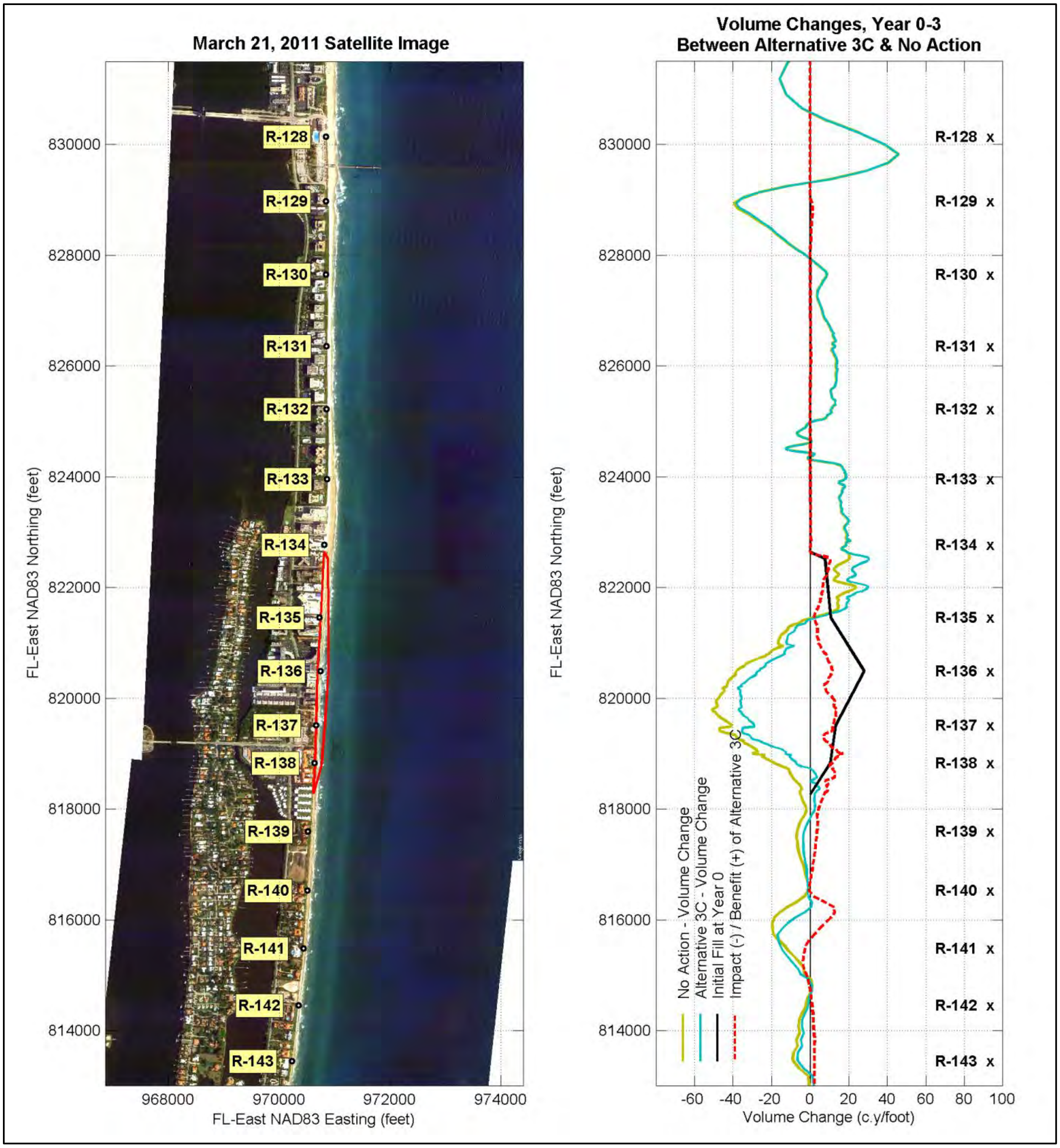

Figure 5-21. Volume Changes to Alternative 3C.

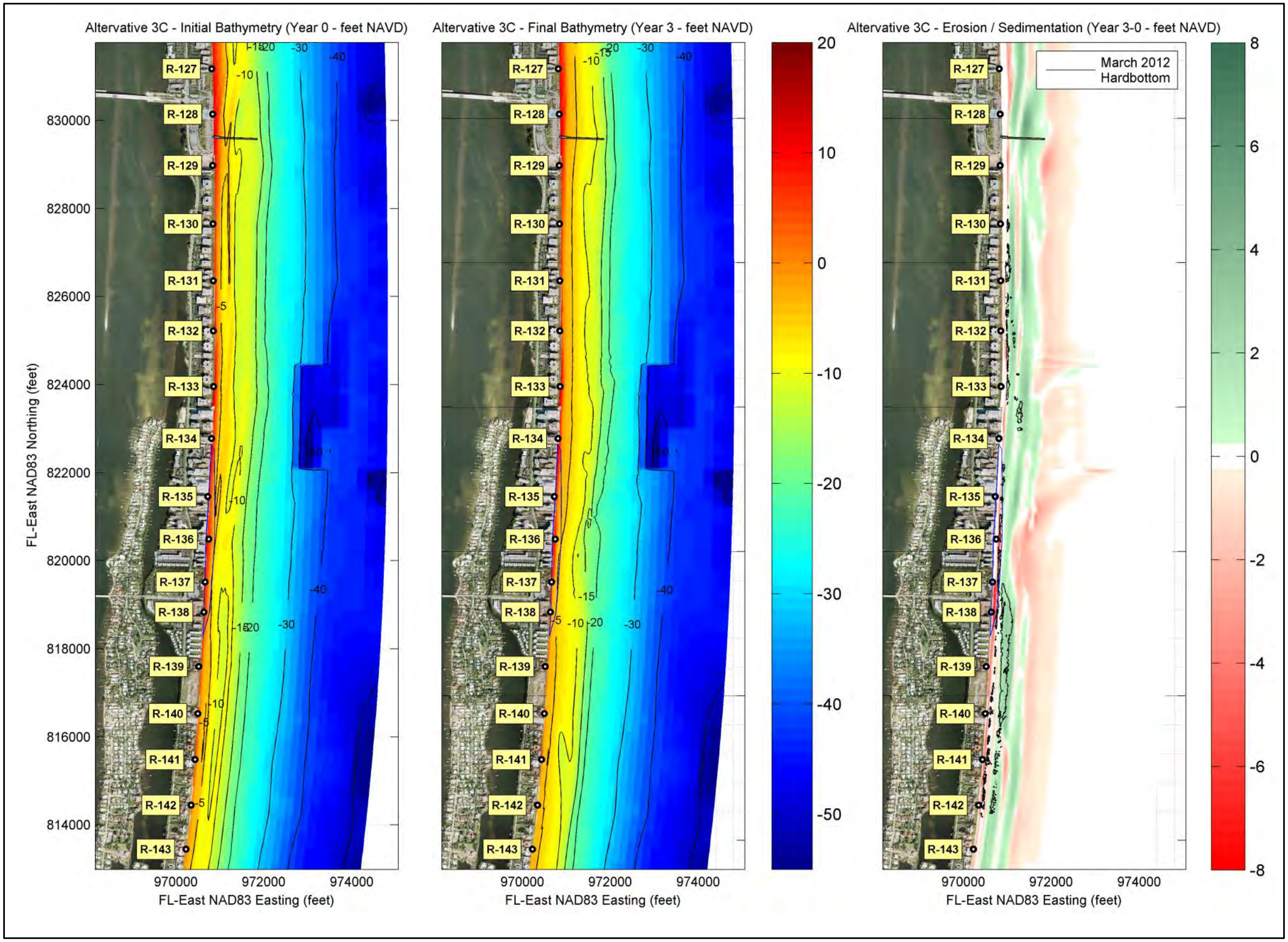

Figure 5-22. Erosion/Sedimentation after 3 years of simulation, Alternative 3C.

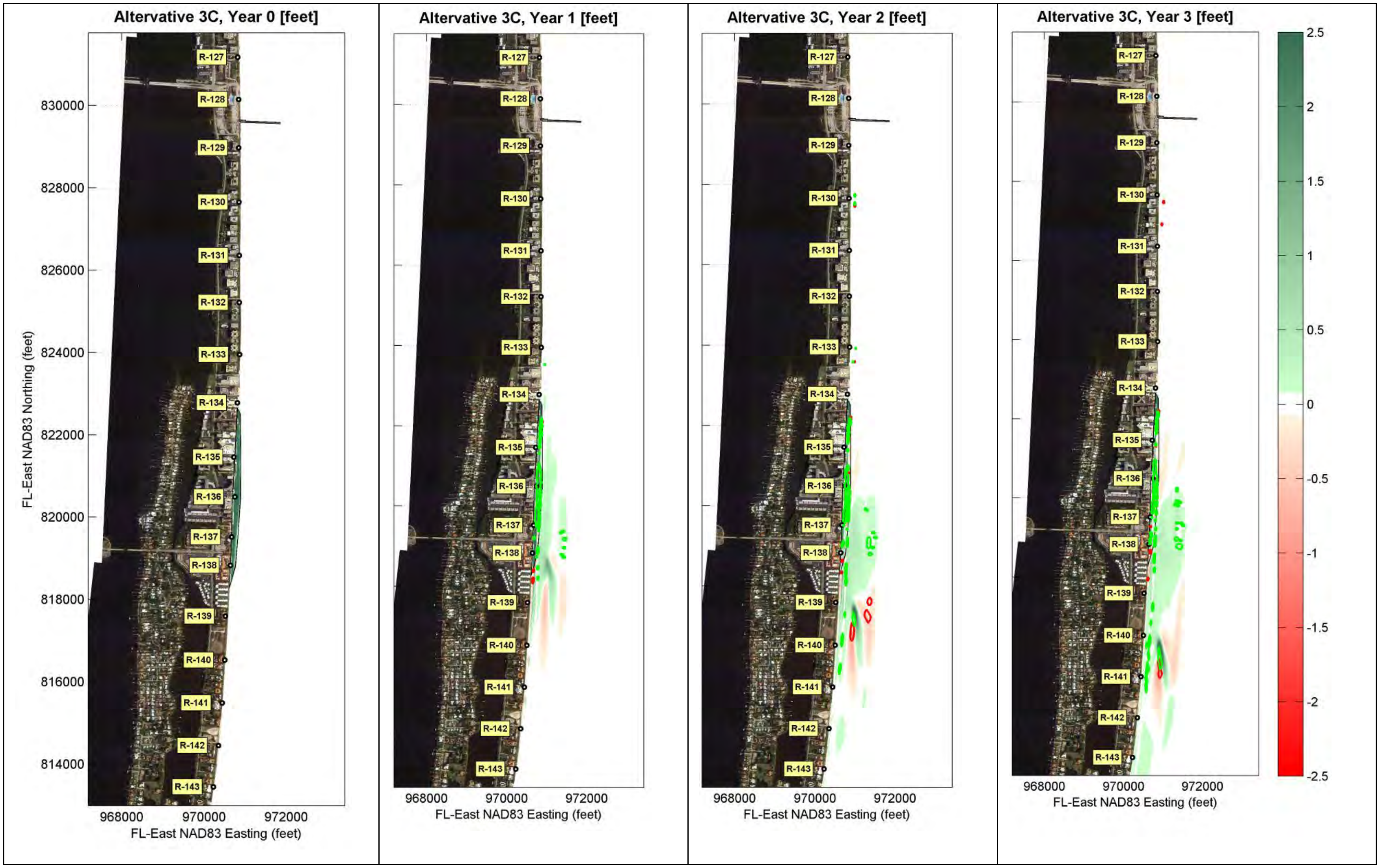

Figure 5-23. Temporal evolution of beach nourishment for Alternative 3C, compared to No Action scenario.

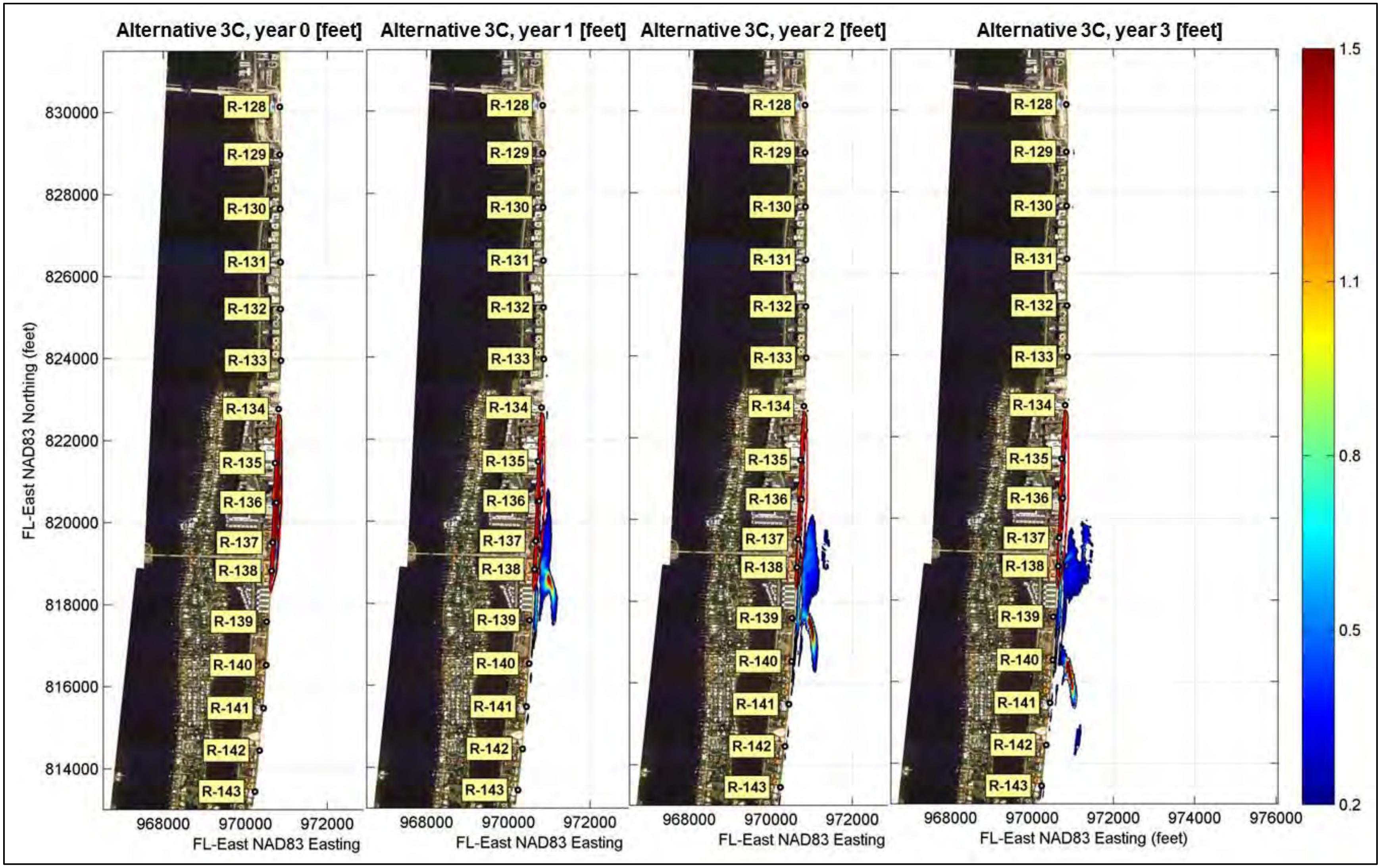

Figure 5-24. Sediment Accumulation greater than 0.2 ft for Alternative 3C.

5.5. Alternative 4 - The Town of Palm Beach Preferred Project and County Increased Sand Volume Project without Shoreline Protection Structures

Alternative 4 includes the placement of 225,900 cubic yards of sand between R-129-210 and R-138+551. Model results for Alternative 4 are shown in Figure 5-26 through Figure 5-28. The sedimentation patterns north of R-134 are similar to Alternative 3, which is expected given that the fill volumes north of R-134 were maintained for Alternative 4. South of R-134 larger fill volumes were included as compared to Alternative 3. The larger fill volumes resulted in increased coverage of sedimentation areas within the County's project area as compared to Alternative 3.

At the end of the 3 year simulation period, there was an estimated coverage of 12.15 acres of hardbottom and an exposure of 0.67 acres attributed to the alternative as depicted in Figure 5-27. The net change in hardbottom at the end of the simulation period (exposure minus coverage) as a result of the project is estimated to be -11.48 acres.

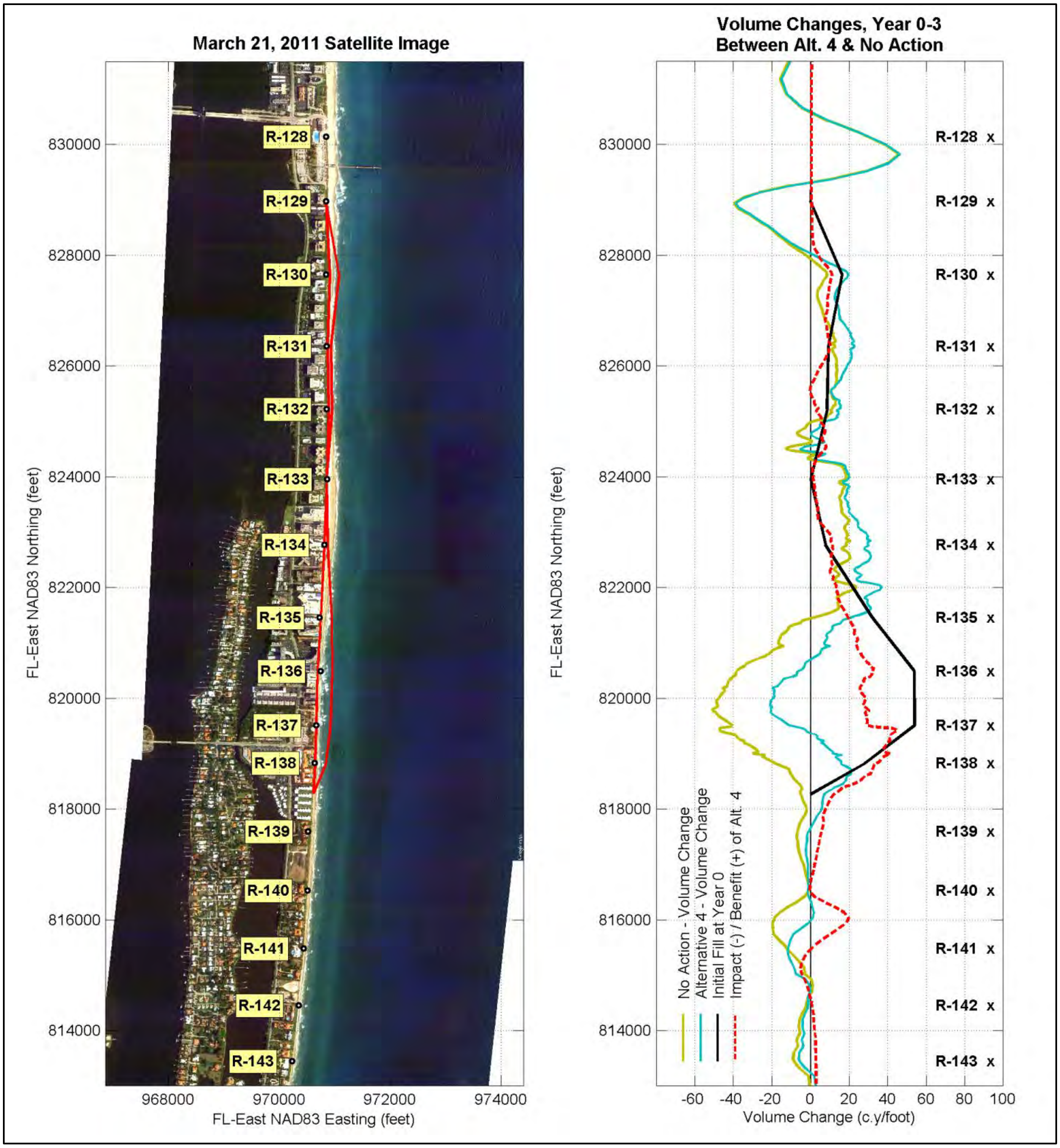

Figure 5-25. Volume Changes to Alternative 4.

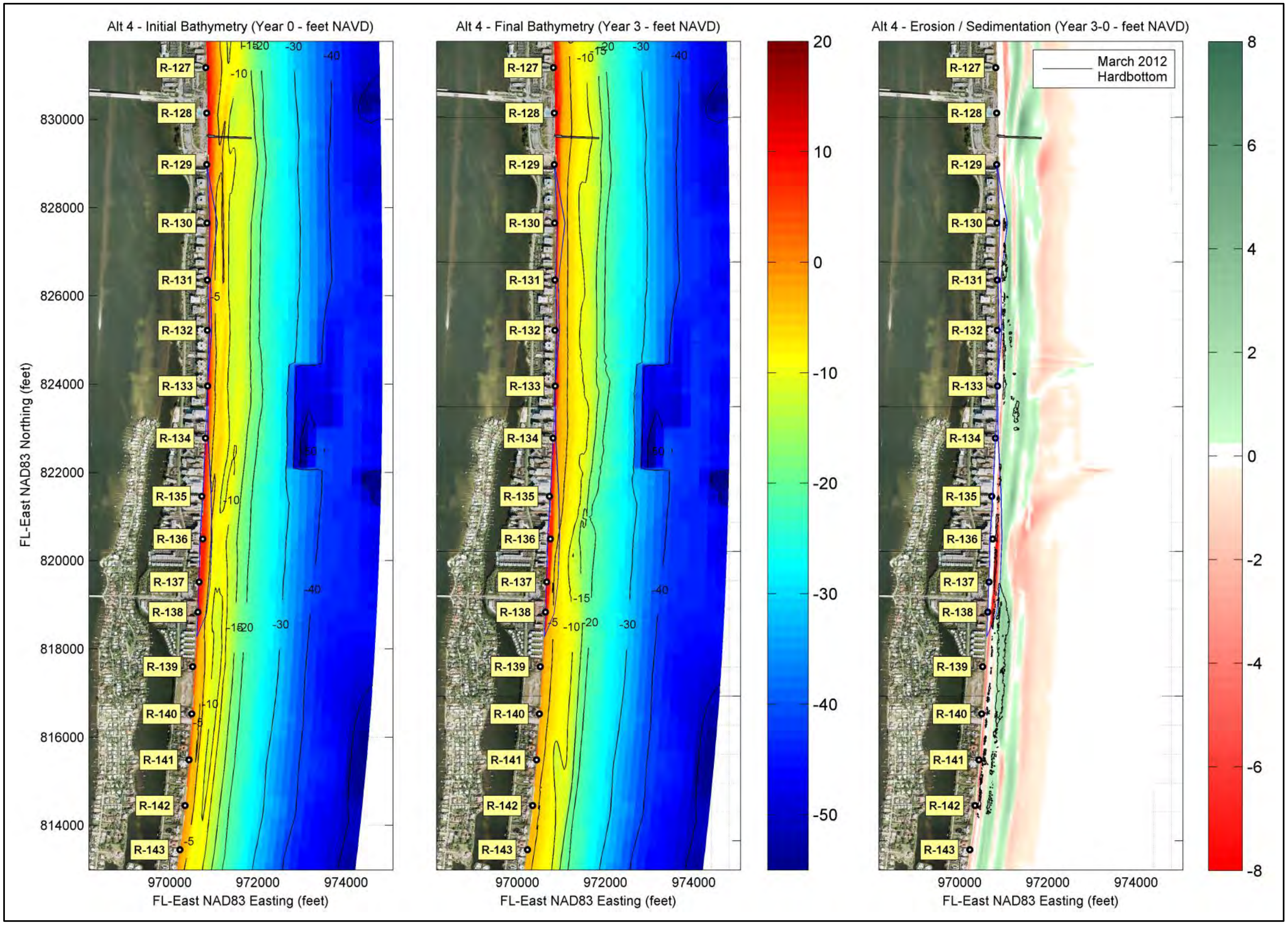

Figure 5-26. Erosion/Sedimentation after 3 years of simulation, Alternative 4.

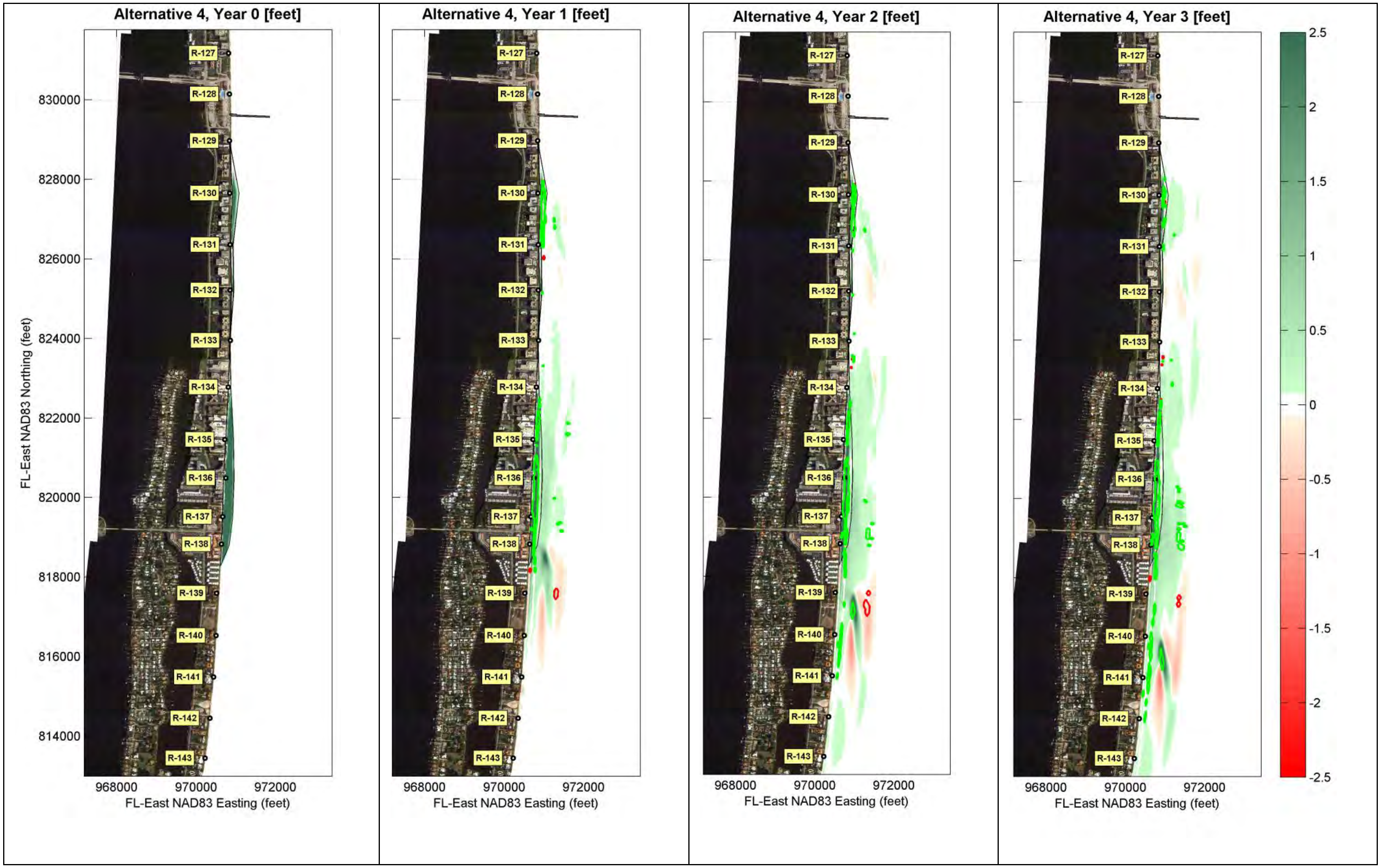

Figure 5-27. Temporal evolution of erosion (red) / sedimentation (green) for Alternative 4.

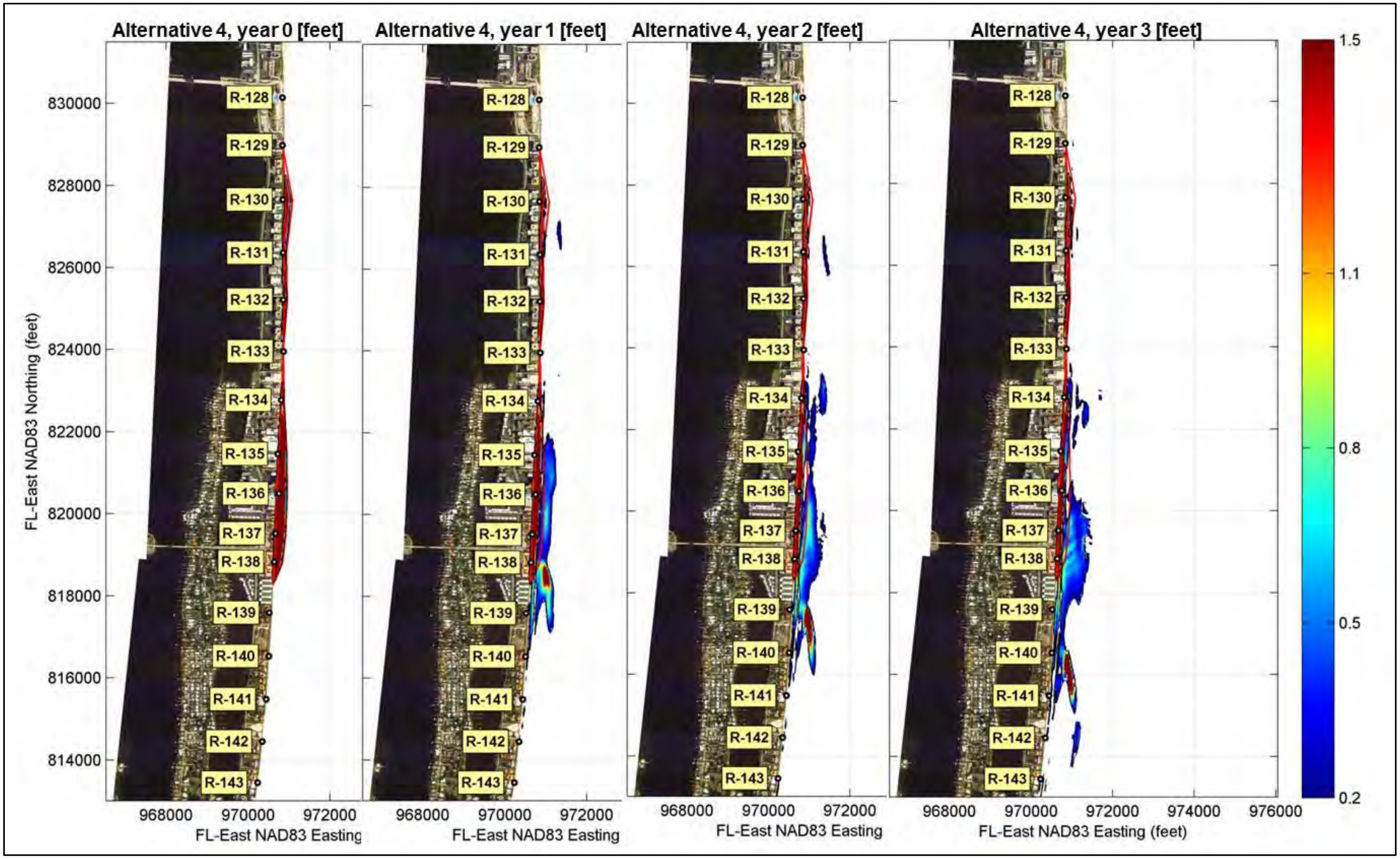

Figure 5-28. Sediment Accumulation greater than 0.2 ft for Alternative 4.

5.6. Alternative 5 - The Town of Palm Beach Increased Sand Volume Project and County Preferred Project

Alternative 5 places seven groins between R-135+160 and R-137+422 and 164,500 cubic yards of fill material between R-129-210 and R-138+551. Model results given in Alternative 5 appear in Figure 5-29 through Figure 5-32. The fill volume north of R-134+135 is increased as compared to Alternative 3, while the fill volume to the south is the same as Alternative 2. The sedimentation areas in the Town of Palm Beach's portion of the project increased as compared to Alternative 3.

At the end of the 3 year simulation period, there was an estimated coverage of 10.09 acres of hardbottom and an exposure of 3.44 acres attributed to the alternative as depicted in Figure 5-31. The net change in hardbottom at the end of the simulation period (exposure minus coverage) as a result of the project is estimated to be -6.64 acres.

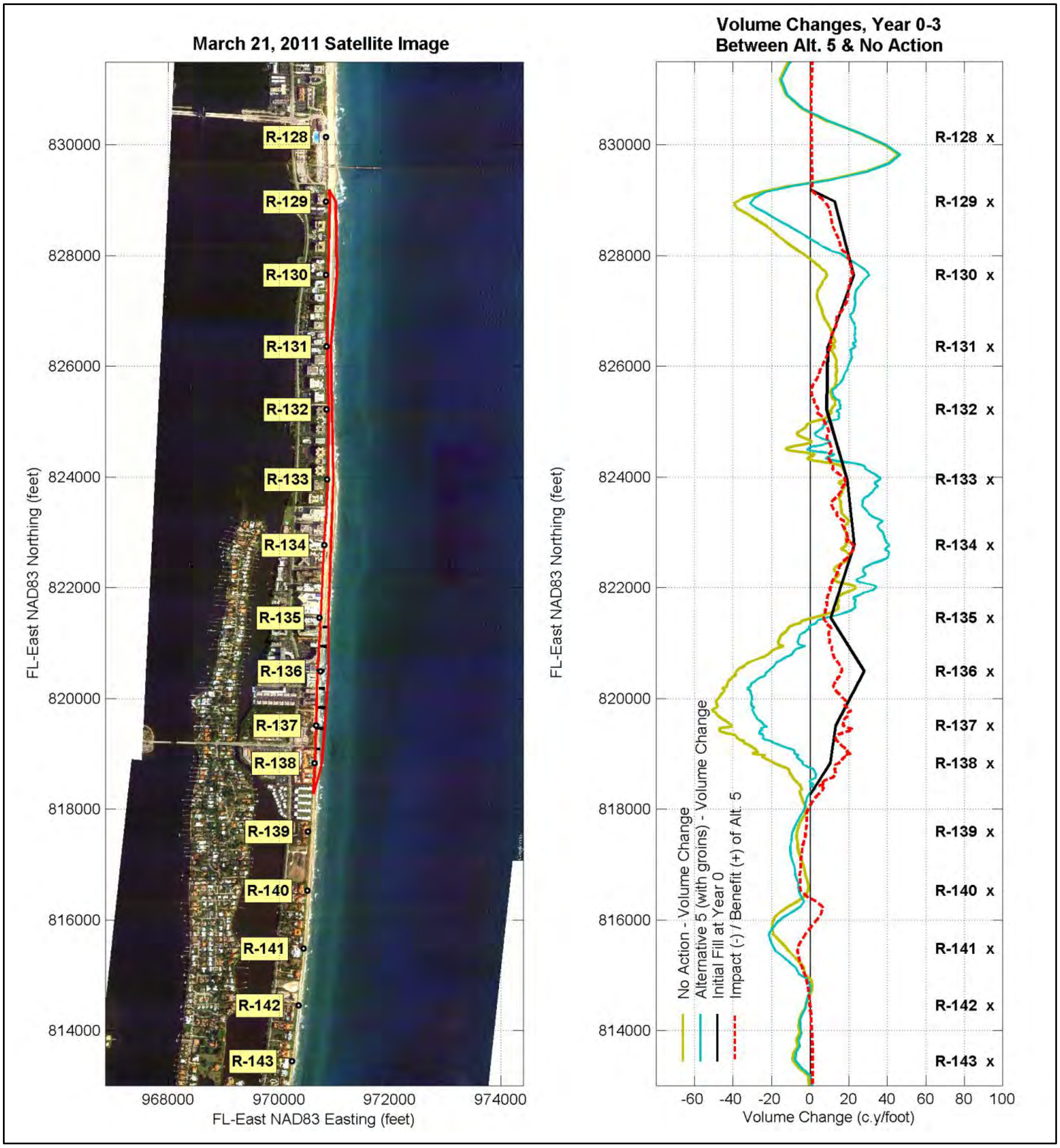

Figure 5-29. Volume Changes, Alternative 5.

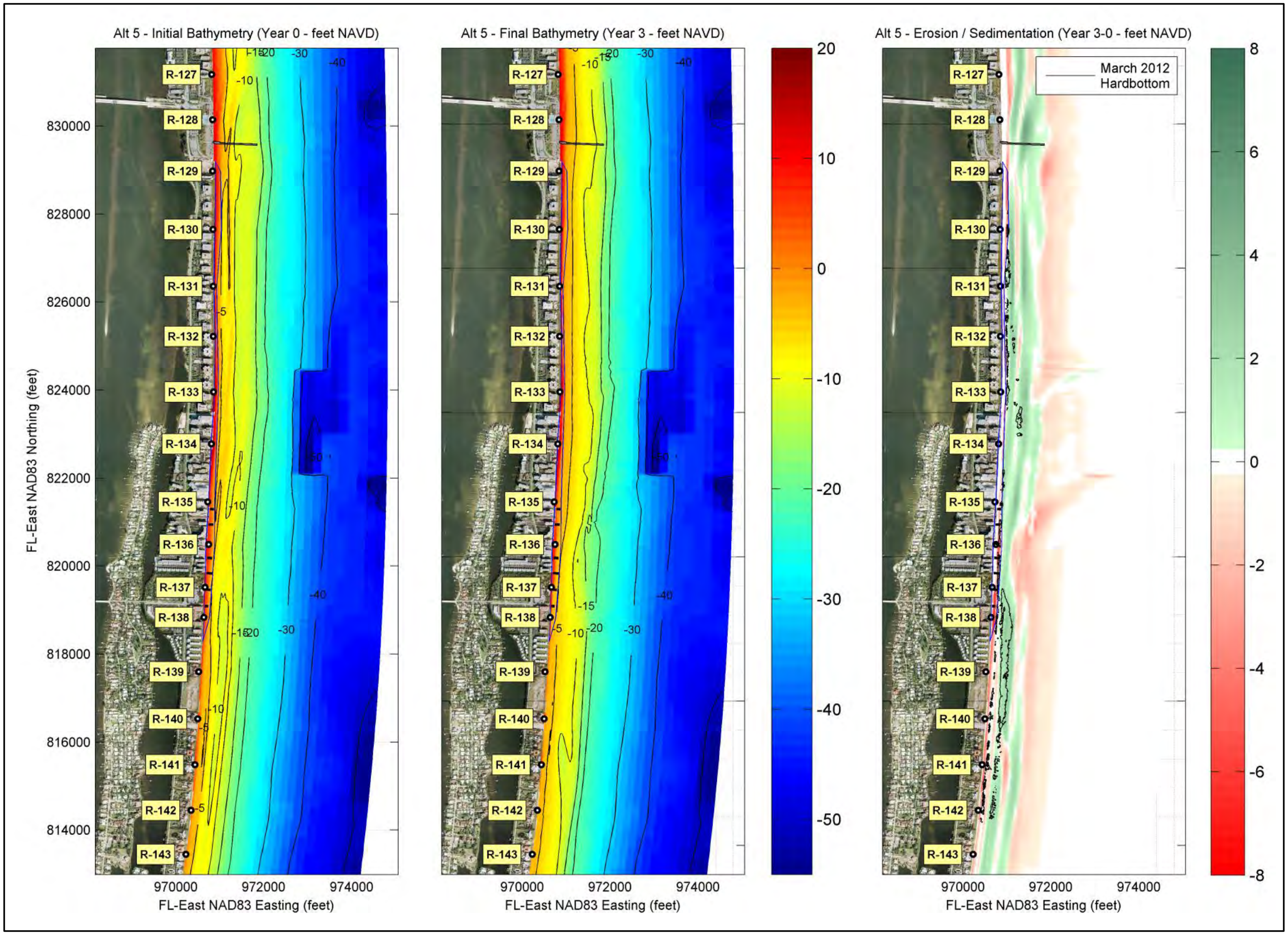

Figure 5-30. Erosion/Sedimentation after 3 years of simulation, Alternative 5.

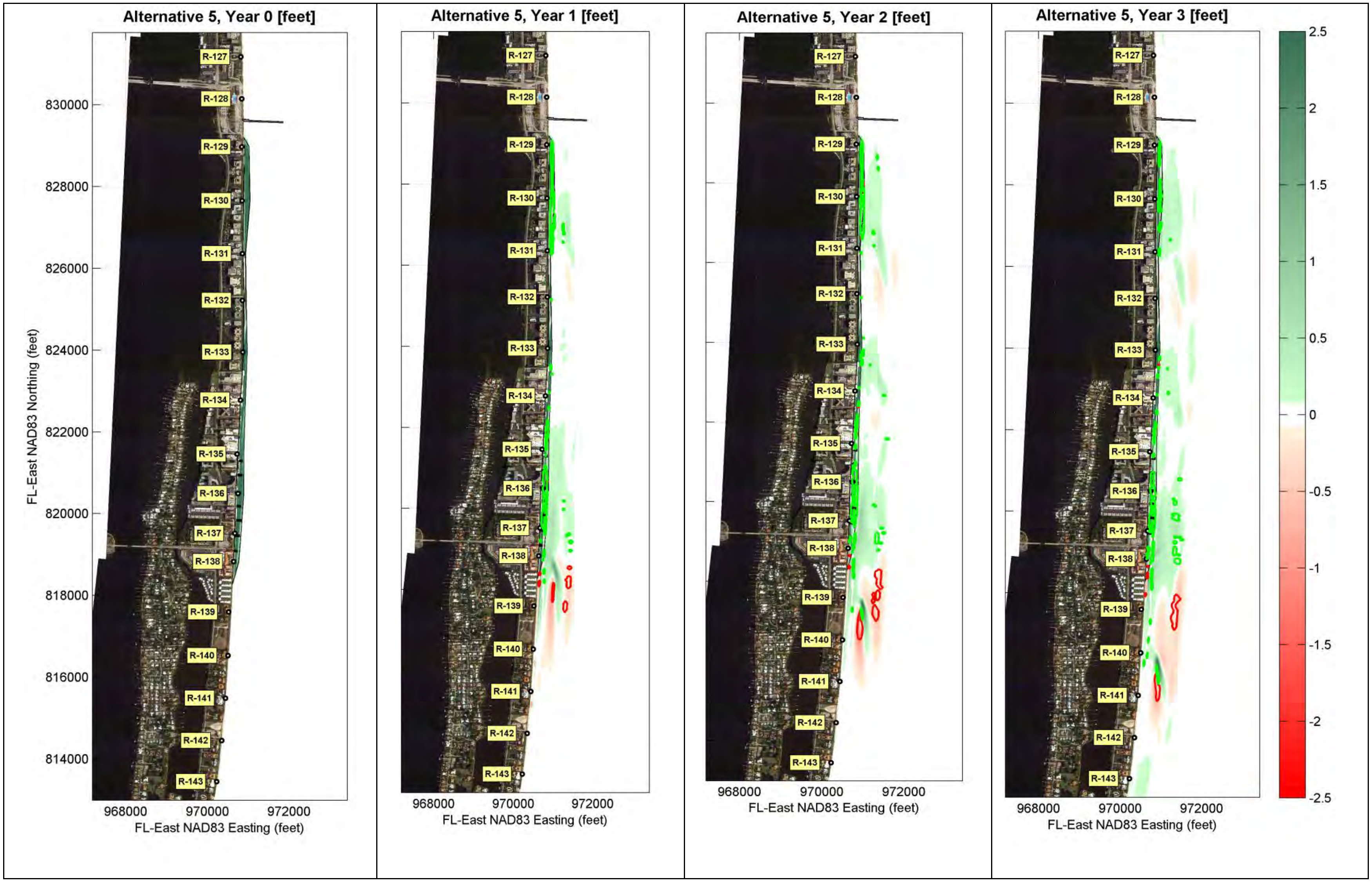

Figure 5-31. Temporal evolution of erosion (red) / sedimentation (green) for Alternative 5.

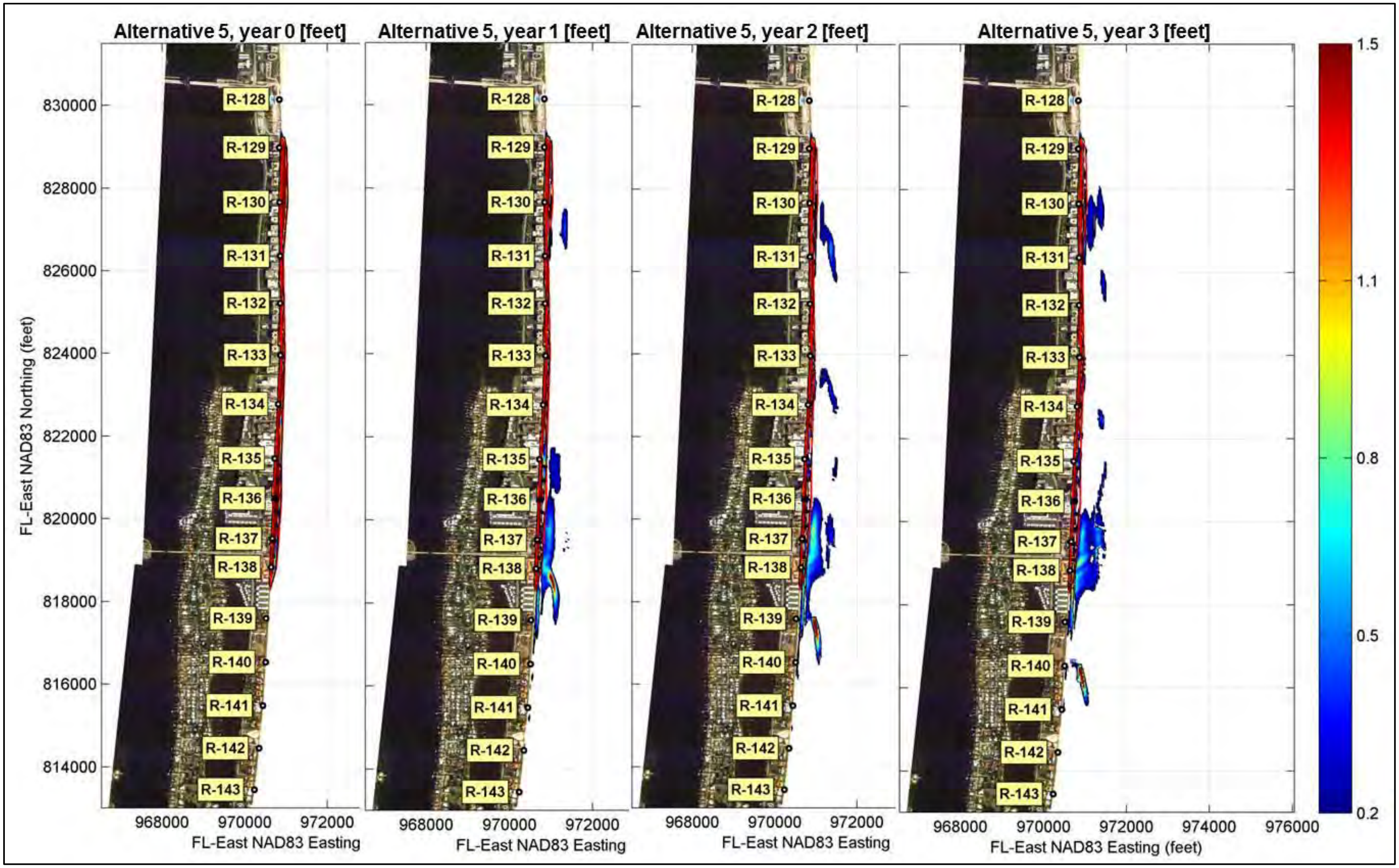

Figure 5-32. Sediment Accumulation greater than 0.2 ft for Alternative 5.

5.7. Alternative 6 - The Town of Palm Beach Increased Sand Volume Project and County Increased Sand Volume without Shoreline Protection Structures Project

5.7.1. Combined Action

Alternative 6 includes the increased sand volume north of R-134+135 modeled for Alternative 5 and the increased volume south of R-134+135 modeled for Alternative 4. Model results given in Alternative 6 appear in Figure 5-33 through Figure 5-36. Alternative 6 shows the greatest coverage of sedimentation areas greater than 0.2 feet as compared to Alternatives 2 through 5.

At the end of the 3 year simulation period, there was an estimated coverage of 13.43 acres of hardbottom and an exposure of 0.44 acres attributed to the alternative as depicted in Figure 5-35. The net change in hardbottom at the end of the simulation period (exposure minus coverage) as a result of the project is estimated to be -12.99 acres.

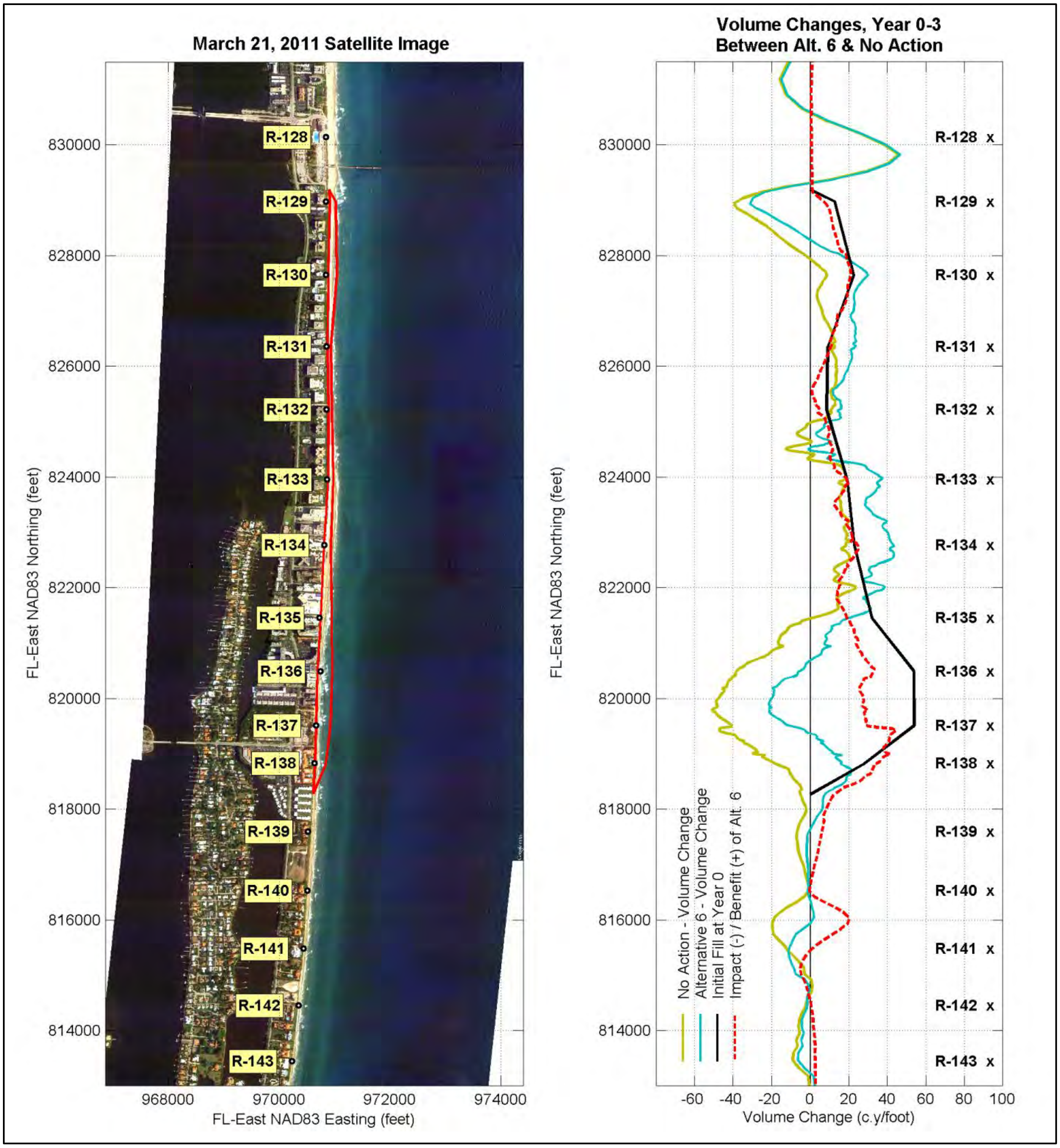

Figure 5-33. Volume Changes, Alternative 6.

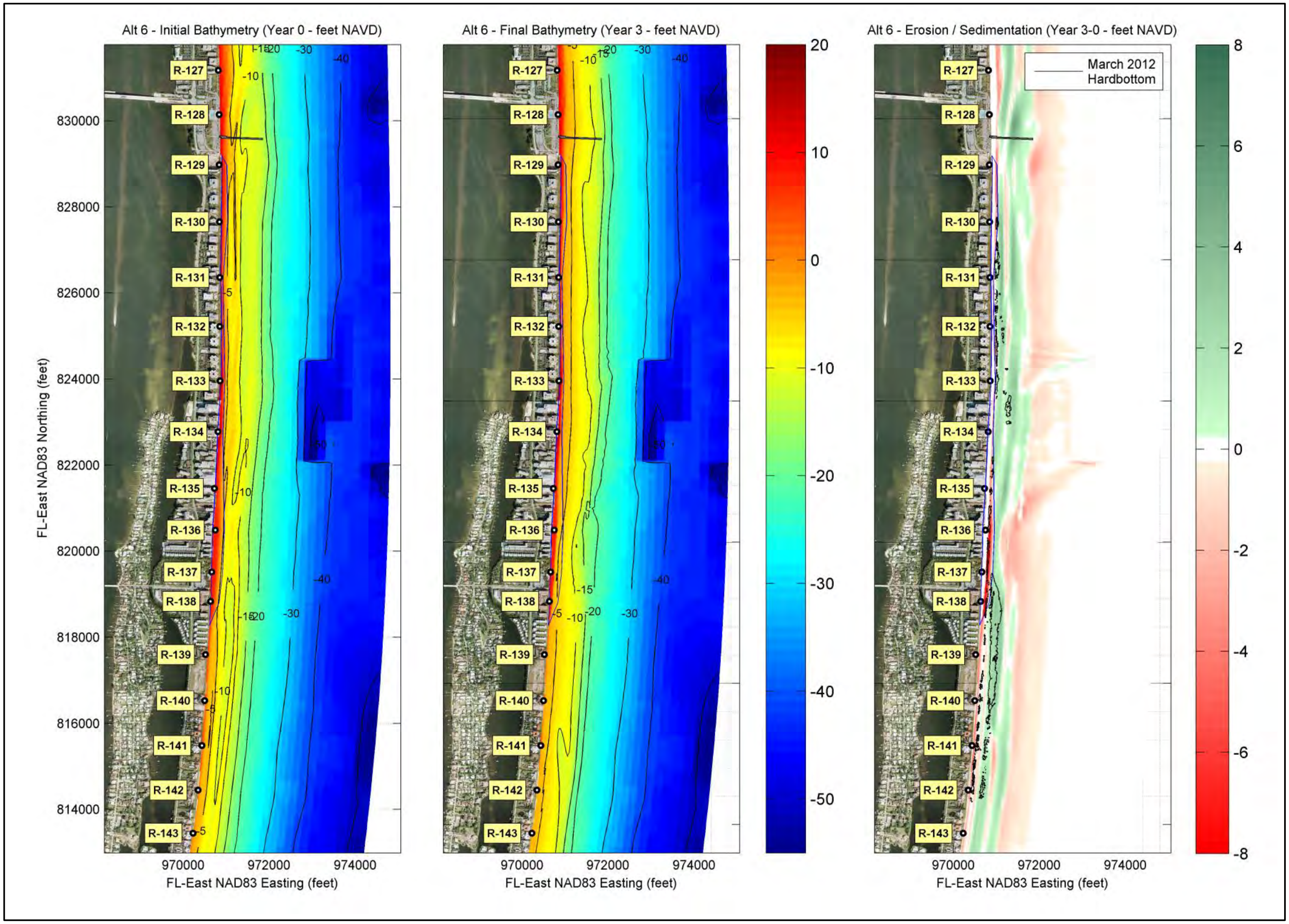

Figure 5-34. Erosion/Sedimentation after 3 years of simulation, Alternative 6.

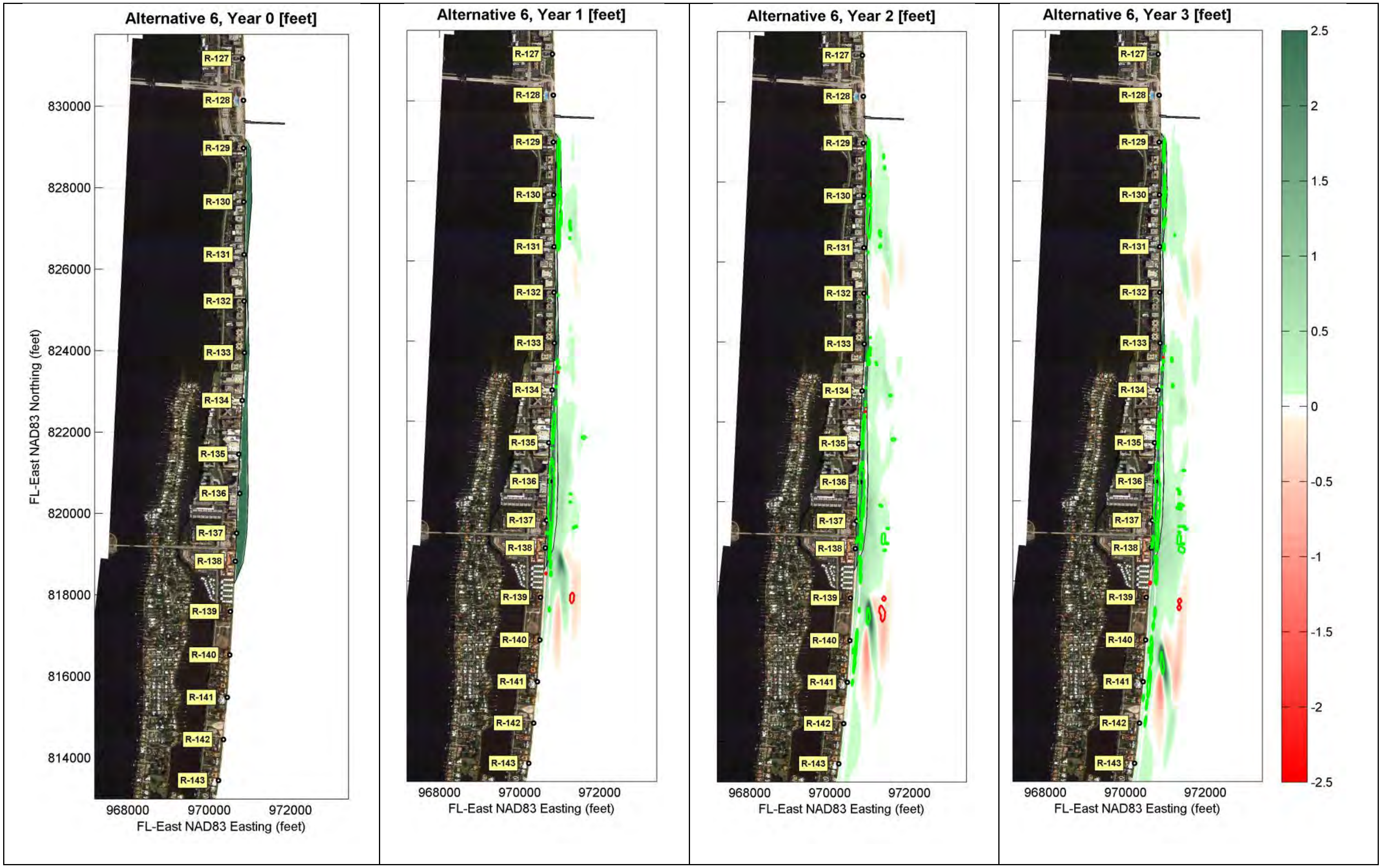

Figure 5-35. Temporal evolution of erosion (red) / sedimentation (green) for Alternative 6, compared to No Action scenario.

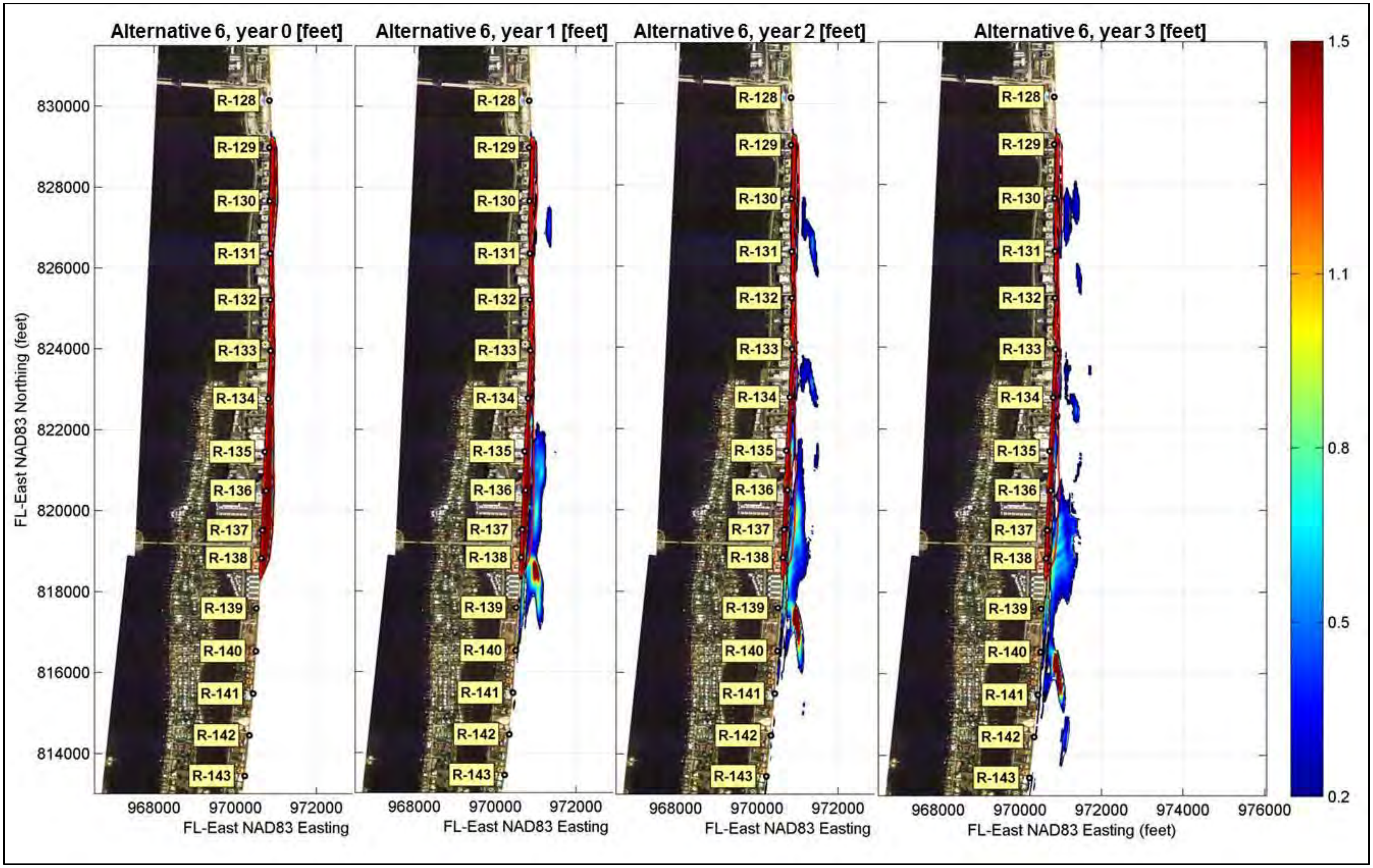

Figure 5-36. Sediment Accumulation greater than 0.2 ft for Alternative 6.

5.7.2. Separated Actions

Alternative 6T (Town of Palm Beach portion of alternative)

Alternative 6T presents a sand placement of 101,000 cubic yards along R-129 and R-134+135. Model results for Alternative 6T are shown in Figure 5-37 through Figure 5-40. The results show that the sedimentation areas greater than 0.2 feet within the Town of Palm Beach are less as compared to Alternative 6. This suggests that the fill placed to the south within the County for Alternative 6 may spread into the Town of Palm Beach limits.

At the end of the 3 year simulation period, there was an estimated coverage of 2.29 acres of hardbottom and an exposure of 0.08 acres attributed to the alternative as depicted in Figure 5-39. The net change in hardbottom at the end of the simulation period (exposure minus coverage) as a result of the project is estimated to be -2.21 acres.

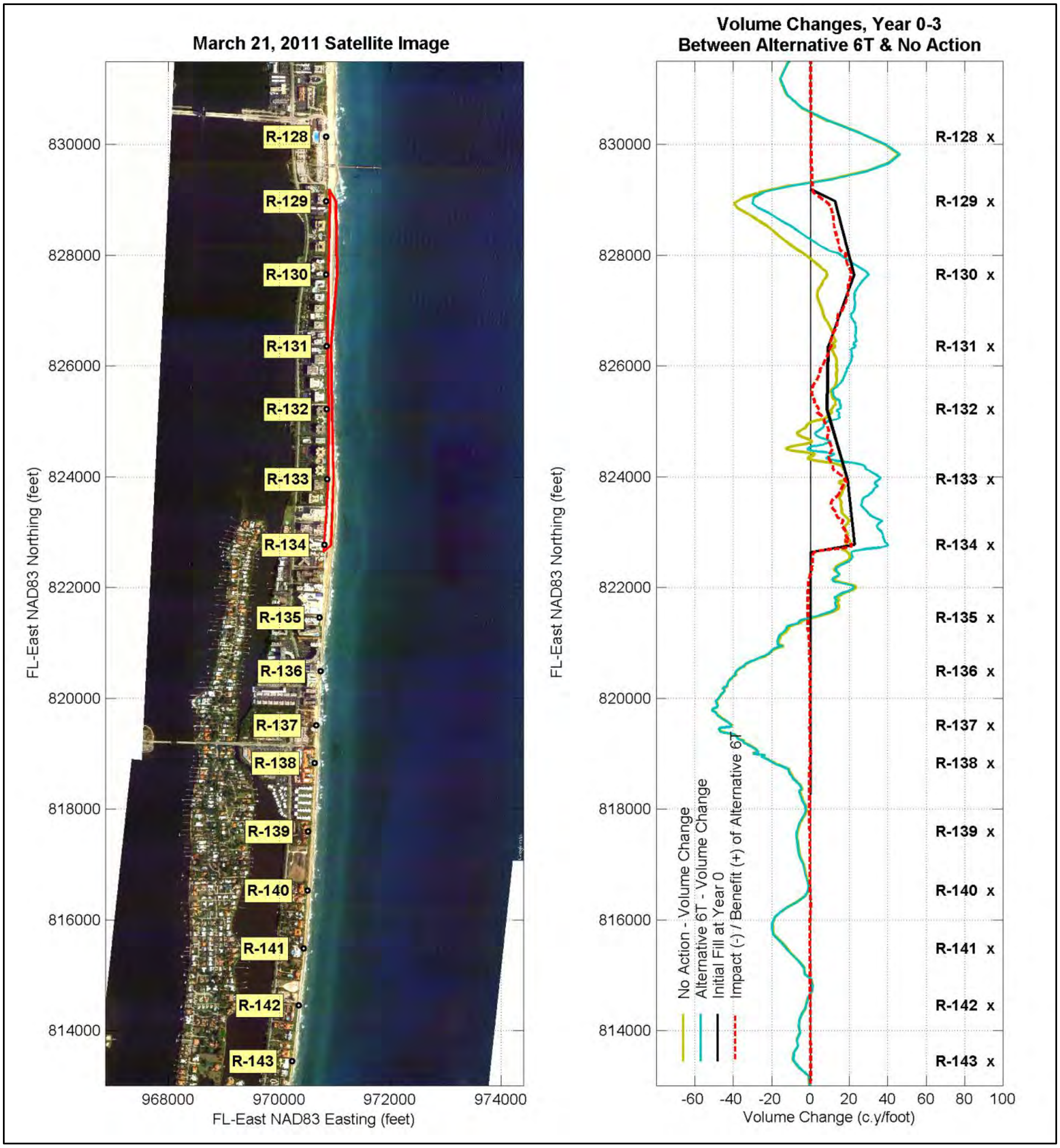

Figure 5-37. Volume Changes, Alternative 6T.

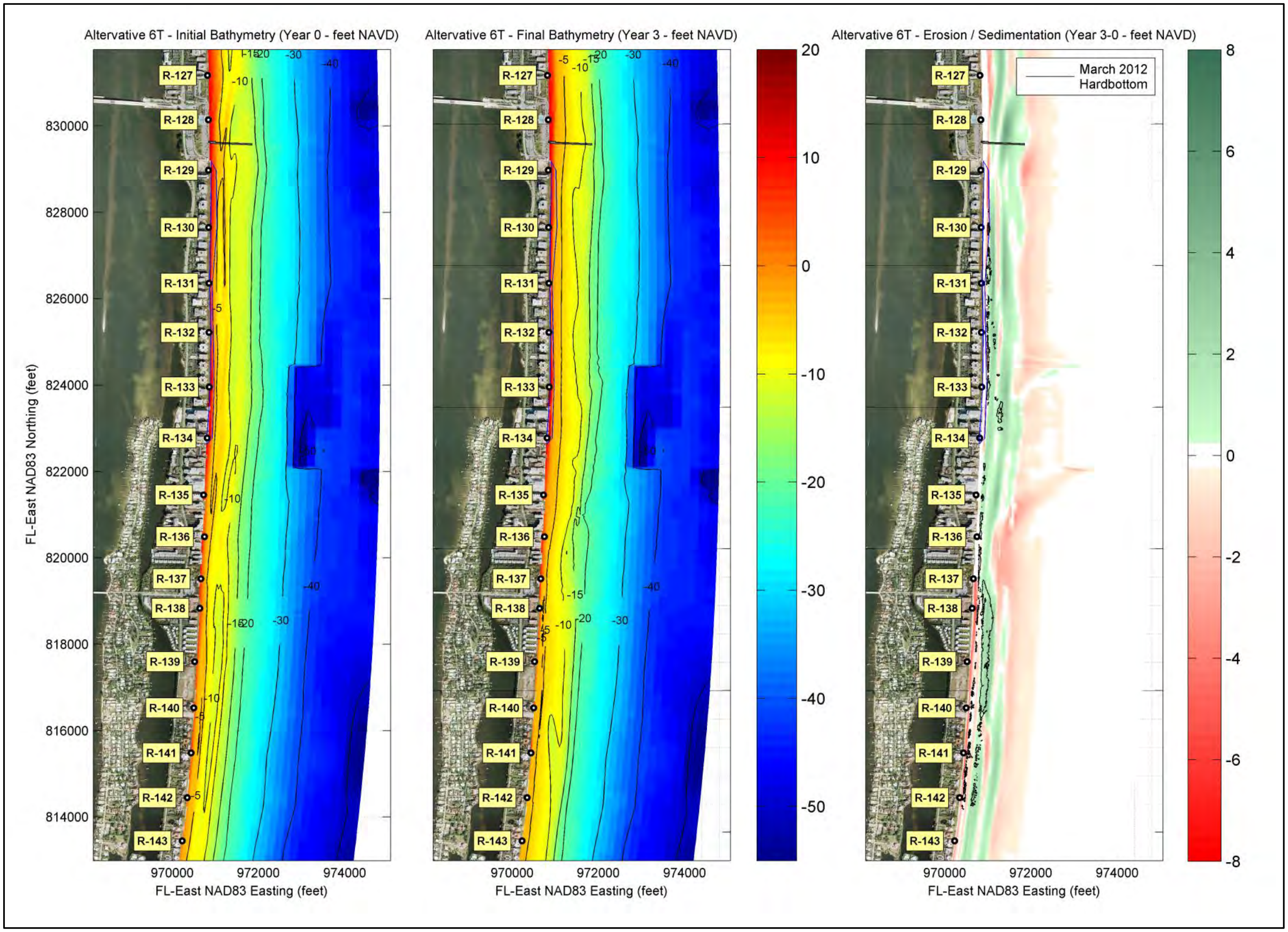

Figure 5-38. Erosion/Sedimentation after 3 years of simulation, Alternative 6T.

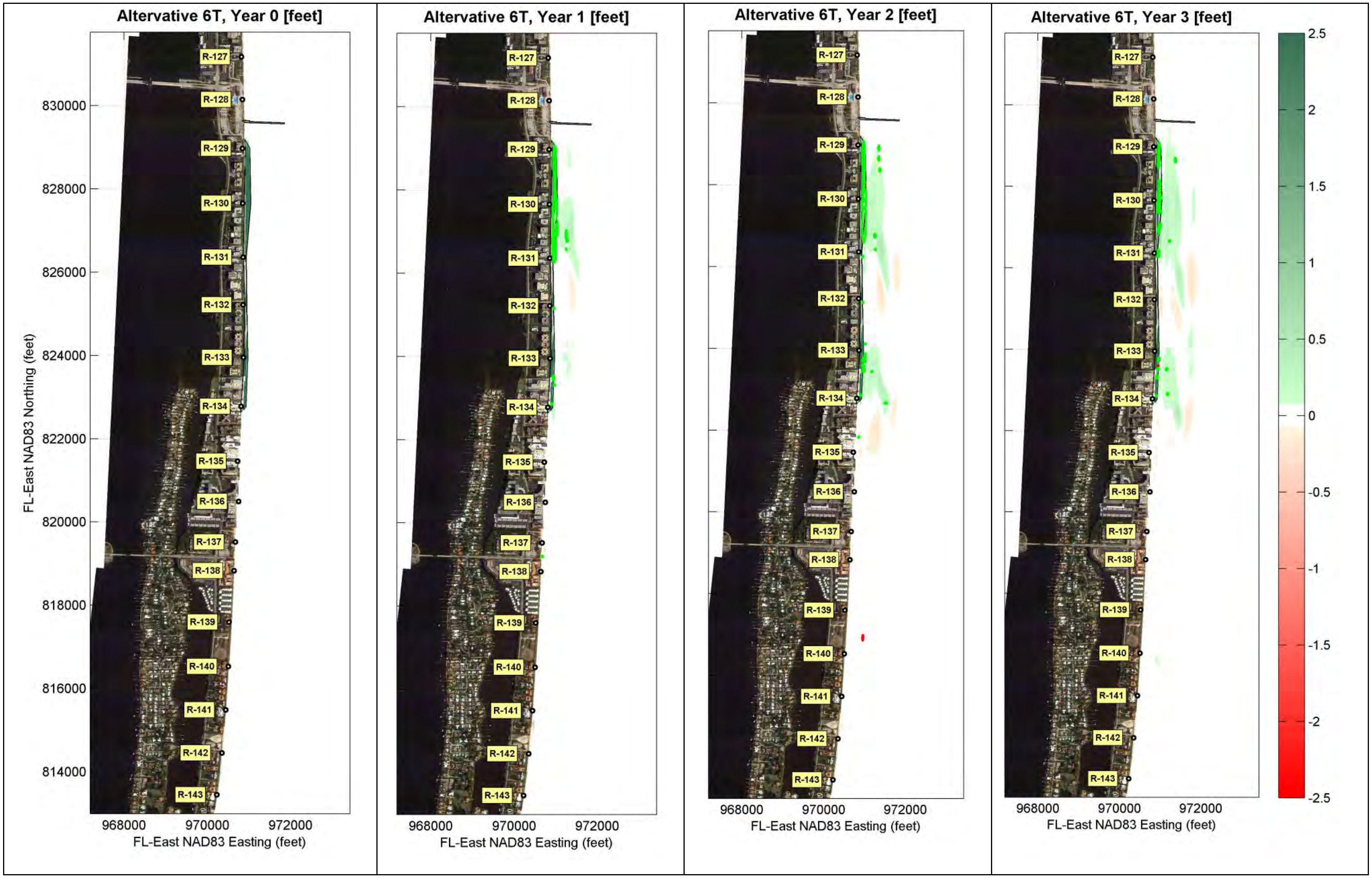

Figure 5-39. Temporal evolution of erosion (red) / sedimentation (green) for Alternative 6T, compared to No Action scenario.

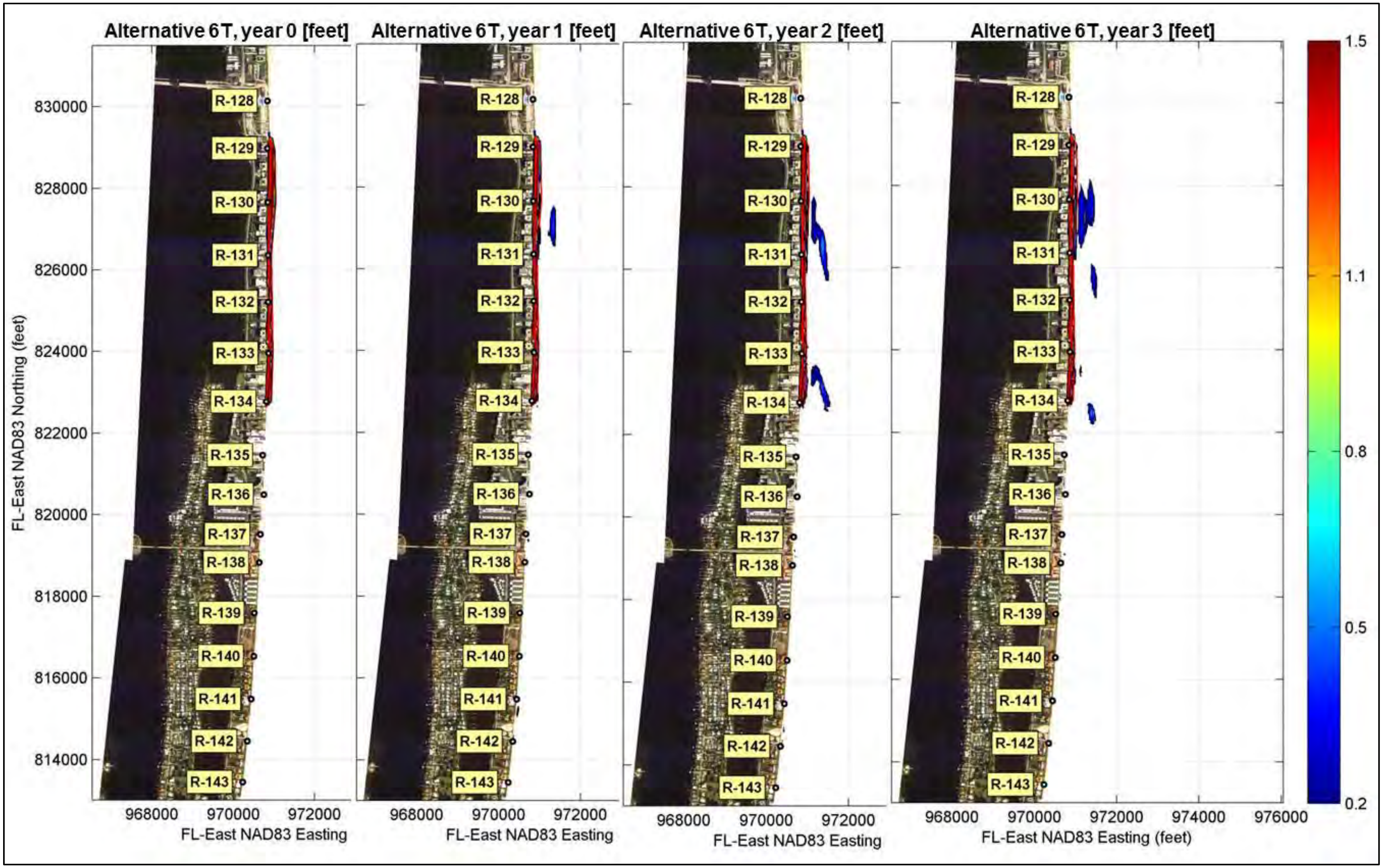

Figure 5-40. Sediment Accumulation greater than 0.2 ft for Alternative 6T.

Alternative 6C (County portion of alternative)

Alternative 6C presents a sand placement of 172,000 cubic yards along R-134+135 and R-138+551. Model results for Alternative 6C are shown in Figure 5-41 through Figure 5-44. The sedimentation areas greater than 0.2 feet indicate that a majority of the areas are located offshore and downdrift of the County's project area, but some spreading to the north into the Town of Palm Beach is shown.

At the end of the 3 year simulation period, there was an estimated coverage of 11.26 acres of hardbottom and an exposure of 0.48 acres attributed to the alternative as depicted in Figure 5-43. The net change in hardbottom at the end of the simulation period (exposure minus coverage) as a result of the project is estimated to be -10.77 acres.

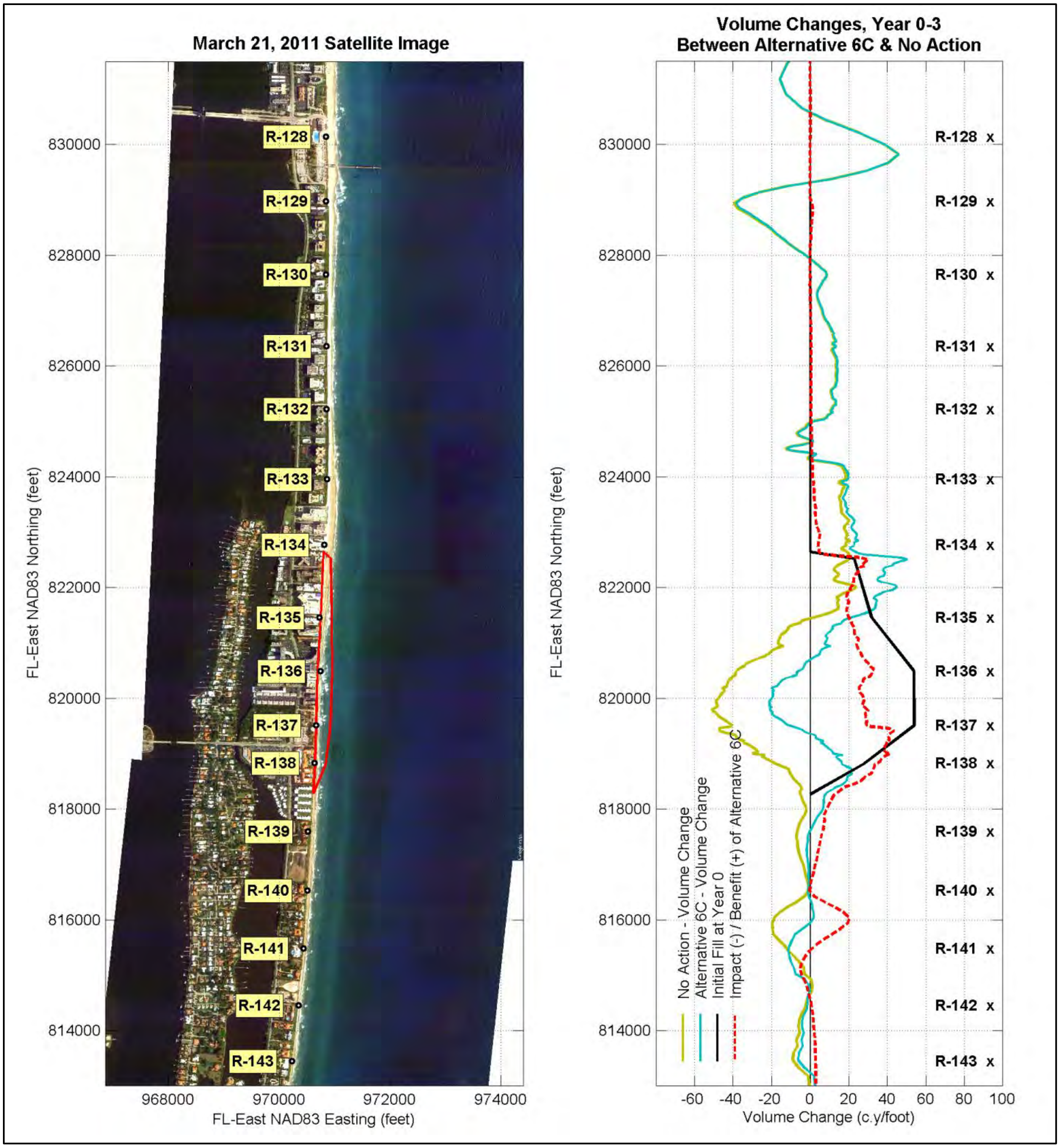

Figure 5-41. Volume Changes, Alternative 6C.

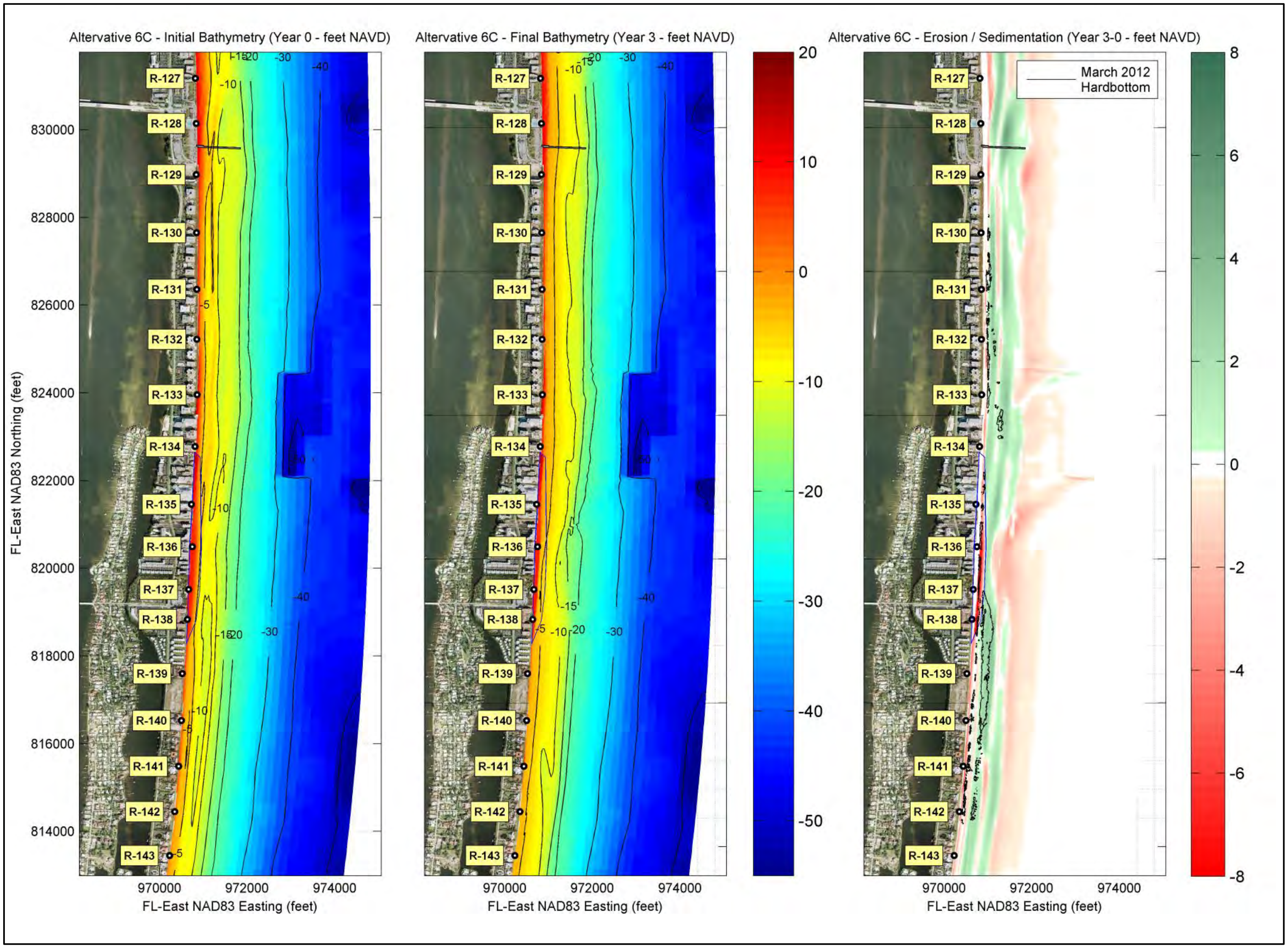

Figure 5-42. Erosion/Sedimentation after 3 years of simulation, Alternative 6C.

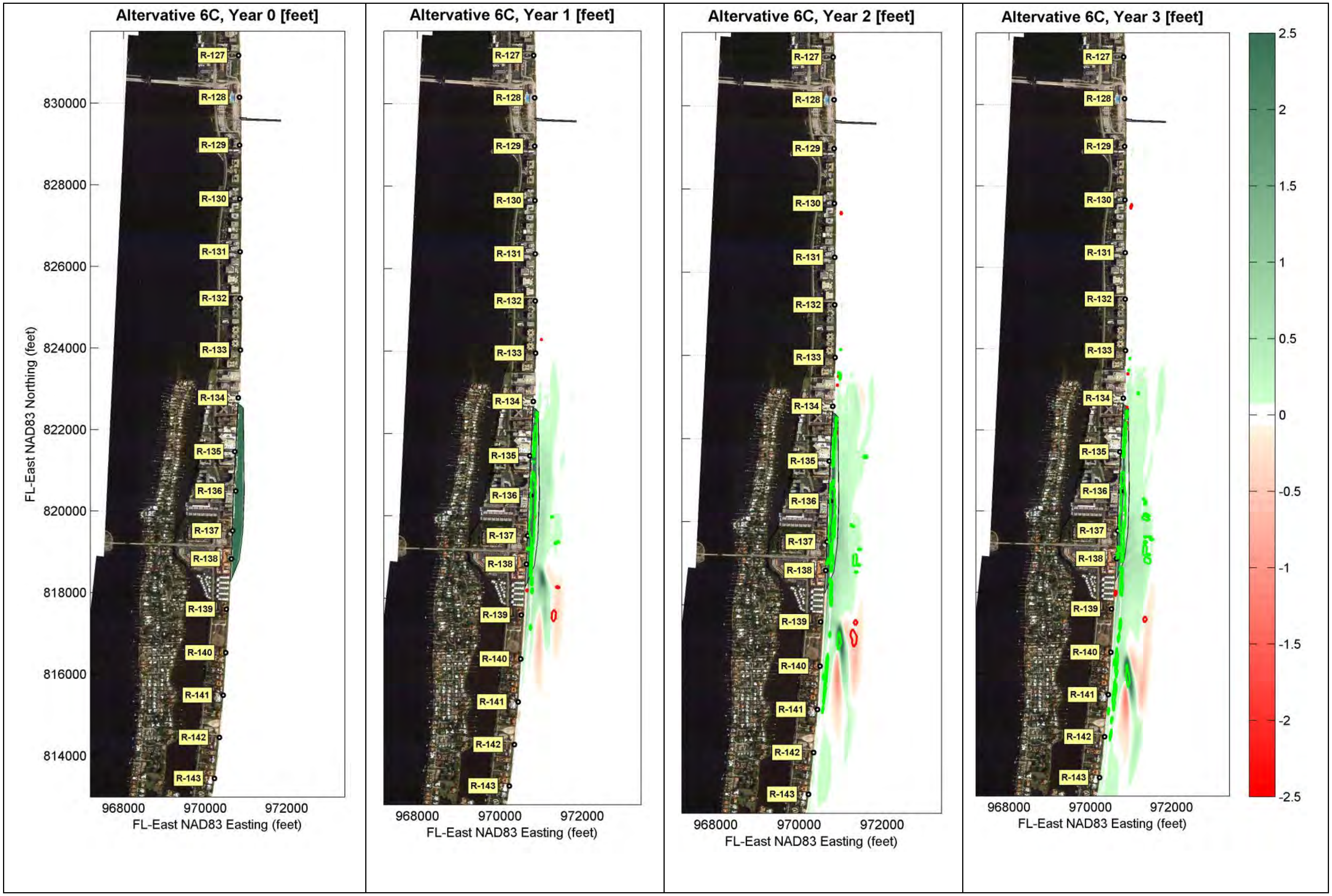

Figure 5-43. Temporal evolution of erosion (red) / sedimentation (green) for Alternative 6C, compared to No Action scenario.

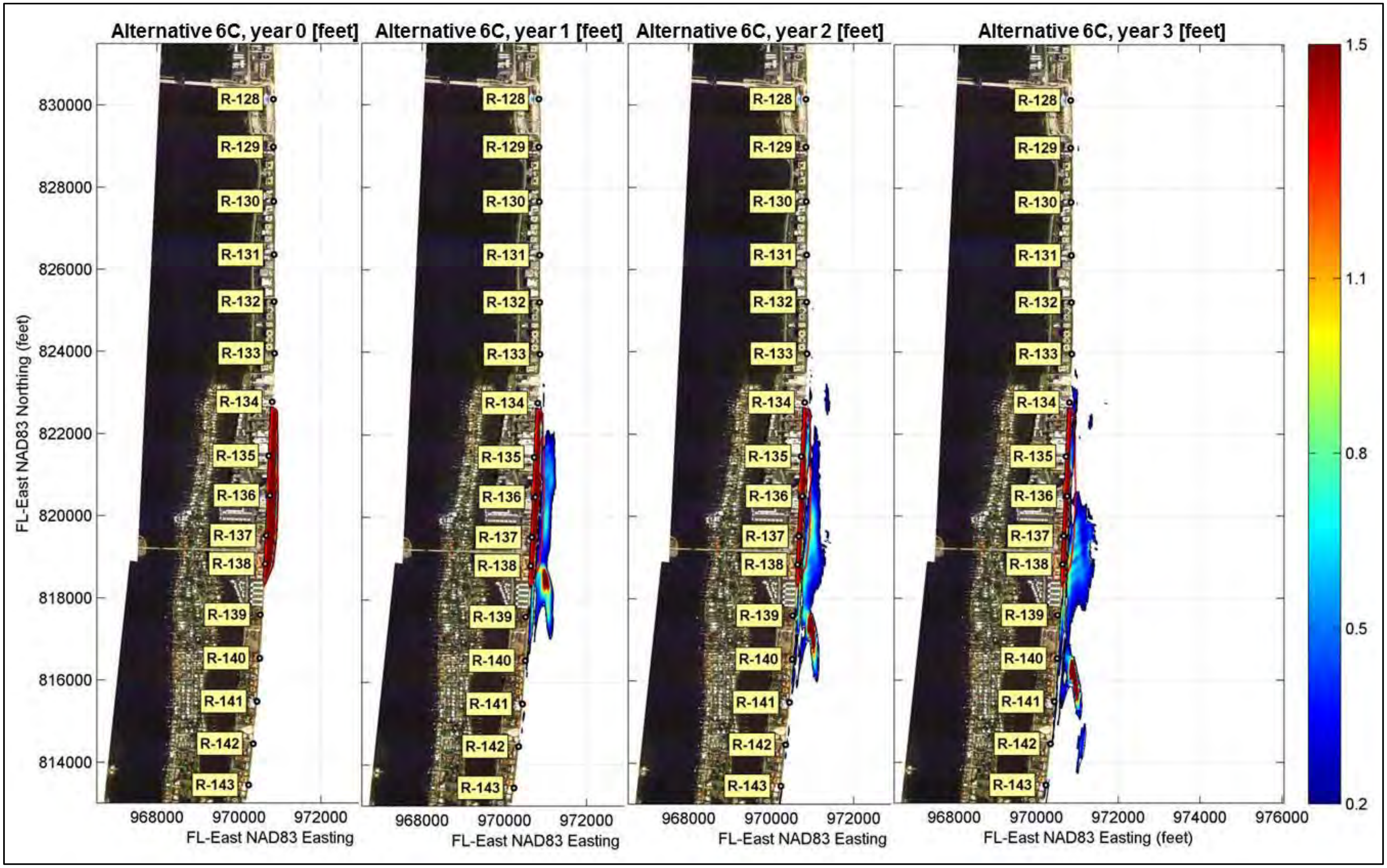

Figure 5-44. Sediment Accumulation greater than 0.2 ft for Alternative 6C.

5.8. Alternative 7

5.8.1. Combined Action

Alternative 7 places seven groins between monuments R-135+160 and R-137+422, and two T-heads located between R-132+556 and R-133+269. In addition, the alternative includes the placement of approximately 401,600 cubic yards of sand between R-129-210 and R-138+551 monuments. Model results given in Alternative 7 appear in Figure 5-45 through Figure 5-48.

North of R-134+135, Alternative 7 contains the largest fill volume as compared to Alternatives 2 through 6. South of R-134+135, the fill volume is the same as Alternative 2. The increased fill volume results in sedimentation greater than 0.2 feet throughout the Town of Palm Beach and County. The sedimentation areas extend the furthest north as compared to the other alternatives.

At the end of the 3 year simulation period, there was an estimated coverage of 13.91 acres of hardbottom and an exposure of 3.28 acres attributed to the alternative as depicted in Figure 5-47. The net change in hardbottom at the end of the simulation period (exposure minus coverage) as a result of the project is estimated to be -10.64 acres.

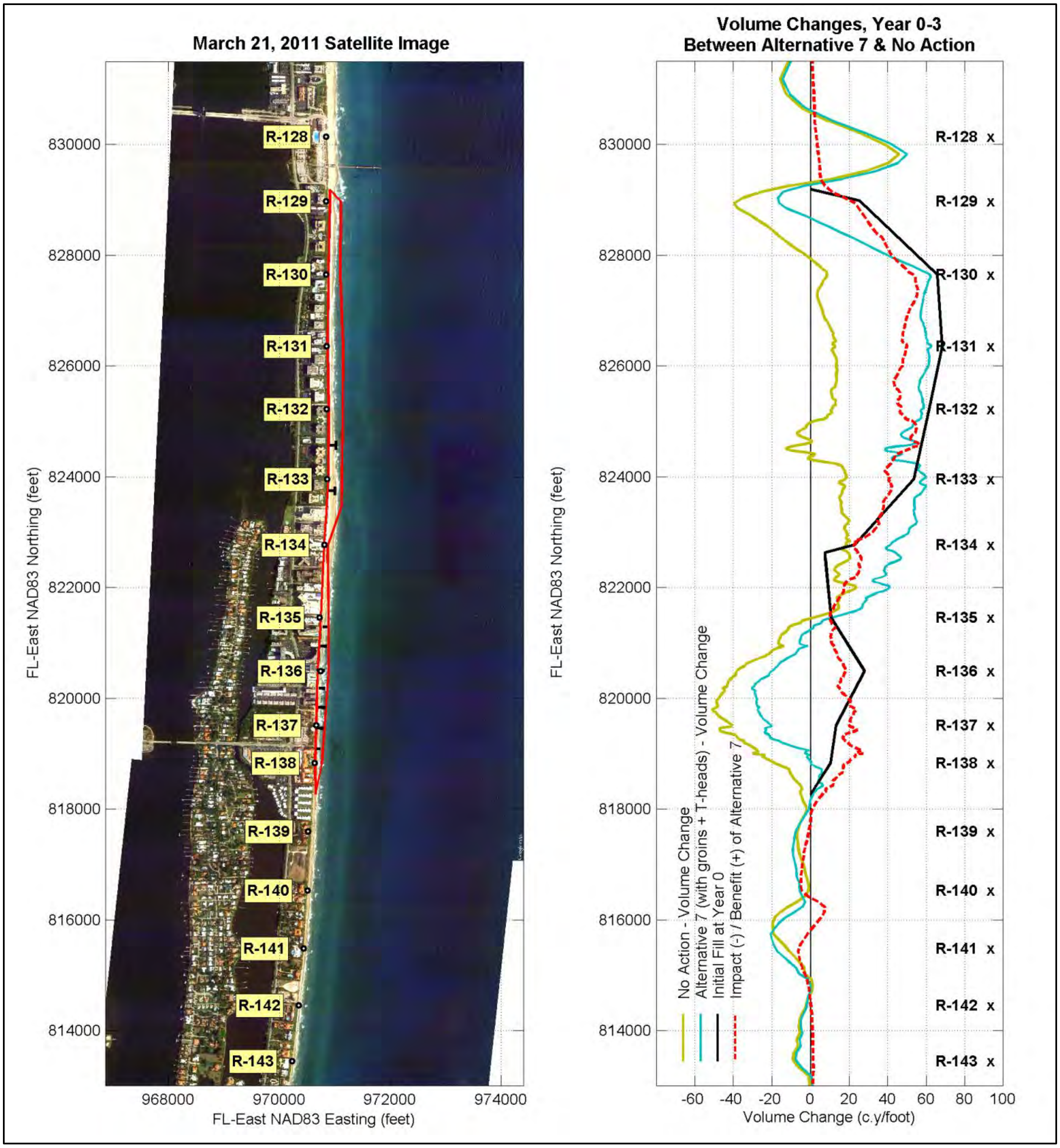

Figure 5-45. Volume Changes, Alternative 7.

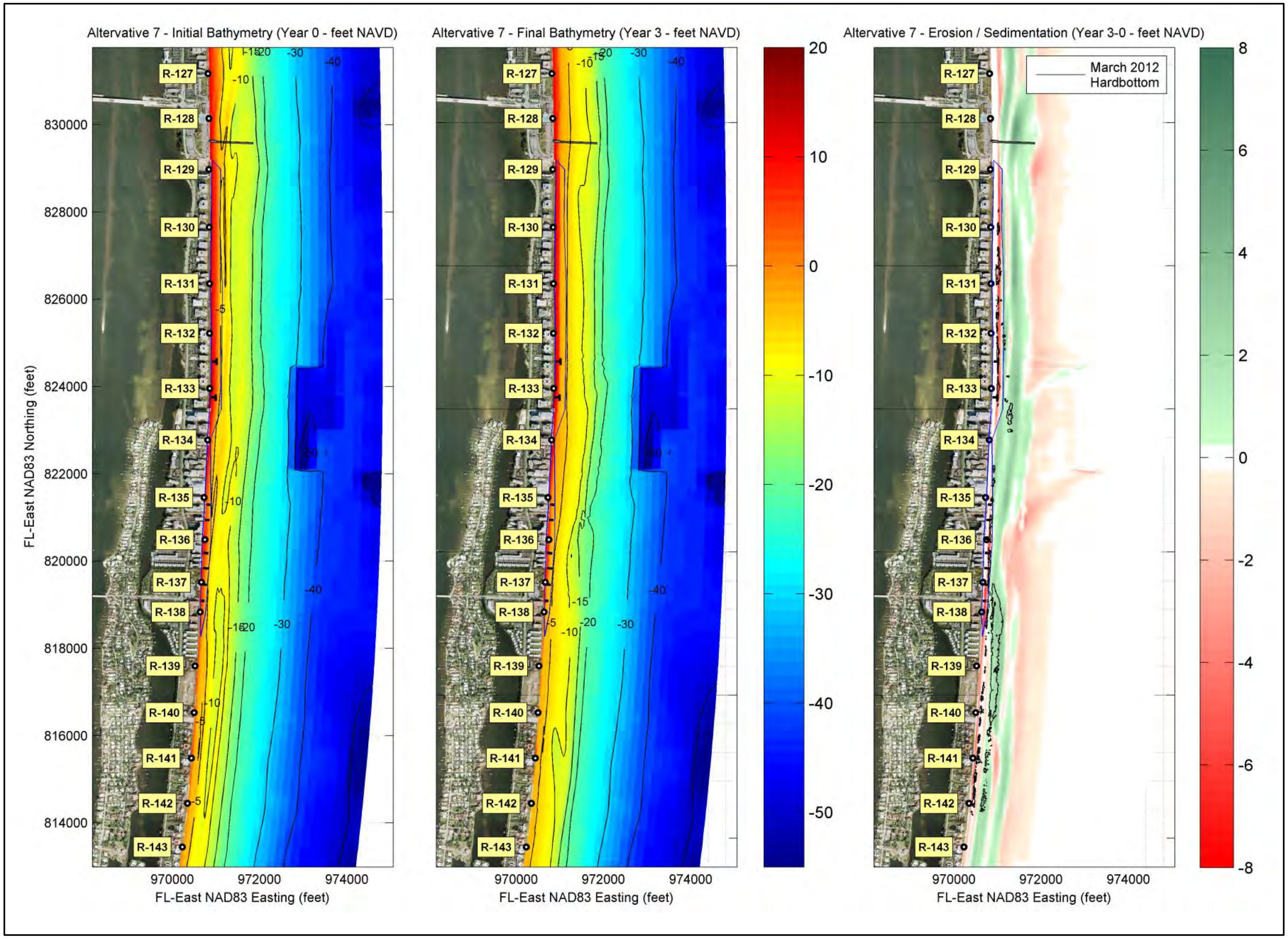

Figure 5-46. Erosion/Sedimentation after 3 years of simulation, Alternative 7.

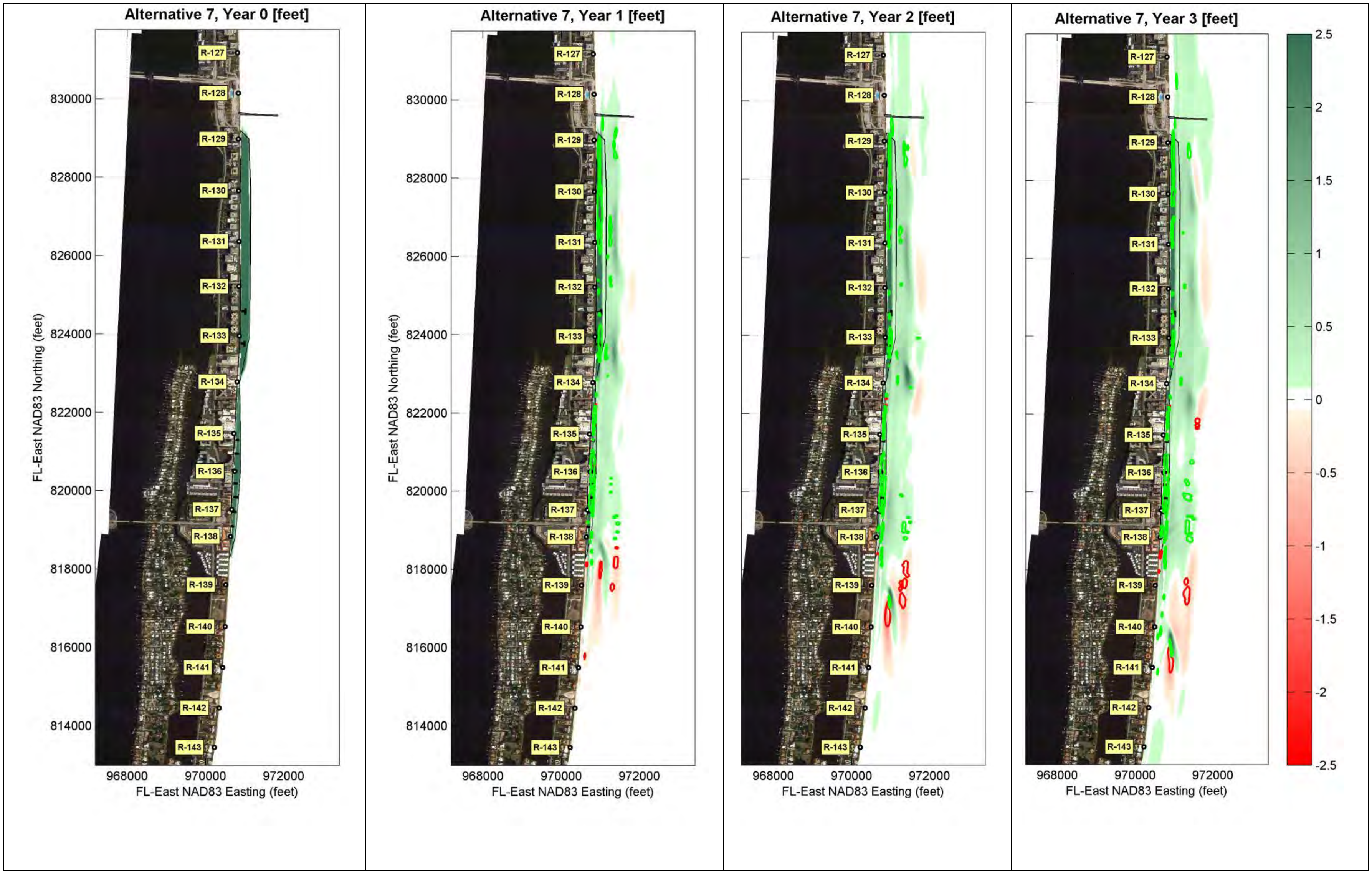

Figure 5-47. Temporal evolution of erosion (red) / sedimentation (green) for Alternative 7, compared to No Action scenario.

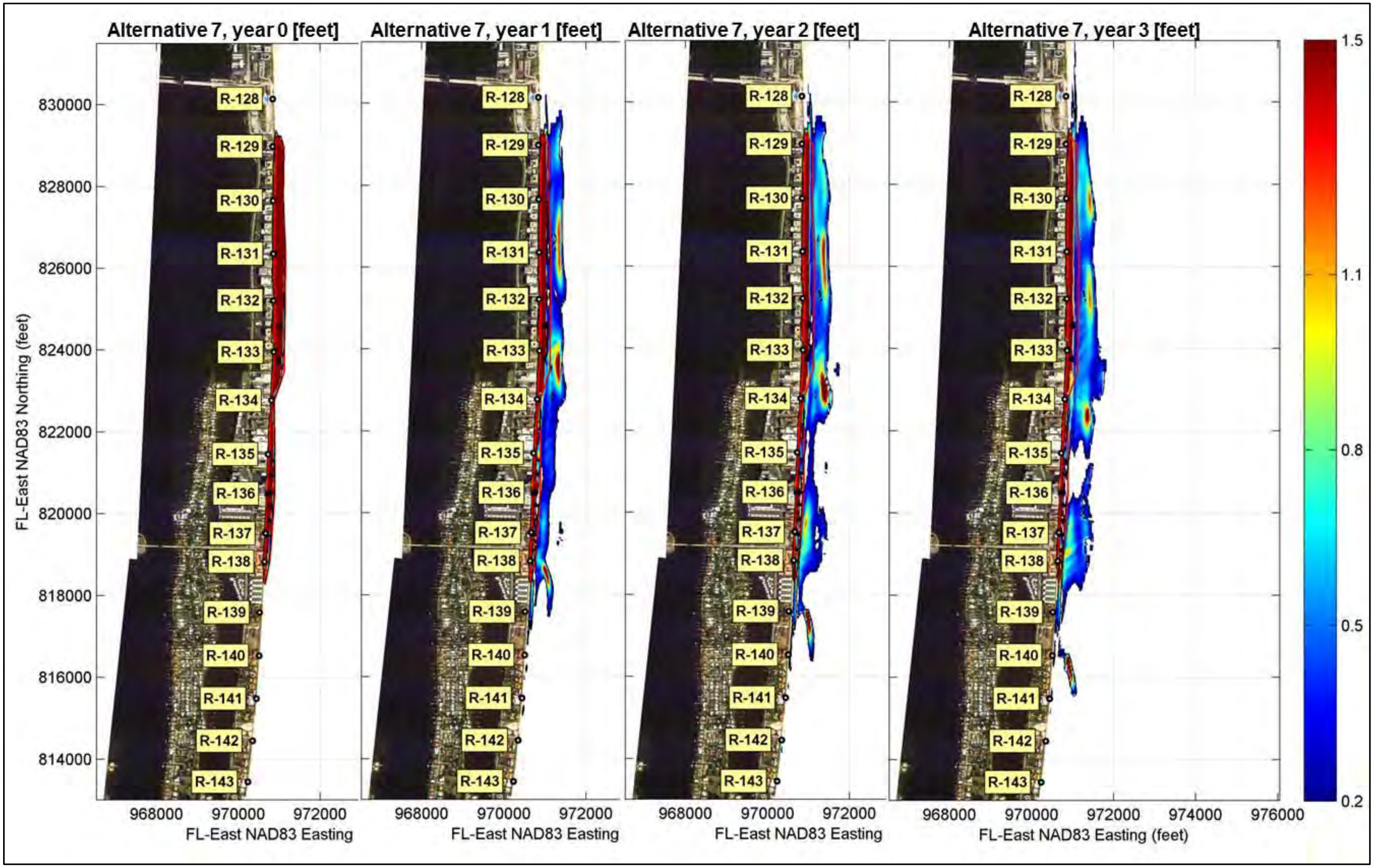

Figure 5-48. Sediment Accumulation greater than 0.2 ft for Alternative 7.

5.8.2. Separated Actions

Alternative 7T (Town of Palm Beach portion of alternative)

Alternative 7T presents a sand placement of 338,072 cubic yards along R-129-210 and R-134+135 and two T-heads located between R-132+556 and R-133+269. Model results for Alternative 7T are shown in Figure 5-49 through Figure 5-52. The sedimentation areas greater than 0.2 feet extend throughout the Town of Palm Beach's project area and into the County. This indicates that some of the sedimentation areas within the County shown in Alternative 7 could be attributed to the fill placed to the north within the Town of Palm Beach.

At the end of the 3 year simulation period, there was an estimated coverage of 6.34 acres of hardbottom and an exposure of 0.80 acres attributed to the alternative as depicted in Figure 5-51. The net change in hardbottom at the end of the simulation period (exposure minus coverage) as a result of the project is estimated to be -5.54 acres.

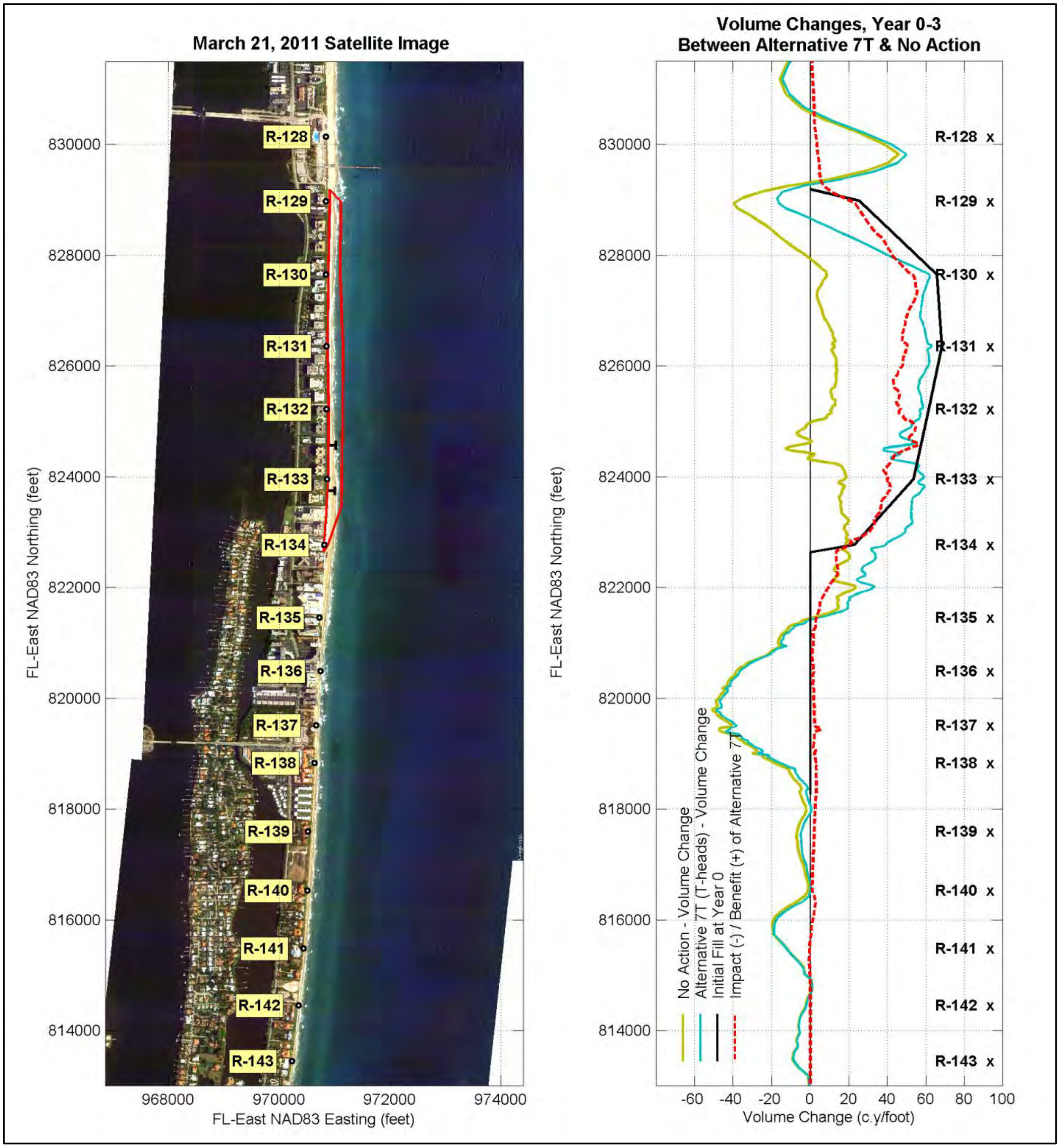

Figure 5-49. Volume Changes, Alternative 7T.

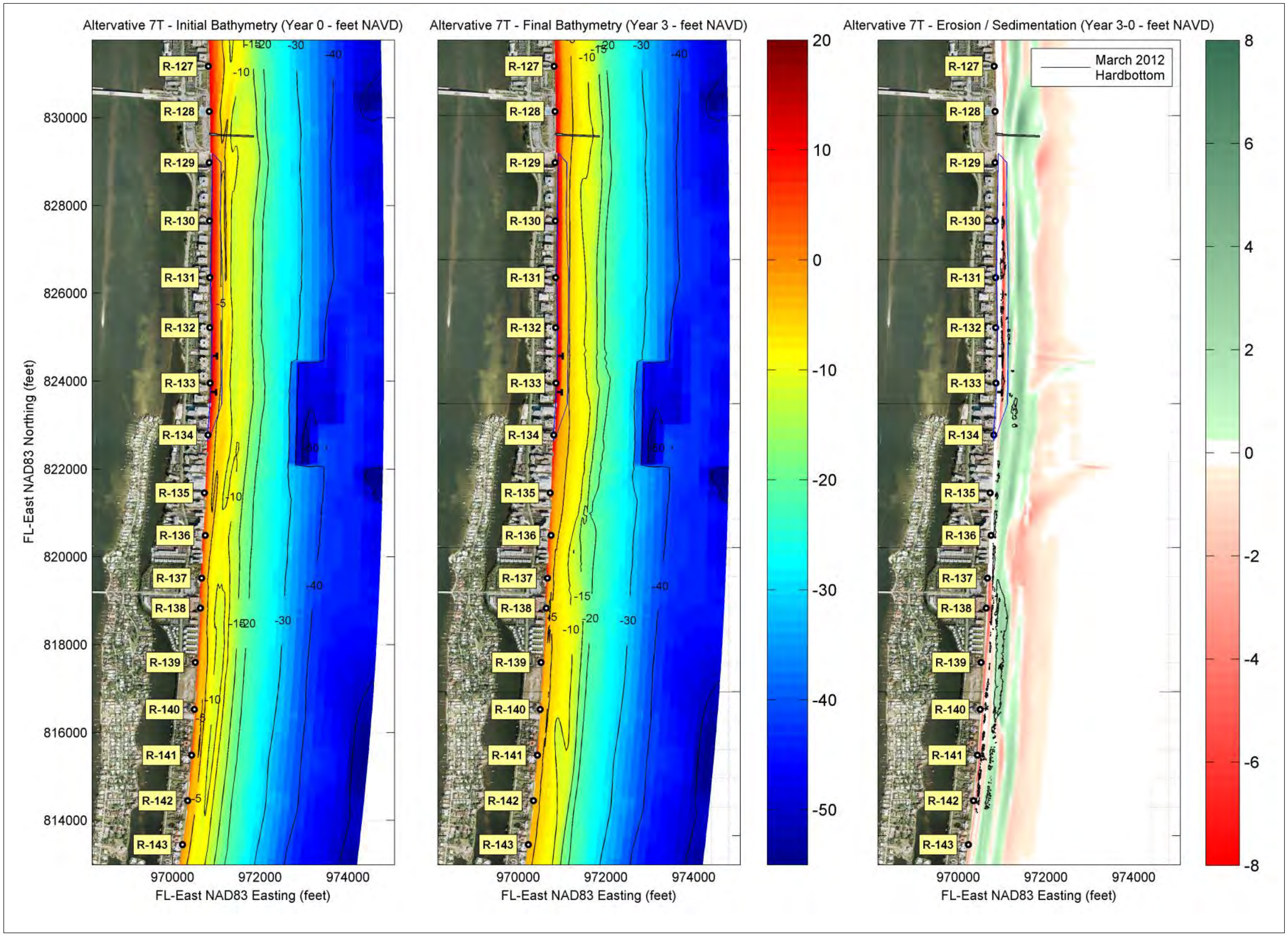

Figure 5-50. Erosion/Sedimentation after 3 years of simulation, Alternative 7T.

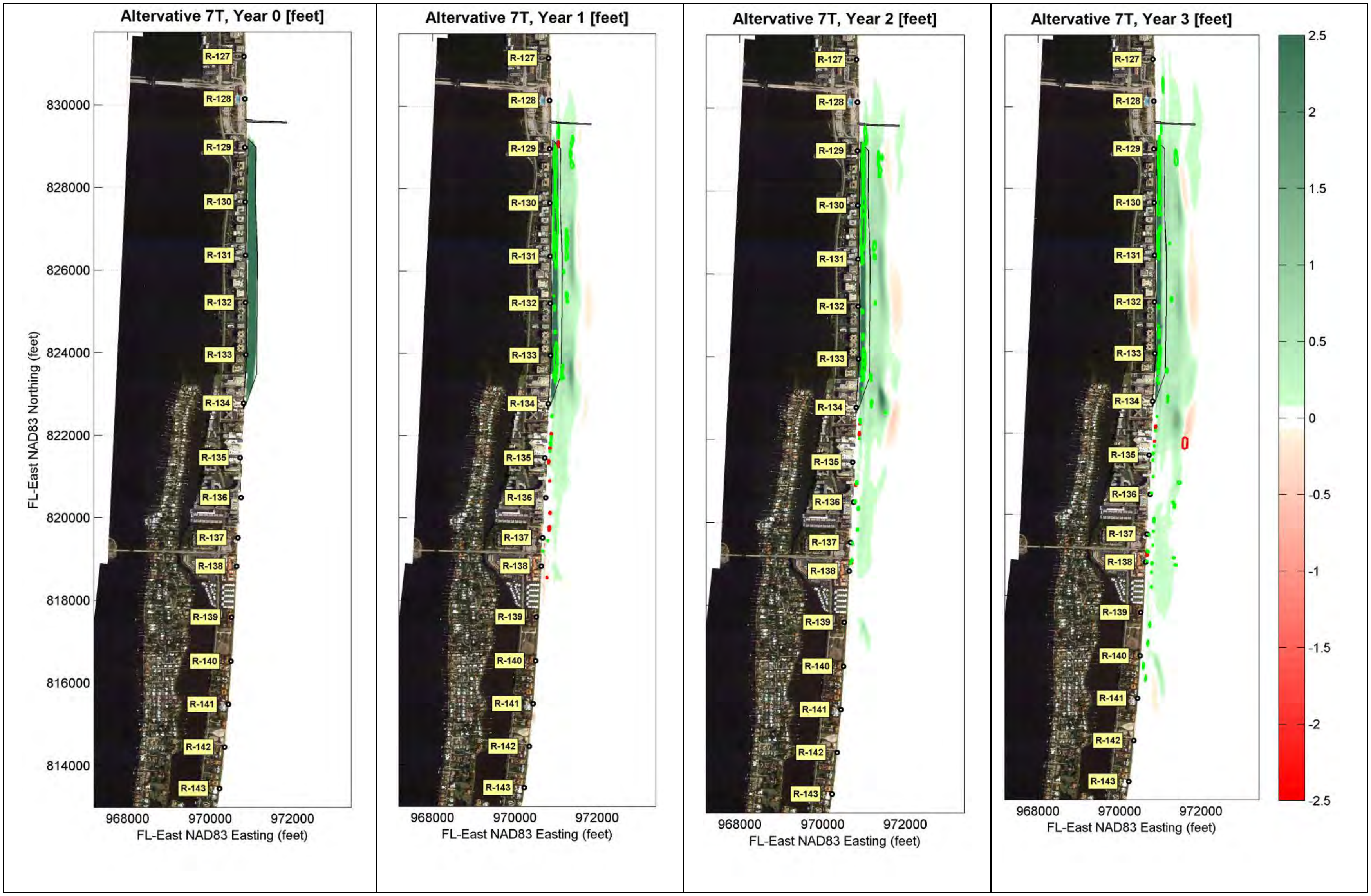

Figure 5-51. Temporal evolution of erosion (red) / sedimentation (green) for Alternative 7T, compared to No Action scenario.

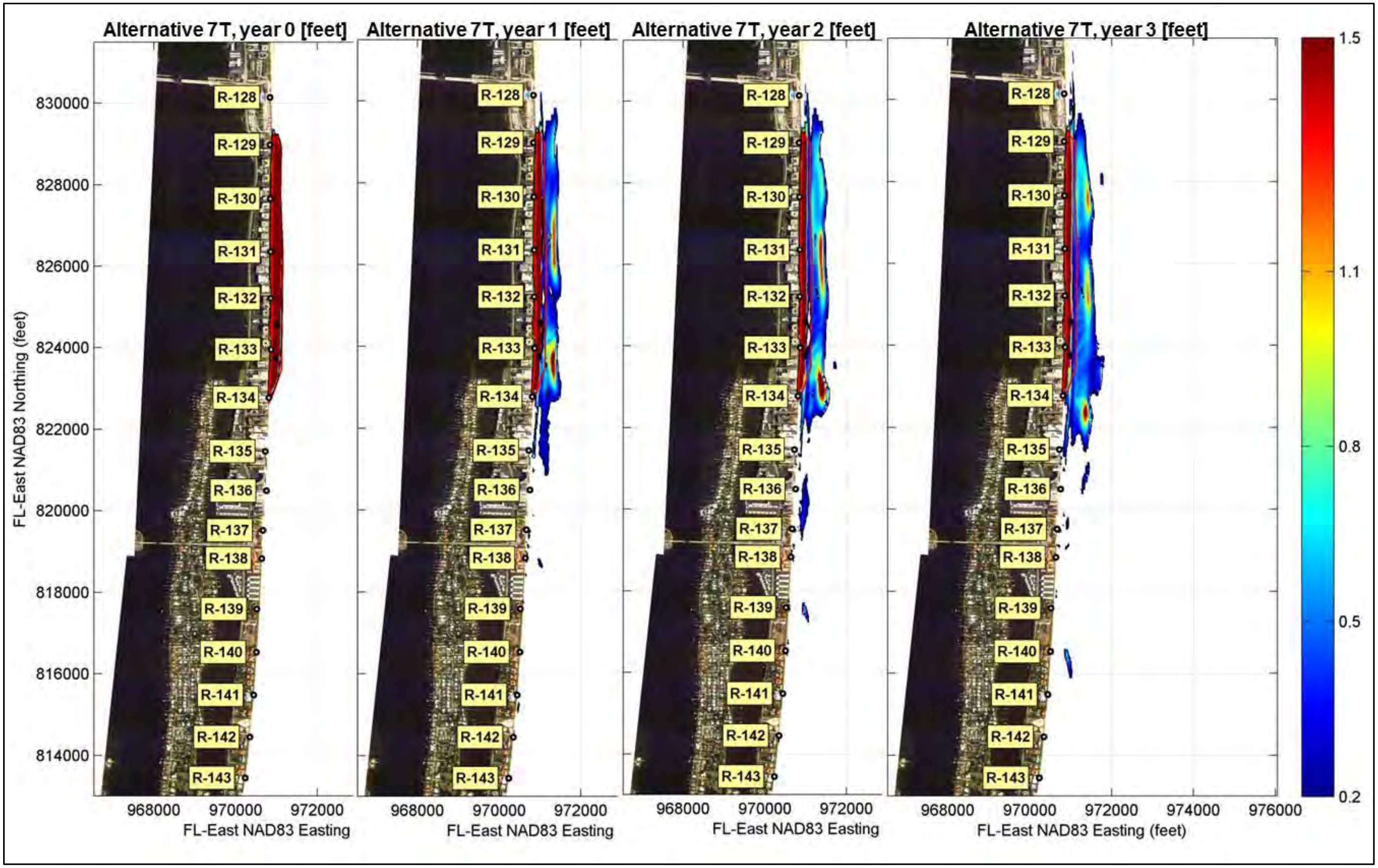

Figure 5-52. Sediment Accumulation greater than 0.2 ft for Alternative 7T.

6.0 SUMMARY AND CONCLUSIONS

A numerical modeling study utilizing Delft3D model was conducted to simulate the proposed Project alternatives and to evaluate the potential hardbottom impact. Seven “combined” alternatives, six “separated” alternatives, and one “No Action” alternative were modeled for a total of thirteen simulations (Table 5-1).

The Delft3D morphological model from previous studies of Southern Palm Beach Island was recalibrated (updated) based on more recent erosion patterns and available data. The performance and impact of each alternative over a 3 year project life was then assessed using the updated calibrated model. The performance and impacts were assessed in terms of volume changes and erosion/sedimentation patterns at 1 year increments during simulation period. The following are the primary findings of the study:

- Greater fill volumes result in increased sedimentation areas and net hardbottom coverage as the fill is redistributed cross shore and transported alongshore.
- Groins retain a portion of the sand that otherwise would be transported downdrift to adjacent beaches. The model indicated that groins within the County for Alternative 2 (and Alternative 2C) resulted in greater sedimentation offshore of the groin field as compared to Alternative 3C with the same fill volume, but less downdrift sedimentation. This is attributed to a greater volume retained within the groins field being redistributed cross shore as opposed to alongshore in the absence of the groins. The net hardbottom coverage was less for Alternative 2 (and Alternative 2C) as compared to Alternative 3C.
- For Alternative 6, the fill placed south of R-134+135 within the County spreads north resulting in increased sedimentation within the Town of Palm Beach.
- For Alternative 7, the fill placed north of R-134+135 within the Town of Palm Beach is transported south resulting in increased sedimentation within the County.

- Alternative 2 resulted in the least area of sedimentation and net hardbottom coverage as compared to the other combined alternatives.

The results of this numerical modeling study should be used in conjunction with other coastal engineering assessments and prudent engineering judgment.

7.0 REFERENCES

Applied Technology & Management, 2012. Town of Palm Beach Town-Wide 2011 Physical Monitoring Report, Applied Technology & Management, West Palm Beach, FL.

Applied Technology & Management, 2013. Town of Palm Beach Town-Wide 2012 Physical Monitoring Report, Applied Technology & Management, West Palm Beach, FL.

Bean-Stuyvesant, 2006. Town of Palm Beach, Phipps Ocean Park (Reach 7) Beach Nourishment Project, After-Dredging Surveys, Bean-Stuyvesant, LLC, Belle Chasse, LA.

Benedet, L., List, J.H., 2008. Evaluation of the physical process controlling beach changes adjacent to nearshore dredge pits. Coastal Engineering volume 55(12). 1224-1236.

Coastal Planning & Engineering, Inc., 2007a. Town of South Palm Beach/Town of Lantana Erosion Control Study, Coastal Planning & Engineering, Inc., Boca Raton, FL.

Coastal Planning & Engineering, Inc., 2007d. Coastal Construction Control Line Permit Application for Town of Palm Beach Southern Dune Repair Project, Coastal Planning & Engineering, Inc., Boca Raton, FL.

Coastal Planning & Engineering, Inc., 2009. 2008 Town of Palm Beach Annual Monitoring, Topographic and Hydrographic Survey Report, Coastal Planning & Engineering, Inc., Boca Raton, FL

Coastal Planning & Engineering, Inc., 2010a. Central Palm Beach County Comprehensive Erosion Control Project, Numerical Calibration of Wave Propagation and Morphology Changes, Coastal Planning & Engineering, Inc., Boca Raton, FL.

Coastal Planning & Engineering, Inc., 2010b. Central Palm Beach County Comprehensive Erosion Control Project, Numerical Calibration of Wave Propagation and Morphology Changes, Appendix 2, Supplemental Model Calibration Discussion, Coastal Planning & Engineering, Inc., Boca Raton, FL.

Coastal Planning & Engineering, Inc., 2011. Central Palm Beach County Comprehensive Erosion Control Project Numerical Modeling of Shore Protection Alternatives, Coastal Planning & Engineering, Inc., Boca Raton, FL.

Coastal Planning & Engineering, Inc., 2013. Central Palm Beach County Comprehensive Erosion Control Project Reformulated Shore Protection Alternatives, Coastal Planning & Engineering, Inc., Boca Raton, FL.

CB&I Coastal Planning & Engineering, Inc., 2014. Southern Palm Beach Island Comprehensive Shoreline Stabilization Project Environmental Impact Statement (EIS) SBEACH Analysis Report. Prepared for U.S. Army Corps of Engineers (USACE)

Deltares, 2011. Delft3D-FLOW Simulation of Multi-Dimensional Hydrodynamic Flows and Transport Phenomena, Including Sediments, User Manual, Part of Hydro-Morphodynamics, Deltares, Delft, the Netherlands.

Florida Department of Environmental Protection, 2013. Beaches and Coastal Systems Data, Historic Shoreline Database, ftp://ftp.dep.state.fl.us/pub/water/beaches/HSSD/ProfileData.

Finkl, C.W., Andrews, J.L., Forrest, B.M., Larenas, M.L., 2008. 2007 Geotechnical Investigations to Identify Sand Resources Offshore of the Town of Palm Beach, Palm Beach County, Florida, Coastal Planning & Engineering, Inc., Boca Raton, FL.

Lesser G.R., Roelvink J.A., Van Kester J.A. T.M., Stelling G.S. 2004. Development and validation of a three-dimensional morphological model. Coastal Engineering 51 (2004) 883– 915.

Lesser, G.R. 2009. An Approach to Medium-Term Coastal Morphological Modeling. TU Delft, PhD Thesis.

National Oceanographic and Atmospheric Administration, 2006. GEODAS Software for Windows, http://www.ngdc.noaa.gov/mgg/gdas/gx_announce.Html.

National Oceanographic and Atmospheric Administration, 2011. Bench Mark Data Sheets, Lake Worth Pier, FL, Station ID: 8722670, http://tidesandcurrents.noaa.gov/.

Palm Beach County, 1993. Environmental Assessment of Coastal Resources in Palm Beach, Lake Worth, South Palm Beach, Lantana, and Manalapan, Palm Beach County, Florida, Palm Beach County, West Palm Beach, FL.

Sea Diversified Inc., 2006. Sea Diversified, Inc. Survey No. 05-784, May 22-26, 2006.

Sea Diversified Inc., 2008. Sea Diversified, Inc. Survey No. 08-1344, December 2008.

Tenix LADS Corporation, 2003. Data Acquisition and Processing Report, High Resolution Hydrographic Survey of the Atlantic Coast of Dade and Palm Beach County, Florida Using Airborne Laser Technology, Tenix LADS Corporation, Biloxi, MS.

U.S. Army Corps of Engineers, 2004. 2004 U.S. Army Corps of Engineers (USACE) Topo/Bathy Lidar: Alabama, Florida, Mississippi and North Carolina, U.S. Army Corps of Engineers Joint Airborne LiDAR Bathymetry Technical Center of Expertise (JALBTCX), Mobile, AL, http://www.csc.noaa.gov/digitalcoast/data/coastallidar.

U.S. Army Corps of Engineers, 2006. USACE 2006 East Coast Topo/Bathy Mapping project, U.S. Army Corps of Engineers Joint Airborne LiDAR Bathymetry Technical Center of Expertise (JALBTCX), Mobile, AL, http://www.csc.noaa.gov/digitalcoast/data/coastallidar.

APPENDIX G-4

DRAFT BOUSS2D MODELING REPORT

This page intentionally left blank.

SOUTHERN PALM BEACH ISLAND COMPREHENSIVE SHORELINE STABILIZATION PROJECT DRAFT BOUSS2D MODELING REPORT

TABLE OF CONTENTS

LIST OF FIGURES

Figure No.

LIST OF TABLES

Table No.

1.0 INTRODUCTION

Under direction of the U.S. Army Corps of Engineers (USACE), CB&I Coastal Planning & Engineering, Inc. (CB&I) assisted in the development of the Southern Palm Beach Island Comprehensive Shoreline Stabilization Project Environmental Impact Statement (EIS). The initial tasks associated with the effort included public scoping and agency coordination to determine what data was necessary to develop the EIS. After review of the data and previous work, the USACE has determined that numerical modeling of breaking waves is required to obtain necessary data that is not currently available.

Concern regarding potential impacts to surfing has previously been expressed in public scoping for projects within the Project Area. In order to evaluate project-related effects on surfing, the BOUSS-2D model was used in this study to simulate waves within the Project Area. BOUSS-2D model was developed by the U.S. Army Corps of Engineers (Nwogu and Demirbilek, 2001) and utilized through the Surface Water Modeling System (SMS) interface (Aquaveo, 2008).

To assess the potential impacts on surfability within the Study Area, a modeling approach was adopted. First, a morphological model (Delft3D) was run to develop the anticipated bathymetry from the coastline response to the alternatives. The bathymetry resulting from the alternatives along with the existing bathymetry were incorporated into the BOUSS-2D model to evaluate the impacts to surfability within the Project Area. In particular, the surfability was evaluated at two popular southern Palm Beach surf spots, Lantana Park and the Lake Worth Pier.

The alternatives that were considered in the analysis included:

- Alternative 1 – No Action Alternative (Status Quo) and referenced herein as the existing conditions.

- Alternative 2 – Applicants' Preferred Project (Proposed Action): Beach and Dune Fill with Shoreline Protection Structures Project

- Alternative 6 – The Town of Palm Beach Increased Sand Volume Project and County Increased Sand Volume without Shoreline Protection Structures Project

- Alternative 7 – Plan was presented by The Coalition to Save Our Shoreline, Inc. (SOS) consisting of beach fill and dune restoration between R129+210 and R134+135 with shoreline protection structures. The sand fill volumes required for the SOS plan are greater than the volumes for Alternative 6 over the same shoreline extents. For the purpose of modeling, Alternative 7 was defined as the SOS plan north of R134+135 and Alternative 2 to the south.

The remainder of the alternatives (Alternatives 3, 4, and 5) did not need to be included in the analysis. They consisted of various combinations of the sand fill volumes and shoreline protection structures comprising Alternatives 2 and 6. Of Alternatives 2 through 6, Alternative 2 required the smallest fill volumes and Alternative 6 required the greatest.

2.0 BACKGROUND

According to Benedet et al. (2007), you can find surfers just about anywhere there is a large body of water with sufficient fetch to allow the generation of surfable waves. Surfing is practiced in the Pacific Nations, North America, South America, Central America, Europe and Asia. Surfing destinations range from Hawaii, Australia and Costa Rica to Ireland, Alaska, Dubai, and even at the North American Great Lakes and the Amazon River tidal bore. Surfing is currently the most popular sport in Australia, the second most popular sport in Brazil, and one of the most popular extreme sports in North America.

The population of surfers around the world has social and economic benefits. Recently, a number of studies are been conducted in terms of impacts of engineering works, creation of surf spots and relation between wave conditions and surfability (e.g. Black, 2001; Black and Mead, 2001, Hutt *et al*. 2001; Scarfe *et al*. 2003 Benedet *et al.*, 2007).

Surfers are traditionally defensive about any activity in the vicinity of their favorite surfing breaks. This behavior may be justified because history shows that their rights have at times been ignored and many surfing breaks have been impacted by coastal modification (Scarfe *et al.*, 2003). Interestingly, some of the most popular surf spots on the east coast of Florida occur near these coastal modifications. For example, the New Smyrna Beach on the south side of Ponce Inlet, the north side of Sebastian Inlet, the north side of Ft. Pierce Inlet, Reef Road south of Palm Beach Inlet, and the south side of the Lake Worth Pier. In this way, the analysis of surfability has become an important issue where an engineering intervention is need.

The most important parameters to analyze surfability are the breaker type, peel angle, peel rate, wave velocity and surfer velocity. Battjes (1974) describes the breaker type as function of Iribarren number:

$$\xi_b = \frac{\tan\alpha}{\sqrt{H_b/L_0}}$$

where: $\tan\alpha$ is the beach slope, H_b is the significant wave height at break, L_0 is the deep water wavelength (~1.56*T^2). According to the author:

Collapsing if $\xi_b > 2.0$

Plunging if $0.4 < \xi_b < 2.0$

Spilling if $\xi_b < 0.4$

Figure 2-1 presents examples of the wave breaker type.

Figure 2-1. Wave breaking type (Benedet, 2007).

In addition to the way wave breaks, it is important to understand the angle the wave breaks related to its crest. If this angle is to sharp, the wave will “close-out”. For optimal surfing conditions the wave has to break gradually along the wave crest. Figure 2-2 presents the peel angle, which is defined as the angle enclosed by the wave crest and the breaker lines (Dafferner and Klein, 2009; Walker, 1974). Knowing the peel angle and the wave velocity (in shallow water $= \sqrt{gh}$) it is possible to calculate the peel rate and surfer velocity.

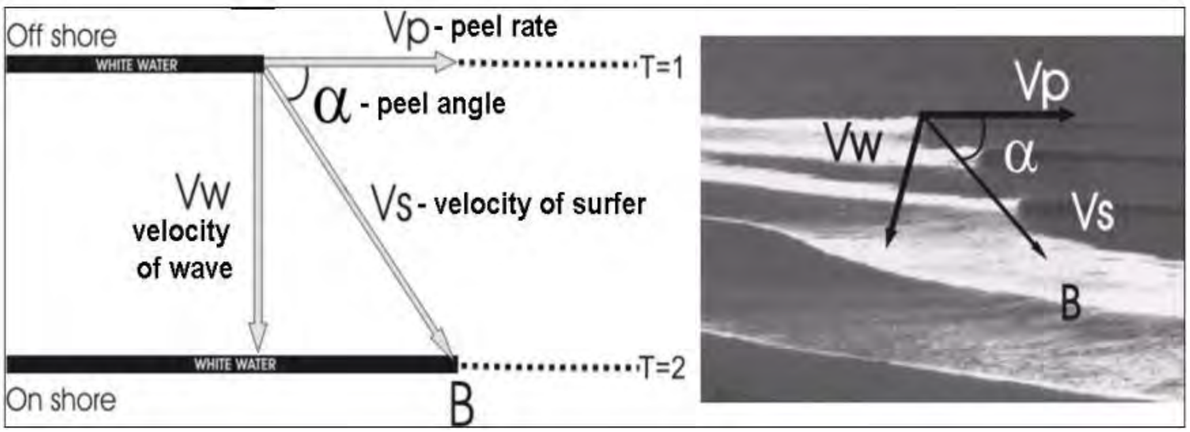

Figure 2-2. Peel angle terminology (Dafferner and Klein, 2009).

Hunt et al. 2001 rated the skill of surfers with respect to peel angle and wave height. Table 2-1 describes presents the rating matrix, while Figure 2-3 presents Hunt’s classification in graphical form. The larger peel angle and smaller the wave height, the easier the wave is to be ridden. Conversely, the smaller the peel angle and larger the wave height, the more difficult the wave becomes to be ridden.

Table 2-1. Rating of the skill of surfers. Ratings are independent of surf break quality or the degree of difficulty of waves (Hunt et al., 2001).

Rating	Description of Rating	Peel Angle Limit (°)	Min/Max Wave Height (m)	Min/Max Wave Height (ft)
1	Beginner surfers not yet able to ride the face of wave and simply moves forward as wave advances	90	0.70/1.00	2.3/3.3
2	Learner surfers able to successfully ride laterally along the crest of a wave	70	0.65/1.50	2.1/4.9
3	Surfers that have developed the skill to generate speed by “pumping” on the face of the wave	60	0.60/2.5	2/8.2
4	Surfers beginning to initiate and execute standard surfing manoeuvres on occasion	55	0.55/4.0	1.8/13.1
5	Surfers able to execute standard surfing manoeuvres consecutively on a single wave	50	0.50/>4.0	1.6/>13.1
6	Surfers able to execute standard surfing manoeuvres consecutively. Executes advanced manoeuvres on occasion	40	0.45/>4.0	1.5/>13.1
7	Top amateur surfers able to consecutively execute advanced manoeuvres	29	0.40/>4.0	1.3/>13.1
8	Professional surfers able to consecutively execute advanced manoeuvres	27	0.35/>4.0	1.1/>13.1
9	Top 44 professional surfers able to consecutively execute advanced manoeuvres	Not reach	0.30/>4.0	1/>13.1
10	Surfers in the future	Not reach	0.30/>4.0	1/>13.1

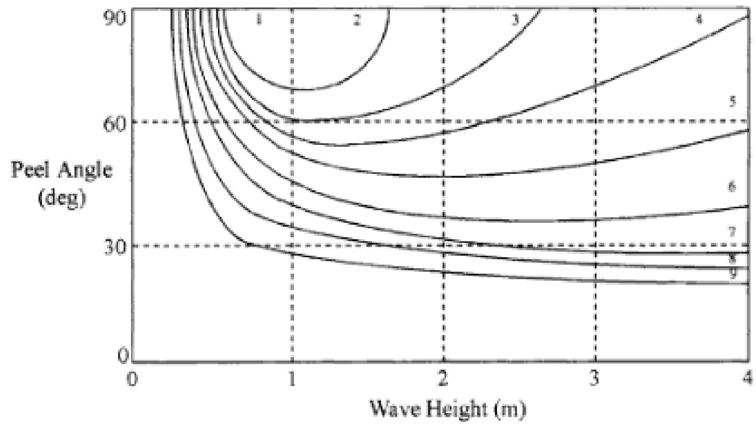

Figure 2-3. Classification of surfing skill rated against peel angle and wave height. (Hunt et al., 2001).

3.0 SURFING IMPACT ANALYSIS

3.1. BOUSS-2D Model Description

BOUSS-2D is a numerical model for simulating the propagation and transformation of waves in coastal regions and harbors based on a time-domain solution of Boussinesq-type equations (Nwogu and Demirbilek, 2001). The governing equations are uniformly valid from deep to shallow water and can simulate most of the phenomena of interest in the nearshore zone and harbor basins including shoaling/refraction over variable topography, reflection/diffraction near structures, energy dissipation due to wave breaking and bottom friction, cross-spectral energy transfer due to nonlinear wave-wave interactions, breaking-induced longshore and rip currents, wave-current interaction and wave interaction with porous structures.

The governing equations in BOUSS-2D are solved in a time domain with a finite-difference method where the water-surface elevation and horizontal velocities are calculated at the grid nodes in a staggered manner. The area of interest is discretized as a rectangular grid. Time-histories of the velocities and fluxes corresponding to incident storm conditions are specified along wave generation boundaries of the grid. The input wave conditions may be periodic (regular) or non-periodic (irregular). Unidirectional or multidirectional sea states can be simulated. Waves propagating out of the computational domain are either absorbed in damping layers placed around the perimeter of the domain or allowed to leave the domain freely. Damping and porosity layers are used to simulate the reflection and transmission characteristics of jetties, breakwaters, and other structures existing in the modeling domain (Demirbilek *et al.*, 2005). Details about BOUSS-2D model are provided in the model theory and examples report (Nwogu and Demirbilek 2001).

The classical form of the Boussinesq equations for wave propagation over water of variable depth was derived by Peregrine (1967). The equations were restricted to relatively shallow water depths, i.e., the water depth, h, had to be less than one-fifth of the wavelength, L, in order to keep errors in the phase velocity to less than 5%. Nwogu (1993) extended the range of applicability of Boussinesq-type equations to deeper water by recasting the equations in terms of the velocity at an arbitrary distance, z, from the still-water elevation, instead of the depth-averaged velocity. The distance from the still-water elevation of the velocity variable becomes a free parameter, which is chosen to optimize the linear dispersion characteristics of the equations.

The optimized form of the equations results in an error of less than 2% for the phase velocity from shallow-water depths up to the deepwater limit (h/L= 0.5). Despite the improvement in the frequency dispersion characteristics, Nwogu's (1993) equations are based on the assumption that the wave heights were much smaller than the water depth. This limits the ability of the equations to describe highly nonlinear waves in shallow water, which led Wei *et al.* (1995) to derive a fully nonlinear form of the equations. The fully nonlinear equations are particularly useful for simulating highly asymmetric waves in shallow water, wave-induced currents, wave setup close to the shoreline, and wave-current interaction. As ocean waves approach the shoreline, they steepen and ultimately break.

The turbulence and currents generated by breaking waves are important driving mechanisms for the transport of sediments and pollutants. Nwogu (1996) extended the fully nonlinear form of the Boussinesq equations to the surf zone, by coupling the mass and momentum equations with a one-equation model for the temporal and spatial evolution of the turbulent kinetic energy produced by wave breaking. The equations have since been modified to include the effects of bottom friction and flow through porous structures (Nwogu and Demirbilek 2001).

The modified equations can simulate most of the hydrodynamic phenomena of interest in coastal regions and harbor basins including:

- Shoaling.
- Refraction.
- Diffraction.
- Full/partial reflection and transmission.
- Bottom friction.
- Nonlinear wave-wave interactions.
- Wave breaking and runup.
- Wave-induced currents.
- Wave-current interaction.

The BOUSS-2D was used to analyze the potential impacts to surfability due to the alternatives as compared to the existing conditions. Surfability was assessed in terms of peel angle, peel rate, wave velocity, and the velocity of the surfer.

3.2. Model setup and simulated scenarios

3.2.1. Model Grid

The potential impacts of the alternatives were analyzed at two important southern Palm Beach surf spots, Lantana Park (hereafter called "Lantana") and Lake Worth Pier (hereafter called "Pier"). A grid with 4 meter resolution was developed as shown by the red box in Figure 3-1. The grid is 1732 meter (X direction) x 5720 meter (Y direction) with a total of 433 x 1730 grid cells.

3.2.2. Bathymetry

Bathymetries for the BOUSS-2D model were developed to represent the beach conditions after the coastal system's natural processes had responded to construction of the alternatives to achieve equilibrium. The temporal evolution of the bathymetries after equilibration was simulated by running the Delft3D morphological model for 3 years after construction for each alternative. The relative changes (greater than 0.2 feet) are shown by the three graphics on the right in Figure 3-2. The relative changes represent the differences between each bathymetry alternative and the existing condition bathymetry (left graphic in Figure 3-2). Within the area of interest at the Lake Worth Pier, Alternatives 2 and 6 did not show differences greater than 0.2 feet, while Alternative 7 showed sedimentation between 2 and 4 feet extending offshore from the shoreline approximately half the length of the Pier. Within the area of interest at Lantana Park, the differences were more evident for all of the alternatives considered with sedimentation up to 1 foot within the surf zone.

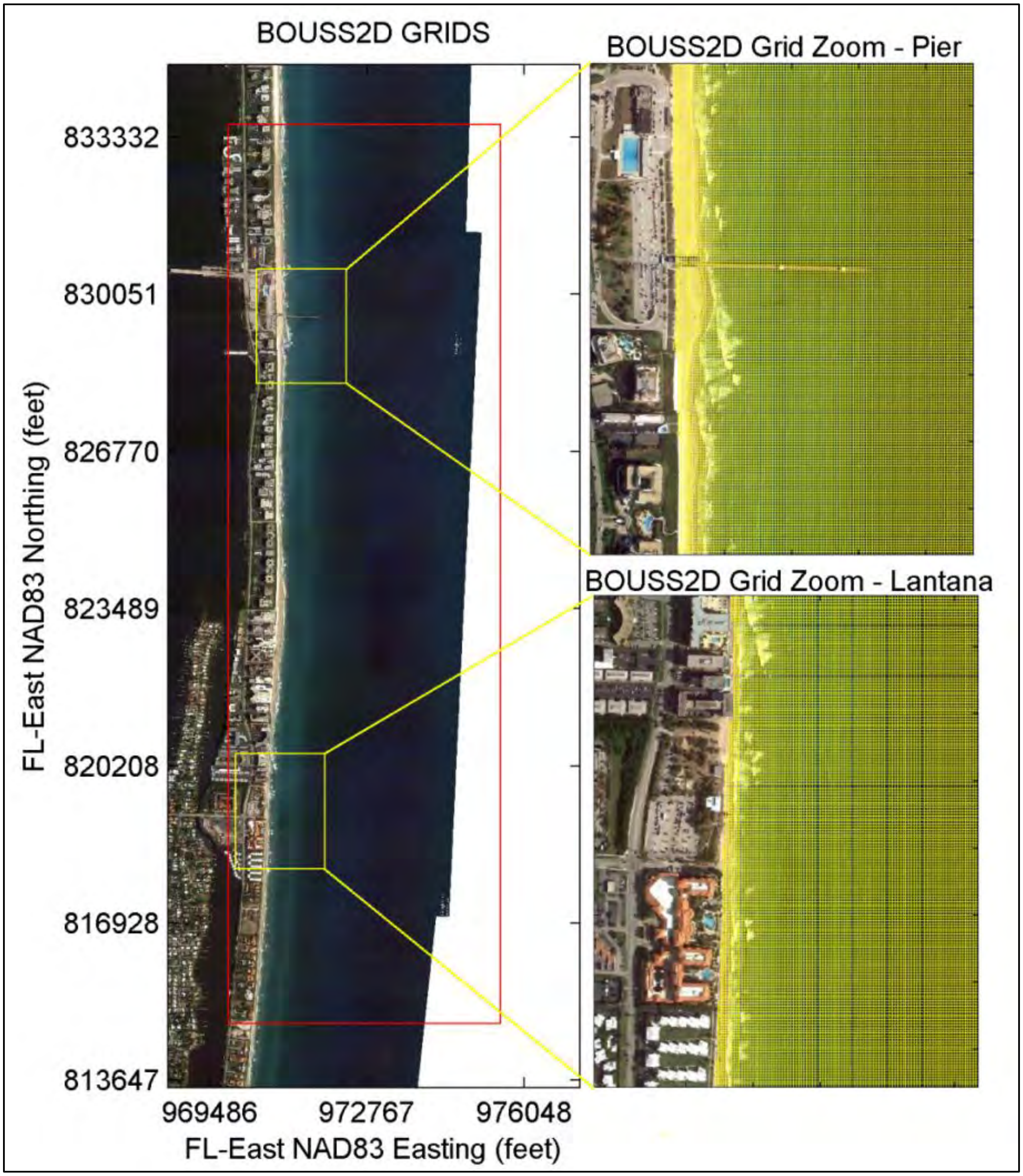

Figure 3-1. Bouss2D grid (red box – left) and zoom at areas of interest – Pier (right top) and Lantana (right bottom).

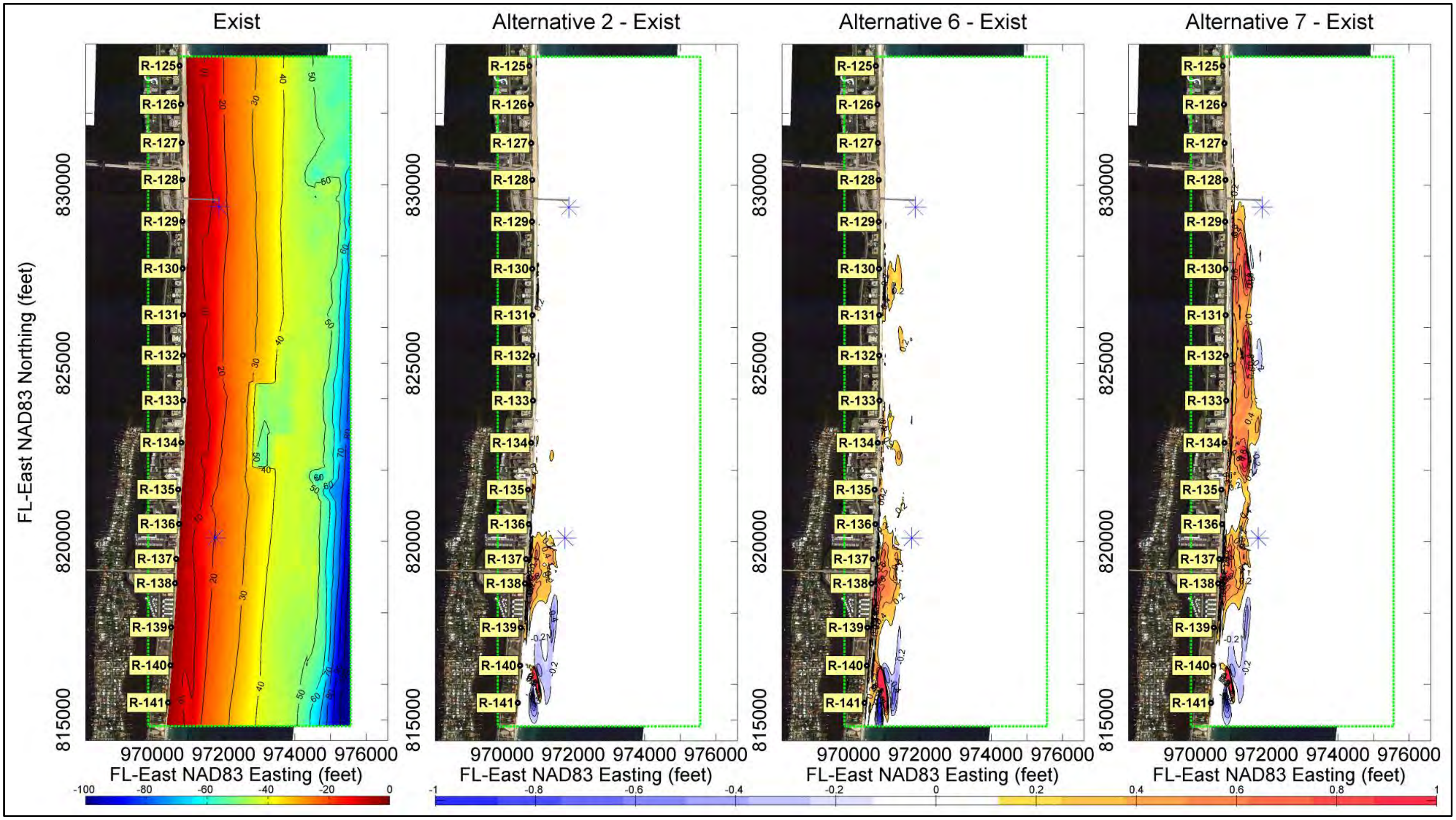

Figure 3-2. Existing bathymetry (left) and differences between alternatives and existing condition. The * represent the points where probes were placed to analyse wave timeseries of Lantana Park and Lake Worth Pier. The green line represents the BOUSS2D grid limits.

3.2.3. Boundary Conditions

According to Nwogu and Demirbilek (2001), to solve the governing equations, appropriate boundary conditions have to be imposed at the boundaries of the computational domain. This requires specification of waves propagating into the domain and the absorption of waves propagating out of the domain. The equations have also been modified to simulate wave interaction with fully/partially reflecting structures within the computational domain. The types of boundaries considered in BOUSS-2D include:

- Fully reflecting or solid wall boundaries.
- External wave generation boundaries.
- Internal wave generation boundaries.
- Wave absorption or damping regions.
- Porous structures.

For the present study, two types of boundary conditions were defined: wave makers and sponge/damp layers (Figure 3-3). According to Nwogu and Demirbilek (2001), waves propagating out of the computational domain should be absorbed in damping regions placed around the perimeter of the computational domain.

The "sponge layers" were set by adjusting the width and reflection coefficient values (Table 3-1). At the north and south boundaries, the layers were defined to minimize reflection (approximately 2.5%) in order to absorb wave energy exiting the grid (Goda, 1985). At the landward boundary, the layer was set to simulate the reflection of the incident wave energy (approximately 20%) as waves interact within the coastline (Goda, 1985).

Figure 3-3. BOUSS-2D boundaries - wavemaker (green), sea sponge layer (blue) land sponge layer (orange).

3.2.4. Waves

The wave scenarios modeled were selected to be representative of conditions conducive for surfing for which the surfing community might expect to experience during a given year. Three wave events were considered to capture the various points of origination.

- Southeast Waves
- Cold Fronts
- Hurricanes

Southeast waves were assumed to represent the typical surfing conditions experienced within the modeling domain. These conditions are characterized as closely spaced, short period waves that provide a minimal ride for surfing. Wave data used in the model to represent the southeast wave event was obtained from CPE-ADCP measurements collected at the Lake Worth Pier between 02/10/2008 to 04/21/2008 (CPE, 2009) The event had a significant wave height (Hs) of 6 feet, period (Tp) of 6.1 seconds, and direction (Dp) of 105°.

Cold fronts, commonly as known as Nor'easters, frequently occur during winter months (October to April) as low pressure systems move offshore of North Carolina and New England. These systems can produce large waves originating from the northeast that propagate south impacting the Study Area. The wave events experienced at the Study Area typically results in longer period swells accompanied by short period wind waves. Depending upon the wind direction and severity of the wind waves, the wave event can provide a relatively long ride as compared to southeast wave events. Wave data used in the model to represent the cold front wave event was obtained from CPE-ADCP measurements collected at the Lake Worth Pier between 02/10/2008 to 04/21/2008 (CPE, 2009). The event had a significant wave height (Hs) of 7.4 feet, period (Tp) of 11 seconds, and direction (Dp) of 64.5°.

Hurricanes generally occur during the summer months (June to November). Depending on the storm track in relation to the Study Area, the systems can produce swells form any direction radiating outward from its center. The wave events experienced can result in long period, high energy swells immediately preceding and/or following the passage of the storm. These ground swells can produce the longest rides experienced within the Study Area. Wave data obtained approximately 12 miles offshore of the Study Area at USACE WIS station ST 63461 over a 30 year period was reviewed (Hubertz, 1992). The highest significant wave height within the record was associated with Hurricane Frances occurring in September 2004. When considering the wind (direction and speed) and swell (direction, height, and period), the best surf conditions were assumed to occur approximately 12 hours prior to landfall of the storm. The conditions characterizing this event were simulated in Delft3D-WAVES in order to determine the wave parameters at

Bouss2D offshore boundary. A summary of simulated wave scenarios are presented in Table 3-1.

Table 3-1. Bouss2D simulated scenarios.

Condition	Wave	Wave Maker				Sponge Beach		Sponge North/South	
		Hs (ft)	Tp (s)	Dir (°)	Spreading (cosine power)	Value	Width (m)	Value	Width (m)
Existing	Southeast	6.0	6.1	105	9	30	0.15	17.0	0.30
	Cold Front	7.4	11.0	65	55	30	0.15	44.1	0.30
	Hurricane Pre Landfall	8.1	13.5	103	14	29	0.15	29.0	0.30
Alt. 2	Southeast	6.0	6.1	105	9	30	0.15	17.0	0.30
	Cold Front	7.4	11.0	65	55	30	0.15	44.1	0.30
	Hurricane Pre Landfall	8.1	13.5	103	14	29	0.15	29.0	0.30
Alt. 6	Southeast	6.0	6.1	105	9	30	0.15	17.0	0.30
	Cold Front	7.4	11.0	65	55	30	0.15	44.1	0.30
	Hurricane Pre Landfall	8.1	13.5	103	14	29	0.15	29.0	0.30
Alt. 7	Southeast	6.0	6.1	105	9	30	0.15	17.0	0.30
	Cold Front	7.4	11.0	65	55	30	0.15	44.1	0.30
	Hurricane Pre Landfall	8.1	13.5	103	14	29	0.15	29.0	0.30

3.2.5. Model Parameters

The model was run for 850 seconds with a timestep of 0.1 s and used the same calibration parameters presented by CPE (2009): The bottom roughness and the Chezy coefficient used in this study are the same as used by the authors at CPE (2009). The Chezy coefficient values used ranged from 30 to 1,000. A Chezy coefficient of 30 is the model default and represents high wave energy dissipation due to bottom friction. A Chezy coefficient of 1,000 is the maximum value allowed by the model, represents small bottom roughness and shows little to no wave energy dissipation. The specific Chezy values utilized during calibration were 30, 350, 650 and 1000. Wave breaking was enabled, and the rest of the parameters were set at the model default values. The authors found that the best value for Chezy coefficient is 1,000. According to Nwogu and Demirbilek (2001), the Smagorinsky number should be kept between 0 and 0.5, with a default value of 0. CPE (2009) found the best value of 0 and this value was used in this study.

4.0 RESULTS

The results of the potential impacts to surfing are divided in two main sections, one section for each surf spots: Lake Worth Pier and Lantana Park. Within each main section, results for the three wave events (Southeast waves, cold front and hurricanes) were included. For each wave event, the significant wave height and wave direction for existing condition were presented followed by the percentage difference of Hs between each alternative and existing condition. Additionally, water surface elevation timeseries were presented followed by the breaker type, water surface elevation and wave breaking for each condition. The peel angle, peel rate, wave velocity and surfer velocity were calculated from BOUSS-2D wave simulations screenshots. The Iribarren number (ξ_b) was calculated from significant wave height at breaking, deep water wave length and beach slope.

4.1. Lake Worth Pier

4.1.1. Southeast Waves (Hs 6 feet, Tp 6.1 s from 105°)

The significant wave height (Hs) for existing condition and the differences between each alternative and the existing condition at Lake Worth Pier are presented in Figure 4-1. Analyzing the wave propagation for existing condition it is observed the reduction of Hs until certain point where the waves start the shoaling process increasing Hs. The effect of the borrow area on the wave propagation is also observed. For this wave case, two wave energy focalization areas are noticed: one between R134 and R135 and another at R132. Two lobes of wave height reduction at each borrow area side are observed as a result of refraction/diffraction.

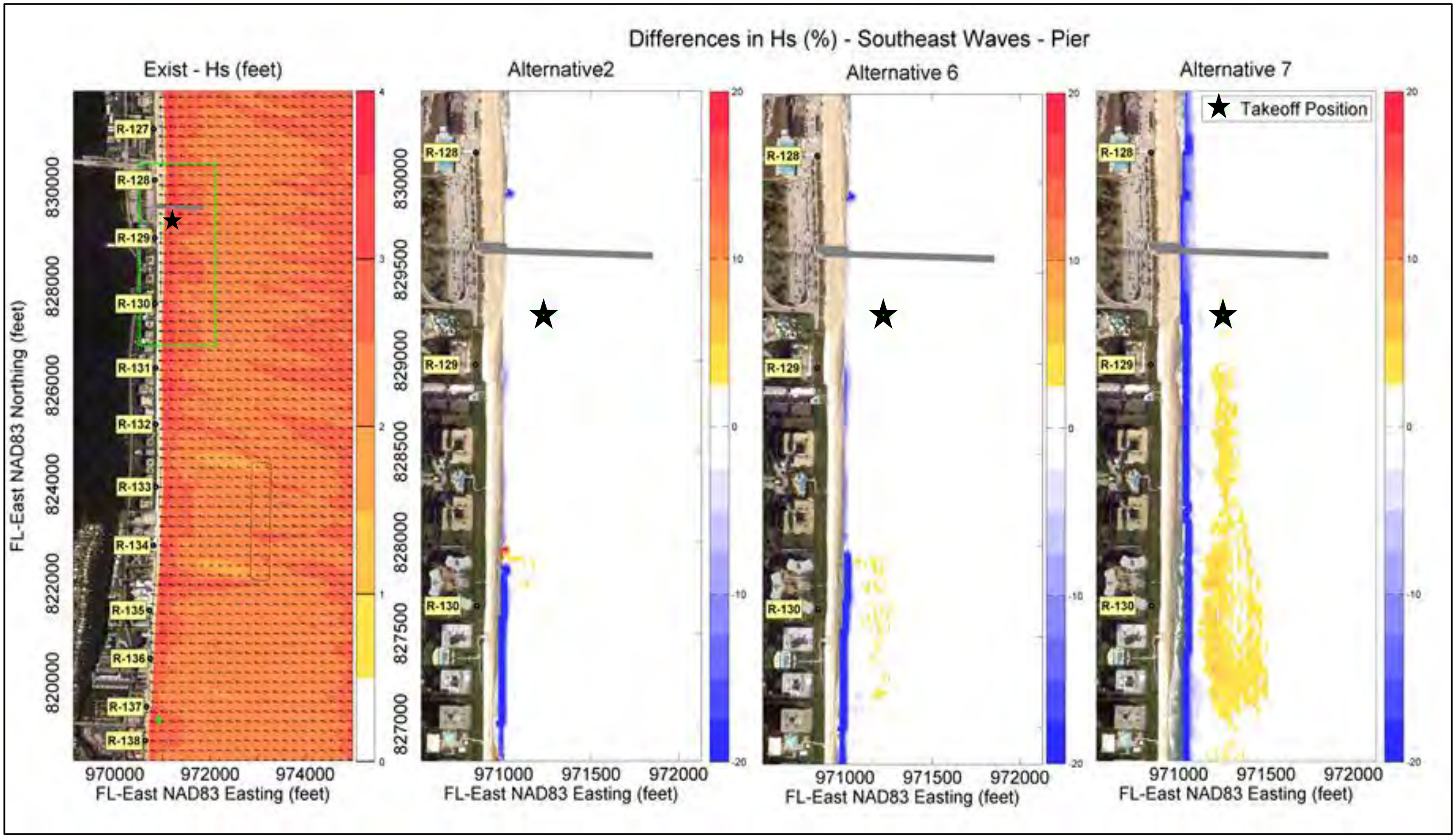

Figure 4-1. Significant wave height for existing condition and differences between each alternative and the existing condition for southeast waves at Lake Worth Pier.

Analyzing the results at the Lake Worth Pier takeoff position (point where the wave starts to break and the surfer would start to surf), it can be observed that for all alternatives there are virtually no changes in Hs. Alternative 7 shows a little variation (~2.5%) south of Lake Worth Pier's takeoff position. Alternative 7 presented the higher Hs increase at this Study Area since this alternative has the higher nourishment volume. A reduction in significant wave height is observed in very shallow water, close to the beach. This reduction should not be an issue for surfing since it happens landward of the surfing area.

Figure 4-2 presents the water surface elevation at Lake Worth Pier for existing and alternatives conditions. The analysis points are presented in Figure 3-2. All alternatives presented very similar timeseries with very small variations, indicating that, at the analyzed points, there will not be significant changes in wave propagation.

BOUSS-2D screenshots of wave simulation results are presented for Pier in Figure 4-3. The parameters calculated from these screenshots are presented in Table 4-1. At the Pier, the breaker type did not change between existing condition and the alternatives. This breaker was classified as a spilling breaker type. The peel angle was 46° (rating of 6) for existing condition. A faster wave section was observed for all alternatives, as evident by the increased peel angle. These peel angles were anticipated to result in "close-outs" ending the ride experienced by the surf. For the same wave velocity, the peel rate increased and consequently, the surfer velocity increased from existing condition to alternatives.

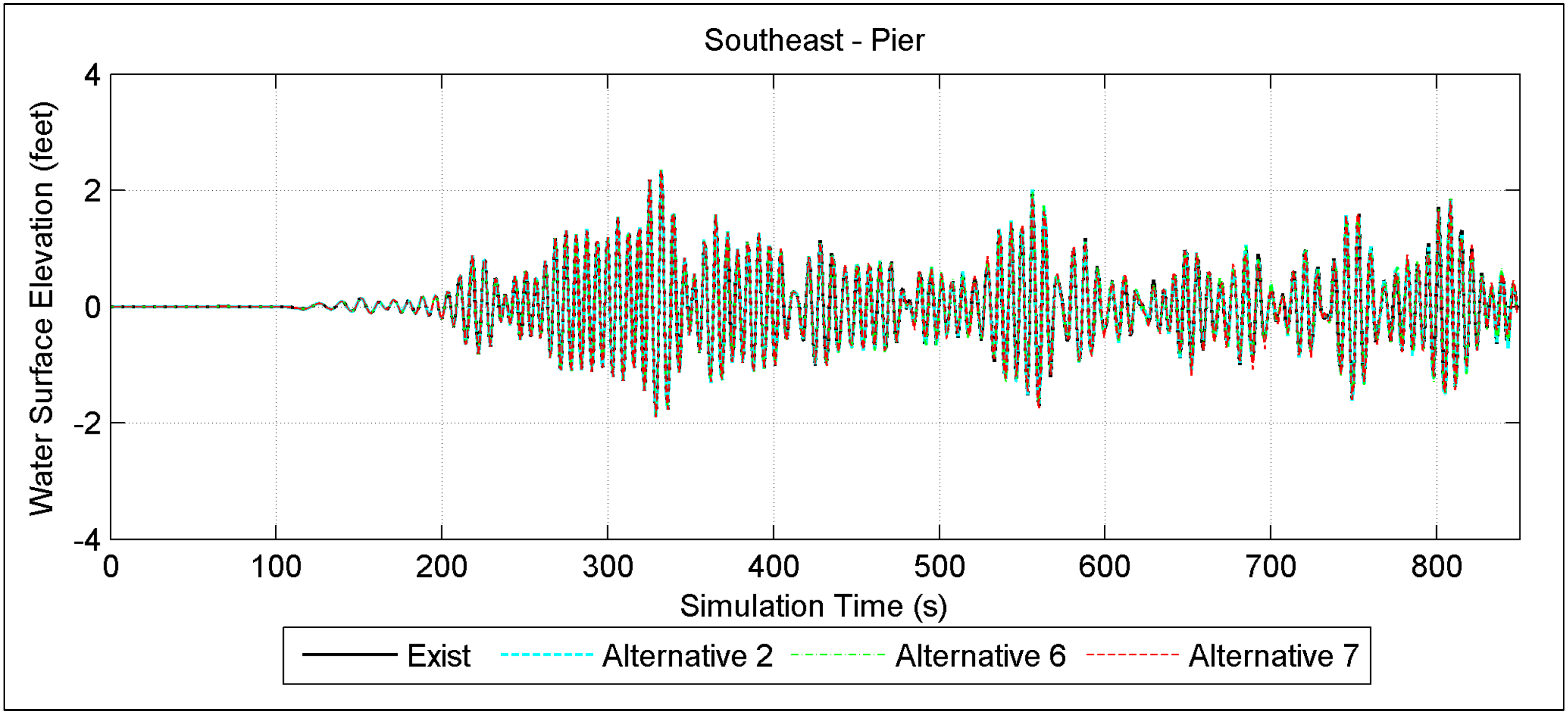

Figure 4-2. Water surface elevation at Lake Worth Pier for southeast waves.

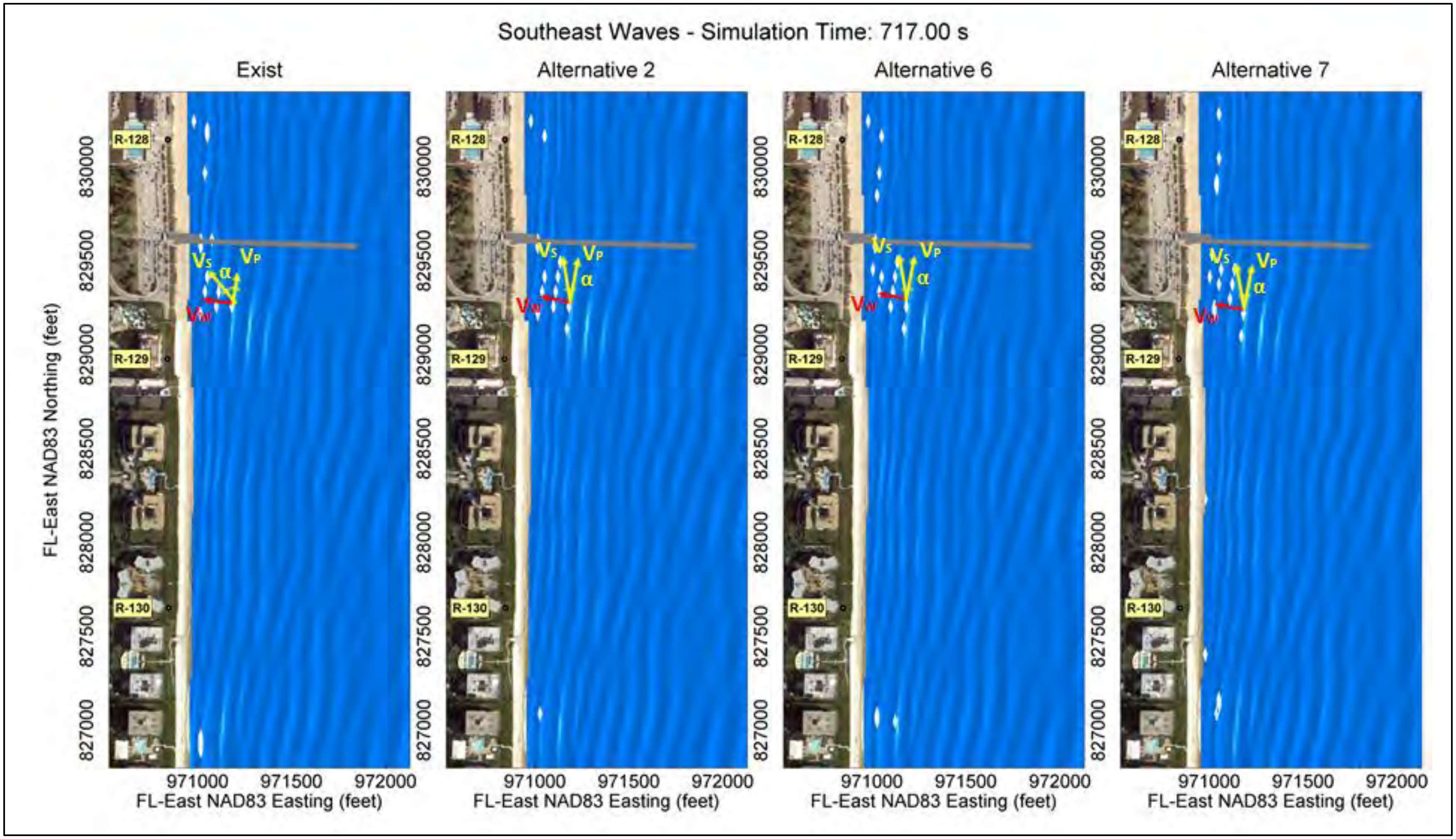

Figure 4-3. Peel angle (α), peel rate (Vp), wave velocity (Vw) and surfer velocity (Vs) identification for southeast waves at the Pier.

Table 4-1. Comparison of existing conditions and alternatives for southeast waves at the Pier.

Condition	ξ_b	Peel angle (°)	Velocity of wave (mph)	Peel rate (mph)	Velocity of surfer (mph)
Existing	0.3	46	9.1	8.7	12.6
Alternative 2	0.2	17	9.3	30.5	31.9
Alternative 6	0.2	16	9.3	32.4	33.7
Alternative 7	0.2	19	9.3	27.0	28.5

4.1.2. Cold Front (Hs 7.4 feet, Tp 11 s from 65°)

For cold front scenarios at Pier, the significant wave height (Hs) for existing condition and the differences between alternatives are presented in Figure 4-4. The wave propagation for existing condition shows shoaling at approximately 1,200 feet from the beach shoreline and it also shows a reduction of Hs, related to wave breaking, at approximately 1,000 feet from the dry beach. Two points of wave focalization are observed, these points are caused by wave refraction/diffraction over the borrow area. One point is located between R132 and R133, and the other at R135. The differences in Hs between alternatives and existing conditions occur only shoreward of wave breaking. This event indicates that the bathymetric changes generated by alternatives do not impact the wave heights at surfing area. Figure 4-4 presents the takeoff position of analyzed waves where it is clear that no changes higher than 2.5% in wave height occur at the takeoff position.

Figure 4-5 presents the water surface elevation at Lake Worth Pier for existing and alternatives conditions at the analysis points presented in Figure 3-2. All alternatives presented very similar timeseries with very small variations, indicating that, at the analyzed points, there will not be significant changes in wave propagation.

BOUSS-2D wave simulations screenshots at Pier are presented in Figure 4-6. The parameters calculated from these screenshots are presented in Table 2-2. The breaker type for Lake Worth Pier for all simulated scenarios and alternatives leads to a Spilling break with ξ_b of 0.3. Existing condition presented the same peel angle and peel rate as Alternatives 2 and 6.

Table 2-2. Comparison of existing and alternatives conditions for cold front at Pier.

Condition	ξ_b	Peel angle (°)	Velocity of wave (mph)	Peel rate (mph)	Velocity of surfer (mph)
Existing	0.3	60	14.2	8.2	16.5
Alternative 2	0.3	60	14.3	8.2	16.5
Alternative 6	0.3	60	14.2	8.2	16.4
Alternative 7	0.3	70	14.2	5.2	15.1

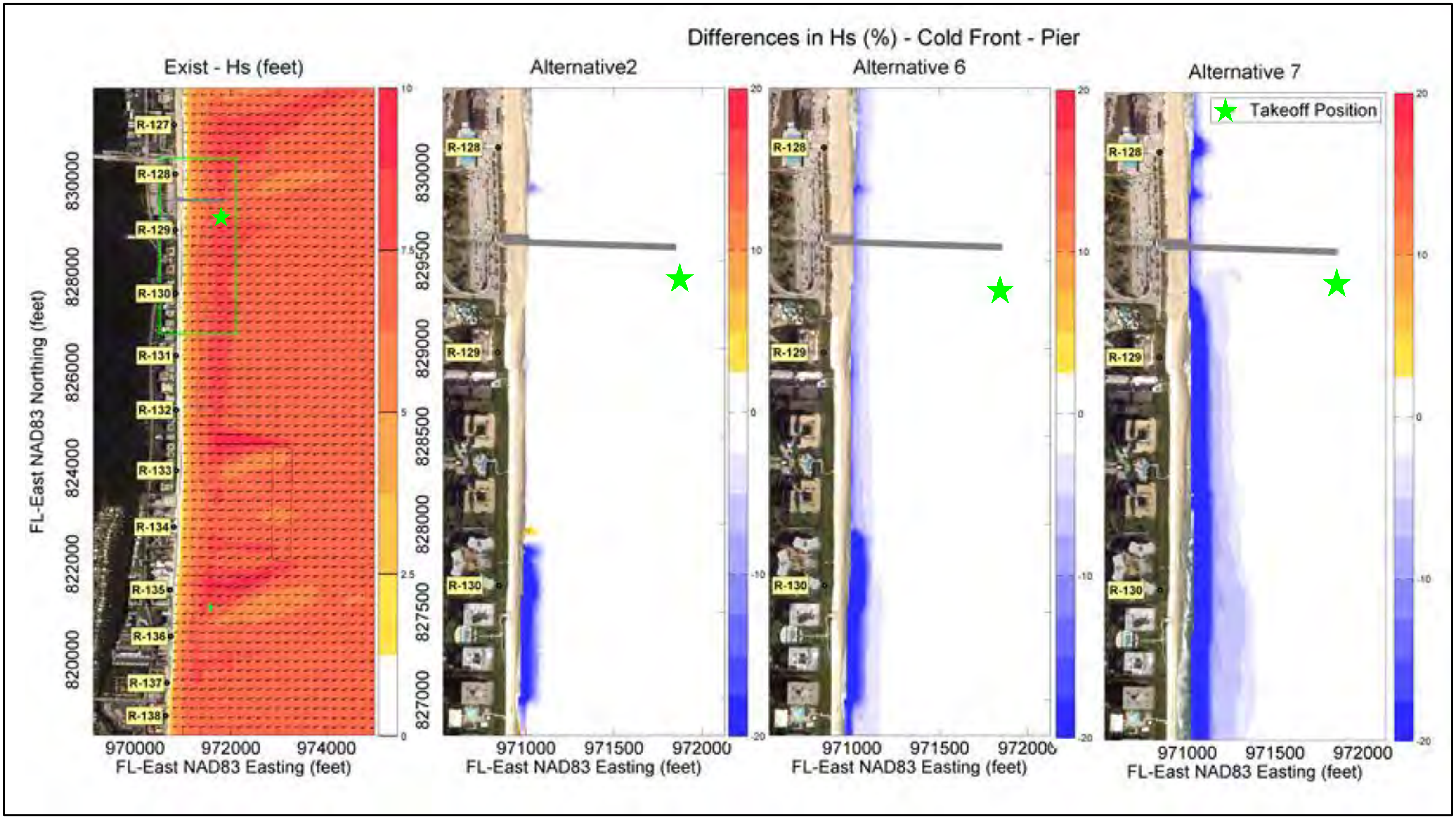

Figure 4-4. Significant wave height for existing condition and differences between each alternative and the existing condition for cold front scenario at Pier.

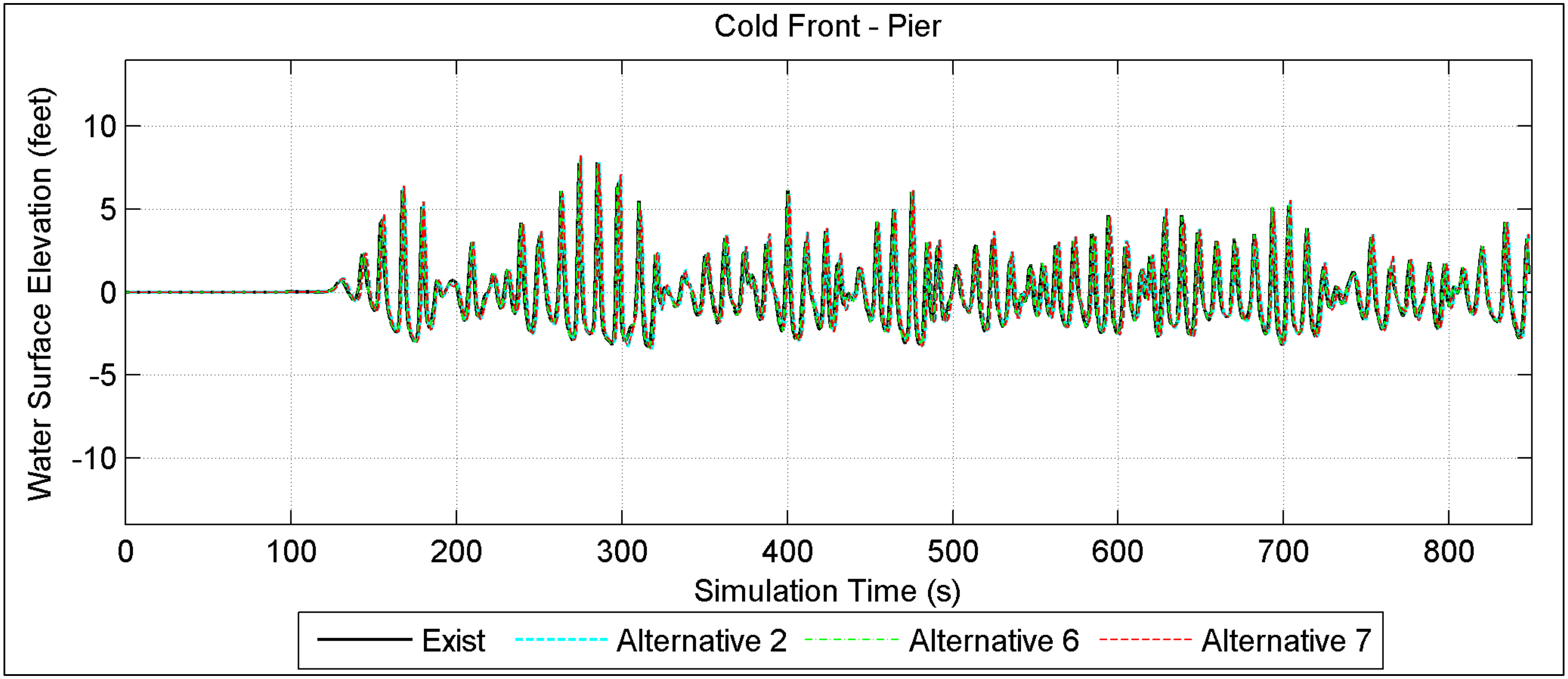

Figure 4-5. Water surface elevation at Pier for cold front.

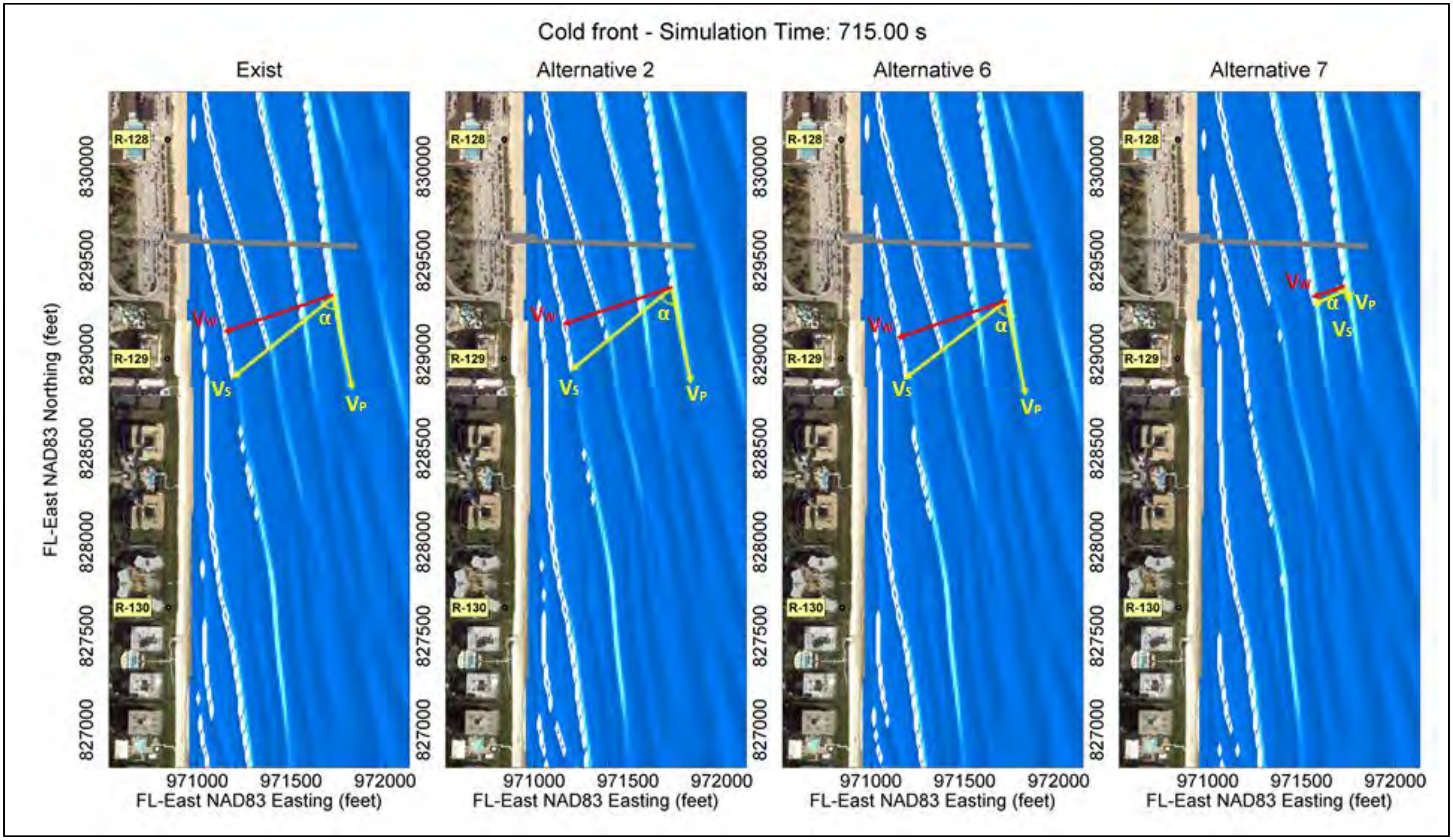

Figure 4-6. Peel angle (α), peel rate (Vp), wave velocity (Vw) and surfer velocity (Vs) identification for cold front at Pier.

4.1.3. Hurricane Pre-Landfall (Hs 8.1 feet, Tp 13.5 s from 103°)

For hurricane pre-landfall scenario, the significant wave height (Hs) for existing condition and the differences between existing and alternatives are presented in Figure 4-7. The wave propagation shows that for this condition, shoaling starts at approximately 2,000 feet from the beach shoreline and the wave breaks at approximately 1,000 feet from dry beach. As for the other wave conditions, for hurricane pre-landfall it is observed an Hs focalization caused by wave refraction/diffraction at the borrow pit. In this case, the wave height is focuses at R132 and between R133 and R134. For all alternatives it is observed a reduction of wave height near the coast due to reduction of depth at that area and increase of bottom friction and/or wave breaking. As Alternative 7 present higher nourishment volumes, the differences are more noticeable in this alternative. This condition presents higher Hs as well as higher wave period compared to the other conditions, the waves will break in deeper water (compared to cold front and southeast waves) and the differences in wave height are not observed at surf areas.

Figure 4-8 presents the water surface elevation at Lake Worth Pier for existing and alternatives conditions, at the analysis points presented in Figure 3-2. All alternatives presented very similar timeseries with very small variations, indicating that at the analyzed points, there will not be significant changes in wave propagation.

Screenshots of hurricane pre-landfall simulations are presented in Figure 4-9. The parameters calculated from these screenshots are presented in Table 4-3. The breaker type for Lake Worth Pier for all simulated scenarios and alternatives are spilling break with ξ_b of 0.3 for all analyzed waves.

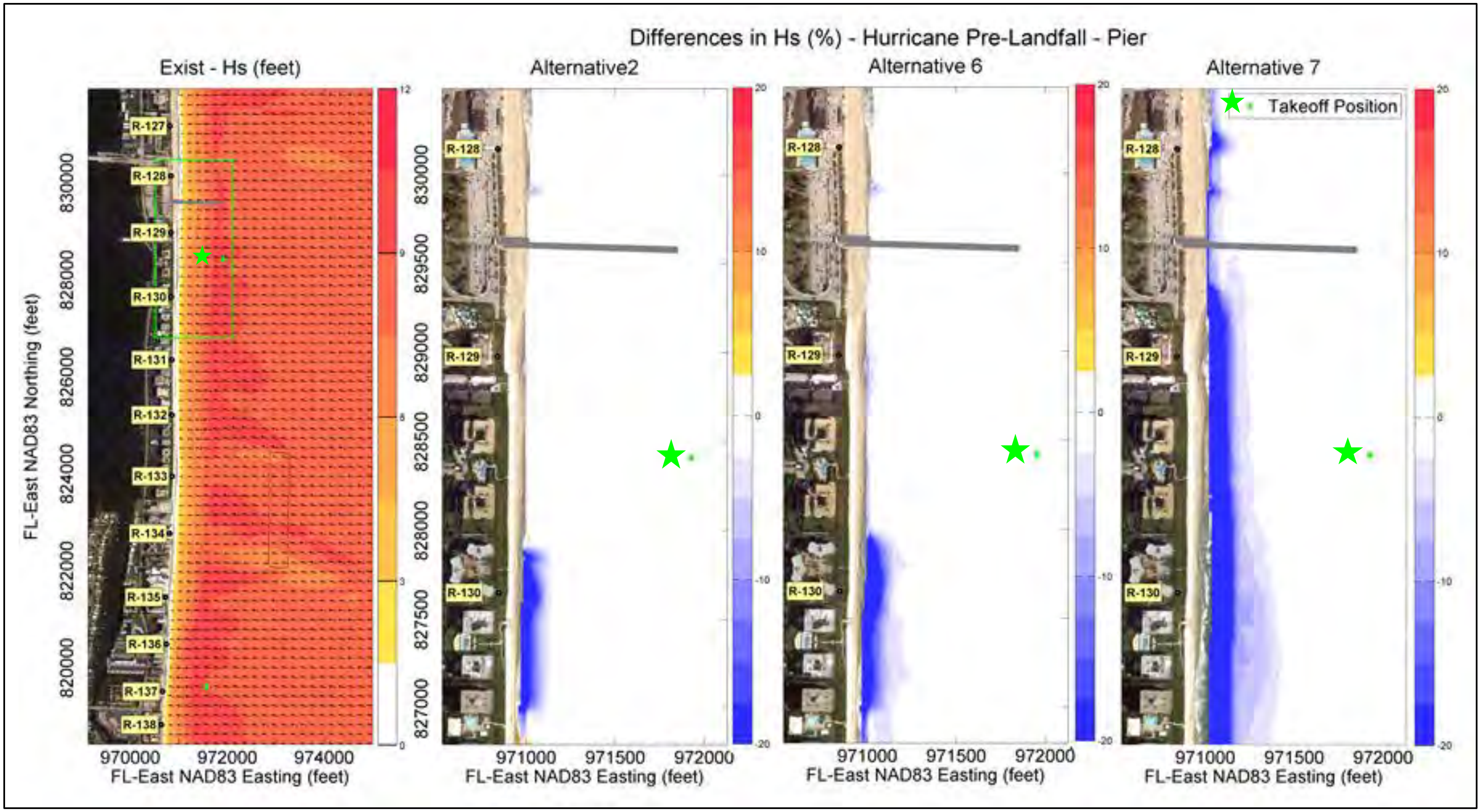

Figure 4-7. Significant wave height for existing condition and differences between each alternative and the existing condition for pre-hurricane at Pier.

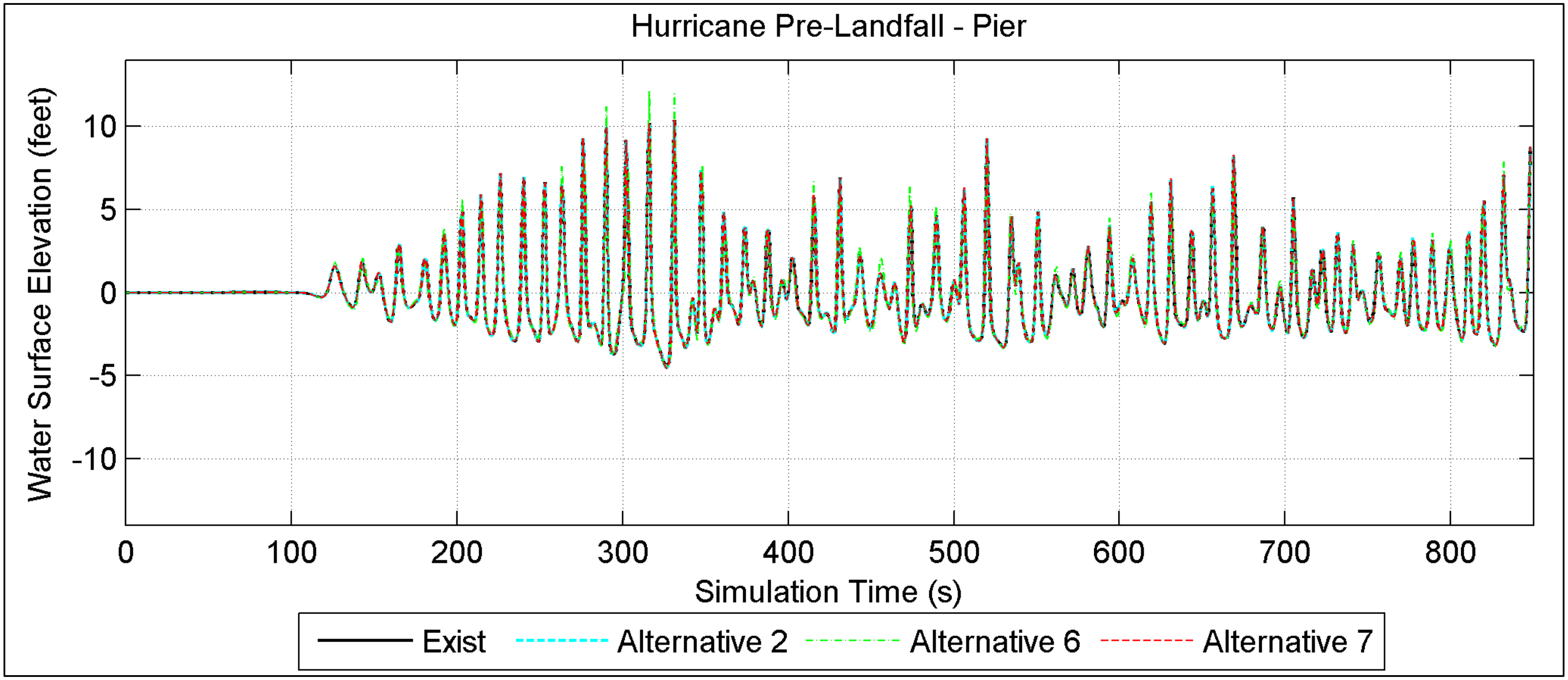

Figure 4-8. Water surface elevation at Pier for hurricane pre-landfall.

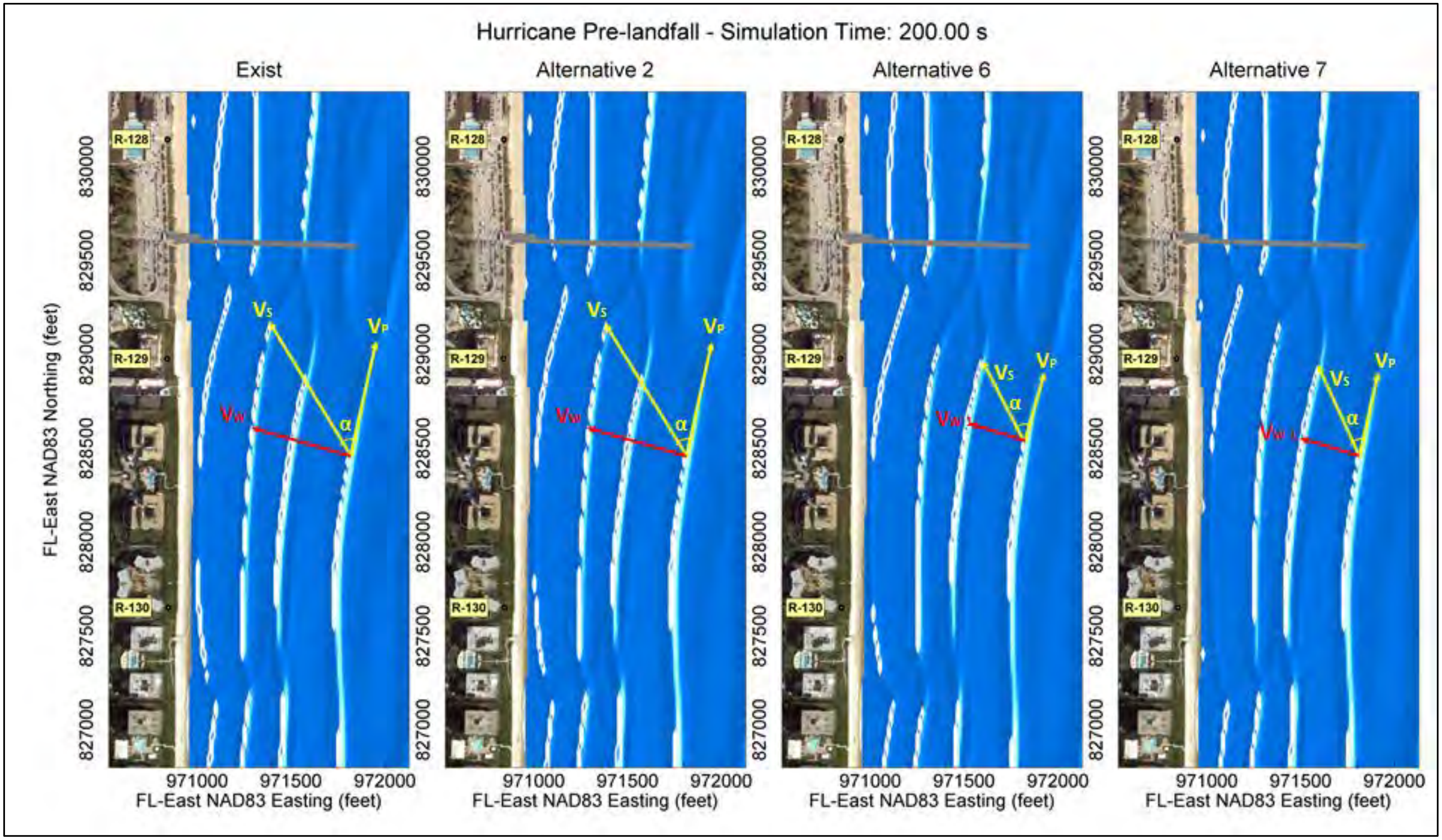

Figure 4-9. Peel angle (α), peel rate (Vp), wave velocity (Vw) and surfer velocity (Vs) identification for hurricane pre-landfall at the Pier.

Table 4-3. Comparison of existing and alternatives conditions for hurricane pre-landfall at Pier.

Condition	ξ_b	Peel angle (°)	Velocity of wave (mph)	Peel rate (mph)	Velocity of surfer (mph)
Existing	0.3	45	15.1	15.1	21.4
Alternative 2	0.3	45	15.4	15.4	21.8
Alternative 6	0.3	42	15.8	17.5	23.6
Alternative 7	0.3	38	15.3	19.6	24.9

4.2. Lantana Park

4.2.1. Southeast Waves (Hs 6 feet, Tp 6.1 s from 105°)

The significant wave height (Hs) for existing condition and the differences between each alternative and the existing condition at Lake Worth Pier are presented in Figure 4-10. Analyzing the impact of alternatives in Hs, it is observed an increasing of significant wave height at Lantana Park area around the takeoff position. This increase in Hs is primarily due to the larger amounts of sediment located where the wave starts to “touch” the bottom before starting its shoaling process.

Figure 4-11 presents the water surface elevation at Lantana Park for existing and alternatives conditions. The analysis points are presented in Figure 3-2. All alternatives presented very similar timeseries with very small variations, indicating that, at the analyzed points, there will not be significant changes in wave propagation.

BOUSS-2D wave simulations screenshots at Lantana are presented in Figure 4-12. The parameters calculated from these screenshots are presented in Table 4-4.

The breaker type at Lantana did not change between the existing condition and the alternatives. For all cases the Iribarren calculated was 0.2, indicating a spilling break type. It is noted that the takeoff position in Alternative 7 is further landward than in other alternatives and the existing condition. This can be due to wave energy dissipation over the bottom. Since Alternative 7 is shallower, the wave dissipates more energy before breaking and this dissipation leads the wave to break closer to the shore. The existing condition and Alternative 2 would be rated a 5 in Hunt *et al.* (2001) classification (see Table 2-1), as compared to a 6 for Alternative 6 and a 7 for Alternative 7. The velocity of wave did not change significantly between alternatives and existing condition.

Table 4-4. Comparison of existing conditions and alternatives for southeast waves at Lantana.

Condition	ξ_b	Peel angle (°)	Velocity of wave (mph)	Peel rate (mph)	Velocity of surfer (mph)
Existing	0.2	54	10.5	7.6	13.0
Alternative 2	0.2	55	10.3	7.2	12.6
Alternative 6	0.2	47	10.4	9.7	14.2
Alternative 7	0.2	26	10.4	21.2	23.6

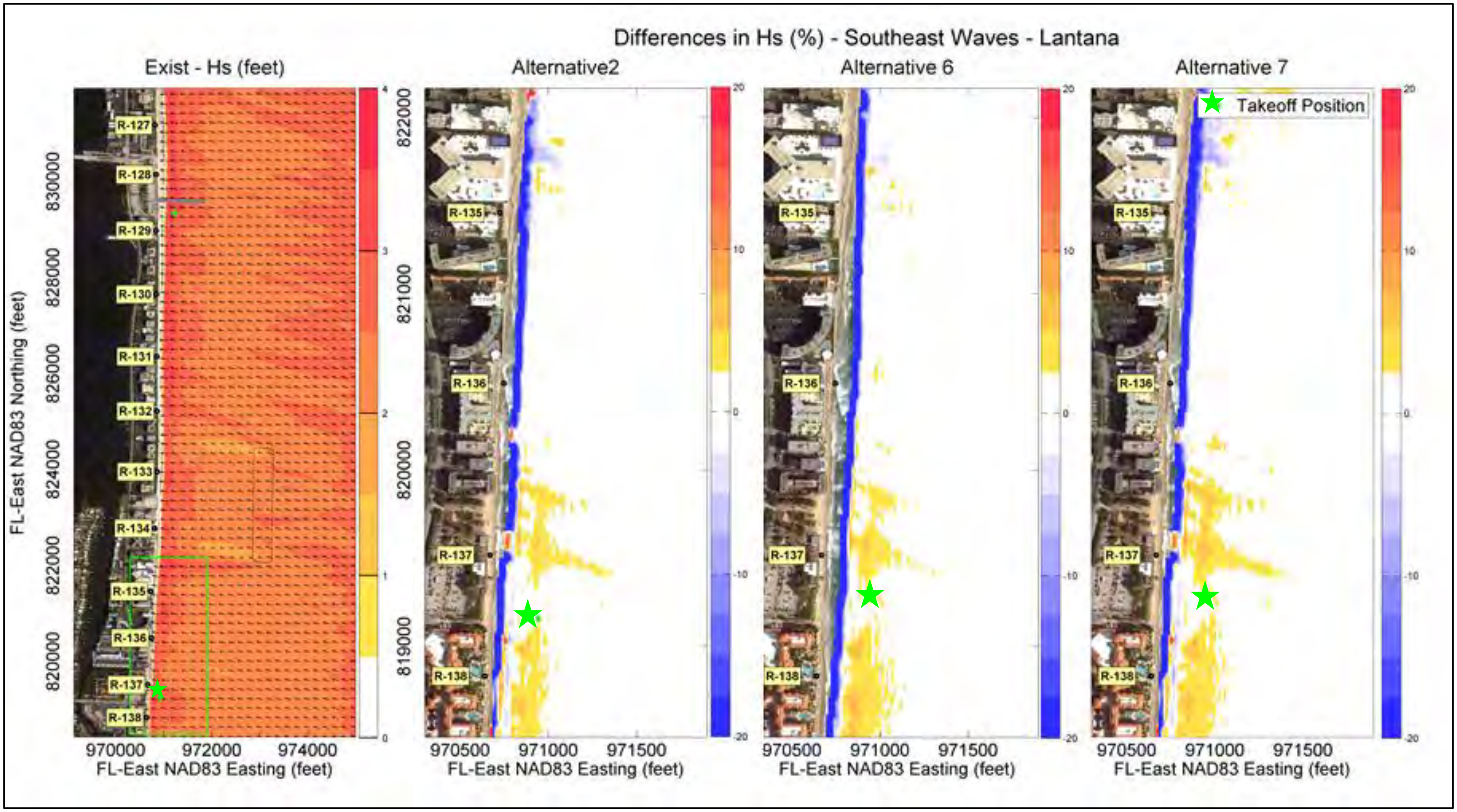

Figure 4-10. Significant wave height for existing condition and differences between each alternative and the existing condition for southeast waves at Lantana Park.

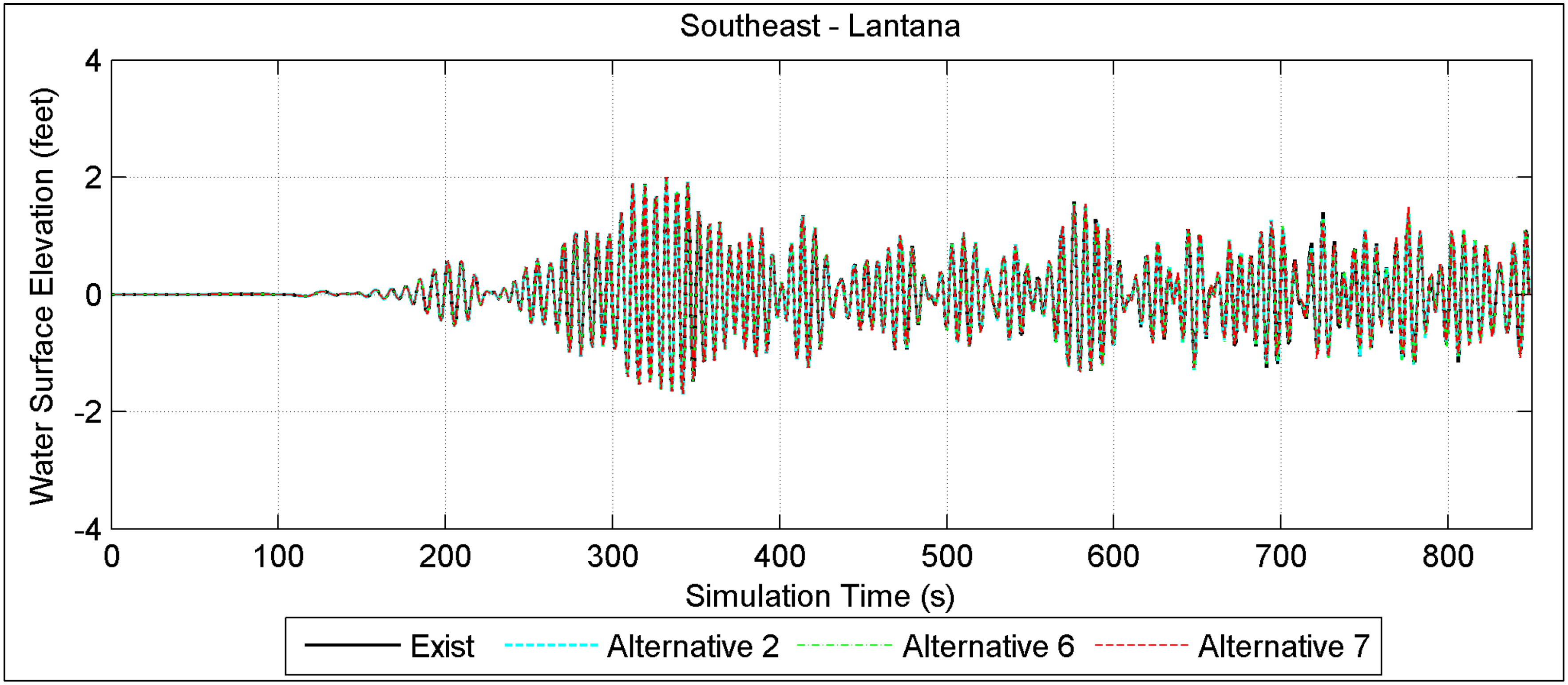

Figure 4-11. Water surface elevation at Lantana Park for southeast waves.

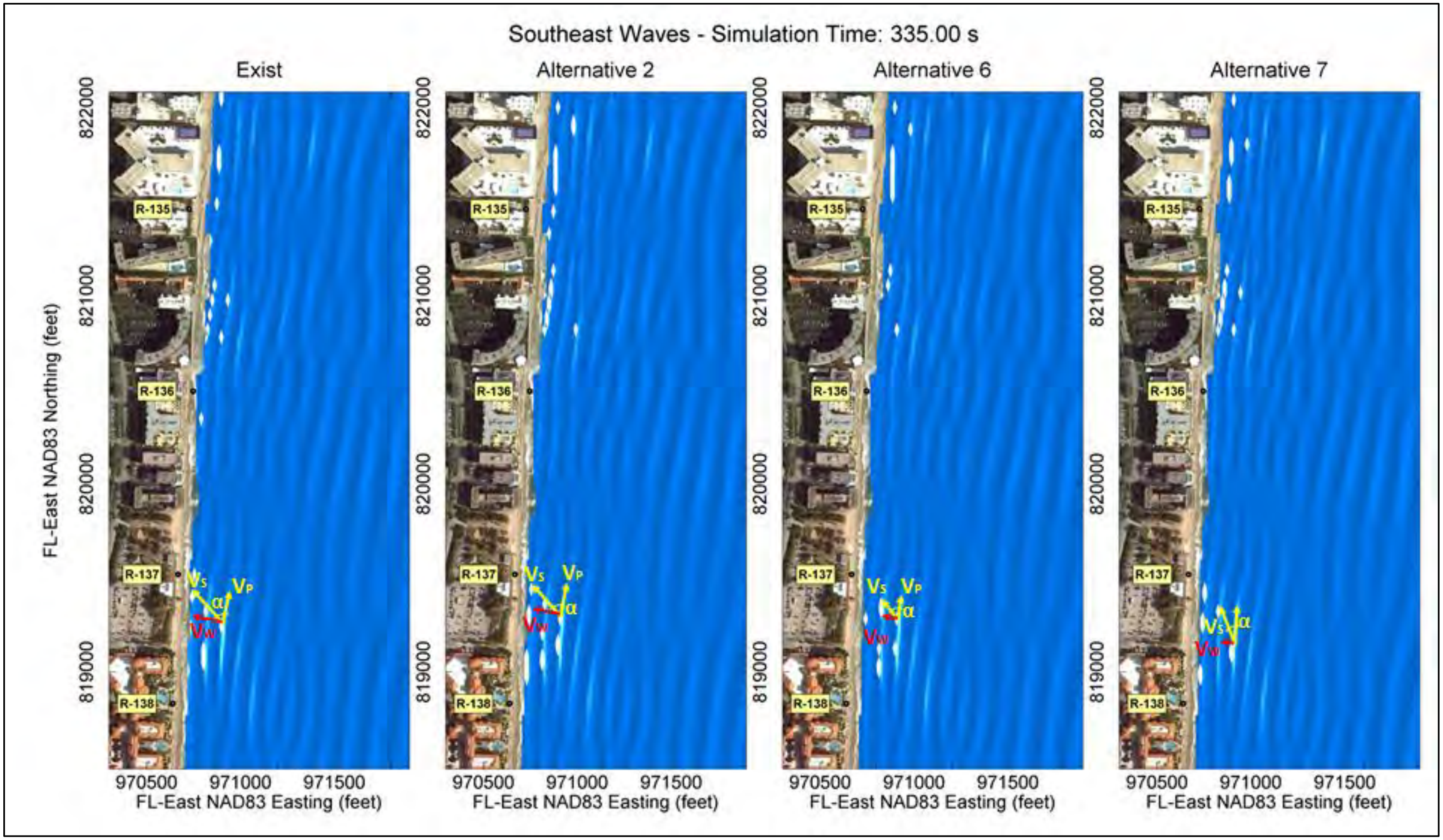

Figure 4-12. Peel angle (α), peel rate (Vp), wave velocity (Vw) and surfer velocity (Vs) identification for southeast waves at Lantana.

4.2.2. Cold Front (Hs 7.4 feet, Tp 11 s from 65°)

For cold front scenarios at Lantana, the significant wave height (Hs) for existing condition and the differences between alternatives are presented in Figure 4-13. The differences in Hs between alternatives and existing conditions occur only shoreward of wave breaking, indicating that the bathymetric changes generated by alternatives does not impact the wave heights at surfing area. Figure 4-13 presents the takeoff position of analyzed waves where it is clear that no changes higher than 2.5% in wave height occur.

Figure 4-14 presents the water surface elevation at Lantana Park for existing and alternatives conditions at the analysis points presented in Figure 3-2. All alternatives presented very similar timeseries with very small variations, indicating that, at the analyzed points, there will not be significant changes in wave propagation.

Bouss2D wave simulations screenshots for cold front waves at Lantana are presented in Figure 4-15. The parameters calculated from these screenshots are presented in Table 4-5. The breaker type for Lantana Beach Park for all simulated scenarios and alternatives leads to a Spilling break with ξ_b of 0.3.

For Lantana, existing condition and Alternatives 2 and 6 are likely for surfers of rating 6 (Hunt *et al.* 2001), Alternative 7 presented a sharper peel angle and it is likely to be surfed by surfers rated as 7 or higher. The velocity of wave for all simulated cases is 15 mph. Alternative 7 increased its surfer velocity to 24.8 mph as a result of peel angle sharpening.

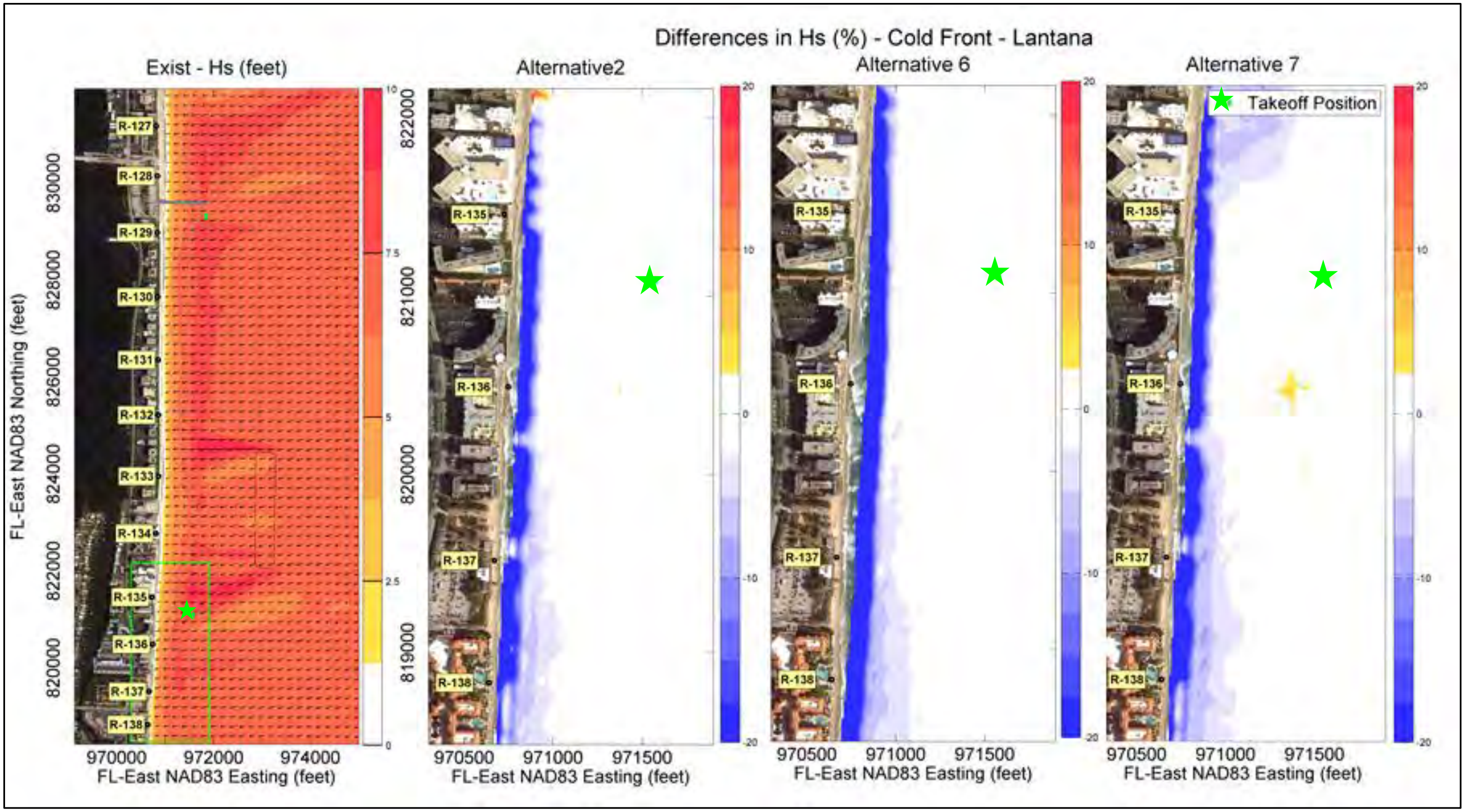

Figure 4-13. Significant wave height for existing condition and differences between each alternative and the existing condition for cold front scenario at Lantana.

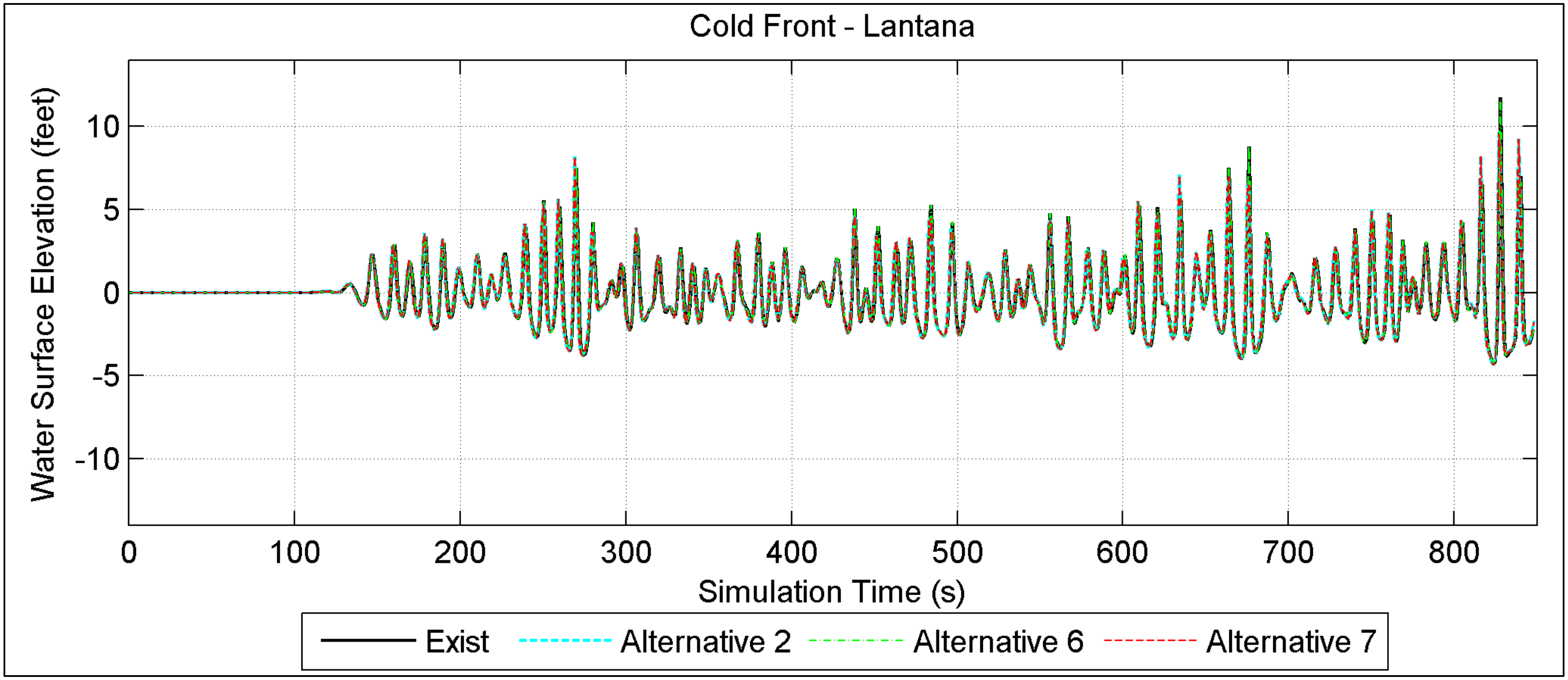

Figure 4-14. Water surface elevation at Lantana for cold front.

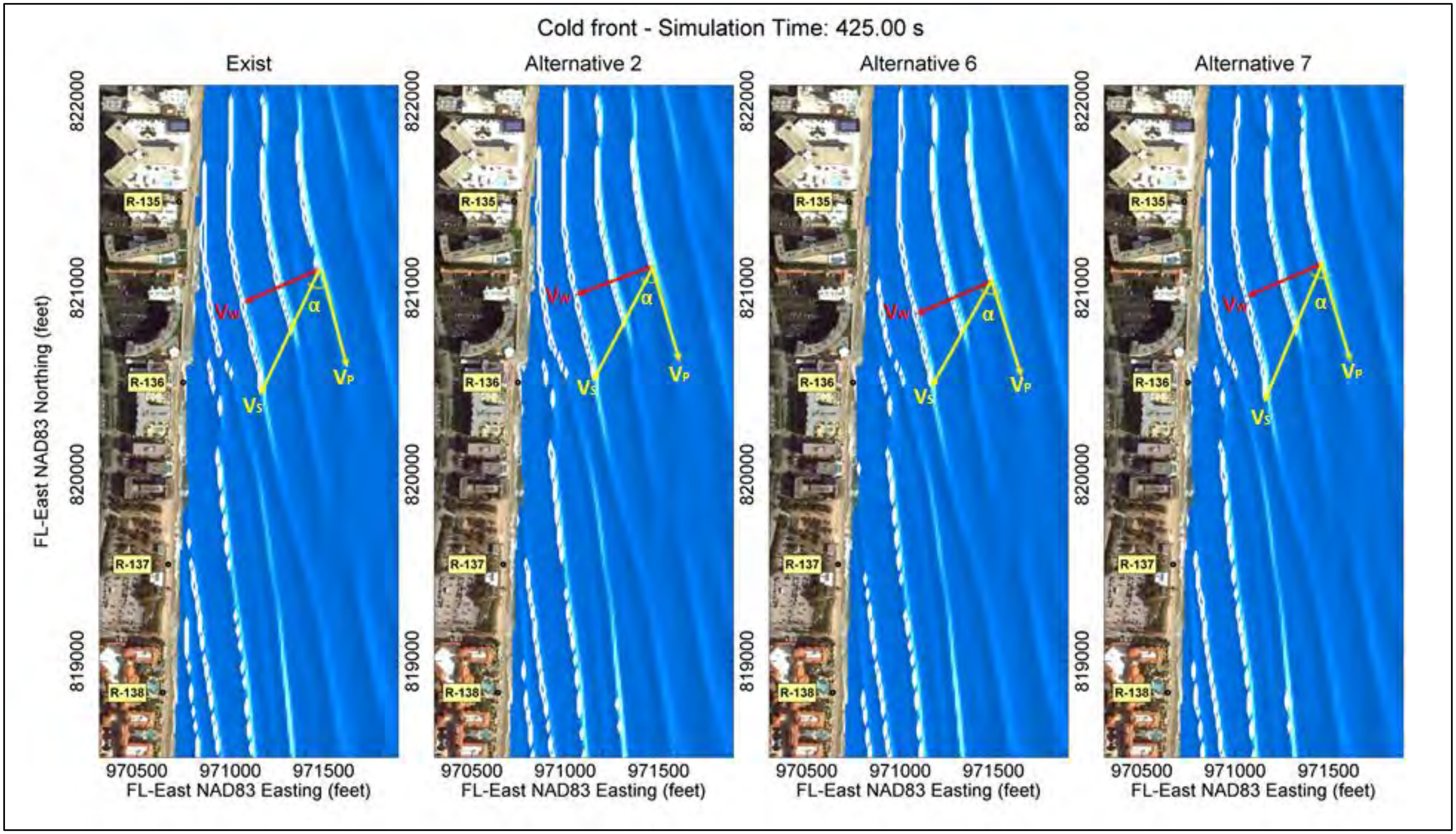

Figure 4-15. Peel angle (α), peel rate (Vp), wave velocity (Vw) and surfer velocity (Vs) identification for cold front at Lantana.

Table 4-5. Comparison of existing and alternatives conditions for cold front at Lantana.

Condition	ξ_b	Peel angle (°)	Velocity of wave (mph)	Peel rate (mph)	Velocity of surfer (mph)
Existing	0.3	40	15.0	17.8	23.3
Alternative 2	0.3	43	15.0	16.0	21.9
Alternative 6	0.3	44	15.0	15.5	21.5
Alternative 7	0.3	37	15.0	19.8	24.8

4.2.3. Hurricane Pre-Landfall (Hs 8.1 feet, Tp 13.5 s from 103°)

Figure 4-16 presents the differences in significant wave height at Lantana. For all alternatives it is observed a reduction of wave height near the coast due to reduction of depth at that area and increase of bottom friction and/or wave breaking. As Alternative 7 present higher nourishment volumes, the differences are more noticeable in this alternative. This condition presents higher Hs as well as higher wave period compared to the other wave conditions. For hurricane pre-landfall condition, the waves break in deeper water (compared to cold front and southeast waves) and the differences in wave height are not observed at surf areas.

Figure 4-17 presents the water surface elevation at Lantana for existing and alternatives conditions, at the analysis points presented in Figure 3-2. All alternatives presented very similar timeseries with very small variations, indicating that at the analyzed points, there will not be significant changes in wave propagation.

Screenshots of hurricane pre-landfall simulations are presented in Figure 4-18. The parameters calculated from these screenshots are presented in Table 4-6. The breaker type for both Lantana Beach Park and Lake Worth Pier for all simulated scenarios and alternatives are spilling break with ξ_b of 0.3 for all analyzed waves.

At Lantana, the peel angle for existing condition is 63°, good for surfers rated as 3 (Hunt *et al*, 2001), for Alternatives 2 (59°), 6 (58°) and 7 (58°), the peel angle decrease a little and it would be good for surfers rated as 4.

Table 4-6. Comparison of existing and alternatives conditions for hurricane pre-landfall at Lantana.

Condition	ξ_b	Peel angle (°)	Velocity of wave (mph)	Peel rate (mph)	Velocity of surfer (mph)
Existing	0.3	63	16.4	8.3	18.4
Alternative 2	0.3	59	16.3	9.8	19.1
Alternative 6	0.3	58	16.4	10.2	19.3
Alternative 7	0.3	58	16.3	10.2	19.3

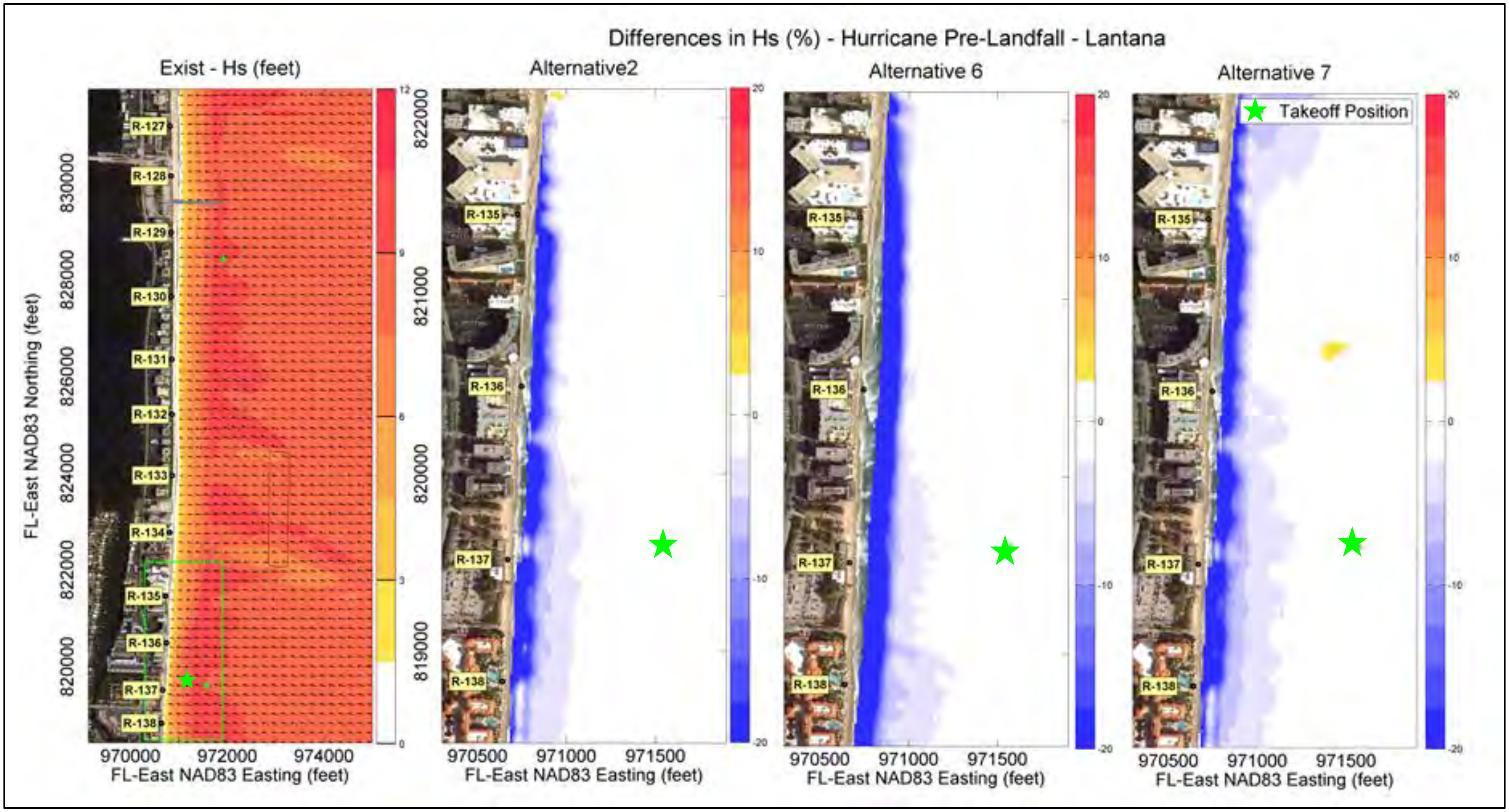

Figure 4-16. Significant wave height for existing condition and differences between each alternative and the existing condition for pre-hurricane at Lantana Park.

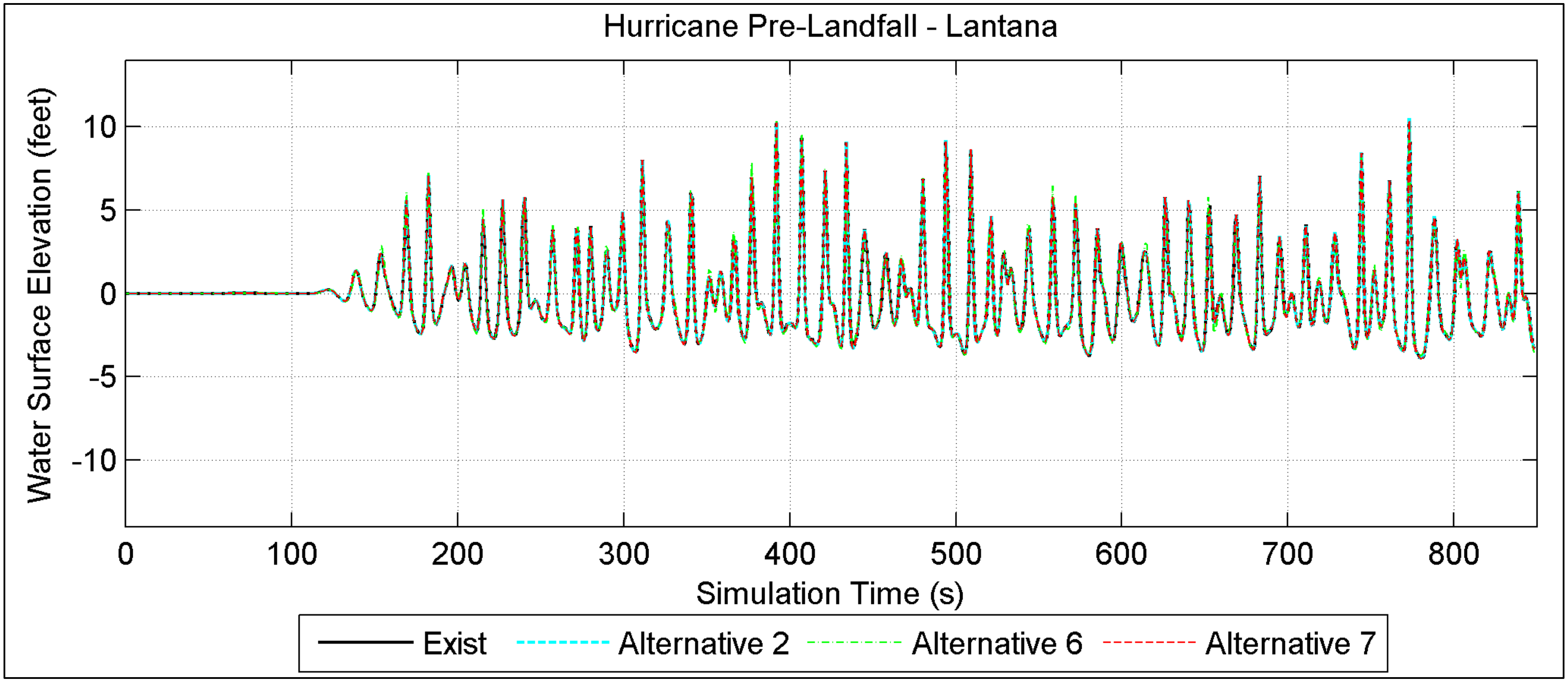

Figure 4-17. Water surface elevation at Lantana for hurricane pre-landfall.

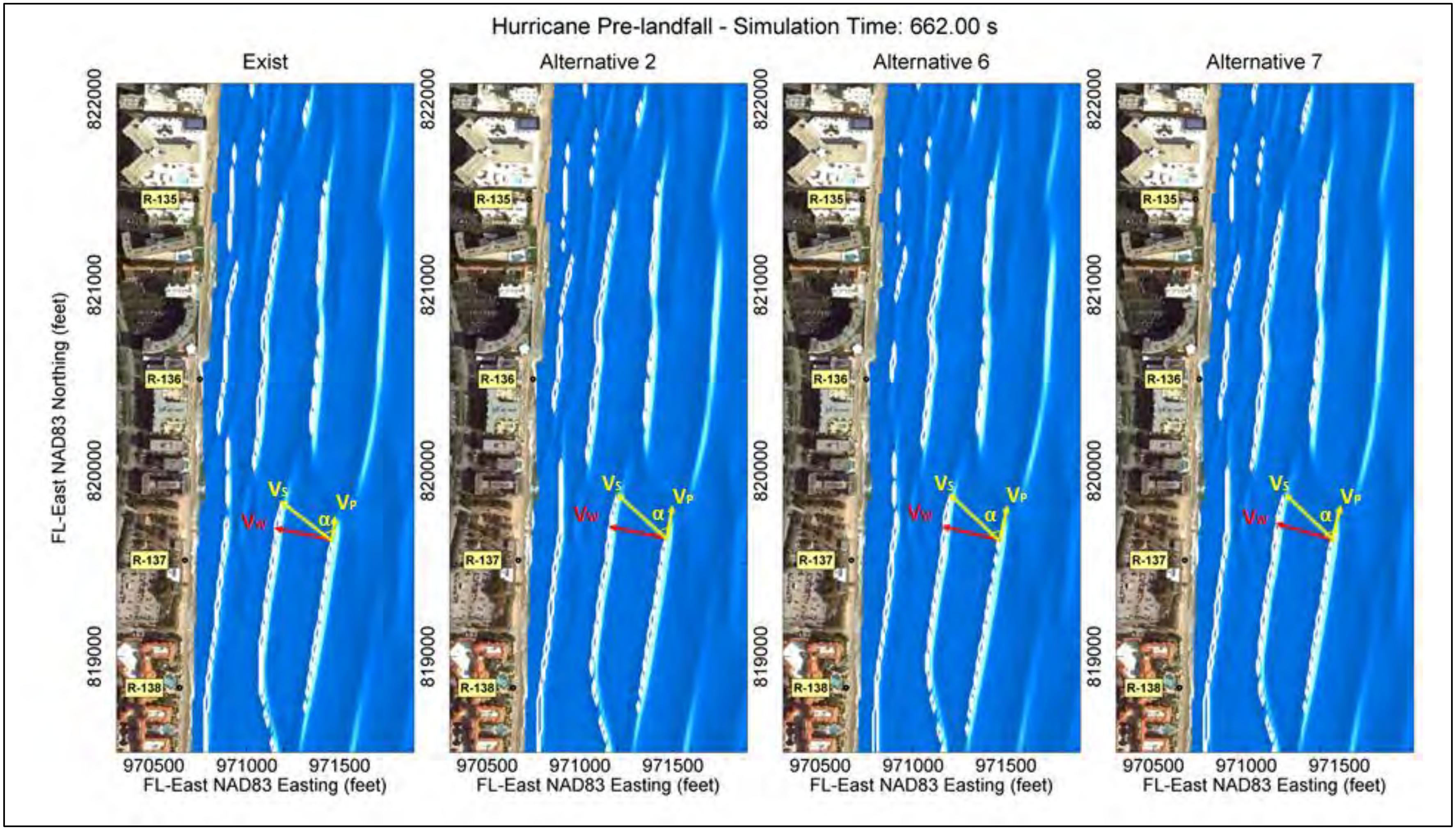

Figure 4-18. Peel angle (α), peel rate (Vp), wave velocity (Vw) and surfer velocity (Vs) identification for hurricane pre-landfall at Lantana.

5.0 SUMMARY AND CONCLUSIONS

A numerical modeling study utilizing BOUSS-2D model was conducted to simulate the potential impacts of Project alternatives to surfability at two points: nearby Lantana Beach Park and at the Lake Worth Pier. Three wave conditions: (i) southeast, (ii) cold front and (iii) hurricane pre-landfall, were used for model verification and model runs. The significant wave height for existing conditions was analyzed as well as the relative differences (%) between existing and alternatives. In addition, the main parameters to assess surfability (Iribarren number ξ_b, peel angle, velocity of wave, peel rate and velocity of surfer) were studied to evaluate the quality of wave for surfing.

The main conclusions of this BOUSS2D study are as follows:

- The minimum skill level required of surfers to surf at the two locations was rated at 5 (out of 10), representing an intermediate skill level.

- Differences of significant wave heights (Hs) between existing and alternatives scenarios were more noticeable for alternatives with higher amount of sediment placement.

- A decrease of wave height was observed near the beach for all alternatives. This decrease would not impact surfing directly since it happened after wave breaking, landward of surfing area.

- The wave condition that showed more impact from the alternatives was the southeast waves. Under this condition (smaller waves with smaller periods) the waves would break close to the beach where the differences in bathymetry (between alternatives and existing) are higher. For hurricane and cold front wave conditions (higher waves with higher periods) the waves would break offshore where the bathymetry presents little or no differences between existing and alternatives.

- An increase of wave height before wave breaking is observed for southeast waves conditions in Alternative 7. This wave height increase is noticed due to the combination of the wave condition used in the model and the bathymetry of Alternative 7. The southeast wave condition have the smallest simulated wave height and period and Alternative 7 presents the highest amount of sediment placed.

- In general, a small variation in peel angle, peel rate and velocity of surfer was observed in all the simulations for the different alternatives. The changes in the surfability at the two locations due to the alternatives were also small.

The results of this numerical modeling study should be used in conjunction with other coastal engineering assessments and prudent engineering judgment.

6.0 LITERATURE CITED

Battjes, J. A., 1974. Surf Similarity. Coastal Engineering. 466-480 p.

Benedet, L., Pierro T., and Henriquez, M., 2007. Impacts of coastal engineering projects on the surfability of sandy beaches. Shore & Beach, Volume 75, No. 4, Fall 2007, American Shore & Beach Preservation Association, Ft. Myers, FL, pp 3-20.

Black, K.P., 2001. Artificial Surfing Reefs for Erosion Control and Amenity; Theory and Application. Special Issue 34 (ICS 2000), Journal of Coastal Research, pp 1-7. 312.

Black, K.P.; and S. Mead 2001 Design of the Gold Coast Artificial Surfing Reef: Surfing Aspects. In: K. Black (ed) Natural and Artificial Reefs for Surfing and Coastal Protection. Special Issue 29 , Journal of Coastal Research, pp 115-130.

Coastal Planning and Engineering, 2009. Boussinesq Wave Modelling for Evaluation of Impact of Proposed Structures on Surfing Conditions. Technical Report. 48p.

Dafferner, G. and da F. Klein, A.H., 2009. "The Relationship Between Morphodynamics and Surfability at Brava Beach, Southern Brazil." Reef Journal, 1(1): 153-161.

Demirbilek, Z., Zundel, A., Nwogu, O., 2005, BOUSS-2D Wave Model in the SMS: 1. Graphical Interface. US Army Corps of Engineers – Engineer Research and Development Center. , Vicksburg, MS.

Goda, Y., 1985. A new method of wave pressure calculation for design of composite breakwater, Proceedings 14th international conference on Coastal, ASCE. Pp 1702-1720.

Hubertz, J.M., 1992, “User’s Guide to the Wave Information Studies (WIS) Wave Model: Version 2.0”, WIS Report 27, US Army Corps of Engineers, Waterways Experiment Station, Vicksburg, MS, 41 pp.

Hutt, J.A.; Black, K.P.; Mead, S.T., 2001. Classification of surf breaks in relation to surfing skill. Journal of Coast Research. SI 29. 66-81 p.

Nwogu, O., 1993. Alternative form of Boussinesq equations for nearshore wave propagation. Journal of Waterway, Port, Coastal and Ocean Engineering, ASCE, 119(6), 618-638.

Nwogu, O., 1996. Numerical prediction of breaking waves and currents with a Boussinesq model. Paper presented at the 25th International Conference on Coastal Engineering, ICCE '96, Orlando, FL.

Nwogu, O., and Demirbilek, Z., 2001. BOUSS-2D: A Boussinesq wave model for coastal regions and harbors. ERDC/CHL TR-01-25, U.S. Army Engineer Research and Development Center, Vicksburg, MS.

Peregrine, D. H., 1967. Long waves on a beach. Journal of Fluid Mechanics 27, 815-827.

Scarfe, B. E., Elwany, M. H. S., Mead, S. T. and Black, K. P., 2003. The science of surfing waves and surfing breaks – A review. Scripps Institution of Oceanography – UC San Diego. Technical Report. 1- 12.

Walker, J.R. 1974. Recreational Surf Parameters, Technical Report 30, Look Laboratory, University of Hawaii, 311 pp

Wei, G., Kirby, J. T., Grilli, S. T., and Subramanya, R., 1995. A fully nonlinear Boussinesq model for surface waves, Part 1, highly nonlinear unsteady waves. Journal of Fluid Mechanics294, 71-92.